1-1-2015

Optimal Control of Epidemics in the Presence of Heterogeneity

Soheil Eshghi
University of Pennsylvania, soheil.eshghi@gmail.com

Optimal Control of Epidemics in the Presence of Heterogeneity

Abstract
We seek to identify and address how different types of heterogeneity affect the optimal control of epidemic processes in social, biological, and computer networks. Epidemic processes encompass a variety of models of propagation that are based on contact between agents. Assumptions of homogeneity of communication rates, resources, and epidemics themselves in prior literature gloss over the heterogeneities inherent to such networks and lead to the design of sub-optimal control policies. However, the added complexity that comes with a more nuanced view of such networks complicates the generalizing of most prior work and necessitates the use of new analytical methods. We first create a taxonomy of heterogeneity in the spread of epidemics. We then model the evolution of heterogeneous epidemics in the realms of biology and sociology, as well as those arising from practice in the fields of communication networks (e.g., DTN message routing) and security (e.g., malware spread and patching). In each case, we obtain computational frameworks using Pontryagin's Maximum Principle that will lead to the derivation of dynamic controls that optimize general, context-specific objectives. We then prove structures for each of these vectors of optimal controls that can simplify the derivation, storage, and implementation of optimal policies. Finally, using simulations and real-world traces, we examine the benefits achieved by including heterogeneity in the control decision, as well as the sensitivity of the models and the controls to model parameters in each case.

Degree Type
Dissertation

Degree Name
Doctor of Philosophy (PhD)

Graduate Group
Electrical & Systems Engineering

First Advisor
Saswati Sarkar

Keywords
Epidemic Routing, Epidemics, Heterogeneity, Optimal Control, Patching, Visibility

Subject Categories
Applied Mathematics | Electrical and Electronics | Epidemiology

OPTIMAL CONTROL OF EPIDEMICS IN THE PRESENCE OF HETEROGENEITY

Soheil Eshghi

A DISSERTATION

in

Electrical and Systems Engineering

Presented to the Faculties of the University of Pennsylvania in Partial Fulfillment of the Requirements for the Degree of Doctor of Philosophy

2015

Supervisor of Dissertation

Saswati Sarkar, Professor of Electrical and Systems Engineering

Graduate Group Chairperson

Alejandro Ribeiro, Rosenbluth Associate Professor of Electrical and Systems Engineering

Dissertation Committee:
Santosh S. Venkatesh, Associate Professor of Electrical and Systems Engineering
George J. Pappas, Joseph Moore Professor and Chair of Electrical and Systems Engineering
Victor M. Preciado, Raj and Neera Singh Assistant Professor of Electrical and Systems Engineering
Olgica Milenkovic, Associate Professor of Electrical and Computer Engineering (University of Illinois at Urbana-Champaign)

*Dedication

This thesis is dedicated first and foremost to my parents, Mahin and Sassan, who have been my bedrock, my guides, and my friends. I am exceptionally grateful to all who have helped me learn, question, and grow.

Acknowledgments

This thesis owes its existence to my advisor, Professor Saswati Sarkar. Her excellent advice and integrity have guided me through my years at Penn, and have shaped my academic approach. I am forever grateful for her dedication to my academic training and rigor. My co-advisor, Professor Santosh S. Venkatesh, has had an equally immense role in this undertaking. His critical eye and simultaneous attention to the big picture and minute detail has been critical to this project, and to my graduate education. I will forever cherish his wonderful lectures.

Thanks are also due to my academic collaborators – first and foremost among them, Dr. M.H.R. (Arman) Khouzani, who mentored me in my first few years at Penn, and introduced me to the topic of epidemic control. I have also had the pleasure of working with, and learning from, Professor Ness Shroff, Dr. Rakesh M. Patil, and Professor Victor M. Preciado. I am also very grateful to the members of my committee, Professor George J. Pappas and Professor Olgica Milenkovic, for their support and insight, which opened up new lines of academic inquiry.

Finally, I am exceptionally grateful for my friends and colleagues here in Philadelphia, who have made my stay here some of the greatest years of my life.

ABSTRACT

OPTIMAL CONTROL OF EPIDEMICS IN THE PRESENCE OF HETEROGENEITY

Soheil Eshghi

Saswati Sarkar

We seek to identify and address how different types of heterogeneity affect the optimal control of epidemic processes in social, biological, and computer networks. Epidemic processes encompass a variety of models of propagation that are based on contact between agents. Assumptions of homogeneity of communication rates, resources, and epidemics themselves in prior literature gloss over the heterogeneities inherent to such networks and lead to the design of sub-optimal control policies. However, the added complexity that comes with a more nuanced view of such networks complicates the generalizing of most prior work and necessitates the use of new analytical methods. We first create a taxonomy of heterogeneity in the spread of epidemics. We then model the evolution of heterogeneous epidemics in the realms of biology and sociology, as well as those arising from practice in the fields of communication networks (e.g., DTN message routing) and security (e.g., malware spread and patching). In each case, we obtain computational frameworks using Pontryagin's Maximum Principle that will lead to the derivation of dynamic controls that optimize general, context-specific objectives. We then prove structures for each of these vectors of optimal controls that can simplify the derivation, storage, and implementation of optimal policies.

Finally, using simulations and real-world traces, we examine the benefits achieved by including heterogeneity in the control decision, as well as the sensitivity of the models and the controls to model parameters in each case.

Contents

[1]Presented in the Information Theory and Applications Workshop (ITA) 2012 and published in the IEEE Transactions on Networking, November 2015 [22].

[2] Presented in IEEE MobiHoc 2012 [44] and published in the IEEE Transactions on Automatic Control, June 2015 [**?**].

[3]Presented at Information Theory and Application Workshop (ITA) 2015 and submitted to IEEE Transactions on Automatic Control, July 2015 [23].

List of Tables

List of Figures

Chapter 1

Overview

1.1 Epidemics & Epidemic Modeling

An epidemic occurs when a disease spreads rapidly among a target population. More generally, any process that involves spreading via interaction can be thought of as an epidemic. Examples of epidemic or epidemic-like processes include the spread of a virus among the human or animal population, malware over a computer network, information over a communication network, and a rumor on social media.

Mathematical models for epidemics, such as those put forth by Daniel Bernoulli [13], predate the germ theory of disease by as much as 100 years. These models, which can be either deterministic or stochastic, seek to track and predict the number of infected individuals. Of these models, deterministic ones have received

the most attention in recent years, both due to their relative analytical straightforwardness and due to limit results which generalize their applicability.[1] It was Hamer [35] who first postulated that the rate of spread of an epidemic is a function of both the populations of infected individuals and those yet to be infected, which is the celebrated mass-action model. This means that the spreading process is non-linear.[2]

Kermack and McKendrick [43] were the first to capture the dynamics of an epidemic through looking at infection states of agents in populations (also known as *compartmental epidemiological models*). Subsequently, these models utilize a mass-action model of interaction to capture the spreading dynamics of the epidemic.[3] In Kermack and McKendrick's original work, agents were divided into 3 compartments based on their infection status (the celebrated SIR epidemic model):

- Infected (I) agents have already contracted the malware,
- Susceptible (S) individuals have yet to contract the malware but are not immune to it,

[1] E.g., those obtained by Kurtz [52] that show an equivalency between the two given some general conditions.

[2] This nonlinearity complicates the analysis of epidemic processes, and leads to interesting behavior such as the Basic Reproduction Number (R_0) threshold results on the terminal spread of an epidemic (c.f., [5]).

[3] These models are very closely related to the Lotka-Volterra predator-prey ecological model (c.f., [63].)

- Recovered (R) agents are not susceptible to the malware, either due to inherent immunity or pre- or post-infection patching.

However, the number and nature of these compartments and their interactions, as well as their interactions with external processes (e.g., birth and death in biological populations), have led to a variety of models that are specific to the behavior of particular epidemics.

While initial work in epidemic modeling was focused on understanding the evolution of an epidemic, intervention policies were soon to follow [36,65,92,93]. These policies seek to stop the spread of an epidemic given limitations on possible actions, such as the limitations that the availability of vaccines, hospital beds, and healthcare workers impose on the control of biological epidemics. Wickwire [93] and Behncke [10] laid the ground-work for most optimal control approaches to date. However, these approaches are limited to homogeneous epidemics, where all nodes are assumed to have the same characteristics (e.g., contact rates, types, importance) and to have identical behavior (i.e., identical control policies).

1.2 Motivating Heterogeneity in Epidemic Models

In practice, however, most epidemics are not homogeneous. Many epidemics spread *non-homogeneously* among the target population, infecting some more frequently and faster than others. In viral epidemics, this can be due to biological, geographical, behavioral, cultural, or socio-economic reasons [17]. We will examine three sources of heterogeneity in turn:

1.2.1 Rate-Heterogeneity

One of the primary ways in which an epidemic can be heterogeneous is when it has different effects and rates of spread in sub-populations.[4] Policies can similarly be non-homogeneous given a dependence on the heterogeneous sub-populations. These sub-populations, or clusters, may result from a variety of reasons, relating to the *nature* of the network:

- **Locality:** In this case, *rate-heterogeneity* arises because contact rates among distant nodes are less than those among closer ones. This is most natural assumption in most types of biologic and social epidemics (i.e., where the epidemic spreads via physical contact) and has led to the study of *ecoepi-*

[4] In literature, these settings have been described by terms such as stratified, structured, clustered, multi-class, multi-type, multi-population, meta-population, demes, heterogeneous, inhomogeneous or spatial epidemic models.

demics [63].

- **Clique/cluster formation:** With the rise of data networks, physical proximity is no longer necessary for the propagation of malware and social epidemics. Users of the same clique can be regarded as the same type with the rate of contact within cliques and across cliques differing depending on the relative sizes of the cliques and their contact rates. Alternately, in cluster (or grid, or volunteer) computing [3], each cluster of CPUs in the cloud constitutes a type. Any two computers in the same cluster can communicate at faster rates than those in different clusters.

- **Behavioral patterns:** In malware epidemics, agents can be clustered based on their security-consciousness, creating safe and risky types based on usage history [99]. Security-savvy users may use more secure protocols, avoid executing untrustworthy code or mass forwarding a received message. The rate of propagation of the malware is therefore the lowest among safe users, higher between safe and risky users, and highest among the risky users. Clustering can also arise naturally in the contexts of technological adoption, fads, opinions [26,79,81], where social contact between adopters of various options and the undecided (infection propagation/ immunization) can lead to their spread.

- **Software/Protocol diversity:** Studies have shown that a network that relies on a homogeneous software/protocol is vulnerable to an attack that exploits a common weakness (e.g., a buffer overflow vulnerability) [56, 69, 94]. In practice, mobile nodes use different operating systems and communication protocols. Such heterogeneities lead to dissimilar rates of propagation of malware among different types, where each type represents a specific OS, platform, software, protocol, etc.

1.2.2 Resource-Heterogeneity

Furthermore, epidemics may spread heterogeneously based on *naturally fluctuating resource-states* in the system that are not inherent to the node (e.g., remaining battery-power in nodes), which leads to fluid types, in contrast to most of the inherent types discussed above. Specifically, the composition of each type of nodes will evolve with time. In these cases, resource constraints limit the ability of particular nodes to perform a certain function, thus stratifying nodes based on their remaining resources. For example, in a Delay-Tolerant Network, or DTN, the ability of a node to relay a message towards its destination depends on its remaining energy reserves. However, message-forwarding consumes energy in the sender and the receiver, which impacts the nodes' future ability to forward further messages. Thus, nodes will be naturally stratified based on the number of messages that they can pass, which is a function of their remaining energy (*stratification*

due to resource-heterogeneity).

1.2.3 Heterogeneity of Epidemics

Finally, multiple epidemics may evolve in tandem, with possible correlations in their infected targets. These epidemics may either: 1) compete for the same nodes, as is the case in multiple strains of a viral epidemic [40, 41] and memes in a world with a limited attention span [91], 2) have an amplifying effect on each others' spread, as is the case with the HIV/TB co-epidemic [38], or 3) they may spread *in conjunction* with each other, where their relative spread is coordinated. In computer networks, this last case can model the case where there are multiple malware types/variants available to the attacker (possibly with different capabilities), and thus the network is attacked by an amalgamation of closely-interlinked malware. For example, variants of a particular malware may execute different policies at certain time as a means of balancing other objectives (e.g., stealth) against the immediate damage that they inflict. In particular, malware such as Stuxnet [53] have had multiple variations that were released at different times with differing functionalities to achieve a unified goal. This is a third type of non-homogeneity - that of the *epidemic* itself.

1.3 Motivation of this work

Models of epidemics need to capture these heterogeneities to be able to form a clear picture of the spreading mechanism.[5] However, prior work has focused on the control of homogeneous epidemics, and thus is deficient in describing real-world epidemics. Multidimensional optimal control formulations, which seek to find optimal *functions* rather than variables, are usually associated with the pitfall of amplifying the complexity of the optimization. This added complexity means that prior approaches will not, in general, yield results for the control of a heterogeneous epidemic. In addition, consideration of heterogeneity will give rise to a wealth of possible structural results for these *vectors of optimal controls* that can be derived and exploited by the controller. Thus, the control of heterogeneous epidemics is a novel, necessary, and natural topic of study that has many real-world applications.

[5]The limit results of Kurtz [52] were extended to the multi-type setting by Ball and Clancey [8], allowing the use of deterministic multi-type models.

1.4 Summary of Contributions

We aim to understand how heterogeneity in contact rates, resources, and epidemics themselves can be leveraged to improve the control of epidemics and epidemic-like processes. In particular:[6]

- In Chapter 2, we seek to derive a theory of the optimal control of *type-heterogeneous* epidemics with a focus on SIR models of malware spread (§1.5). We will concentrate on optimal control policies for classes of defenders that may have different sensitivities to infection (i.e., perceived or real damage) and differing control mechanisms at their disposal.

- In Chapter 3, we aim to develop a theory of optimal control of *resource-heterogeneous* epidemics, focusing on a case where resource-heterogeneity results from differences in the remaining energy of nodes in the process of message delivery in a a Delay-Tolerant Network, or DTN (§1.6). In this case, the resource-state is available to the node, and can be factored into its message-forwarding decision. We concentrate on understanding the structure of these forwarding decisions, as well as their dependence on the energy-states in settings which guarantee a certain Quality of Service (QoS).

[6]Here and subsequently, "We" and "Our" are used in description of the work to acknowledge the contributions of M.H.R. Khouzani, Saswati Sarkar, Santosh S. Venkatesh, and Ness B. Shroff, who contributed to some or all of the work.

- Finally, in Chapter 4, we seek to put forth a theory for the optimal control of cases where the *epidemic* itself is *heterogeneous*. In particular, we investigate stealth-aware optimal spread of malware in §1.7, where there is an inherent heterogeneity to the *infections*. In this case, an attacker balances the need for stealth against the traditional aim of damaging a network, as has been seen in some recent malware [53]. Here, we aim to understand the structure of the optimal decisions of the malware developer, given a range of possible assumptions on the capabilities at their disposal, and to characterize the optimal spread of the epidemic both on its own and in the presence of a network defense mechanism.

We now present each problem in the 3 domains in more detail, and summarize our contributions to each case:

1.5 Rate-Heterogeneity: Optimal Control of Clustered Malware Epidemics

We consider the spread of a malware epidemic in a heterogeneous environment where nodes are stratified based on their respective contact rates. In the environments, immunization/healing/patching policies need to cater to the specific stratum to ensure maximal efficacy. In malware epidemics, as opposed to biological ones, the healing mechanism (i.e., patching) can be replicative, which means that patched nodes may be able to spread the patch to other nodes. This possible secondary spread of immunity also arises in some of the other rate-dependent heterogeneous epidemic models (see §1.2.1). We consider the immunization/healing/patching rates as dynamic controls that evolve with time. The aim of this investigation was to find optimal, custom trade-offs between the damage sustained by the network and the resources spent in patching it against the malware utilizing the heterogeneity in contact-rates among nodes in the network. The gains from these *rate-heterogeneous* approaches, however, usually come at a cost (in terms of computation, storage, sensitivity, etc.) which depends on the nature of the network. Characterizing these costs and the resulting optimal immunization/healing/patching structures determine whether the controller should make use of such mechanisms. We seek to quantify the changes that arise from such an approach as compared to simpler ones that assume a homogeneous net-

work.

Contributions

- We *modeled* the spread of an epidemic in a *rate-heterogeneous* environment by considering logical clusters of nodes where each cluster constitutes a *type*. Nodes of the same type homogeneously mix with a rate specific to that type and nodes of different types contact each other at rates particular to that pair of types, with SIR epidemic dynamics that evolve according to these pairwise contact rates. The model can therefore capture any communication topology between different groups of nodes. To capture a general case of possible responses of the network, we considered both *non-replicative* and *replicative* patching: in the former, some of the hosts are pre-loaded with the patch, which they transmit to the rest. In the latter, each recipient of the patch can also forward the patch to nodes that it contacts by a mechanism similar to the spread of the malware itself. In our model, patching can immunize susceptible nodes and may or may not heal infective nodes. The dynamics of the model can be seen in Fig. 1.1.

- We proposed a formal framework for *computing dynamic optimal* patching policies (patching action within each cluster) for these rate-heterogeneous settings. these policies leverage heterogeneity in the network structure to attain the minimum possible aggregate cost due to the spread of malware

and the overhead of patching. The framework in each case relies on optimal control formulations that cogently capture the effect of the patching rate controls on the state dynamics and their resulting trade-offs. We accomplished this by using a combination of damage functions associated with the controls and a *stratified* mean-field deterministic epidemic model in which nodes were divided into different types. Above and beyond, it can exploit the inhomogeneity in the network to enable a better utilization of the resources. Such higher patching efficacy is achieved by allowing the patching controls to depend on node types, which in turn gives rise to *multidimensional (dynamic)* optimal control formulations. These formulations lead to a solution framework derived from Pontryagin's Maximum Principle, which characterizes necessary conditions for the optimality of vectors of controls.

- We proved that for both non-replicative and replicative settings the optimal control associated with each type has a simple *structure* provided the corresponding patching cost is either concave or convex. These structures were derived using Pontryagin's Maximum Principle and analytic arguments specific to this problem. This derivation reveals that the structure of the optimal control for a specific type depends only on the nature of the corresponding patching cost and not on those of other types. This fact (correspondence of the nature of the optimal patching control in a type to the convexity or concavity of the patching cost in that particular type and not that of others)

is surprising, as the control for each type affects immunization and healing in other types and the spread of the infection in general. Specifically, if the patching cost associated with the control for a given type is concave, irrespective of the nature of the patching costs for other types, the corresponding optimal control turns out to be a bang-bang function with at most one jump: up to a certain threshold time (possibly different for different types) it selects the maximum possible patching rate and subsequently it stops patching altogether. If the patching cost is strictly convex, the decrease from the maximum to the minimum patching rate is continuous rather than abrupt, and monotone. Note that each of these bang-bang controls can be represented by one point (the threshold), and thus the vector of control functions can be expressed as a vector of scalars of the same size, which simplifies their computation and storage. Furthermore, the simplicity of these structures makes them suitable for implementation, while also providing a benchmark for other policies that may require fewer network parameters. The optimal controls were compared to heuristic and homogeneous alternatives over real-world traces and numerical simulations in a variety of sample topologies. As expected, it was seen that as contact rates become more varied within a topology, homogeneous approximations to the optimal controls become very inefficient. This experimentally validated the premise of considering rate-heterogeneity in the choice of the patching controls.

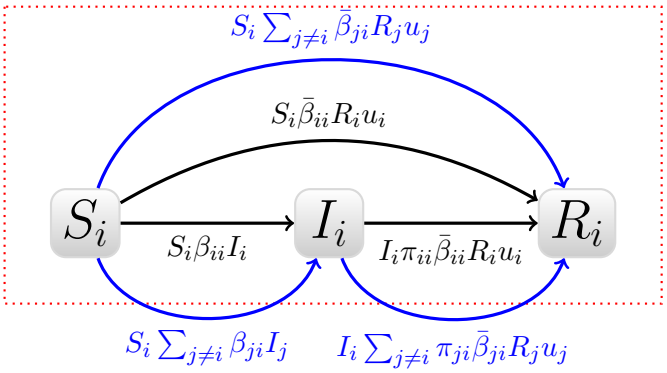

Figure 1.1: This figure captures the SIR dynamics within each agent type, as well as the interactions between types. The numbers on the arrows indicate rates. Blue arrows indicate inter-type contacts, while black ones represent contacts that happen within each type. Notice that the communication rates (denoted by β) between susceptible agents of a certain type i and the infected nodes of type j can be different from their communication rate with recovered notes of the same type, a situation that may arise due to the nature of the system (e.g., in the case of two competing infections) or because of provisions taken by either the attacker or the defender (i.e., $\beta_{ij} \neq \beta_{ji}$). u_j denotes the dynamic control of the defender on the propagation of patches by type j, while π_{ji} (static) represents the extent to which infected agents of type i can be healed by agents of type j.

1.6 Resource-Heterogeneity: Optimal Energy-Aware Epidemic Routing in DTNs

In Delay-Tolerant Networks (DTNs), end-to-end connectivity is rare, and messages have to be passed along by intermediate nodes to reach their destination. Most importantly, message forwarding consumes energy in the intermediate nodes, which is critical as in many cases their energy supplies are non-replenishable (e.g., where communication devices are carried by disaster relief personnel and soldiers, or where they can be mounted on wandering animals). These forwarding decisions leave different nodes with different remaining energies at each time-instant, leading to an exploitable *resource-heterogeneity* in the network. This message forwarding process can accordingly be *controlled* to achieve certain objectives in terms of both the delivery of the message and the resources of the network. A fundamental question in this realm is how to balance quality of service (i.e., the probability that the message reaches its destination in a timely manner) against the use of network resources (such as node battery power and bandwidth). It is of practical importance to see whether it is possible to derive optimal controls that depend on readily-measurable resource-states of nodes (such as battery power), and to quantify the effects of this trade-off and the benefits of incorporating the additional information in the decision.

Contributions

- We *modeled* message transmission in a DTN as a *resource-state heterogeneous* controllable SI epidemic, where the forwarding policies in each node constitute the controls. We defined a node that had received a copy of the message and is not its destination as an *infective* (I) and a (non-destination) node that had not yet received a copy of the message as a *susceptible* (S). When an infective node contacts a susceptible at time t, the message is transmitted with a certain forwarding probability if the infective (transmitter) and susceptible (receiver) have at least s and r units of energy (s and r being the energy necessary for transmission and reception of the message). Stratifying the nodes based on their energy resource-state, we defined $S_i(t)$ (respectively, $I_i(t)$) to be the *fraction* of nodes that are susceptible (respectively, infective) and that have i energy units at time t. At any given time, each node can observe its own level of available energy, and *its forwarding decision should, in general, utilize such information*. Thus, the forwarding decision in our model is dependent on the forwarding node's remaining energy: upon an instance of contact between a susceptible node of energy i and an infective node of energy j, the message is forwarded with probability $u_j(t)$ ($0 \leq u_j(t) \leq 1$). We took these probabilities to be our controls $\mathbf{u}(t) = \big(u_s(t), u_{s+1}(t), \ldots, u_B(t)\big)$. If the message is forwarded, the susceptible node of energy i transforms to an infective node with $i - r$ energy units, and the infective node of energy j

likewise to an infective node with $j - s$ energy units. If a message-carrying node that has sufficient energy for one transmission contacts the destination that has yet to receive the message, the message is always forwarded to the destination. These dynamics can be seen in Fig. 1.2. We modeled the evolution of these fractions (states) using epidemiological differential equations that rely on mean-field approximation of Markov processes. Subsequently, we formulated the trade-off between energy conservation and likelihood of timely delivery as a dynamic energy-dependent optimal control problem: at any given time, each node chooses its forwarding probability based on its current remaining energy. Since the number of relay nodes with the message increases and residual energy reserves decrease with transmissions and receptions, the forwarding probabilities vary with time. Thus, they must be chosen so as to control the evolution of network states, which capture both the fraction of nodes holding a copy of the message and the remaining battery reserves of the nodes.

- We sought to *compute* dynamic forwarding probabilities (*optimal controls*) that optimize objective functions penalizing energy depletion subject to enforcing timely message delivery. These dynamic forwarding probabilities constituted our optimal controls. The resulting optimal control problem is solved using Pontryagin's Maximum Principle, which leads to a computational framework for the optimal controls.

- Utilizing the above framework combined with arguments specific to this context, we characterized the *structures* of these resource-dependent optimal controls (i.e., forwarding decisions) and showed that they follow simple rules that can be computed in a computationally efficient manner.

  Our first result was to prove that dynamic optimal controls follow simple threshold-based rules. That is, a node in possession of a copy of the message forwards the message to nodes it encounters that have not yet received it until a certain threshold time that depends on its current remaining energy. Calculating these thresholds is much simpler than solving the general problem and can be done once at the source node of the message. Subsequently, they can be added to the message as a small overhead. Each node that receives the message can retrieve the threshold times and forward the message if its age is less than the threshold entry of the node's residual energy level. The execution of the policy at each node is therefore simple and based only on local information.

  Our second result was to characterize the nature of the dependence of the thresholds on the energy levels. Intuitively, the less energy a node has, the more reluctant it should be to transmit the message, as the transmission will drive it closer to critically low battery levels. However, our investigations revealed that this intuition can only be confirmed when the penalties associated with low final remaining energies are convex. In particular, we

constructed a viable case with non-convex costs where the optimal thresholds did not follow this intuition.

Our optimal control provided a missing *benchmark* for forwarding policies in large networks in which no information about the mobility pattern of the individual nodes is available and a minimum QoS is desired. This benchmark allowed me to observe the sub-optimality of some simpler heuristic policies, and to identify parameter ranges in which they perform close to the optimal. Furthermore, we showed that the optimal controls were robust to estimation errors in their parameters and synchronization, and that they performed much better than heuristics in cases with more energy heterogeneity and starker penalties on energy mis-utilization. Finally, we showed that these optimal controls extended the number of messages a network could transmit before exhaustion, which is a measure of network lifetime.

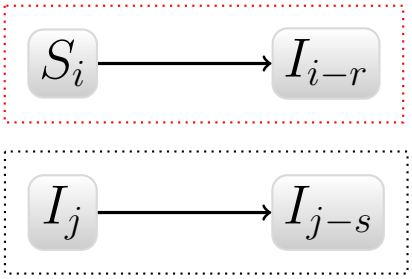

Figure 1.2: This figure captures how the message transmission upon contact changes the energy levels of nodes, as well as infecting the susceptible node. The dotted boxes represent the two agents in which the simultaneous transformations that result from a message transmission occur. The susceptible agent becomes an infective while losing r units of power, while the infecting agent spends s units of energy to send the message.

1.7 Epidemic-Heterogeneity: Visibility-Aware Malware Epidemics

Multiple epidemics may spread simultaneously in a network, leading to a third type of heterogeneity: *epidemic heterogeneity*. In particular, malware epidemics differ from biological ones in that multiple variants of an epidemic can spread in a *coordinated* manner. Furthermore, these epidemics can be designed to respond to triggers and to act in such a way as to maximize a certain utility for the malware designer, perhaps even factoring the response of the defender (controlled evolution). This creates challenges for security professionals who have to understand the motivations and methods of these malware designers. The malware

designer's control, in this model, is to dynamically tune the mix of the malware variants to achieve a certain objective. Thus, the designer's decision to spread the epidemic will be dependent on the particular variant, leading to *heterogeneous control structures*.

Specifically, a new generation of malware, one that eschews damage to the network to maintain stealth, has led to new challenges in computer network security. These "surgical" strikes seek to minimize visibility, as awareness can lead the intended target to cease communication (e.g., by quarantining the targets). Stuxnet, for example, was designed to attack a specific control software used in centrifuges [25] and did not steal or manipulate data, or receive any command instructions from remote sources so as to maintain stealth [53] (cf. Duqu, Flame, and Gauss [11]). Yet, it was discovered and remedied after it spread outside its target area [76]. Thus there is a new trade-off for the attacker — that between stealth and damage. That is, if the malware spreads too fast, it will also be detected and remedied fast, so a slower spread may mean that it can cause more aggregate damage. Thus, in contrast to many other epidemiological contexts, aggressive policies may not be optimal.

In particular, we consider the case where two variants of a single malware spread in a network. One spreads aggressively in every contact, and is thus visible to the network due to its communications, while the other passive variant does not spread subsequent to infecting a node. Coordinating distributed attacks comes

at the cost of added visibility due to communication and is susceptible the timing errors in the hosts. Thus, we focus on the case where distributed nodes that are infected are not asked to coordinate, as was the case in Stuxnet. The natural question that arises is to characterize the structure of optimal malware variant mix that the attacker will spread at each instant depending on their goal structures and the communication mechanisms that they may have at their disposal.

Contributions

- We *modeled* a network under attack by these two variants of a malware. Depending on their infection status, nodes could be divided into 4 groups: 1) *Germinators* (G) that are a fixed (potentially very small) fraction of the nodes that are the only nodes under the direct control of the attacker, 2) *Susceptibles* (S) that are nodes that have not received any variant of the malware, 3) *Zombies* (Z) that have received the aggressive malware variant and will continue to propagate it indiscriminately, and 4) *Passives* (P) that have received the passive variant of the malware, and thus do not propagate it any further. Both zombies and passives can contribute to damaging the network through the execution of malicious code. Zombies, however, are potentially visible to the network as they have to communicate with other nodes to spread the message. To capture the visibility-conscious malware designer's decision to spread either of the potent-yet-visible or less-potent-

but-less-visible variants of a malware at each time instant, we proposed a mathematical formulation for the state dynamics governing interaction between nodes in these 4 groups. This model characterizes how nodes in these groups transform from one state to the other, as well as the impact of the attacker's control. In this model, the germinators, at each encounter with a susceptible, decide whether to turn it into a zombie or a passive, or to leave it as a susceptible. We also investigated the case where we added a further mechanism of interaction whereby the germinators, upon contact with zombies, can turn them into passives (i.e., stopping them from spreading the message any further). Finally, we formulated state dynamics that account for the network's defense strategy. Once a defender becomes aware of a malware outbreak, she can ask nodes to limit their effective contacts as a means to limit the spread of malware. This, however, comes at a cost of stopping legitimate communication within the network. For a pictorial representation of these 3 dynamics, see Fig. 1.3. We quantified the damage inflicted by the malware through characterizing an overall damage function consisting of an efficacy function of the aggregate number of zombies and passives, and a visibility function of the number of zombies. In the first two models described above, the attacker chooses controls that maximize this damage. In the latter model, the effect of visibility is built into the network dynamics, as we allow the network to choose a policy based on the fraction

of zombies, and so the attacker is only directly concerned with maximizing efficacy. In these settings, the network can choose quarantine policies that are either affine or logistic in the number of zombies.

- We sought to *compute* dynamic malware-spread mixes (*optimal controls*) that the malware designer would employ to optimally balance her objectives of maximum damage and minimum visibility given the variety of possible mechanisms available to the defender. These dynamic decisions, which determined the probability that each variant will be spread at each encounter between a germinator and a susceptible, constituted our optimal controls. The resulting optimal control problem is solved using Pontryagin's Maximum Principle, which leads to a computational framework for the optimal controls.

- We showed that the attacker's optimal strategy in all of these models follows a certain *structure*: the germinators only create zombies up to a certain time, and then only create passives (including by halting zombies) from then on. That is, the optimal controls are *bang-bang* (i.e., only taking their minimal and maximum values) with only one jump. It is interesting to note that in each of the variations we considered, our analysis revealed that all the controls switch at the same point, a fact that was not at all clear *a priori*. Thus the entire control space could be described by one time-point, a fact that is invaluable for deriving the optimal controls computationally.

Furthermore, the controls were easy to implement as the infectives need to be programmed with just one time instant for all of their controls. After completely characterizing the optimal controls, we investigated the effect of the network's estimation errors in the latter model for network response. We demonstrated that the model performs reasonably well even when there are small errors in the network's estimation of the number of zombies, which it uses to determines its response to the malware epidemic.

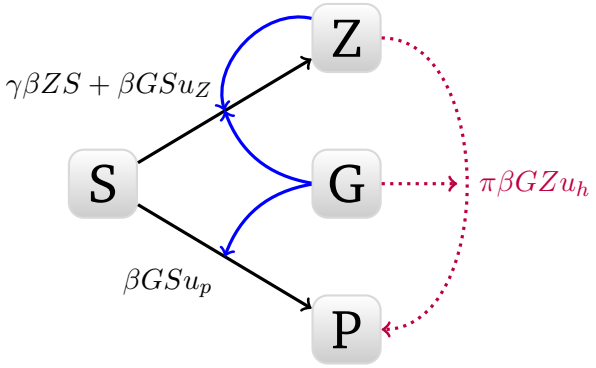

Figure 1.3: The solid black arrows show the dynamics in the visibility-aware epidemic model with no halting (the ability to make zombies into passive agents upon contact). The red arrows show the additional mechanism that affects the case where halting is assumed in the model. Finally, in the case with network defense, β is replaced by $\beta(Z)$, which is a function of the number of zombies (i.e., the visibility of the epidemic). Note that the population of G never changes, and the arrows emanating from it show that some changes happen when a germinator agent encounters another type of agent. As before, the numbers beside the arrows denote rates of transition.

1.8 Literature review and positioning of our contributions

1.8.1 Rate Heterogeneity

Epidemic models, and especially SIR epidemic models, have been used extensively to model the spread of malware and the propagation of information in computer networks, beginning from Murray [66] and Kephart and White [42]. Recent work on malware and information epidemics has focused on how these epidemics can be controlled [1, 50, 58]. However, the work on the propagation of information (such as [1,58]) has focused on two-hop routing with no adversaries, which does not apply to malware defense and a host of other applications such as technology adoption. On the other hand, works on malware defense, such as [50] have modeled healing and immunization as contact-independent exogenous processes that are uniform among all nodes, which are very limiting assumptions. Recognizing the constraints of the defender, works such as [45, 46] have included the cost of patching in the aggregate damage of the malware and have characterized the optimal dynamic patching policies that attain desired trade-offs between the patching efficacy and the extra taxation of network resources. Similarly, Li *et al.* [57] and Altman *et al.* [2] have characterized optimal dynamic transmission control policies for two-hop and multi-hop messages. These results, however, critically

rely on the *homogeneous* mixing assumption: that all pairs of nodes have identical expected inter-contact times. Thus, there will only be one optimal control for the system. While this assumption may serve as an approximation in cases where detailed information about the network is unavailable, studies [16, 55, 64, 71, 89] show that the spread of malware in mobile networks can be very inhomogeneous, owing primarily to the non-uniform distribution of nodes. Thus, a uniform action may be sub-optimal.

To the best of our knowledge, our work was the first that considers the control of a general stratified epidemic and provides analytical structural guarantees for a dynamic patching.[7] Our model is general enough to capture any clustering of the nodes with arbitrary inter-contact rates of interaction and to allow different methods of type specification. Owing to the heterogeneity of nodes, it becomes necessary to have differing controls for different strata (types), leading to a *vector* of controls as opposed to the *single* control that was derived for *homogeneous* users in prior literature. Deriving structure results for a vector of controls requires analytical arguments that are quite different from those employed for a single control. The simple structure results described for the optimal policies have not been established in the context of (static or dynamic) control of *heterogeneous* epidemics. The power of our analytical results is in the extensive generality of our model.

[7] Li *et al.* [58] consider a 2-type epidemic, but with no control. All other prior work has assumed *one uniform control* for one set of *homogeneous* users.

1.8.2 Resource Heterogeneity

The literature on message routing in DTNs is extensive [1, 7, 9, 19, 20, 60, 61, 67, 68, 82–84, 88, 90, 96]. Most notably, Vahdat and Becker [88] present a policy where each node propagates the message to all of its neighbors simultaneously ("Epidemic Routing"), while Spyropoulos *et al.* [84] propose spreading a specific number of copies of the message initially and then waiting for the recipients of these copies to deliver the message to the destination ("Spray and Wait"). Wang and Wu [90] present "Optimized Flooding", where flooding is stopped once the total probability of message delivery exceeds a threshold. Singh *et al.* [83] and Altman *et al.* [1] identify optimal and approximately optimal message forwarding policies in the class of policies that do not take the distribution of node energies into account. In summary, the state of the art in packet forwarding in DTNs comprises of heuristics that ignore energy constraints [60, 88, 96], those that consider only overall energy consumption but provide no analytic performance guarantees [9, 19, 61, 68, 84, 90], and those that do not utilize the energy available *to each node* in making forwarding decisions [1, 7, 20, 67, 82, 83]. An efficient forwarding strategy can use knowledge of the distribution of energy among nodes to its advantage, and this motivates the design of dynamic energy-dependent controls which are the subject of this work.

To the best of our knowledge, our work was the first work that considers message routing in DTNs as a *resource-heterogeneous* optimal forwarding problem

where the forwarding decision of a node is based on its remaining energy. Furthermore, the optimal structures derived for the forwarding decisions are also a contribution of the work, given the difficulties posed by vectors of controls. Next, the threshold ordering results for the optimal controls, obtained for convex costs, are without precedent in proposition and analysis. Finally, the counter-example provided shows that convexity is a relatively strong sufficient condition for this ordering phenomenon.

1.8.3 Epidemic Heterogeneity

Multiple interacting epidemics that spread among a single population have been considered in the fields of biology [40, 41] and sociology [91]. In these models, these epidemics either compete for a limited pool of susceptible nodes, or cause the susceptibles to become more vulnerable to other epidemics. However, in all these contexts, there is no mechanism to coordinate the actions of competing epidemics. In the realm of malware, on the other hand, such a coordination among multiple epidemics can not only exist, but can be intrinsic to the attack strategy of a malware designer. Furthermore, in the majority of malware epidemic models, e.g., [27, 34, 51, 62, 77, 98], two things have generally been assumed: 1- that the attacker's sole aim is to maximize the spread of the malware, and 2- that they have a mechanism to control the malware in the future (through a timer in the code, for example– for a similar framework, see [22]). As we described, these two

assumptions are no longer true for the emerging generation of malware. Thus, the model presented for the spread of visibility-heterogeneous malware variants has no precedent in literature. Accordingly, the questions we asked and the solutions we obtained are substantially different to prior work. The closest work to this topic was by Khouzani and Sarkar [47]. However, their model differs from mine in two key ways: 1) They assume that the malware can control the transmission range of infected nodes, while in this problem, we assume that the control affects the mix of malware variants and that the communication ranges of nodes are outside the malware's control, perhaps even being controlled by the defender as a mitigation mechanism. Thus, the control and the trade-off to the malware designer is fundamentally different. 2) The models for defense are also different: In their model, patching is the major defense of the network and starts as soon as the epidemic spreads. This may not be the case for an emerging stealthy epidemic like Stuxnet that is very large and extremely hard to decipher, let alone mitigate [15,95]. In our model, the network only becomes aware of the malware as it becomes more visible (i.e., as the visible variant spreads). Furthermore, we examine at a case where the network can defend itself by choosing the communication ranges of nodes as a decreasing function of the visibility of the malware, which is a form of quarantine. In addition to these two key differences, in our models the malware designer only requires synchronized actions from a fixed number of nodes that are under its control from the outset. This decreases the risks of de-

tection and policy implementation errors arising from coordinating synchronized distributed actions among a varying set of nodes, which is necessary in Khouzani and Sarkar's model.

To the best of our knowledge, our work was the first work that considers the problem of multiple coordinated malware variants spreading in a network (malware *epidemic heterogeneity*). Furthermore, the consideration of stealth as a means of stratification of the epidemics and as a goal of the malware designer is also without precedent. The optimal structures that are presented for the optimal malware spreading probabilities also constitute a contribution of the work. The simple structure of these optimal controls - that at each time, the spread of only one variant of the malware is encouraged, with only one abrupt transition in the preferred malware - holds for all the models presented. This means that it is reasonable for a network defender to assume this simple action structure for the actions of the malware. Finally, the numerical simulations show that the model is not sensitive to estimation errors in the fraction of visible malware (zombies) on the part of the network defender, and thus the simple defense structures assumed in the latter model can be a reasonable starting point in the derivation of optimal stable defense strategies for the network.

Chapter 2

Rate-Heterogeneity: Optimal Patching in Clustered Malware Epidemics[1]

2.1 Introduction

Differing communication rates among multiple types/clusters of agents constitute the most obvious type of heterogeneity that inherently affects the spreading of most epidemics. This is especially relevant where there is an opportunity to leverage this heterogeneity to develop better type-dependent epidemic control policies. In particular, we focus on the spread of malware (and specifically, worms)

[1]Presented in the Information Theory and Applications Workshop (ITA) 2012 and published in the IEEE Transactions on Networking, November 2015 [22].

in computer networks, where there are multiple factors that cause heterogeneity, e.g., locality, IP space, platform.

Worms (self-propagating malicious codes) are a decades-old threat in the realm of the Internet. Worms undermine the network in various ways: they can eavesdrop on and analyze traversing data, access privileged information, hijack sessions, disrupt network functions such as routing, etc. Although the Internet is the traditional arena for trojans, spyware, and viruses, the current boom in mobile devices, combined with their spectacular software and hardware capabilities, has created a tremendous opportunity for future malware. Mobile devices communicate with each other and with computers through myriad means – Bluetooth or Infrared when they are in close proximity, multimedia messages (MMS), mobile Internet, and peer to peer networks. Current smart-phones are equipped with operating systems, CPUs, and memory powerful enough to execute complex codes. Wireless malware such as *cabir*, *skulls*, *mosquito*, *commwarrior* have already sounded the alarm [72]. It has been theoretically predicted [89] that it is only a matter of time before major malware outbreaks are witnessed in the wireless domain.

Malware spreads when an infective node *contacts*, i.e., communicates with, a susceptible node, i.e., a node without a copy of the malware and vulnerable to it. This spread can be countered through patching [97]: the vulnerability utilized by the worm can be fixed by installing security patches that immunize the

susceptible and potentially remove the malware from the infected, hence simultaneously healing and immunizing infective nodes. However, the distribution of these patches burdens the limited resources of the network, and can wreak havoc on the system if not carefully controlled. In wired networks, the spread of *Welchia*, a counter-worm to thwart *Blaster*, rapidly destabilized important sections of the Internet [54]. Resource constraints are even more pronounced in wireless networks, where bandwidth is more sensitive to overload, and nodes have limited energy reserves.

We propose a formal framework for deriving *dynamic optimal* patching policies that leverage heterogeneity in the network structure to attain the minimum possible aggregate cost due to the spread of malware and the overhead of patching. We assume arbitrary (potentially non-linear) functions for the cost rates of the infective nodes. We consider both *non-replicative* and *replicative* patching: in the former, some of the hosts are pre-loaded with the patch, which they transmit to the rest. In the latter, each recipient of the patch can also forward the patch to nodes that it contacts by a mechanism similar to the spread of the malware itself. In our model, patching can immunize susceptible nodes and may or may not heal infective nodes. The framework in each case relies on optimal control formulations that cogently capture the effect of the patching rate controls on the state dynamics and their resulting trade-offs. We accomplish this by using a combination of damage functions associated with the controls and a *stratified*[2] mean-field

[2]Known by other terms such as structured, clustered, multi-class, multi-type, multi-population,

deterministic epidemic model in which nodes are divided into different types. Nodes of the same type homogeneously mix with a rate specific to that type, and nodes of different types contact each other at rates particular to that pair of types. The model can therefore capture any communication topology between different groups of nodes. Above and beyond, it can exploit the inhomogeneity in the network to enable a better utilization of the resources. Such higher patching efficacy is achieved by allowing the patching controls to depend on node types, which in turn leads to *multidimensional (dynamic)* optimal control formulations.

Multidimensional optimal control formulations, particularly those in the solution space of functions rather than variables, are usually associated with the pitfall of amplifying the complexity of the optimization. An important contribution of this work, therefore, is to prove that for both non-replicative and replicative settings the optimal control associated with each type has a simple structure provided the corresponding patching cost is either concave or convex. These structures are derived using Pontryagin's Maximum Principle and analytic arguments specific to this problem, another of our contributions. This derivation reveals that the structure of the optimal control for a specific type depends only on the nature of the corresponding patching cost and not on those of other types. This holds even though the control for each type affects immunization and healing in other types and the spread of the infection in general. Specifically, if the patching cost

compartmental epidemic models, and sometimes loosely as heterogeneous, inhomogeneous or spatial epidemic models.

associated with the control for a given type is concave, irrespective of the nature of the patching costs for other types, the corresponding optimal control turns out to be a bang-bang function with at most one jump: up to a certain threshold time (possibly different for different types) it selects the maximum possible patching rate and subsequently it stops patching altogether. If the patching cost is strictly convex, the decrease from the maximum to the minimum patching rate is continuous rather than abrupt, and monotone. To the best of our knowledge, such simple structure results have not been established in the context of (static or dynamic) control of *heterogeneous* epidemics. Furthermore, the simplicity of these structures makes them suitable for implementation, while also providing a benchmark for other policies that may require fewer network parameters. Our numerical calculations reveal a series of interesting behaviors of optimal patching policies for different sample topologies.

To the best of our knowledge, this is the first work that considers a stratified epidemic and provides analytical structural guarantees for a dynamic patching.[3] Our model is general enough to capture any clustering of the nodes with arbitrary inter-contact rates of interaction and to allow different methods of type specification. Owing to the heterogeneity of nodes, we are compelled to have differing controls for different strata (types), leading to a *vector* of controls as opposed to the *single* control that was derived for *homogeneous* users in prior literature. De-

[3]Li *et al.* [58] consider a 2-type epidemic, but with no control. All other prior work has assumed *one uniform control* for one set of *homogeneous* users.

riving structure results for a vector of controls requires analytical arguments that are quite different from those employed for a single control. The power of our analytical results is in the extensive generality of our model.

First, we develop our system dynamics and objectives (§2.2) and characterize optimal non-replicative (§2.3) and replicative (§2.4) patching. We then analyze an alternate objective (§2.5) and present numerical simulation of our results (§2.6).

2.2 System Model and Objective Formulation

In this section we describe and develop the model of the state dynamics of the system as a general *stratified* epidemic for both non-replicative (§2.2.1) and replicative (§2.2.2) patching, motivate the model (§2.2.3), formulate the aggregate cost of patching, and cast this resource-aware patching as a *multi-dimensional* optimal control problem (§2.2.5). This formulation relies on a key property of the state dynamics which we isolate in §2.2.4. We develop solutions in this model framework and present our main results in §2.3 and §2.4.

Our models are based on mean-field limits of Poisson contact processes for which path-wise convergence results have been shown (c.f. [52, p.1], [32]).

2.2.1 Dynamics of non-replicative patching

A node is **infective** if it has been contaminated by the malware, **susceptible** if it is vulnerable to the infection but not yet infected, and **recovered** if it is immune to the malware. An infective node spreads the malware to a susceptible one while transmitting data or control messages. The network consists of nodes that can be stratified into M different *types*[4]. The population of these types need not be equal. A node of type i contacts another of type j at rate $\beta_{ij}^{(N)}$.

There are $N_i = \alpha_i N$ ($\alpha_i > 0$) nodes of type i in the network, among which $n_i^S(t)$, $n_i^I(t)$ and $n_i^R(t)$ are respectively in the susceptible, infective and recovered states at time t. Let the corresponding fractions be $S_i(t) = n_i^S(t)/N_i$, $I_i(t) = n_i^I(t)/N_i$, and $R_i(t) = n_i^R(t)/N_i$. We assume that during the course of the epidemic, the populations of each type, N_i, are stable and do not change with time. Therefore, for all t and all i, we have $S_i(t) + I_i(t) + R_i(t) = 1$.

Amongst each type, a pre-determined set of nodes, called *dispatchers*, are pre-loaded with the appropriate patch. Dispatchers can transmit patches to both susceptible and infective nodes, *immunizing* the susceptible and possibly *healing* the infective; in either case successful transmission converts the target node to the recovered state. In *non-replicative* patching (as opposed to *replicative* patching-see §2.2.2) the recipient nodes of the patch do not propagate it any further.[5] Dis-

[4] equivalently, *clusters, segments, populations, categories, classes, strata*).

[5] This may be preferred if the patches themselves can be contaminated and cannot be reliably

patchers of type i contact nodes of type j at rate $\bar{\beta}_{ij}^{(N)}$, which may be different from the contact rate $\beta_{ij}^{(N)}$ of the malware between these two types. Examples where contact rates may be different include settings where the network manager may utilize a higher priority option for the distribution of patches, ones where the malware utilizes legally restricted means of propagation not available to dispatchers, or ones where the patch is not applicable to all types, with the relevant $\bar{\beta}_{ij}^{(N)}$ now being zero. The number of dispatchers of type i, which is fixed over time in the non-replicative setting, is $N_i R_i^0$, where $0 < R_i^0 < 1$.

Place the time origin $t = 0$ at the earliest moment the infection is detected and the appropriate patches generated. Suppose that at $t = 0$, for each i, an initial fraction $0 \leq I_i(0) = I_i^0 \leq 1$ of nodes of type i are infected. At the onset of the infection, the dispatchers ($R_i(0) = R_i^0$) are the only agents immune to the malware. In view of node conservation, it follows that $S_i(0) = S_i^0 = 1 - I_i^0 - R_i^0$.

At any given t, any one of the $n_i^S(t)$ susceptibles of type i may be infected by any of the $n_j^I(t)$ infectives of type j at rate $\beta_{ji}^{(N)}$. [6] Thus, susceptibles of type i are transformed to infectives (of the same type) at an aggregate rate of $n_i^S(t) \sum_j \beta_{ji}^{(N)} n_j^I(t)$ by contact with infectives of any type.

The system manager regulates the resources consumed in the patch distribution by dynamically controlling the rate at which dispatchers contact susceptible

authenticated.

[6] Susceptibles of type i may be contacted by infectives of type j at a higher rate, and it is possible that not all contacts lead to infection.

and infective nodes. For each j, let the control function $u_j(t)$ represent the rate of transmission attempts of dispatchers of type j at time t. We suppose that the controls are non-negative and bounded,

$$0 \leq u_j(\cdot) \leq u_{j,\max}. \tag{2.2.1}$$

We will restrict consideration to control functions $u_j(\cdot)$ that have a finite number of points of discontinuity. We say that a control (vector) $\mathbf{u}(t) = \big(u_1(t), \ldots, u_M(t)\big)$ is *admissible* if each $u_j(t)$ has a finite number of points of discontinuity.

Given the controls $u_1(\cdot), \ldots, u_M(\cdot)$, susceptibles of type i are transformed to recovered nodes of the same type at an aggregate rate of $n_i^S(t) \sum_j \bar{\beta}_{ji}^{(N)} n_j^R(0) u_j(t)$ by contact with dispatchers of any type. A subtlety in the setting is that the dispatcher may find that the efficacy of the patch is lower when treating infective nodes. This may model situations, for instance, where the malware attempts to prevent the reception or installation of the patch in an infective host, or the patch is designed only to remove the vulnerability that leaves nodes exposed to the malware but does not remove the malware itself if the node is already infected. We capture such possibilities by introducing a (type-dependent) coefficient $0 \leq \pi_{ji} \leq 1$ which represents the efficacy of patching an infective node: $\pi_{ji} = 0$ represents one extreme where a dispatcher of type j can only immunize susceptibles but can not heal infectives of type i, while $\pi_{ji} = 1$ represents the other extreme where contact with a dispatcher of type j both immunizes and heals nodes of type i equally well; we also allow π_{ij} to assume intermediate values between the above extremes. An

infective node transforms to the recovered state if a patch heals it; otherwise, it remains an infective. Infective nodes of type i accordingly recover at an aggregate rate of $n_i^I(t)\sum_{j=1}^{M}\pi_{ji}\bar{\beta}_{ji}^{(N)}n_j^R(0)u_j(t)$ by contact with dispatchers.

In the large (continuum) population regime, suppose that the two limits $\beta_{ij} := \lim_{N\to\infty}\alpha_i N\beta_{ij}^{(N)}$ and $\bar{\beta}_{ij} := \lim_{N\to\infty}\alpha_i N\bar{\beta}_{ij}^{(N)}$ exist. We say that a type j is a *neighbor* of a type i if $\beta_{ij} > 0$, and $S_j(t) > 0$ (i.e., infected nodes of type i can contact nodes of type j). There is now a natural notion of a topology that is inherited from these rates with types as vertices and edges between neighboring types. Figure 2.1 illustrates some simple topologies. For a given topology inherited from the

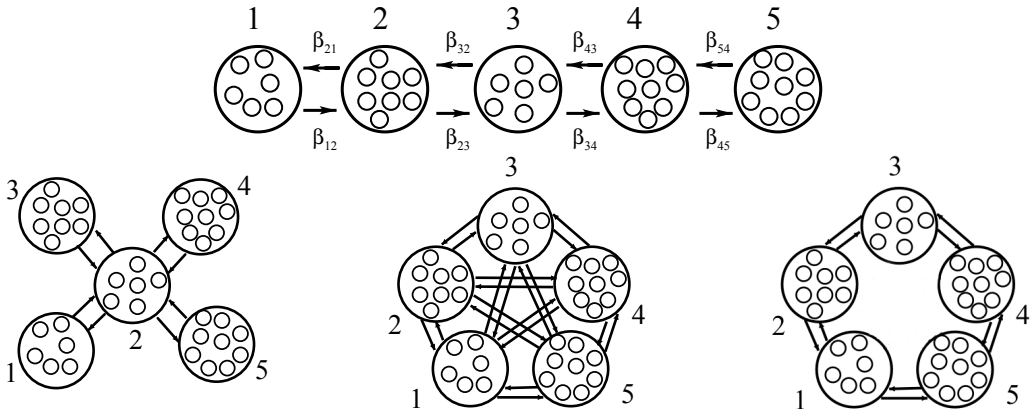

Figure 2.1: Four sample topologies of 5 hotspot regions: linear, star, complete, and ring. For instance, nodes of hotspot 1 in the linear topology can only communicate with nodes of hotspots 1 (at rate β_{11}) and 2 (at rate β_{12}).

rates $\{\beta_{ij}, 1 \le i,j \le M\}$ there is now another natural notion, that of *connectivity*:

we say that type j is connected to type i if, for some k, there exists a sequence of types $i = s_1 \mapsto s_2 \mapsto \ldots \mapsto s_{k-1} \mapsto s_k = j$ where type s_{l+1} is a neighbor of type s_l for $1 \leq l < k$. We assume that each type is either initially infected ($I_i(0) > 0$), or is connected to an initially infected type. We also assume that for every type i such that $R_i^0 > 0$, there exists a type j for which $\bar{\beta}_{ij} > 0$, i.e., type i can immunize nodes of at least one type, and there exist types k and l for which $\beta_{ki} > 0$ and $\beta_{il} > 0$, $S_l(0) > 0$, i.e., the infection can spread to and from that type. (In most settings we may expect, naturally, that $\beta_{ii} > 0$ and $\bar{\beta}_{ii} > 0$.)

Thus, we have:[7]

$$\dot{S}_i = -\sum_{j=1}^{M} \beta_{ji} I_j S_i - S_i \sum_{j=1}^{M} \bar{\beta}_{ji} R_j^0 u_j, \tag{2.2.2a}$$

$$\dot{I}_i = \sum_{j=1}^{M} \beta_{ji} I_j S_i - I_i \sum_{j=1}^{M} \pi_{ji} \bar{\beta}_{ji} R_j^0 u_j, \tag{2.2.2b}$$

where, by writing $\mathbf{S}(t) = \big(S_1(t), \ldots, S_M(t)\big)$, $\mathbf{I}(t) = \big(I_1(t), \ldots, I_M(t)\big)$, and $\mathbf{R}^0(t) = \big(R_1^0(t), \ldots, R_M^0(t)\big)$ in a compact vector notation, the initial conditions and state constraints are given by

$$\mathbf{S}(0) = \mathbf{S}^0 \succeq \mathbf{0}, \quad \mathbf{I}(0) = \mathbf{I}^0 \succeq \mathbf{0}, \tag{2.2.3}$$

$$\mathbf{S}(t) \succeq \mathbf{0}, \quad \mathbf{I}(t) \succeq \mathbf{0}, \quad \mathbf{S}(t) + \mathbf{I}(t) \preceq \mathbf{1} - \mathbf{R}^0. \tag{2.2.4}$$

In these expressions $\mathbf{0}$ and $\mathbf{1}$ represent vectors all of whose components are 0 and 1 respectively, and the vector inequalities are to be interpreted as component-wise inequalities. Note that the evolution of $\mathbf{R}(t)$ need not be explicitly considered

[7] We use dots to denote *time* derivatives throughout, e.g., $\dot{S}(t) = dS(t)/dt$.

since at any given time, node conservation gives $R_i(t) = 1 - S_i(t) - I_i(t)$. We henceforth drop the dependence on t and make it implicit whenever we can do so without ambiguity.

2.2.2 Dynamics of replicative patching

In the replicative setting, a recipient of the patch can forward it to other nodes upon subsequent contact. Thus, recovered nodes of type i are added to the pool of dispatchers of type i, whence the fraction of dispatchers of type i grows from the initial $R_i(0) = R_i^0$ to $R_i(t)$ at time t. This should be contrasted with the non-replicative model in which the fraction of dispatchers of type i is fixed at R_i^0 for all t.

The system dynamics equations given in (2.2.2) for the non-replicative setting now need to be modified to take into account the growing pool of dispatchers. While in the non-replicative case we chose the pair $\big(\mathbf{S}(t), \mathbf{I}(t)\big)$ to represent the system state, in the replicative case it is slightly more convenient to represent the system state by the explicit triple $\big(\mathbf{S}(t), \mathbf{I}(t), \mathbf{R}(t)\big)$. The system dynamics are now governed by:

$$\dot{S}_i = -\sum_{j=1}^{M} \beta_{ji} I_j S_i - S_i \sum_{j=1}^{M} \bar{\beta}_{ji} R_j u_j, \tag{2.2.5a}$$

$$\dot{I}_i = \sum_{j=1}^{M} \beta_{ji} I_j S_i - I_i \sum_{j=1}^{M} \pi_{ji} \bar{\beta}_{ji} R_j u_j, \tag{2.2.5b}$$

$$\dot{R}_i = S_i \sum_{j=1}^{M} \bar{\beta}_{ji} R_j u_j + I_i \sum_{j=1}^{M} \pi_{ji} \bar{\beta}_{ji} R_j u_j, \tag{2.2.5c}$$

with initial conditions and state constraints given by

$$\mathbf{S}(0) = \mathbf{S}^0 \succeq \mathbf{0}, \quad \mathbf{I}(0) = \mathbf{I}^0 \succeq \mathbf{0}, \quad \mathbf{R}(0) = \mathbf{R}^0 \succeq \mathbf{0}, \tag{2.2.6}$$

$$\mathbf{S}(t) \succeq \mathbf{0}, \quad \mathbf{I}(t) \succeq \mathbf{0}, \quad \mathbf{R}(t) \succeq \mathbf{0}, \quad \mathbf{S}(t) + \mathbf{I}(t) + \mathbf{R}(t) = \mathbf{1}. \tag{2.2.7}$$

The assumptions on controls and connectivity are as in §2.2.1.

2.2.3 Motivation of the models and instantiations

We now motivate the stratified epidemic models (2.2.2) and (2.2.5) through examples, instantiating the types in each context.

Proximity-based spread—heterogeneity through locality

The overall roaming area of the nodes can be divided into regions (e.g., hotspots, office/residential areas, central/peripheral areas) of different densities (fig. 2.1). One can therefore stratify the nodes based on their locality, i.e., each type corresponds to a region. IP eavesdropping techniques (using software such as `AirJack`, `Ethereal`, `FakeAP`, `Kismet`, etc.) allow malware to detect new victims in the vicinity of the host. Distant nodes have more attenuated signal strength (i.e., lower SINR) and are therefore less likely to be detected. Accordingly, malware (and also patch) propagation rates β_{ij} (respectively $\bar{\beta}_{ij}$) are related to the local densities of the nodes in each region and decay with an increase in the distance between regions i and j: typically β_{ii} exceeds β_{ij} for $i \neq j$, likewise for $\bar{\beta}_{ij}$. The same phenomenon was observed for malware such as `cabir` and `lasco` that use Bluetooth

and Infrared to propagate.

Heterogeneity through software/protocol diversity

A network that relies on a homogeneous software/protocol is vulnerable to an attack that exploits a common weakness (e.g., a buffer overflow vulnerability). Accordingly, inspired by the natural observation that *the chances of survival are improved by heterogeneity*, increasing the network's heterogeneity without sacrificing inter-operability has been proposed as a defense mechanism [94]. In practice, mobile nodes use different operating systems and communication protocols, e.g., `Symbian`, `Android`, `iOS`, `RIM`, `webOS`, etc. Such heterogeneities lead to dissimilar rates of propagation of malware amongst different types, where each type represents a specific OS, platform, software, protocol, etc. In the extreme case, the malware may not be able to contaminate nodes of certain types. The patching response should take such inhomogeneities into account in order to optimally utilize network resources, since the rate of patching can also be dissimilar among different types.

Heterogeneity through available IP space

Smart-phone trojans like `skulls` and `mosquito` spread using Internet or P2P networks. In such cases the network can be decomposed into *autonomous systems* (ASs) with each type representing an AS [59]. A worm either scans IP addresses uniformly randomly or uses the IP masks of ASs to restrict its search domain and

increase its rate of finding new susceptible nodes. In each of these cases the contact rates differ between different AS's depending on the actual number of assigned IPs in each IP sub-domain and the maximum size of that IP sub-domain.

Heterogeneity through differing clique sizes

Malware that specifically spreads in social networks has been recorded in the past few years [24]. Examples include `Samy` in MySpace in 2005 and `Koobface` in MySpace and Facebook in 2008. `Koobface`, for instance, spread by delivering (contaminated) messages to the "friends" of an infective user. MMS based malware such as `commwarrior` can also utilize the contact list of an infective host to access new handsets. In such cases the social network graph can be approximated by a collection of friendship *cliques*.[8] Users of the same clique can be regarded as the same type with the rate of contact within cliques and across cliques differing depending on the relative sizes of the cliques.[9]

[8] A clique is a maximal complete sub-graph of a graph [14, p. 112].

[9] In MMS/E-mail, types typically depend on the nature of social contact, while in Bluetooth, types are naturally based on distance to the center of the cluster, as nodes that are closer are more likely to contact each other. Wang *et al.* [89] examine the spreading patterns of viruses through both these mechanism with the same assumption as our work in terms of the underlying variable behind the spread (proximity for Bluetooth and social ties for MMS). Furthermore, our model is general enough to even capture the hybrid spread of a virus that the authors investigate. In that case, the types would be based on both distance to the center of the cluster *and* the nature of the social contact.

Cloud-computing—heterogeneity through cluster sizes

In cluster (or grid, or volunteer) computing [3], each cluster of CPUs in the cloud constitutes a type. Any two computers in the same cluster can communicate at faster rates than those in different clusters. These contact rates depend on the communication capacity of connecting lines as well as the relative number of computers in each cluster.

Clustered epidemics in technology adoption, belief-formation over social media and health care

We now elaborate on the application of our clustered epidemics model in these diverse set of contexts. First consider a rivalry between two technologies or companies for adoption in a given population, e.g., Android and iPhone, or cable and satellite television. Individuals who are yet to choose either may be considered as susceptibles and those who have chosen one or the other technology would be classified as either infective or recovered depending upon their choice. Dispatchers constitute the promoters of a given technology (the one whose subscribers are denoted as recovered). Awareness about the technology and subsequent subscription to either may spread through social contact between infectives and susceptibles (infection propagation in our terminology), and dispatchers and the rest (patching in our terminology). Immunization of a susceptible corresponds to her adoption of the corresponding technology, while healing of an infective corre-

sponds to an alteration in her original choice. The stratifications may be based on location or social cliques, and the control $\mathbf{u}$ would represent promotion efforts, which would be judiciously selected by the proponent of the corresponding technology. Patching may either be replicative or non-replicative depending on whether the newly subscribed users are enticed to attract more subscribers by referral rewards. Similarly, clustered epidemics may be used to model belief management over social media, where infective and recovered nodes represent individuals who have conflicting persuasions and susceptibles represent those who are yet to subscribe to either doctrine. Last, but not least, the susceptible-infective-recovered classification and immunization/healing/infection have natural connotations in the context of a biological epidemic. Here, the dispatchers correspond to health-workers who administer vaccines and/or hospitalization and the stratification is based on location. Note that in this context, patching can only be non-replicative.

2.2.4 Key observations

A natural but nevertheless important observation is that if the initial conditions are non-negative, then the system dynamics (2.2.2) and (2.2.5) yield unique states satisfying the positivity and normalization constraints (2.2.4) and (2.2.7), respectively.

Theorem 1. The dynamical system (2.2.2) (respectively (2.2.5)) with initial con-

ditions (2.2.3) (respectively, (2.2.6)) has a unique state solution $\big(\mathbf{S}(t), \mathbf{I}(t)\big)$ (respectively $\big(\mathbf{S}(t), \mathbf{I}(t), \mathbf{R}(t)\big)$) which satisfies the state constraints (2.2.4) (respectively, (2.2.7)). For all $t > 0$, $I_i(t) > 0$; $R_i(t) > 0$ if $R_i(0) > 0$; and $S_j(t) > 0$ if and only if $S_j(0) \neq 0$. For each j such that $S_j(0) = 0$, $S_j(t') = 0$ for all $t' \in (0, T]$.

Proof of Theorem 1

We use the following general result :

Lemma 1. Suppose the vector-valued function $\mathbf{f} = (f_i, 1 \leq i \leq 3M)$ has component functions given by quadratic forms $f_i(t, \mathbf{x}) = \mathbf{x}^T Q_i(t)\mathbf{x} + {p_i}^T\mathbf{x}$ $(t \in [0, T]$; $\mathbf{x} \in \mathbb{S})$, where $\mathbb{S}$ is the set of $3M$-dimensional vectors $\mathbf{x} = (x_1, \ldots, x_{3M})$ satisfying $\mathbf{x} \geq \mathbf{0}$ and $\forall j \in \{1, \ldots, M\}; x_j + x_{M+j} + x_{2M+j} = 1$, $Q_i(t)$ is a matrix whose components are uniformly, absolutely bounded over $[0, T]$, as are the elements of the vector p_i. Then, for an $3M$-dimensional vector-valued function $\mathbf{F}$, the system of differential equations

$$\begin{gathered} \dot{\mathbf{F}} = \mathbf{f}(t, \mathbf{F}) \qquad (0 < t \leq T) \\ \text{subject to initial conditions } \mathbf{F}(0) \in \mathbb{S} \end{gathered} \tag{2.2.8}$$

has a unique solution, $\mathbf{F}(t)$, which varies continuously with the initial conditions $\mathbf{F}_0 \in \mathbb{S}$ at each $t \in [0, T]$.

This follows from a standard result in the theory of ordinary differential equations [78, Theorem A.8, p. 419] given that $\mathbf{f}(t, \mathbf{F})$ is comprised of quadratic and linear forms and is thus Lipschitz over $[0, T] * \mathbb{S}$.

Proof of Theorem 1: We write $\mathbf{F}(0) = \mathbf{F}_0$, and in a slightly informal notation, $\mathbf{F} = \mathbf{F}(t) = \mathbf{F}(t, \mathbf{F}_0)$ to acknowledge the dependence of $\mathbf{F}$ on the initial value $\mathbf{F}_0$.

We first verify that $\mathbf{S}(t) + \mathbf{I}(t) + \mathbf{R}(t) = \mathbf{1}$ for all t in both cases. By summing the left and right sides of the system of equations (2.2.2) and the $\dot{R}_i$ equation that was left out (respectively the two sides of equations (2.2.5)), we see that in both cases for all i, $\big(\dot{S}_i(t) + \dot{I}_i(t) + \dot{R}_i(t)\big) = 0$, and, in view of the initial normalization $\big(S_i(0) + I_i(0) + R_i(0)\big) = 1$, we have $\big(S_i(t) + I_i(t) + R_i(t)\big) = 1$ for all t and all i.

We now verify the non-negativity condition. Let $\mathbf{F} = (F_1, \ldots, F_{3M})$ be the state vector in $3M$ dimensions whose elements are comprised of $(S_i, 1 \leq i \leq M)$, $(I_i, 1 \leq i \leq M)$ and $(R_i, 1 \leq i \leq M)$ in some order. The system of equations (2.2.2) can thus be represented as $\dot{\mathbf{F}} = \mathbf{f}(t, \mathbf{F})$, where for $t \in [0, T]$ and $\mathbf{x} \in \mathbb{S}$, the vector-valued function $\mathbf{f} = (f_i, 1 \leq i \leq 3M)$ has component functions $f_i(t, \mathbf{x}) = \mathbf{x}^T Q_i(t)\mathbf{x} + {p_i}^T\mathbf{x}$ in which (i) $Q_i(t)$ is a matrix whose non-zero elements are of the form $\pm\beta_{jk}$, (ii) the elements of $p_i(t)$ are of the form $\pm\bar{\beta}_{jk}R_j^0 u_j$ and $\pm\bar{\beta}_{jk}\pi_{jk}R_j^0 u_j$, whereas (2.2.5) can be represented in the same form but with (i) $Q_i(t)$ having elements $\pm\beta_{jk}$, $\pm\bar{\beta}_{jk}u_j$, and $\pm\bar{\beta}_{jk}\pi_{jk}u_j$, and (ii) $p_i = \mathbf{0}$. Thus, the components of $Q_i(t)$ are uniformly, absolutely bounded over $[0, T]$. Lemma 1 establishes that the solution $\mathbf{F}(t, \mathbf{F}_0)$ to the systems (2.2.2) and (2.2.5) is unique and varies continuously with the initial conditions $\mathbf{F}_0$; it clearly varies continuously with time. Next, using elementary calculus, we show in the next paragraph that if $\mathbf{F}_0 \in \mathbf{Int}\,\mathbb{S}$ (and, in particular, each component of $\mathbf{F}_0$ is positive), then

each component of the solution $\mathbf{F}(t, \mathbf{F}_0)$ of (2.2.2) and (2.2.5) is positive at each $t \in [0, T]$. Since $\mathbf{F}(t, \mathbf{F}_0)$ varies continuously with $\mathbf{F}_0$, therefore $\mathbf{F}(t, \mathbf{F}_0) \geq \mathbf{0}$ for all $t \in [0, T]$, $\mathbf{F}_0 \in \mathbb{S}$, which completes the overall proof.

Accordingly, let the S_i, I_i, and R_i component of $\mathbf{F}_0$ be positive. Since the solution $\mathbf{F}(t, \mathbf{F}_0)$ varies continuously with time, there exists a time, say $t' > 0$, such that each component of $\mathbf{F}(t, \mathbf{F}_0)$ is positive in the interval $[0, t')$. The result follows trivially if $t' \geq T$. Suppose now that there exists $t'' < T$ such that each component of $\mathbf{F}(t, \mathbf{F}_0)$ is positive in the interval $[0, t'')$, and at least one such component is 0 at t''.

We first examine the non-replicative case. We show that such components can not be S_i for any i and subsequently rule out I_i and R_i for all i. Note that $u_j(t), I_j(t), S_j(t)$ are bounded in $[0, t'']$ (recall $(S_j(t) + I_j(t) + R_j(t)) = 1$, $S_j(t) \geq 0$, $I_j(t) \geq 0$, $R_j(t) \geq 0$ for all $j \in \{1, \ldots, M\}, t \in [0, t'']$). From (2.2.2a) $S_i(t'') = S_i(0) e^{-\int_0^{t''} \sum_{j=1}^{M} (\beta_{ji} I_j(t) + \bar{\beta}_{ji} R_j^0 u_j(t))\, dt}$. Since all $u_j(t), I_j(t)$ are bounded in $[0, t'']$, $S_i(0) > 0, R_j^0 \geq 0$, and $\beta_{ji}, \bar{\beta}_{ji} \geq 0$, therefore $S_i(t'') > 0$. Since $S_i(t) > 0$, $I_i(t) \geq 0$ for all $i, t \in [0, t'']$, and $\beta_{ji} \geq 0$, from (2.2.2b), $\dot{I}_i \geq -I_i \sum_{j=1}^{M} \pi_{ji} \bar{\beta}_{ji} R_j^0 u_j$ for all i in the interval $[0, t'']$. Thus, $I_i(t'') \geq I_i(0) e^{-\int_0^{t''} \sum_{j=1}^{M} \pi_{ji} (\bar{\beta}_{ji} R_j^0 u_j(t))\, dt}$. Since all $u_j(t), I_j(t), S_j(t)$ are bounded in $[0, t'']$, and $I_i(0) > 0$, $\bar{\beta}_{ji}, \pi_{ji} \geq 0$, it follows that $I_i(t'') > 0$ for all $i \geq 0$. Finally, $R_i(t'') > 0$ because $R_i(0) > 0$ and $\dot{R}_i(t) \geq 0$ from the above, so $R_i(t) \geq R_i^0$, and $S_i(t) + I_i(t) \leq 1 - R_i^0$ for all t and i. This contradicts the definition of t'' and in turn implies that $\mathbf{F}(t, \mathbf{F}_0) > 0$ for all $t \in [0, T]$,

$\mathbf{F}_0 \in$ **Int** $\mathbb{S}$.

The proof for the replicative case is similar, with the difference that R_i^0 is replaced with R_i, which is itself bounded.

Since the control and the unique state solution $\mathbf{S}(t)$, $\mathbf{I}(t)$ are non-negative, (2.2.2a, 2.2.5a) imply that $\mathbf{S}(t)$ is a non-increasing function of time. Thus, $S_j(t) = 0$ if $S_j(0) = 0$ for any j. Using the argument in the above paragraph and starting from a $t' \in [0, T)$ where $S_j(t') > 0$, $I_j(t') > 0$, or $R_j(t') > 0$, it may be shown respectively that $S_j(t) > 0$, $I_j(t) > 0$, and $R_j(t) > 0$ for all $t > t'$. All that remains to show now is:

Lemma 2. There exists $\epsilon > 0$ such that $\mathbf{I}(t) > 0$ for $t \in (0, \epsilon)$.

Let $d(i, j)$ be the *distance* from type j to type i (i.e., for all i, $d(i, i) = 0$ and for all pairs (i, j), $d(i, j) = 1+$ minimum number of types in a path from type j to type i). Now, define $d(i, U) := \min_{j \in U} d(i, j)$, where $U := \{\, i : I_i^0 > 0 \,\}$. Since we assumed that every type i is either in U or is connected to a type in U, $d(i, U) < M$ for all types i.

Let $\delta > 0$ be a time such that for all types i such that $d(i, U) = 0$ (the initially infected types),we have $I_i(t) > 0$ for $t \in [0, \delta)$. Thus, proving Lemma 3 below will be equivalent to proving Lemma 2, given an appropriate scaling of δ.

Lemma 3. For all i and for all integers $r \geq 0$, if $d(i, U) \leq r$, then $I_i(t) > 0$ for $t \in (\frac{r}{M}\delta, T)$.

Proof: By induction on r.

Base case: $r = 0$. If $d(i, U) = 0$, this means that the type is initially infected, and thus $I_i(t) > 0$ for $t \in (0, T)$ by definition. Therefore the base case holds.

Induction step: Assume that the statement holds for $r = 0, \ldots, k$ and consider $r = k + 1$. Since $(\frac{k+1}{M}\delta, T) \subset (\frac{k}{M}\delta, T)$, we need to examine types i such that $d(i, U) = k+1$. In equation (2.2.2b) at $t = \frac{k+1}{M}\delta$, the first sum on the right involves terms like $I_j(\frac{k+1}{M}\delta)S_i(\frac{k+1}{M}\delta)$ where j is a neighbor of i, while the second sum involves terms like $I_i(\frac{k+1}{M}\delta)u_j(\frac{k+1}{M}\delta)$. Since $d(i, U) = k+1$, there exist neighbors j of i such that $d(j, U) = k$, and therefore $I_j(t) > 0$ for $t \in [\frac{k+1}{M}\delta, T)$ (by the induction hypothesis). Hence since $S_i^0 > 0$ and $\beta_{ji} > 0$ (i and j being neighbors), for such t, $\dot{I}_i(t) > -I_i(t)\sum_{j=1}^{M} \pi_{ji}\bar{\beta}_{ji}R_j^0 u_j(t) \geq -GI_i(t)$, where $G \geq 0$ is an upperbound on the sum (continuous functions are bounded on a closed and bounded interval). Thus $I_i(t) > I_i(\frac{k+1}{M}\delta)e^{-Kt} > 0$, completing the proof for $r = k + 1$. ■

2.2.5 The optimality objective

The network seeks to minimize the overall cost of infection and the resource overhead of patching in a given operation time window $[0, T]$. At any given time t, the system incurs costs at a rate $f\big(\mathbf{I}(t)\big)$ due to the malicious activities of the malware[10]. For instance, the malware may use infected hosts to eavesdrop, analyze, misroute, alter, or destroy the traffic that the hosts generate or relay. We suppose that $f(\mathbf{0}) = 0$ and make the natural assumption that the scalar function $f(\mathbf{I})$ is

[10] This is a standard assumption in the field of epidemics, e.g., Rowthorn *et al.* [74], and Sethi and Staats [80])

increasing and differentiable with respect to each I_i. The simplest natural candidate for $f(\mathbf{I})$ is of the form $\sum_{i=1}^{M} f_i(I_i)$; in this setting each f_i is a non-decreasing function of its argument representing the cost of infection for type i which is in turn determined by the criticality of the data of that type and its function.[11] The network also benefits at the rate of $L\big(\mathbf{R}(t)\big)$, i.e., incurs a cost at the rate of $-L\big(\mathbf{R}(t)\big)$, due to the removal of uncertainty about the state of the nodes being patched. The inclusion of $L(\mathbf{R})$ allows the framework to capture domains such as belief propagation and technology adoption, where there are gains associated with the fraction of recovered nodes at each instant. We suppose that the scalar function $L(\mathbf{R})$ is non-decreasing and differentiable with respect to each R_i (e.g., allowing constant or zero functions).

In addition to the cost of infection, each dispatcher burdens the network with a cost by consuming either available bandwidth, energy reserves of the nodes (e.g., in communication and computing networks), or money (e.g., in technology adoption, propaganda, health-care) to disseminate the patches. Suppose dispatchers of type i incur cost at a rate of $R_i^0 h_i(u_i)$. We suppose that the overhead of extra resource (bandwidth or energy or money) consumption at time t is then given by a sum of the form $\sum_{i=1}^{M} R_i^0 h_i(u_i)$. The scalar functions $h_i(\cdot)$ represent how much resource is consumed for transmission of the patch by nodes of each type and how significant this extra taxation of resources is for each type. Naturally enough, we

[11] Such differences themselves may be a source of stratification. In general, different types need not exclusively reflect disparate mixing rates.

assume these functions are non-decreasing and satisfy $h_i(0) = 0$ and $h_i(\gamma) > 0$ for $\gamma > 0$. We assume, additionally, that each h_i is twice differentiable. Following the same lines of reasoning, the corresponding expression for the cost of replicative patching is of the form $\sum_{i=1}^{M} R_i h_i(u_i)$. In problems that arise from the field of computer networks, such as malware propagation and cloud computing, we would expect to have concave $h_i(\cdot)$, as the marginal effort required to spread the epidemic at a contact opportunity would be expected to rise negligibly. For example, in a Delay-Tolerant Network, every contact between a transmitting recovered and another node would already involve beaconing and the exchange of messages that identify the state of the nodes, and transmitting the patch more frequently would just affect the part of the transmission cost that is to do with the patch itself. However, when looking at social networks, for example, asking a user to spread a message more often can lead to reluctance on its part, and this would justify $h_i(\cdot)$ that are convex. We therefore allow for both convex and concave $h_i(\cdot)$ functions.

With the arguments stated above, the aggregate cost for non-replicative patching is given by an expression of the form

$$J_{non-rep} = \int_0^T \left(f(\mathbf{I}) - L(\mathbf{R}) + \sum_{i=1}^{M} R_i^0 h_i(u_i) \right) dt, \tag{2.2.9}$$

while for replicative patching, the aggregate cost is of the form

$$J_{rep} = \int_0^T \left(f(\mathbf{I}) - L(\mathbf{R}) + \sum_{i=1}^{M} R_i h_i(u_i) \right) dt. \tag{2.2.10}$$

Problem Statement: The system seeks to minimize the aggregate cost **(A)** in (2.2.9) for non-replicative patching (2.2.2, 2.2.3) and **(B)** in (2.2.10) for replicative patching (2.2.5, 2.2.6) by an appropriate selection of an optimal admissible control $\mathbf{u}(t)$.

In this setting, it is clear that by a scaling of $\bar{\beta}_{ji}$ and $h_j(\cdot)$, we can assume WLoG that $u_{j,\max} = 1$.

It is worth noting that any control in the non-replicative case can be emulated in the replicative setting: this is because the fraction of the dispatchers in the replicative setting is non-decreasing, hence at any time instance, a feasible $u^{rep}(t)$ can be selected such that $R_i(t)u_i^{rep}(t)$ is equal to $R_i^0 u_i^{non-rep}(t)$. This means that the minimum cost of replicative patching is always less than the minimum cost of its non-replicative counterpart. Our numerical results will show that this improvement is substantial. However, replicative patches increase the risk of patch contamination: the security of a smaller set of known dispatchers is easier to manage than that of a growing set whose identities may be ambiguous. Hence, in a nutshell, if there is a dependable mechanism for authenticating patches, replicative patching ought to be the preferred method, otherwise one needs to evaluate the trade-off between the risk of compromised patches and the efficiency of the patching.

2.3 Optimal Non-Replicative Patching

2.3.1 Numerical framework for computing optimal controls

The main challenge in computing the optimal state and control functions $\big((\mathbf{S},\mathbf{I}),\mathbf{u}\big)$ is that while the differential equations (2.2.2) can be solved once the optimal controls $\mathbf{u}(\cdot)$ are known, an exhaustive search for an optimal control is infeasible as there are an uncountably infinite number of control functions. *Pontryagin's Maximum Principle (PMP)* provides an elegant technique for solving this seemingly intractable problem (c.f. [85]). Referring to the integrand in (2.2.9) as $\xi_{non-rep}$ and the RHS of (2.2.2a) and (2.2.2b) as ν_i and μ_i, we define the Hamiltonian to be

$$\mathcal{H} = \mathcal{H}(\mathbf{u}) := \xi_{non-rep} + \sum_{i=1}^{M} (\lambda_i^S \nu_i + \lambda_i^I \mu_i), \tag{2.3.1}$$

where the *adjoint* (or *costate*) functions λ_i^S and λ_i^I are continuous functions that for each $i = 1 \dots M$, and at each point of continuity of $\mathbf{u}(\cdot)$, satisfy

$$\dot{\lambda}_i^S = -\frac{\partial \mathcal{H}}{\partial S_i}, \quad \dot{\lambda}_i^I = -\frac{\partial \mathcal{H}}{\partial I_i}, \tag{2.3.2}$$

along with the final (i.e., transversality) conditions

$$\lambda_i^S(T) = 0, \quad \lambda_i^I(T) = 0. \tag{2.3.3}$$

Then PMP implies that the optimal control at time t satisfies

$$\mathbf{u} \in \arg\min_{\mathbf{v}} \mathcal{H}(\mathbf{v}) \tag{2.3.4}$$

where the minimization is over the space of admissible controls (i.e., $H(u) = \min_v H(v)$).

In economic terms, the adjoint functions represent a shadow price (or imputed value); they measure the marginal worth of an increment in the state at time t when moving along an optimal trajectory. Intuitively, in these terms, λ_i^I ought to be positive as it represents the additional cost that the system incurs per unit time with an increase in the fraction of infective nodes. Furthermore, as an increase in the fraction of the infective nodes has worse long-term implications for the system than an increase in the fraction of the susceptibles, we anticipate that $\lambda_i^I - \lambda_i^S > 0$. The following result confirms this intuition. It is of value in its own right but as its utility for our purposes is in the proof of our main theorem of the following section, we will defer its proof (to §2.3.3) to avoid breaking up the flow of the narrative at this point.

Lemma 4. The positivity constraints $\lambda_i^I(t) > 0$ and $\lambda_i^I(t) - \lambda_i^S(t) > 0$ hold for all $i = 1, \ldots, M$ and all $t \in [0, T)$.

The abstract maximum principle takes on a very simple form in our context. Using the expression for $\xi_{non-rep}$ from (2.2.9) and the expressions for ν_i and μ_i from (2.2.2), trite manipulations show that the minimization (2.3.4) may be ex-

pressed in the much simpler (nested) scalar formulation

$$u_i(t) \in \arg\min_{0 \le x \le 1} \psi_i(x,t) \qquad (1 \le i \le M); \tag{2.3.5}$$

$$\psi_i(x,t) := R_i^0(h_i(x) - \phi_i(t)x); \tag{2.3.6}$$

$$\phi_i := \sum_{j=1}^{M} \bar{\beta}_{ij}\lambda_j^S S_j + \sum_{j=1}^{M} \bar{\beta}_{ij}\pi_{ij}\lambda_j^I I_j. \tag{2.3.7}$$

Equation (2.3.5) allows us to characterize u_i as a function of the state and adjoint functions at each time instant. Plugging into (2.2.2) and (2.3.2), we obtain a system of (non-linear) differential equations that involves only the state and adjoint functions (and not the control $\mathbf{u}(\cdot)$), and where the initial values of the states (2.2.3) and the final values of the adjoint functions (2.3.3) are known. Numerical methods for solving *boundary value* nonlinear differential equation problems may now be used to solve for the state and adjoint functions corresponding to the optimal control, thus providing the optimal controls using (2.3.5).

We conclude this section by proving an important property of $\phi_i(\cdot)$, which we will use in subsequent sections.

Lemma 5. For each i, $\phi_i(t)$ is a decreasing function of t.

Proof. We examine the derivative of $\phi_i(t)$; we need expressions for the derivatives of the adjoint functions towards that end. From (2.3.1), (2.3.2), at any t at which

$\mathbf{u}$ is continuous, we have:

$$\dot{\lambda}_i^S = -\frac{\partial L(\mathbf{R})}{\partial R_i} - (\lambda_i^I - \lambda_i^S)\sum_{j=1}^{M}\beta_{ji}I_j + \lambda_i^S\sum_{j=1}^{M}\bar{\beta}_{ji}R_j^0 u_j,$$

$$\dot{\lambda}_i^I = -\sum_{j=1}^{M}\left((\lambda_j^I - \lambda_j^S)\beta_{ij}S_j\right) + \lambda_i^I\sum_{j=1}^{M}\pi_{ji}\bar{\beta}_{ji}R_j^0 u_j - \frac{\partial L(\mathbf{R})}{\partial R_i} - \frac{\partial f(\mathbf{I})}{\partial I_i}. \qquad (2.3.8)$$

Using (2.3.7), (2.3.8) and some reassembly of terms, at any t at which $\mathbf{u}$ is continuous, $\dot{\phi}_i(t) = -\sum_{j=1}^{M}\bar{\beta}_{ij}\Bigg[S_j\frac{\partial L(\mathbf{R})}{\partial R_j} + \pi_{ij}I_j\left(\frac{\partial L(\mathbf{R})}{\partial R_j} + \frac{\partial f(\mathbf{I})}{\partial I_j}\right) + \sum_{k=1}^{M}(1 + \pi_{ij})\lambda_j^I\beta_{kj}S_jI_k + \sum_{k=1}^{M}\pi_{ij}I_jS_k\beta_{jk}(\lambda_k^I - \lambda_k^S)\Bigg]$. The assumptions on $L(\cdot)$ and $f(\cdot)$ (together with Theorem 1) show that the first two terms inside the square brackets on the right are always non-negative. Theorem 1 and Lemma 4 (together with our assumptions on π_{ij}, β_{ij} and $\bar{\beta}_{ij}$) show that the penultimate term is positive for $t > 0$ and the final term is non-negative. It follows that $\dot{\phi}_i(t) < 0$ for every $t \in (0, T)$ at which $\mathbf{u}(t)$ is continuous. As $\phi_i(t)$ is a continuous function of time and its derivative is negative except at a finite number of points (where $\mathbf{u}$ may be discontinuous), it follows indeed that, as advertised, $\phi_i(t)$ is a decreasing function of time. □

2.3.2 Structure of optimal non-replicative patching

We are now ready to identify the structure of optimal controls $(u_1(t), \ldots, u_M(t))$:

Theorem 2. Predicated on the existence of an optimal control, for types i such that $R_i^0 > 0$: if $h_i(\cdot)$ is concave, then the optimal control for type i has the following structure: $u_i(t) = 1$ for $0 < t < t_i$, and $u_i(t) = 0$ $t_i < t \leq T$, where $t_i \in [0, T)$. If

$h_i(\cdot)$ is strictly convex then the optimal control for type i, $u_i(t)$ is continuous and has the following structure: $u_i(t) = 1$ for $0 < t < t_i^1$, $u_i(t) = 0$ for $t_i^2 < t \leq T$, and $u_i(t)$ strictly decreases in the interval $[t_i^1, t_i^2]$, where $0 \leq t_i^1 < t_i^2 \leq T$.

Notice that if $R_i^0 = 0$ in (2.2.2), the control u_i is irrelevant and can take any arbitrary admissible value. Intuitively, at the onset of the epidemic, a large fraction of nodes are susceptible to the malware ("potential victims"). Bandwidth and power resources should hence be used maximally in the beginning (in all types), rendering as many infective and susceptible nodes robust against the malware as possible. In particular, there is no gain in deferring patching since the efficacy of healing infective nodes is less than that of immunizing susceptible nodes (recall that $\pi_{ij} \leq 1$). While the non-increasing nature of the optimal control is intuitive, what is less apparent is the characteristics of the decrease, which we establish in this theorem. For concave $h_i(\cdot)$, nodes are patched at the maximum possible rate until a time instant when patching stops abruptly, while for strictly convex $h_i(\cdot)$, this decrease is continuous. It is instructive to note that the structure of the optimal action taken by a type only depends on its own patching cost and not on that of its neighbors. This is somewhat counter-intuitive as the controls for one type affect the infection and recovery of other types. The timing of the decrease in each type differs and depends on the location of the initial infection as well as the topology of the network, communication rates, etc.

Proof. For non-linear concave $h_i(\cdot)$, (2.3.5) requires the minimization of the (non-linear concave) difference between a non-linear concave function of a scalar variable x and a linear function of x at all time instants; hence the minimum can only occur at the end-points of the interval over which x can vary. Thus all that needs to be done is to compare the values of $\psi_i(x,t)$ for the following two candidates: $x = 0$ and $x = 1$. Note that $\psi_i(0,t) = 0$ at all time instants and $\psi_i(1,t)$ is a function of time t. Let

$$\gamma_i(t) := \psi_i(1,t) = R_i^0 h_i(1) - R_i^0 \phi_i(t). \tag{2.3.9}$$

Then the optimal u_i satisfies the following condition:

$$u_i(t) = \begin{cases} 1 & \gamma_i(t) < 0 \\ \\ 0 & \gamma_i(t) > 0 \end{cases} \tag{2.3.10}$$

From the transversality conditions in (2.3.3) and the definition of $\phi_i(t)$ in (2.3.7), for all i, it follows that $\phi_i(T) = 0$. From the definition of the cost term, $h_i(1) > 0$, hence, since $R_i^0 > 0$, therefore $\gamma_i(T) > 0$. Thus the structure of the optimal control predicted in the theorem for the strictly concave case will follow from (2.3.10) if we can show that $\gamma_i(t)$ is an increasing function of time t, as that implies that it can be zero at most at one point t_i, with $\gamma_i(t) < 0$ for $t < t_i$ and $\gamma_i(t) > 0$ for $t > t_i$. From (2.3.9), γ_i will be an increasing function of time if ϕ_i is a decreasing function of time, a property which we showed in Lemma 5.

If $h_i(\cdot)$ is linear (i.e., $h_i(x) = K_i x$, $K_i > 0$, since $h_i(x) > 0$ for $x > 0$), $\psi_i(x,t) = R_i^0 x(K_i - \phi_i(t))$ and from (2.3.5), the condition for an optimal u_i is:

$$u_i(t) = \begin{cases} 1 & \phi_i(t) > K_i \\ \\ 0 & \phi_i(t) < K_i \end{cases} \tag{2.3.11}$$

But from (2.3.3), $\phi_i(T) = 0 < K_i$ and as by Lemma 5, $\phi_i(t)$ is decreasing, it follows that $\phi_i(t)$ will be equal to K_i at most at one time instant $t = t_i$, with $\phi_i(t) > 0$ for $t < t_i$ and $\phi_i(t) < 0$ for $t > t_i$. This, along with (2.3.11), concludes the proof of the theorem for the concave case.

We now consider the case where $h_i(\cdot)$ is strictly convex. In this case, the minimization in (2.3.5) may also be attained at an interior point of $[0,1]$ (besides 0 and 1) at which the partial derivative of the right hand side with respect to x is zero. Hence,

$$u_i(t) = \begin{cases} 1 & 1 < \eta(t) \\ \\ \eta(t) & 0 < \eta(t) \leq 1 \\ \\ 0 & \eta(t) \leq 0. \end{cases} \tag{2.3.12}$$

where $\eta(t)$ is such that $\left.\dfrac{dh_i(x)}{dx}\right|_{(x=\eta(t))} = \phi_i(t)$.

Note that $\phi_i(t)$ is a continuous function due to the continuity of the states and adjoint functions. We showed that it is also a decreasing function of time (Lemma 5). Since $h_i(\cdot)$ is double differentiable, its first derivative is continuous, and since it is strictly convex, its derivative is a strictly increasing function of its argument.

Therefore, $\eta(t)$ must be a continuous and decreasing function of time, as per the predicted structure. □

2.3.3 Proof of Lemma 4

Proof. From (2.3.8) and (2.3.3), at time T we have:

$$\lambda_i^I|_{t=T} = (\lambda_i^I - \lambda_i^S)|_{t=T} = 0,$$
$$\lim_{t\uparrow T} \dot{\lambda}_i^I = -\frac{\partial L(\mathbf{R})}{\partial R_i}(T) - \frac{\partial f(\mathbf{I})}{\partial I_i}(T) < 0$$
$$\lim_{t\uparrow T}(\dot{\lambda}_i^I - \dot{\lambda}_i^S) = -\frac{\partial f(\mathbf{I})}{\partial I_i}(T) < 0$$

Hence, $\exists\ \epsilon > 0$ s.t. $\lambda_i^I > 0$ and $(\lambda_i^I - \lambda_i^S) > 0$ over $(T-\epsilon, T)$.

Now suppose that, going backward in time from $t = T$, (at least) one of the inequalities is first violated at $t = t^*$ for i^*, i.e., for all i, $\lambda_i^I(t) > 0$ and $(\lambda_i^I(t) - \lambda_i^S(t)) > 0$ for all $t > t^*$ and either (A) $(\lambda_{i^*}^I(t^*) - \lambda_{i^*}^S(t^*)) = 0$ or (B) $\lambda_{i^*}^I(t^*) = 0$ for some $i = i^*$. Note that from continuity of the adjoint functions $\lambda_i^I(t^*) \geq 0$ and $(\lambda_i^I(t^*) - \lambda_i^S(t^*)) \geq 0$ for all i.

We investigate case (A) first. We have:[12] $(\dot{\lambda}_{i^*}^I - \dot{\lambda}_{i^*}^S)(t^{*+}) = -\frac{\partial f(\mathbf{I})}{\partial I_{i^*}} - \sum_{j=1}^M [(\lambda_j^I - \lambda_j^S)\beta_{i^*j}S_j] - \lambda_{i^*}^I \sum_{j=1}^M \bar{\beta}_{ji^*}(1-\pi_{ji^*})R_j^0 u_j$. First of all, $-\partial f(\mathbf{I})/\partial I_{i^*} < 0$. The other two terms are non-positive, due to the definition of t^* and $\pi_{ij} \leq 1$. Hence, $(\dot{\lambda}_{i^*}^I - \dot{\lambda}_{i^*}^S)(t^{*+}) < 0$, which is in contradiction with Property 1 of real-valued functions, proved in [50]:

[12] $g(t_0^+) := \lim_{t\downarrow t_0} g(t)$ and $g(t_0^-) := \lim_{t\uparrow t_0} g(t)$. The RHS of the equation is evaluated at $t = t^*$ due to continuity.

Property 1. Let $g(t)$ be a continuous and piecewise differentiable function of t. If $g(t_0) = L$ and $g(t) > L$ ($g(t) < L$) for all $t \in (t_0, t_1]$. Then $\dot{g}(t_0^+) \geq 0$ (respectively $\dot{g}(t_0^+) \leq 0$).

On the other hand, for case (B) we have:[12] $\dot{\lambda}_{i^*}^I(t^{*+}) = -\frac{\partial L(\mathbf{R})}{\partial R_{i^*}} - \frac{\partial f(\mathbf{I})}{\partial I_{i^*}} - \sum_{j=1}^{M}[(\lambda_j^I - \lambda_j^S)\beta_{i^*j}S_j]$, which is negative since $-\partial L(\mathbf{R})/\partial R_{i^*} \leq 0$, $-\partial f(\mathbf{I})/\partial I_{i^*} < 0$, and from the definition of t^* (for the third term). This contradicts Property 1 and the claim follows. □

2.4 Optimal Replicative Patching

2.4.1 Numerical framework for computing the optimal controls

As in the non-replicative setting, we develop a numerical framework for calculation of the optimal solutions using PMP, and then we establish the structure of the optimal controls.

For every control $\tilde{\mathbf{u}}$, we define $\tau_i(\mathbf{I}(0), \mathbf{S}(0), \mathbf{R}(0), \tilde{\mathbf{u}}) \in [0, T]$ as follows: If $R_i(0) > 0$, and therefore $R_i(t) > 0$ for all $t > 0$ due to Theorem 1, we define $\tau_i(\mathbf{I}(0), \mathbf{S}(0), \mathbf{R}(0), \tilde{\mathbf{u}})$ to be 0. Else, $\tau_i(\mathbf{I}(0), \mathbf{S}(0), \mathbf{R}(0), \tilde{\mathbf{u}})$ is the maximum t for which $R_i(t) = 0$. It follows from Theorem 1 that $R_i(t) = 0$ for all $t \leq \tau_i(\mathbf{I}(0), \mathbf{S}(0), \mathbf{R}(0), \tilde{\mathbf{u}})$ and all i such that $R_i(0) = 0$, and $R_i(t) > 0$ for all $\tau_i(\mathbf{I}(0), \mathbf{S}(0), \mathbf{R}(0), \tilde{\mathbf{u}}) < t \leq T$. We begin with the hypothesis that there exists at least one optimal control, say $\tilde{\mathbf{u}} \in \mathcal{U}^*$, and construct a control $\mathbf{u}$ that chooses $u_i(t) := 0$ for

$t \leq \tau_i(\mathbf{I}(0), \mathbf{S}(0), \mathbf{R}(0), \tilde{\mathbf{u}})$ and $u_i(t) := \tilde{u}_i(t)$ for $t > \tau_i(\mathbf{I}(0), \mathbf{S}(0), \mathbf{R}(0), \tilde{\mathbf{u}})$. Clearly, the states $\mathbf{S}(t), \mathbf{I}(t), \mathbf{R}(t)$ corresponding to $\tilde{\mathbf{u}}$ also constitute the state functions for $\mathbf{u}$, as the state equations only differ at $t = 0$, a set of measure zero. Thus, $\mathbf{u}$ is also an optimal control, and $\tau_i(\mathbf{I}(0), \mathbf{S}(0), \mathbf{R}(0), \tilde{\mathbf{u}}) = \tau_i(\mathbf{I}(0), \mathbf{S}(0), \mathbf{R}(0), \mathbf{u})$ for each i. Henceforth, for notational convenience, we will refer to $\tau_i(\mathbf{I}(0), \mathbf{S}(0), \mathbf{R}(0), \tilde{\mathbf{u}})$, $\tau_i(\mathbf{I}(0), \mathbf{S}(0), \mathbf{R}(0), \mathbf{u})$ as τ_i. Note that the definition of this control completely specifies the values of each u_i in $[0, T]$.

Referring to the integrand of (2.2.10) as ξ_{rep} and the RHS of equations (2.2.5 a,b,c) as ν_i, μ_i and ρ_i the Hamiltonian becomes:

$$\mathcal{H} = \mathcal{H}(\mathbf{u}) := \xi_{rep} + \sum_{i=1}^{M} [(\lambda_i^S \nu_i + \lambda_i^I \mu_i + \lambda_i^R \rho_i), \tag{2.4.1}$$

where the *adjoint* functions $\lambda_i^S, \lambda_i^I, \lambda_i^R$ are continuous functions that at each point of continuity of $\mathbf{u}(\cdot)$ and for all $i = 1 \dots M$, satisfy

$$\dot{\lambda}_i^S = -\frac{\partial \mathcal{H}}{\partial S_i}, \ \dot{\lambda}_i^I = -\frac{\partial \mathcal{H}}{\partial I_i}, \ \dot{\lambda}_i^R = -\frac{\partial \mathcal{H}}{\partial R_i}, \tag{2.4.2}$$

with the final constraints:

$$\lambda_i^S(T) = \lambda_i^I(T) = \lambda_i^R(T) = 0. \tag{2.4.3}$$

According to PMP, any optimal controller must satisfy:

$$\mathbf{u} \in \arg\min_{\mathbf{v}} \mathcal{H}(\mathbf{v}), \tag{2.4.4}$$

where the minimization is over the set of admissible controls.

Using the expressions for ξ_{rep} from (2.2.10) and the expressions for ν_i, μ_i and ρ_i from (2.2.5), it can be shown that the vector minimization (2.4.4) can be expressed as a scalar minimization

$$u_i(t) \in \arg\min_{0 \le x \le 1} \psi_i(x,t) \qquad (1 \le i \le M); \tag{2.4.5}$$

$$\psi_i(x,t) := R_i(t)(h_i(x) - \phi_i(t)x); \tag{2.4.6}$$

$$\phi_i := \sum_{j=1}^{M} \bar{\beta}_{ij}(\lambda_j^S - \lambda_j^R)S_j + \sum_{j=1}^{M} \pi_{ij}\bar{\beta}_{ij}(\lambda_j^I - \lambda_j^R)I_j. \tag{2.4.7}$$

Equation (2.4.5) characterizes the optimal control u_i as a function of the state and adjoint functions at each instant. Plugging the optimal u_i into the state and adjoint function equations (respectively (2.2.5) and (2.4.2)) will again leave us with a system of (non-linear) differential equations that involves only the state and adjoint functions (and not the control $\mathbf{u}(\cdot)$), the initial values of the states (2.2.6) and the final values of the adjoint functions (2.4.3). Similar to the non-replicative case, the optimal controls may now be obtained (via (2.4.5)) by solving the above system of differential equations.

We conclude this subsection by stating and proving some important properties of the adjoint functions (Lemma 6 below) and $\phi_i(\cdot)$ (Lemma 7 subsequently), which we use later.

First, from (2.4.3), $\psi_i(0,t) = 0$, hence (2.4.5) results in $\psi_i(u_i,t) \le 0$. Furthermore, from the definition of τ_i, if $t \le \tau_i$, $(h_i(u_i(t)) - \phi_i(t)u_i(t)) = 0$, and if $t > \tau_i$,

$(h_i(u_i(t)) - \phi_i(t)u_i(t)) = \dfrac{\psi_i(u_i,t)}{R_i(t)} \leq 0$, so for all t,

$$\alpha_i(u_i,t) := (h_i(u_i(t)) - \phi_i(t)u_i(t)) \leq 0. \tag{2.4.8}$$

Lemma 6. For all $t \in [0,T)$ and for all i, we have $(\lambda_i^I - \lambda_i^S) > 0$ and $(\lambda_i^I - \lambda_i^R) > 0$.

Using our previous intuitive analogy, Lemma 6 implies that infective nodes are always worse for the evolution of the system than either susceptible or healed nodes, and thus the marginal price of infectives is greater than that of susceptible and healed nodes at all times before T. As before, we defer the proof of this lemma (to §2.4.3) to avoid breaking up the flow of the narrative. We now state and prove Lemma 7.

Lemma 7. For each i, $\phi_i(t)$ is a decreasing function of t, and $\dot{\phi}_i(t^+) < 0$ and $\dot{\phi}_i(t^-) < 0$ for all t.

Proof. $\phi_i(t)$ is continuous everywhere (due to the continuity of the states and adjoint functions) and differentiable whenever $\mathbf{u}(\cdot)$ is continuous. At any t at which $\mathbf{u}(\cdot)$ is continuous, we have: $\dot{\phi}_i(t) = \sum_{j=1}^{M} \bar{\beta}_{ij}[(\dot{\lambda}_j^S - \dot{\lambda}_j^R)S_j + (\lambda_j^S - \lambda_j^R)\dot{S}_j + \pi_{ij}(\dot{\lambda}_j^I - \dot{\lambda}_j^R)I_j + \pi_{ij}(\lambda_j^I - \lambda_j^R)\dot{I}_j]$.

From (2.4.1) and the adjoint equations (2.4.2), at points of continuity of the

control, we have:

$$\begin{aligned}
\dot{\lambda}_i^S =& -(\lambda_i^I - \lambda_i^S)\sum_{j=1}^{M}\beta_{ji}I_j - (\lambda_i^R - \lambda_i^S)\sum_{j=1}^{M}\bar{\beta}_{ji}R_j u_j,\\
\dot{\lambda}_i^I =& -\frac{\partial f(\mathbf{I})}{\partial I_i} - \sum_{j=1}^{M}(\lambda_j^I - \lambda_j^S)\beta_{ij}S_j - (\lambda_i^R - \lambda_i^I)\sum_{j=1}^{M}\pi_{ji}\bar{\beta}_{ji}R_j u_j,\\
\dot{\lambda}_i^R =& \frac{\partial L(\mathbf{R})}{\partial R_i} + u_i\sum_{j=1}^{M}\bar{\beta}_{ij}(\lambda_j^S - \lambda_j^R)S_j + u_i\sum_{j=1}^{M}\pi_{ij}\bar{\beta}_{ij}(\lambda_j^I - \lambda_j^R)I_j\\
& - h_i(u_i) = \frac{\partial L(\mathbf{R})}{\partial R_i} - \alpha_i(u_i, t).
\end{aligned} \tag{2.4.9}$$

Therefore, after some regrouping and cancellation of terms, at any t, we have

$$\begin{aligned}
-\dot{\phi}_i(t^+) =& \sum_{j=1}^{M}\bar{\beta}_{ij}[(1-\pi_{ij})\sum_{k=1}^{M}(\lambda_j^I - \lambda_j^R)\beta_{kj}I_k S_j + \pi_{ij}\frac{\partial f(\mathbf{I})}{\partial I_j}I_j\\
& + (S_j + \pi_{ij}I_j)(\frac{\partial L(\mathbf{R})}{\partial R_j} - \alpha_i(u_i, t)) + \pi_{ij}I_j\sum_{k=1}^{M}(\lambda_k^I - \lambda_k^S)\beta_{jk}S_k].
\end{aligned}$$

Now, since $0 \leq \pi_{ij} \leq 1$, the assumptions on $\bar{\beta}_{ij}$, β_{ki} and β_{il}, Theorem 1, and Lemma 6 all together imply that the sum of the first and last terms of the RHS will be positive. The second and third terms will be non-negative due to the definitions of $f(\cdot)$ and $L(\cdot)$ and (2.4.8). So $\dot{\phi}_i(t^+) < 0$ for all t. The proof for $\dot{\phi}_i(t^-) < 0$ is exactly as above. In a very similar fashion, it can be proved that $\dot{\phi}_i(t) < 0$ at all points of continuity of $\mathbf{u}(\cdot)$, which coupled with the continuity of $\phi_i(t)$ shows that it is a decreasing function of time. □

2.4.2 Structure of optimal replicative dispatch

Theorem 3. If an optimal control exists, for types i such that $R_i(t) > 0$ for some t: if $h_i(\cdot)$ is concave for type i, the optimal control for type i has the following

structure: $u_i(t) = 1$ for $0 < t < t_i$, and $u_i(t) = 0$ for $t_i < t \leq T$, where $t_i \in [0, T)$. If $h_i(\cdot)$ is strictly convex, the optimal control for type i, $u_i(t)$ is continuous and has the following structure: $u_i(t) = 1$ for $0 < t < t_i^1$, $u_i(t) = 0$ for $t_i^2 < t \leq T$, and $u_i(t)$ strictly decreases in the interval $[t_i^1, t_i^2]$, where $0 \leq t_i^1 < t_i^2 \leq T$.

Notice that for i such that $R_i(t) = 0$ for all t, the control $u_i(t)$ is irrelevant and can take any arbitrary value. We first prove the theorem for $t \in [\tau_i, T]$, and then we show that $\tau_i \in \{0, T\}$, completing our proof.

Proof: First consider an i such that $h_i(\cdot)$ is concave and non-linear. Note that hence $\psi_i(x, t)$ is a non-linear concave function of x. Thus, the minimum can only occur at extremal values of x, i.e., $x = 0$ and $x = 1$. Now $\psi_i(0, t) = 0$ at all times t, so to obtain the structure of the control, we need to examine $\psi_i(1, t)$ at each $t > \tau_i$. Let $\gamma_i(t) := \psi_i(1, t) = R_i(t)(h_i(1) - \phi_i(t))$ be a function of time t. From (2.4.5), the optimal u_i satisfies:

$$u_i(t) = \begin{cases} 1 & \gamma_i(t) < 0, \\ \\ 0 & \gamma_i(t) > 0. \end{cases} \tag{2.4.10}$$

We now show that $\gamma_i(t) > 0$ for an interval $(t_i, T]$ for some t_i, and $\gamma_i(t) < 0$ for $[\tau_i, t_i)$ if $t_i > \tau_i$. From (2.4.3) and (2.4.7), $\gamma_i(T) = h_i(1)R_i(T) > 0$. Since $\gamma_i(t)$ is a continuous function of its variable (due to the continuity of the states and adjoint functions), it will be positive for a non-zero interval leading up to $t = T$. If $\gamma_i(t) > 0$ for all $t \in [\tau_i, T]$, the theorem follows. Otherwise, from continuity, there must exist a $t = t_i > \tau_i$ such that $\gamma_i(t_i) = 0$. We show that for $t > t_i$, $\gamma_i(t) > 0$,

from which it follows that $\gamma_i(t) < 0$ for $t < t_i$ (by a contradiction argument). The theorem will then follow from (2.4.10).

Towards establishing the above, we show that $\dot{\gamma}_i(t^+) > 0$ and $\dot{\gamma}_i(t^-) > 0$ for any t such that $\gamma_i(t) = 0$. Hence, there will exist an interval $(t_i, t_i + \epsilon)$ over which $\gamma_i(t) > 0$. If $t_i + \epsilon \geq T$, then the claim holds, otherwise there exists a $t = t_i^{'} > t_i$ such that $\gamma_i(t_i^{'}) = 0$ and $\gamma_i(t) \neq 0$ for $t_i < t < t_i^{'}$ (from the continuity of $\gamma_i(t)$). So $\dot{\gamma}_i(t_i^{'-}) > 0$, which contradicts a property of real-valued functions (proved in [50]), establishing the claim:

Property 2. If $g(x)$ is a continuous and piecewise differentiable function over $[a, b]$ such that $g(a) = g(b)$ while $g(x) \neq g(a)$ for all x in (a, b), $\frac{dg}{dx}(a^+)$ and $\frac{dg}{dx}(b^-)$ cannot be positive simultaneously.

We now show that $\dot{\gamma}_i(t^+) > 0$ and $\dot{\gamma}_i(t^-) > 0$ for any $t > \tau_i$ such that $\gamma_i(t) = 0$. Due to the continuity of $\gamma_i(t)$ and the states, and the finite number of points of discontinuity of the controls, for any $t > \tau_i$ we have $\dot{\gamma}_i(t^+) = (\dot{R}_i(t^+)\frac{\gamma_i(t)}{R_i(t)} - R_i(t)\dot{\phi}_i(t^+))$ and $\dot{\gamma}_i(t^-) = (\dot{R}_i(t^-)\frac{\gamma_i(t)}{R_i(t)} - R_i(t)\dot{\phi}_i(t^-))$. If $\gamma_i(t) = 0$, then $\dot{\gamma}_i(t^+) = -R_i(t)\dot{\phi}_i(t^+)$ and $\dot{\gamma}_i(t^-) = -R_i(t)\dot{\phi}_i(t^-)$, which are both positive from Lemma 7 and Theorem 1, and thus the theorem follows.

The proofs for linear and strictly convex $h_i(\cdot)$'s are virtually identical to the corresponding parts of the proof of Theorem 2 and are omitted for brevity; the only difference is that in the linear case we need to replace R_i^0 with $R_i(t)$. The following lemma, proved in §2.4.4, completes the proof of the theorem.

Lemma 8. For all $0 \leq i \leq B$, $\tau_i \in \{0, T\}$. ■

2.4.3 Proof of Lemma 6

Proof. First, from (2.4.7) and (2.4.3), we have $\phi_i(T) = 0$, which, combined with (2.4.6) results in $\psi_i(x, T) = R_i(T)h_i(x)$. Since either $R_i(T) > 0$ or $\tau_i > T$, (2.4.5) and the definition of u_i result in $u_i(T) = 0$, as all other values of x would produce a positive $\psi_i(x, T)$. Therefore, $h_i(u_i(T)) = 0$.

The rest of the proof has a similar structure to that of Lemma 4. $(\lambda_i^I - \lambda_i^S)|_{t=T} = 0$ and $\lim_{t\uparrow T}(\dot{\lambda}_i^I - \dot{\lambda}_i^S) = -\partial f(\mathbf{I})/\partial I_i < 0$, for all i. Also, for all i, $(\lambda_i^I - \lambda_i^R)|_{t=T} = 0$ and $\lim_{t\uparrow T}(\dot{\lambda}_i^I - \dot{\lambda}_i^R) = -\partial f(\mathbf{I})/\partial I_i - \partial L(\mathbf{R})/\partial R_i + h_i(u_i(T)) < 0$, since $h_i(u_i(T)) = 0$.

Hence, $\exists\ \epsilon > 0$ such that $(\lambda_i^I - \lambda_i^S) > 0$ and $(\lambda_i^I - \lambda_i^R) > 0$ over $(T - \epsilon', T)$.

Now suppose that (at least) one of the inequalities is first[13] violated at $t = t^*$ for i^*, i.e., for all i, $(\lambda_i^I(t) - \lambda_i^S(t)) > 0$ and $(\lambda_i^I(t) - \lambda_i^R(t)) > 0$ for all $t > t^*$, and either (A) $(\lambda_{i^*}^I(t^*) - \lambda_{i^*}^S(t^*)) = 0$, or (B) $(\lambda_{i^*}^I(t^*) - \lambda_{i^*}^R(t^*)) = 0$ for some i^*. Note that from continuity of the adjoint functions, $(\lambda_i^I(t^*) - \lambda_i^S(t^*)) \geq 0$, and $(\lambda_i^I(t^*) - \lambda_i^R(t^*)) \geq 0$ for all i.

Case (A): Here, we have:[14]

$$(\dot{\lambda}_{i^*}^I - \dot{\lambda}_{i^*}^S)(t^{*+}) = -\frac{\partial f(\mathbf{I})}{\partial I_{i^*}} - \sum_{j=1}^{M}(\lambda_j^I - \lambda_j^S)\beta_{i^*j}S_j - (\lambda_{i^*}^I - \lambda_{i^*}^R)\sum_{j=1}^{M}\bar{\beta}_{ji^*}(1 - \pi_{ji^*})R_j u_j.$$

First of all, $-\partial f(\mathbf{I})/\partial I_{i^*} < 0$. Also, the second and third terms are non-positive,

[13] Going backward in time from $t = T$.

[14] The RHS of the equation is evaluated at $t = t^*$ due to continuity.

according to the definition of t^*. Hence, $(\dot{\lambda}^I_{i^*} - \dot{\lambda}^S_{i^*})(t^{*+}) < 0$, which contradicts Property 1, therefore case (A) does not arise.

Case (B): In this case, we have:[14]

$$(\dot{\lambda}^I_{i^*} - \dot{\lambda}^R_{i^*})(t^{*+}) = -\frac{\partial f(\mathbf{I})}{\partial I_{i^*}} - \frac{\partial L(\mathbf{R})}{\partial R_{i^*}} - \sum_{j=1}^{M}(\lambda^I_j - \lambda^S_j)\beta_{i^*j}S_j + \alpha_{i^*}(u_{i^*}, t).$$

We have $-\partial f(\mathbf{I})/\partial I_{i^*} < 0$ and $-\partial L(\mathbf{R})/\partial R_{i^*} \leq 0$. Also, $-(\lambda^I_{i^*} - \lambda^S_{i^*}) \sum_{j=1}^{M} \beta_{ji^*}S_j$ is non-positive, according to the definition of t^*, and α_{i^*} will be non-negative due to (2.4.8). This shows $(\dot{\lambda}^I_{i^*} - \dot{\lambda}^R_{i^*})(t^{*+}) < 0$, contradicting Property 1, and so case (B) does not arise either, completing the proof. □

2.4.4 Proof of Lemma 8

Proof. We start by creating another control $\bar{\mathbf{u}}$ from $\mathbf{u}$ such that for every i, for every $t \leq \tau_i$, $\bar{u}_i(t) := 1$, and for every $t > \tau_i$, $\bar{u}_i(t) := u_i(t)$. We prove by contradiction that $\tau_i(\mathbf{I}(0), \mathbf{S}(0), \mathbf{R}(0), \bar{\mathbf{u}}) \in \{0, T\}$ for each i. Since $\bar{u}_i \not\equiv u_i$ only in $[0, \tau_i]$ and $R_i(t) = 0$ for $t \in (0, \tau_i]$ when $\mathbf{u}$ is used, the state equations can only differ at a solitary point $t = 0$, and therefore both controls result in the same state evolutions. Thus, for each i, $\tau_i(\mathbf{I}(0), \mathbf{S}(0), \mathbf{R}(0), \bar{\mathbf{u}}) = \tau_i(\mathbf{I}(0), \mathbf{S}(0), \mathbf{R}(0), \mathbf{u})$, and $\tau_i(\mathbf{I}(0), \mathbf{S}(0), \bar{\mathbf{u}})$ may be denoted as τ_i as well. The lemma therefore follows.

For the contradiction argument, assume that the control is $\bar{\mathbf{u}}$ and that $\tau_i \in (0, T)$ for some i. Our proof relies on the fact that if $\bar{u}_i(t') = 0$ at some $t' \in (0, T)$, then $\bar{u}_i(t) = 0$ for $t > t'$, which follows from the definition of $\bar{\mathbf{u}}$ and prior results in the proof of Theorem 3.

For $t \in [0, \tau_i]$, since $R_i(t) = 0$ in this interval, (2.2.5c) becomes:

$$\dot{R}_i = \sum_{j=1, j\neq i}^{M} \bar{\beta}_{ji}(S_i + \pi_{ji} I_i) R_j \bar{u}_j = 0 \tag{2.4.11}$$

in this interval. Since all terms in $\sum_{j=1,j\neq i}^{M} \bar{\beta}_{ji}(S_i + \pi_{ji} I_i) R_j \bar{u}_j$ are non-negative, for each $j \neq i$ we must either have (i) $\bar{\beta}_{ji}(S_i(t) + \pi_{ji} I_i(t)) = 0$ for some $t \in [0, \tau_i]$, or (ii) $R_j(t)\bar{u}_j(t) = 0$ for all $t \in [0, \tau_i]$.

(i) Here, either $\bar{\beta}_{ji} = 0$; or $(S_i(t) + \pi_{ji} I_i(t)) = 0$, and hence due to Theorem 1, $S_i(t) = 0$ and $\pi_{ji} I_i(t) = 0$. In the latter case, from Theorem 1, $S_i(0) = 0$ and $\pi_{ji} = 0$. and therefore for all $t > 0$, we will have $\bar{\beta}_{ji}(S_i + \pi_{ji} I_i) R_j \bar{u}_j = 0$.

(ii) We can assume $\bar{\beta}_{ji}(S_i(t) + \pi_{ji} I_i(t)) > 0$ for all $t \in (0, \tau_i]$. For such j, if $\tau_j < \tau_i$, $R_j(t) > 0$ for $t \in (\tau_j, \tau_i]$, therefore $\bar{u}_j(t) = 0$ for such t. Due to the structure results obtained for the interval $[\tau_j, T]$ in Theorem 3, $\bar{u}_j(t) = 0$ for all $t > \tau_j$, and therefore $\bar{\beta}_{ji}(S_i + \pi_{ji} I_i) R_j \bar{u}_j = 0$ for all $t > 0$.

Now, since $M < \infty$, the set $W = \{\tau_k : \tau_k > 0, k = 1, \ldots, M\}$ must have a minimum $\omega_0 < T$. Let $L(\omega_0) = \{k \in \{1, \ldots, M\} : \tau_k = \omega_0\}$. Let the second smallest element in W be ω_1. Using the above argument, the values of $R_k(t)$ for $t \in [\omega_0, \omega_1]$ for all $k \in L(\omega_0)$ would affect each other, but not R_i's for i such that $\tau_i > 0$, $i \notin L(\omega_0)$. Furthermore, in this interval for $k \in L(\omega_0)$ we have $\dot{R}_k = \sum_{g \in L(\omega_0)} \bar{\beta}_{gk}(S_g + \pi_{gk} I_i) R_g \bar{u}_g$, with $R_k(\omega_0) = 0$. We see that for all $k \in L(\omega_0)$, replacing $R_k(t) = 0$ in the RHS of equation (2.2.5) gives us $\dot{R}_k(t) = 0$, a compatible LHS, while not compromising the existence of solutions for all other states. An application of Theorem 1 for $t \in [\omega_0, \omega_1]$ and $\bar{u}$ shows that this is the

unique solution of the system of differential equations (2.2.5). This contradicts the definition of τ_k, completing the proof of the lemma. □

2.5 An Alternative Cost Functional

Recall that in our objective function, the cost of non-replicative patching was defined as $\sum_{i=1}^{M} R_i^0 h_i(u_i)$ (respectively $\sum_{i=1}^{M} R_i h_i(u_i)$ for the replicative case), which corresponds to a scenario in which the dispatchers are charged for every instant they are immunizing/healing (distributing the patch), irrespective of the number of nodes they are delivering patches to. This represents a *broadcast* cost model where each transmission can reach all nodes of the neighboring types. In an alternative *unicast* scenario, different transmissions may be required to deliver the patches to different nodes. This model is particularly useful if the dispatchers may only transmit to the nodes that have not yet received the patch.[15] Hence, the cost of patching in this case can be represented by: $\sum_{i=1}^{M}\sum_{j=1}^{M} R_i^0 \bar{\beta}_{ij}(S_j + I_j)p(u_i)$ (for the replicative case: $\sum_{i=1}^{M}\sum_{j=1}^{M} R_i \bar{\beta}_{ij}(S_j + I_j)p(u_i)$), where $p(.)$ is an increasing

[15]This can be achieved by keeping a common database of nodes that have successfully received the patch, or by implementing a turn-taking algorithm preventing double targeting. Note that we naturally assume that the network does not know with a priori certainty which nodes are infective, and hence it cannot differentiate between susceptibles and infectives. Consequently, even when $\pi_{ij} = 0$, i.e., the system manager knows the patch cannot remove the infection and can only immunize the susceptible, still the best it may be able to do is to forward the message to any node that has not yet received it.

function. More generally, the patching cost can be represented as a sum of the previously seen cost (§2.2.5) and this term.

For non-replicative patching, if all $h_i(\cdot)$ and $p(\cdot)$ are concave, then Theorem 2 will hold if for all pairs (i,j), $\pi_{ij} = \pi_j$ (i.e., healing efficacy only depends on the type of an infected node, not that of the immunizer). The analysis will change in the following ways: A term of $R_i^0 p(u_i) \sum_{j=1}^{M} \bar{\beta}_{ij}(S_j + I_j)$ is added to (2.3.6), and subsequently to (2.3.9) (with $u_i = 1$ in the latter case). Also, (2.3.8) is modified by the subtraction of $\sum_{j=1}^{M} \bar{\beta}_{ji} R_j^0 p(u_j)$ from the RHS of both equations. This leaves $\dot{\lambda}_i^I - \dot{\lambda}_i^S$ untouched, while subtracting a positive amount from $\dot{\lambda}_i^I$, meaning that Lemma 4 still holds. As $\phi_i(t)$ was untouched, this means that Lemma 5 will also hold. Thus the RHS of $\dot{\gamma}_i$ is only modified by the subtraction of $\sum_{j,k=1}^{M} \bar{\beta}_{ij}(S_j + \pi_j I_j)\bar{\beta}_{kj} R_k^0 \left(p(u_k) - u_k p(1)\right)$ which is a positive term, as for any continuous, increasing, concave function $p(\cdot)$ such that $p(0) = 0$, we have $ap(b) \geq bp(a)$ if $a \geq b \geq 0$, since $\frac{p(x)}{x}$ is increasing. This yields: $(p(u_k) - u_k p(1) \geq 0)$. Therefore the conclusion of Theorem 2 holds. Similarly, it may be shown that Theorem 2 also holds for strictly convex $h_i(\cdot)$ provided $p(\cdot)$ is linear.

For the replicative case, if $p(\cdot)$ is linear ($p(x) = Cx$) and again $\pi_{ij} = \pi_j$ for all (i,j), Theorem 3 will hold. The modifications of the integrand and ψ_i are as above. The adjoint equations (2.4.9) are modified by the subtraction of $\sum_{j=1}^{M} C\bar{\beta}_{ji} R_j u_j$ from $\dot{\lambda}_i^I$ and $\dot{\lambda}_i^I$, and the subtraction of $C u_i \sum_{j=1}^{M} \bar{\beta}_{ij}(S_j + I_j)$ from $\dot{\lambda}_i^R$. Due to the simultaneous change in ψ_i, however, we still have $\dot{\lambda}_i^R = \partial L(\mathbf{R})/\partial R_i - \alpha_i(u_i, t)$.

Therefore, Lemma 6 still holds, as $\dot{\lambda}_i^I - \dot{\lambda}_i^S$ is unchanged, and a positive amount is subtracted from $\dot{\lambda}_i^I - \dot{\lambda}_i^R$. We absorb $\sum_{j=1}^{M} C\bar{\beta}_{ij}(S_j + I_j)$ into $\phi_i(t)$, where all the $p(\cdot)$ terms in $\dot{\phi}_i$ will cancel out, leaving the rest of the analysis, including for Lemmas 7 and 8, to be the same. The theorem follows.

2.6 Numerical Investigations

In this section, we numerically investigate the optimal control policies for a range of malware and network parameters and examine its performance in a real-world traces. [16] We first present an example of our optimal policy (§2.6), and then we examine its behavior in some sample topologies (§2.6). Subsequently, we present 4 heuristics that are likely to arise in practice and show the cost improvements the optimal policy is likely to show(§2.6) and demonstrate the relative benefits of replicative, as opposed to non-replicative, patching (§2.6). For an emerging epidemic, the initial conditions and the contact rates β_{ij} may not immediately be known. However, these parameters can be estimated by the network by looking at the empiric contact frequencies of a small number of nodes. Furthermore, nodes may have synchronization issues that affect the implementation of a time-sensitive policy. In §2.6, we investigate the optimal policy's robustness to errors in estimation of the initial states, mixing rates, and in the synchronization of the node clocks. Finally, in §2.6, we examine how our optimal policy performs on a

[16] For our calculations, we used *C* and *MATLAB* programming.

real trace of mobility and communication.

Recalling the notion of topologies presented in §2.2.1 (in the paragraph before (2.2.2)), we consider **four** topologies: *linear*, ring, *star* and *complete*, as was illustrated in Fig. 2.1. We assume $\beta_{ii} = \beta = 0.223$ for all i.[17] The value of β_{ij}, $i \neq j$ is equal to $X_{Coef} \cdot \beta$ if link ij is part of the topology graph, and zero otherwise. It should be noted that $\beta_{ij} * T$ denotes the average number of contacts between nodes of regions i and j within the time period, and thus β and T are dependent variables. For simplicity, we use equal values for $\beta_{ji}, \beta_{ij}, \bar{\beta}_{ij}$, $\bar{\beta}_{ji}$ for all i, j (i.e., $\beta_{ji} = \beta_{ij} = \bar{\beta}_{ij} = \bar{\beta}_{ji}$), and set $\pi_{ij} = \pi$ for all i, j. We examine two different aggregate cost structures for non-replicative patching:[18]

$$\text{(type-A) - } \int_0^T \left(K_I \sum_{i=1}^{M} I_i(t) + K_u \sum_{i=1}^{M} R_i^0 u_i(t) \right) dt \tag{2.6.1}$$

and

$$\text{(type-B) - } \int_0^T \left(K_I \sum_{i=1}^{M} I_i(t) + K_u \sum_{i=1}^{M} R_i^0 u_i(t)(S_i(t) + I_i(t)) \right) dt \tag{2.6.2}$$

(described in §2.2.5 and §2.5 respectively). For replicative patching, R_i^0 in both cost types is replaced with $R_i(t)$. The parameters for all simulations are summarized in Table 2.1.

[17] This specific value of β is chosen to match the average inter-meeting times from the numerical experiment reported in [37].

[18] $f_i(\cdot)$, $h_i(\cdot)$, and $p(\cdot)$ are linear and identical for all i, and $l_i(\cdot) = 0$.

Table 2.1: Simulation parameters: Here, REP shows whether the patching is replicative, X_C is X_{Coef}, and C is cost type. In all cases, $K_I = 1$. Dashed parameters are simulation variables.

FIG.	TOP.	REP	π	M	T	C	X_C	$\mathbf{R}^0$	$\mathbf{I}^0$	K_U
2.2	LIN.	N	-	3	35	A	0.1	$\{0.2\}_1^M$	0.3,$\{0\}_2^M$	0.5
2.3	LIN.	N	-	10	35	A	-	$\{0.2\}_1^M$	0.3,$\{0\}_2^M$	0.5
2.4	STAR	N	-	-	35	B	0.1	$\{0.2\}_1^M$	0.6,$\{0\}_2^M$	0.2
2.5	LIN.	Y	1	-	35	A	0.1	$\{0.2\}_1^M$	0.2,$\{0\}_2^M$	0.2
2.6	COMP.	Y	1	-	35	A	0.1	$\{0.2\}_1^M$	0.3,$\{0\}_2^M$	0.2
2.7A	RING	N	1	4	10	A	0.2	0.05, $\{0.01\}_2^M$	0.1,$\{0\}_2^M$	0.01
2.7B	RING	N	0	4	35	A	0.1	$\{0.1\}_1^M$	0.4,$\{0\}_2^M$	0.07
2.7C	RING	N	1	4	20	A	0.5	$\{0.01\}_1^M$	0.05,$\{0\}_2^M$	0.01

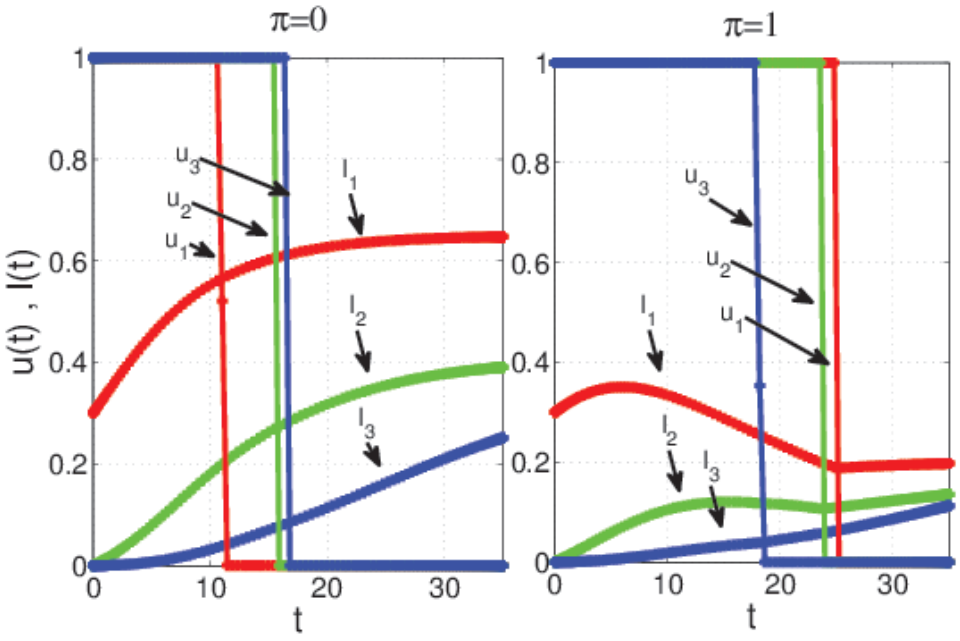

Figure 2.2: Optimal patching policies and corresponding levels of infection in a three region linear topology. Note how the infection that initially only exists in region 1 spreads in region 1 and then to region 2, and finally to region 3.

Numeric Example

First, in Fig. 2.2 we have depicted an example of the optimal dynamic patching policy along with the corresponding evolution of the infection as a function of time for a simple 3-region linear topology. For $\pi = 0$ the levels of infection are non-decreasing, whereas for $\pi = 1$ they may go down as well as up (due to healing).

Effects of Topology

We study the *drop-off* times (the time thresholds at which the bang-bang optimal patching halts) in different regions for linear and star topologies.

Fig. 2.3 reveals two different patterns for $\pi = 0$ and $\pi = 1$ in a linear topology. For $\pi = 0$, a middle region is patched for the longest time, whereas for $\pi = 1$, as we move away from the origin of the infection (region 1), the drop-off point decreases. This is because for $\pi = 0$, patching can only benefit the network by recovering susceptibles. In regions closer to the origin, the fraction of susceptibles decreases quickly, making continuation of the patching comparatively less beneficial. In the middle regions, where there are more salvageable susceptibles, patching should be continued for longer. For regions far from the origin, patching can be stopped earlier, as the infection barely reaches them within the time horizon of consideration. For $\pi = 1$, patching is able to recover both susceptible and infective nodes. Hence, the drop-off times depend only on the exposure to the infection, which decreases with distance from the origin. As X_{Coef} is increased, the drop-off points when $\pi = 1$ get closer together. Intuitively, this is because higher cross-mixing rates have a homogenizing effect, as the levels of susceptible and infective nodes in different region rapidly become comparable. Also, Fig. 2.3 reveals that as X_{Coef} increases and more infection reaches farther regions, they are patched for longer, which agrees with our intuition.

We next investigate a star configuration where the infection starts from a pe-

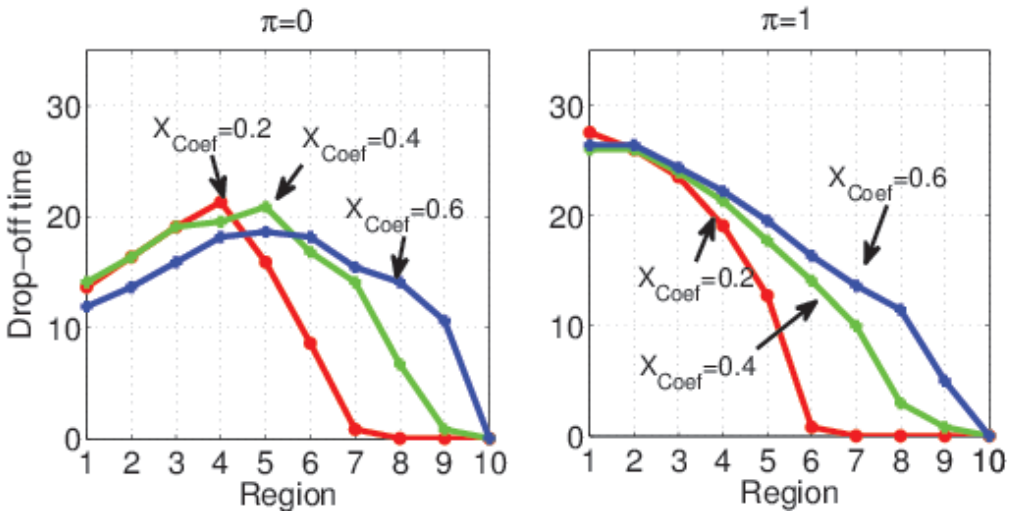

Figure 2.3: Drop-off times in a linear topology for $X_{Coef} = 0.2, 0.4, 0.6$.

ripheral region (region 1 in the star in Fig. 2.1). Fig. 2.4 reveals the following interesting phenomenon: although the central region is the only one that is connected to all the regions, for $\pi = 0$, it is patched for shorter lengths of time compared to the peripherals. In retrospect, this is because only susceptible nodes can be patched and their number at the central region drops quickly due to its interactions with all the peripheral regions, rendering patching inefficient relatively swiftly. As expected, this effect is amplified with higher numbers of peripheral regions. For $\pi = 1$, on the other hand, the central region is patched for the longest time. This is because the infective nodes there can infect susceptible nodes in all regions, and hence the patching, which can now heal the infectives as well, does not stop until it heals almost all of infective nodes in this region.

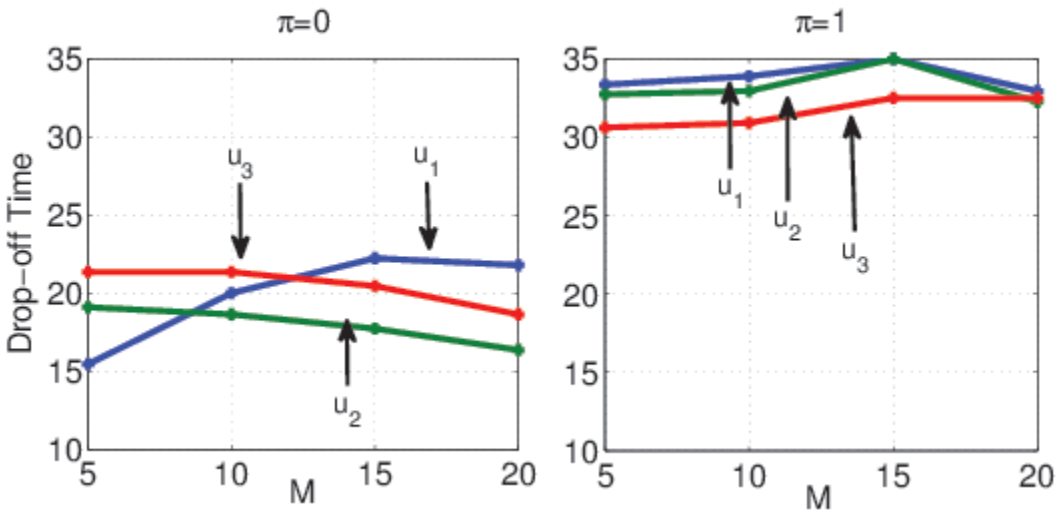

Figure 2.4: Drop-off times in the star topology.

Cost Comparison

Next, in order to evaluate the efficacy of our optimal dynamic heterogeneous patching, which we henceforth refer to as *Stratified Dynamic* (S.D.), we compare our aggregate cost against those of four alternative policies.

In the simplest alternative policy, all regions use identical patching intensities that do not change with time. We then select this fixed and static level of patching so as to minimize the aggregate cost among all possible choices. We refer to this policy as *Static* (St.). The aggregate cost may be reduced if the static level of the patching is allowed to be distinct for different regions. These values (still fixed over time) are then independently varied and the optimum combination is selected. We refer to this policy as *Stratified Static* (S. St.). The third policy we implement is a *homogeneous* approximation to the heterogeneous network.

Specifically, the whole network is approximated by a single region model with an inter-contact rate equal to the *mean* pairwise contact rate of the real system. The optimal control is derived based on this model and applied across all regions to calculate the aggregate cost. We call this policy *Simplified Homogeneous* (S. H.). The simplified homogeneous policy is a special case of Spatially Static (Sp. St.) policies: Sp. St. policies optimize a *single* jump-point for a bang-bang control to be applied to *all* types in the topology.

Fig. 2.5 depicts the aggregate costs of all five policies for a linear topology and intra-type β_{ii} and inter-type contact rates β_{ij} constant. As we can clearly observe, our stratified policy achieves the least cost, outperforming the rest. For example for $M \geq 3$ regions, our policy outperforms the best static policies by 40% and for $M = 5$, it betters the homogeneous approximation by 100%, which shows that our results about the structure of the optimal control can result in large cost improvements. When the number of regions is small, S. H. and Sp. St. perform better than S. St., all of which obviously outperform St. However, as the number of regions increases and the network becomes more spatially heterogeneous, the homogeneous approximation, and all uniform controls in general, worsen and the S. St. policy quickly overtakes them as the best approximation to the optimal. In this case, the cost of the two stratified policies does not change noticeably as the number of types is increased. While this is an attribute of the simulation settings (and in particular, the linear topology), in general, S.D. and S.St. are the only

two policies that can optimize controls in direct accordance with the topology. Therefore the extent of their cost variations is less as the number of types is varied compared to the other heuristics. In the particular case of Fig. 2.5, the fraction of recovered in each type increases much faster due to the increased number of interactions, and thus less patching needs to be carried out in that type (less intensity for the stratified static case, and for a shorter period in the stratified dynamic policy). However, these effects are countered by the rising number of elements in the cost function, leading to a seemingly constant cost. For $\pi = 0$, a similar performance gap is observed. Specifically, as discussed, optimal drop-off times for this problem should vary based on the distance from the originating region, a factor that the Sp. St., S. H., and St. policies ignore.

We now present some general observations for which we do not present figures due to space constraints. From our observations, the relative performance of the optimal becomes better as the heterogeneity among the nodes increases, both in terms of topology and in terms of states. Fig. 2.3 is typical for the intermediate parameter range where the optimal stratified dynamic policy is not on or off all the time. For example, the optimal performs better (relative to the heuristics) in a linear topology as opposed to a complete topology (which has identical contact rates among all pairs of types). Furthermore, for example, if the initial fraction of infectives is high in all types and we have no healing ($\pi = 0$), or the time period is too short relative to the contact rates, the patch cannot spread much beyond its

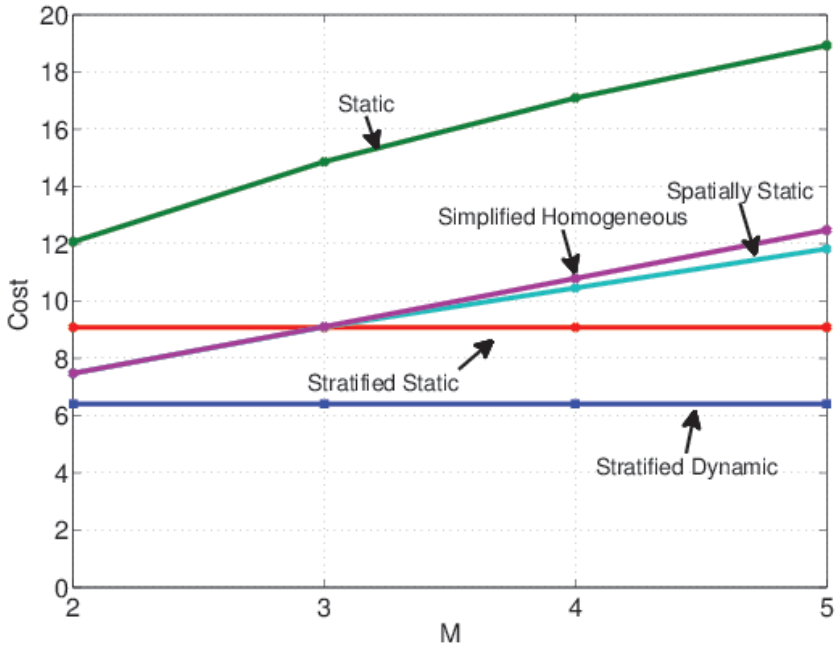

Figure 2.5: Cost of heuristics vs. the optimal policy, linear topology.

original nodes, and thus all policies perform at around the same level. Finally, if the cost of infection is very high or very low relative to immunization, the optimal stratified dynamic policy will be one (respectively, zero) at all times, a control that can be replicated by the constrained heuristics, and thus the gains in performance are muted.

Replicative vs. Non-replicative Patching

We already know that optimal replicative patching will outperform optimal non-replicative patching. We examine the extent of the difference through numerical computation. In Fig. 2.6, we see the aggregate cost of optimal replicative and non-replicative patching in a complete topology as a function of the size of the

network for $M \leq 11$. Here, even for such modest sizes, replicative patching can be 60% more efficient than non-replicative patching, a significant improvement. This is especially true for the complete topology and other edge-dense topologies, as in replicative patching, the patch can spread in ways akin to the malware.

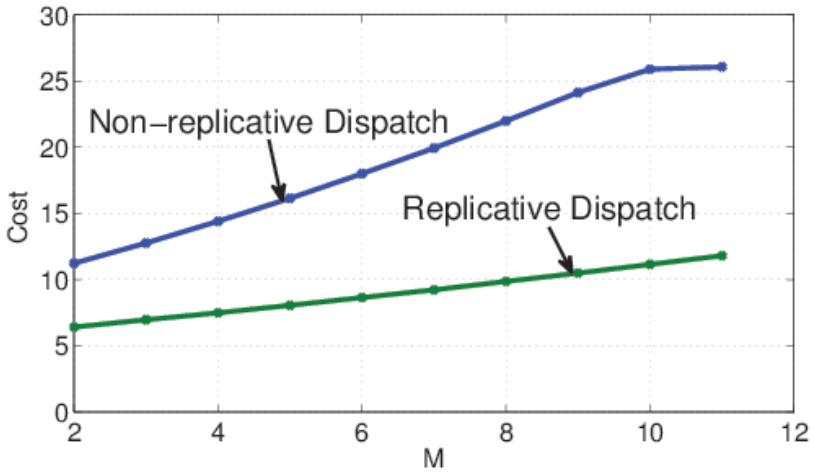

Figure 2.6: Replicative and non-replicative patch cost, complete topology.

Robustness

In this section, we simulated the robustness of our optimal control to errors in the determination of the initial states (Fig. 2.7a), the contact rates (Fig. 2.7b), and the synchronization of the node clocks (Fig. 2.7c). In Fig. 2.7a, the system estimates the number of susceptibles and infectives of an emerging epidemic in a ring topology of size M=3 with an unbiased, uniformly distributed error. It then uses this estimated network to calculate optimal controls which it applies in the real settings. It can be seen that a maximum estimation error of 15% leads to a

mean cost deficiency of only 5%. This performance was replicated across differing network sizes and values of the initial parameters. In Fig. 2.7b, the system estimates the mean contact rates of an emerging epidemic in a ring topology of size M=4 with an unbiased, uniformly distributed error. It then uses this estimated topology to calculate optimal controls which it applies in the real settings. It can be seen that an unbiased maximum estimation error of 25% changes the mean costs by less than 1%. This remarkable robustness was seen with a range of sizes and initial parameters. In Fig. 2.7c, it was assumed that the optimal controls for a ring topology of size M=4 had been calculated and passed on to nodes whose clocks have unbiased, uniformly distributed shifts from the reference, who then implement the bang-bang policy. Here, we plot the mean cost difference as a function of the ratio of the maximum magnitude of the synchronization error to the resolution at which the drop-off times of the optimal control were calculated, and observe that the cost barely changes even when this ratio approaches one (and the synchronization error is of the magnitude of the decision instants).

From these results, it can be seen that the optimal control is very robust to errors in these parameters, and thus can be implementable in networks where these parameters are initially unknown and have to be estimated. We have, in each case, compared the performance of the optimal control to the heuristic which is most robust to those specific types of errors - the Simplified Homogeneous (Sp. St.) approximation for errors in the determination of the initial states and the

contact rates (errors in which will get averaged out among the types), and the Stratified Static (S. St.) heuristic for clock synchronization errors, as this heuristic does not depend on the clocks of the nodes and is inherently robust to such errors.

Real-World Trace

In this section, we calculated the optimal control (and the relevant heuristics) for a network topology derived from a real-world trace: Bluetooth data from volunteers at the SigComm '09 conference [70]. We calculated the optimal control and the heuristics for a topology with constant contact rates derived from the trace, and with one randomly chosen infective and one recovered person per each type. We applied the controls to the real proximity data of the participants over 50 runs to find the cost differential and the variance (Table 2.2).

The SigComm '09 data set includes "Bluetooth encounters, opportunistic messaging, and social profiles of 76 users of MobiClique application at SIGCOMM 2009". The participants from each country constitute a "type" for categorization. We chose 5 types, as there were five nationalities with more than 2 participants, and calculated their per-day contact rate. Patching was replicative with $\pi = 1$, $K_I = 1$, and $K_U = 0.05$. Note that in this instance, the stratified dynamic policy still outperforms all other heuristics by 15%. It is interesting to note that even the Sp. St. policy significantly outperforms the homogeneous approximation S. H., which underscores the benefits of considering node heterogeneity.

Table 2.2: MEAN AND VARIANCE OF THE COST OF THE POLICIES ON THE SIGCOMM09 TRACE OVER 50 RUNS.

SIGCOMM09	MEAN	VARIANCE
S.D.	0.4052	0.1090
S. H.	0.6914	0.2711
S. ST.	0.8829	0.0204
SP. ST.	0.4609	0.0781
ST.	1.1667	0.0285

2.7 Conclusion

We presented a general model for patch dissemination in a rate-heterogeneous network in the mean-field regime that can capture the core of many different types of real-world networks. We proved that optimal controls for each type have a simple structure that can be easily computed, stored, and executed in many cases of practical importance. The derived optimal controls are observed to be robust to errors in model parameter estimation, and perform better than heuristics derived from practice on simulations and traces.

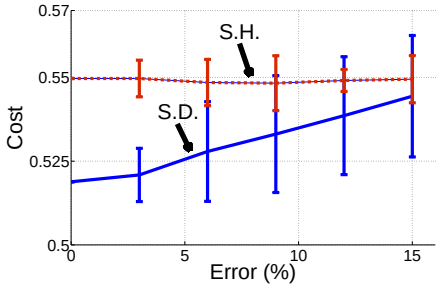

(a) Initial condition estimation errors

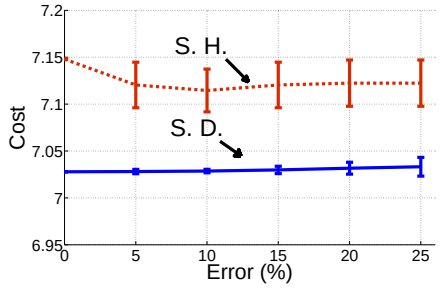

(b) Contact rate estimation errors

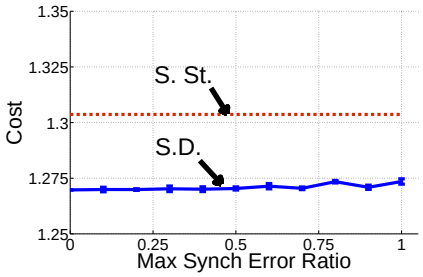

(c) Node synchronization errors

Figure 2.7: Effect of errors in initial condition estimation 2.7a, contact rate estimation 2.7b, and node synchronization 2.7c on the mean cost of the optimal dynamic policy and the most robust heuristic. An error % of γ for the contact rate β, for example, means that the estimate is uniformly distributed in $[(1-\gamma)\beta, (1+\gamma)\beta]$. Error-bars represent the cost variance over 25 runs.

Chapter 3

Resource-Heterogeneity: Optimal Energy-Aware Epidemic Routing in DTNs [1]

3.1 Introduction

An epidemic may also be constrained by the resources it needs from the infected population in order to spread. These resources (e.g., wealth in the spread of a fad) may fluctuate as a result of the spread of the epidemic, leading to a stratification of nodes based on their relative amount of remaining resources, and thus their ability to be affected by, and spread, the epidemic. As opposed to the inherent types of

[1] Presented in IEEE MobiHoc 2012 [44] and published in the IEEE Transactions on Automatic Control, June 2015 [**?**].

the previous chapter, these *resource-dependent* types are fluid. In particular, in this chapter we focus on the spread of a message in a Delay-Tolerant Network (DTN), where the act of sending and receiving the message consumes energy in both nodes, and thus induces an energy-heterogeneity in the system that affects the epidemic's spread in the future.

Delay-Tolerant Networks have been envisioned for civilian disaster response networks, military networks, and environmental surveillance, e.g., where communication devices are carried by disaster relief personnel and soldiers, or where they can be mounted on wandering animals. These networks are comprised of mobile nodes whose communication range is much smaller than their roaming area, and therefore messages are typically relayed by intermediate nodes at times of spatial proximity. Relaying messages consumes a significant amount of energy in the sending and receiving nodes. However, mobile nodes in DTNs typically have limited battery reserves and replacing/recharging the batteries of drained nodes is usually infeasible or expensive. Simple epidemic forwarding depletes the limited energy reserves of nodes, while conservative forwarding policies jeopardize the timely delivery of the message to the destination. Hence, there is an inherent trade-off between timely message delivery and energy conservation.

The literature on message routing in DTNs is extensive [1, 7, 9, 19, 20, 60, 61, 67, 68, 82–84, 88, 90, 96]. Most notably, Vahdat and Becker [88] present a policy where each node propagates the message to all of its neighbors simultaneously

("Epidemic Routing"), while Spyropoulos *et al.* [84] propose spreading a specific number of copies of the message initially and then waiting for the recipients of these copies to deliver the message to the destination ("Spray and Wait"). Wang and Wu [90] present "Optimized Flooding", where flooding is stopped once the total probability of message delivery exceeds a threshold. Singh *et al.* [83] and Altman *et al.* [1] identify optimal and approximately optimal message forwarding policies in the class of policies that do not take the distribution of node energies into account. In summary, the state of the art in packet forwarding in DTNs comprises of heuristics that ignore energy constraints [60, 88, 96], those that consider only overall energy consumption but provide no analytic performance guarantees [9, 19, 61, 68, 84, 90], and those that do not utilize the energy available *to each node* in making forwarding decisions [1, 7, 20, 67, 82, 83] (we describe some of these policies in more detail in §3.4). An efficient forwarding strategy can use knowledge of the distribution of energy among among nodes to its advantage, and this motivates the design of dynamic energy-dependent controls which are the subject of this work.

We start by formulating the trade-off between energy conservation and likelihood of timely delivery as a dynamic energy-dependent optimal control problem: at any given time, each node chooses its forwarding probability based on its current remaining energy. Since the number of relay nodes with the message increases and residual energy reserves decrease with transmissions and recep-

tions, the forwarding probabilities vary with time. Thus, they must be chosen so as to control the evolution of network states, which capture both the fraction of nodes holding a copy of the message and the remaining battery reserves of the nodes. We model the evolution of these states using epidemiological differential equations that rely on mean-field approximation of Markov processes, and seek dynamic forwarding probabilities (*optimal controls*) that optimize objective functions penalizing energy depletion subject to enforcing timely message delivery (§§3.2.1,3.2.2).

Our first result is to prove that dynamic optimal controls follow simple easy-to-implement threshold- based rules (§3.3, Theorem 5). That is, a node in possession of a copy of the message forwards the message to nodes it encounters that have not yet received it until a certain threshold time that depends on its current remaining energy. Calculating these thresholds is much simpler than solving the general problem and can be done once at the source node of the message. Subsequently, they can be added to the message as a small overhead. Each node that receives the message can retrieve the threshold times and forward the message if its age is less than the threshold entry of the node's residual energy level. The execution of the policy at each node is therefore simple and based only on local information.

Our second result is to characterize the nature of the dependence of the thresholds on the energy levels. Intuitively, the less energy a node has, the more reluc-

tant it should be to transmit the message, as the transmission will drive it closer to critically low battery levels. However, our investigations reveal that this intuition can only be confirmed when the penalties associated with low final remaining energies are convex (§3.3, Theorem 6), and does not hold in general otherwise.

Finally, our optimal control provides a missing *benchmark* for forwarding policies in large networks in which no information about the mobility pattern of the individual nodes is available and a minimum QoS is desired. This benchmark allows us to observe the sub-optimality of some simpler heuristic policies, and to identify parameter ranges in which they perform close to the optimal (§3.4).

3.2 System Model

We assume a low-load scenario in which only one message is propagated in the network within a terminal time T. This message has a single destination and it is sufficient for a copy of the message to be delivered to its destination by the terminal time. We use the deterministic mean-field (i.e., for large numbers of nodes) regime which models state evolution using a system of differential equations. Such models have been shown to be acceptable approximations both analytically and empirically for large and fast-moving mobile wireless networks [44]. In §3.2.1, we develop our system dynamics model based on mean-field deterministic ODEs. Subsequently, in §3.2.2 we consider two classes of utility functions that cogently combine a penalty for the impact of the policy on the residual en-

ergy of the nodes with guarantees for the QoS of the forwarding policy.

3.2.1 System Dynamics

We begin with some definitions: a node that has received a copy of the message and is not its destination is referred to as an *infective*; a (non-destination) node that has not yet received a copy of the message is called a *susceptible*. The maximum energy capacity of all nodes is B units. A message transmission between a pair of nodes consumes s units of energy in the transmitter and r units in the receiver, independent of their total energy level. Naturally, $r \leq s$. When an infective node contacts a susceptible at time t, the message is transmitted with a certain forwarding probability if the infective (transmitter) and susceptible (receiver) have at least s and r units of energy. If either does not have the respective sufficient energy, transmission will not occur.

Two nodes contact each other at rate $\hat{\beta}$. We assume that inter-contact times are exponentially distributed and uniform among nodes, an assumption common to many mobility models (e.g., Random Walker, Random Waypoint, Random Direction, etc. [33]). Moreover, it is shown in [33] that

$$\hat{\beta} \propto \frac{\text{average rel. node speeds} \times \text{communication ranges}}{\text{the roaming area}}. \tag{3.2.1}$$

Assuming $t = 0$ mark the moment of message generation, we define $S_i(t)$ (respectively, $I_i(t)$) to be the *fraction* of nodes that are susceptible (respectively, infective) and that have i energy units at time t. Hence for $t \in [0, T]$: $\sum_{i=0}^{B} (S_i(t) + I_i(t)) =$

1.

At any given time, each node can observe its own level of available energy, and its forwarding decision should, in general, utilize such information. Hence, upon an instance of contact between a susceptible node with i units of energy and an infective node with j units of energy at time t, as long as $i \geq r$ **and** $j \geq s$, the message is forwarded with probability $u_j(t)$ ($0 \leq u_j(t) \leq 1$). We take these probabilities to be our controls $\mathbf{u}(t) = \big(u_s(t), u_{s+1}(t), \ldots, u_B(t)\big) \in \mathcal{U}$, where $\mathcal{U}$ is the set of piecewise continuous controls with left-hand limits at each $t \in (0, T]$, and right-hand limits at each $t \in [0, T)$. If the message is forwarded, the susceptible node transforms to an infective node with $i - r$ energy units, and the infective node likewise to an infective node with $j - s$ energy units. We assume that once an infective contacts another node, the infective can identify (through a low-load exchange of control messages) whether the other node has a copy of the message (i.e., is infective), or does not (i.e., is susceptible), whether the contacted node is a destination and also whether it has enough energy to receive the message. We assume that the dominant mode of energy consumption is the transmission and reception of the message, and that each exchange of the control messages consumes an insignificant amount of energy. If a message-carrying node that has sufficient energy for one transmission contacts the destination that has yet to receive the message, the message is always forwarded to the destination.

Let N be the total number of nodes and define $\beta := N\hat{\beta}$. Following (3.2.1), $\hat{\beta}$

is inversely proportional to the roaming area, which scales with N. Hence, if we can define a density of nodes, β has a nontrivial value. The system dynamics in this regime over any finite interval can be approximated thus, except at the finite points of discontinuity of $\mathbf{u}$ ([31, Theorem 1]):

$$\dot{S}_i = \begin{cases} -\beta S_i \sum_{j=s}^{B} u_j I_j & (r \le i \le B), \quad (3.2.2a) \\ 0 & (0 \le i < r), \quad (3.2.2b) \end{cases}$$

$$\dot{I}_i = \begin{cases} -\beta u_i I_i \sum_{j=r}^{B} S_j & (B-r < i \le B), \quad (3.2.2c) \\ -\beta u_i I_i \sum_{j=r}^{B} S_j + \beta S_{i+r} \sum_{j=s}^{B} u_j I_j & (B-s < i \le B-r), \quad (3.2.2d) \\ -\beta u_i I_i \sum_{j=r}^{B} S_j + \beta S_{i+r} \sum_{j=s}^{B} u_j I_j + \beta u_{i+s} I_{i+s} \sum_{j=r}^{B} S_j & (s \le i \le B-s), \quad (3.2.2e) \\ \beta S_{i+r} \sum_{j=s}^{B} u_j I_j + \beta u_{i+s} I_{i+s} \sum_{j=r}^{B} S_j & (0 \le i < s). \quad (3.2.2f) \end{cases}$$

Note that in the above differential equations and in the rest of this work, whenever not ambiguous, the dependence on t is made implicit. We now explain each of these equations:[2]

[2]We consider protocols where a destination receives at most one copy of the message by the terminal time. The system dynamics hold if we allow the reception of multiple copies because isolated transmissions have no effect on the mean-field regime.

(3.2.2a): The rate of decrease in the fraction of susceptible nodes with energy level $i \geq r$ is proportional to the rate of contacts between these nodes and transmitting infective nodes with energy level equal to or higher than s.

(3.2.2b): Susceptibles with less than r units of energy cannot convert to infectives.

The rate of change in infectives of energy level i is due to three mechanisms:

1. Transmitting infectives of energy level i convert to infectives with energy level $i - s$ upon contact with susceptibles that have sufficient energy for message exchange. This conversion happens due to the energy consumed in transmitting the message, resulting in a decrease in infectives of energy level i.

2. Susceptibles with energy level $i + r$ are transformed to infectives of energy level i upon contact with transmitting infectives that have at least s units of energy, swelling the ranks of infectives of energy level i. This conversion occurs due to the energy consumed in receiving the message.

3. Transmitting infectives of energy level $i + s$ convert to infectives with energy level i upon contact with susceptibles that have sufficient energy for message exchange, adding to the pool of infectives of energy level i. Like 1, this is due to the energy consumed in transmitting the message.

Now, given that energy levels are upper-bounded by B:

I If $B - r < i \leq B$, only mechanism 1 is possible, as $i + s \geq i + r > B$, ruling out 2 and 3 respectively. This results in (3.2.2c).

II If $B - s < i \leq B - r$, only mechanisms 1 and 2 are possible, as $i + s > B$ rules out 3, leading to (3.2.2d).

III If $s \leq i \leq B - s$, all three mechanisms are in play, resulting in (3.2.2e).

IV If $0 \leq i < s$, only mechanisms 2 & 3 remain, as $i - s < 0$ rules out 1. Thus, we have (3.2.2d).

We consider continuous state solutions $\mathbf{S}(t) = \big(S_0(t), \ldots, S_B(t)\big)$, $\mathbf{I}(t) = \big(I_0(t), \ldots, I_B(t)\big)$ to the dynamical system (3.2.2) subject to initial conditions

$$\mathbf{S}(0) = \mathbf{S}_0 := (S_{00}, \ldots, S_{0B}),\ \mathbf{I}(0) = \mathbf{I}_0 := (I_{00}, \ldots, I_{0B}). \tag{3.2.3}$$

We naturally assume that the initial conditions satisfy $\mathbf{S}(0) \geq \mathbf{0}$, $\mathbf{I}(0) \geq \mathbf{0}$, and $\sum_{i=0}^{B} \big(S_i(0) + I_i(0)\big) = 1$ (vector inequalities are to be interpreted component-wise throughout).

We say that a state solution $(\mathbf{S}(t), \mathbf{I}(t))$ for the system (3.2.2) is *admissible* if the non-negativity and normalization conditions

$$\mathbf{S}(t) \geq \mathbf{0}, \quad \mathbf{I}(t) \geq \mathbf{0}, \quad \sum_{i=0}^{B} (S_i(t) + I_i(t)) = 1, \tag{3.2.4}$$

are satisfied for all $t \in [0, T]$. We next show that states satisfying (3.2.2) are admissible and unique for any $\mathbf{u} \in \mathcal{U}$:

Theorem 4. Suppose the initial conditions satisfy $\mathbf{S}(0) \geq \mathbf{0}$, $\mathbf{I}(0) \geq \mathbf{0}$, and $\sum_{i=0}^{B}\big(S_{0i} + I_{0i}\big) = 1$, and suppose $\mathbf{u}(t) = \big(u_s(t), u_{s+1}(t), \ldots, u_B(t)\big)$ is any system of piecewise continuous controls. Then the dynamical system (3.2.2) has a unique state solution $(\mathbf{S}(t),\ \mathbf{I}(t))$, which is admissible. If $I_i(t') > 0$ for any i (respectively, $S_j(t') > 0$ for any j) and $t' \in [0, T)$, $I_i(t) > 0$ (respectively $S_j(t) > 0$) for all $t > t'$. Also, for each j, $S_j(t') = 0$ for all $t' \in (0, T]$ if $S_j(0) = 0$.

In our proof, we use the following general result:

Lemma 9. Suppose the vector-valued function $\mathbf{f} = (f_i, 1 \leq i \leq N)$ has component functions given by quadratic forms $f_i(t, \mathbf{x}) = \mathbf{x}^T Q_i(t)\mathbf{x} \quad (t \in [0, T];\ \mathbf{x} \in \mathbb{S})$, where $\mathbb{S}$ is the set of N-dimensional vectors $\mathbf{x} = (x_1, \ldots, x_N)$ satisfying $\mathbf{x} \geq \mathbf{0}$ and $\sum_{i=1}^{N} x_i = 1$, and $Q_i(t)$ is a matrix whose components are uniformly, absolutely bounded over $[0, T]$. Then, for an N-dimensional vector-valued function $\mathbf{F}$, the system of differential equations

$$\begin{gathered} \dot{\mathbf{F}}(t) = \mathbf{f}(t, \mathbf{F}) \qquad (0 < t \leq T) \\ \text{subject to initial conditions } \mathbf{F}(0) \in \mathbb{S} \end{gathered} \tag{3.2.5}$$

has a unique solution, $\mathbf{F}(t)$, which varies continuously with the initial conditions $\mathbf{F}_0 \in \mathbb{S}$ at each $t \in [0, T]$.

This follows from standard results in the theory of ordinary differential equations [78, Theorem A.8, p. 419] given the observation that $\mathbf{f}(t, \mathbf{F})$ is comprised of quadratic forms and is thus Lipschitz over $[0, T] * \mathbb{S}$.

Proof. We write $\mathbf{F}(0) = \mathbf{F}_0$, and in a slightly informal notation, $\mathbf{F} = \mathbf{F}(t) =$

$\mathbf{F}(t, \mathbf{F}_0)$ to acknowledge the dependence of $\mathbf{F}$ on the initial value $\mathbf{F}_0$.

We first verify the normalization condition of the admissibility criterion. By summing the left and right sides of the system of equations (3.2.2) we see that $\sum_{i=0}^{B}\big(\dot{S}_i(t) + \dot{I}_i(t)\big) = 0$, and, in view of the initial normalization $\sum_{i=0}^{B}\big(S_i(0) + I_i(0)\big) = 1$, we have $\sum_{i=0}^{B}\big(S_i(t) + I_i(t)\big) = 1$ for all t.

We now verify the non-negativity condition. Let $\mathbf{F} = (F_1, \ldots, F_N)$ be the state vector in $N = 2(B+1)$ dimensions whose elements are comprised of $(S_i, 0 \leq i \leq B)$ and $(I_i, 0 \leq i \leq B)$ in some order. The system of equations (3.2.2a)–(3.2.2f) can thus be represented as $\dot{\mathbf{F}} = \mathbf{f}(t, \mathbf{F})$, where for $t \in [0, T]$ and $\mathbf{x} \in \mathbb{S}$, the vector-valued function $\mathbf{f} = (f_i, 1 \leq i \leq N)$ has component functions $f_i(t, \mathbf{x}) = \mathbf{x}^T Q_i(t)\mathbf{x}$ in which $Q_i(t)$ is a matrix whose non-zero elements are of the form $\pm\beta u_k(t)$. Thus, the components of $Q_i(t)$ are uniformly, absolutely bounded over $[0, T]$. Lemma 9 establishes that the solution $\mathbf{F}(t, \mathbf{F}_0)$ to the system (3.2.2a)–(3.2.2f) is unique and varies continuously with the initial conditions $\mathbf{F}_0$; it clearly varies continuously with time. Next, using elementary calculus, we show in the next paragraph that if $\mathbf{F}_0 \in$ **Int** $\mathbb{S}$ (and, in particular, each component of $\mathbf{F}_0$ is positive), then each component of the solution $\mathbf{F}(t, \mathbf{F}_0)$ of (3.2.2a)–(3.2.2f) is positive at each $t \in [0, T]$.[3] Since $\mathbf{F}(t, \mathbf{F}_0)$ varies continuously with $\mathbf{F}_0$, it follows that $\mathbf{F}(t, \mathbf{F}_0) \geq \mathbf{0}$ for all $t \in [0, T]$, $\mathbf{F}_0 \in \mathbb{S}$, which completes the overall proof.

Accordingly, let each component of $\mathbf{F}_0$ be positive. Since the solution $\mathbf{F}(t, \mathbf{F}_0)$

[3]Throughout this chapter, we use positive for strictly positive, etc.

varies continuously with time, there exists a time, say $t' > 0$, such that each component of $\mathbf{F}(t, \mathbf{F}_0)$ is positive in the interval $[0, t')$. The result follows trivially if $t' \geq T$. Suppose now that there exists $t'' < T$ such that each component of $\mathbf{F}(t, \mathbf{F}_0)$ is positive in the interval $[0, t'')$, and at least one component is 0 at t''. We first show that such components can not be S_i for any $i \geq 0$ and subsequently rule out I_i for all $i \geq 0$. Note that $u_j(t), I_j(t), S_j(t)$ are bounded in $[0, t'']$ (recall $\sum_{j=0}^{B} (S_j(t) + I_j(t)) = 1, S_j(t) \geq 0, I_j(t) \geq 0$ for all $j, t \in [0, t'']$). First, let $r \leq i \leq B$. From (3.2.2a), $S_i(t'') = S_i(0) e^{-\beta \int_0^{t''} \sum_{j=s}^{B} u_j(t) I_j(t)\, dt}$. Since all $u_j(t), I_j(t)$ are bounded in $[0, t'']$, and $S_i(0) > 0$, $\beta > 0$, therefore $S_i(t'') > 0$. From (3.2.2b), $S_i(t'') = S_i(0) > 0$ for $0 \leq i < r$. Thus, $S_i(t'') > 0$ for all i. Since $S_i(t) > 0$, $I_i(t) \geq 0$ for all $i, t \in [0, t'']$, from (3.2.2c) – (3.2.2e), $\dot{I}_i \geq -\beta u_i I_i \sum_{j=r}^{B} S_j$ for all $i \geq s$ in the interval $[0, t'']$. Thus, $I_i(t'') \geq I_i(0) e^{-\beta \int_0^{t''} u_i(t) \sum_{j=r}^{B} S_j(t)\, dt}$. Since all $u_j(t), I_j(t), S_j(t)$ are bounded in $[0, t'']$, and $I_i(0) > 0, \beta > 0$, it follows that $I_i(t'') > 0$ for all $i \geq s$. Finally, since $S_i(t) > 0, I_i(t) \geq 0$ for all $i, t \in [0, t'']$, from (3.2.2f), it follows that $\dot{I}_i \geq 0$ for all $i < s$, $t \in [0, t'']$. Thus, $I_i(t'') \geq I_i(0) > 0$ for all $i < s$. This contradicts the definition of t'' and in turn implies that $\mathbf{F}(t, \mathbf{F}_0) > 0$ for all $t \in [0, T]$, $\mathbf{F}_0 \in$ **Int** $\mathbb{S}$.

Since the control and the unique state solution $\mathbf{S}(t)$, $\mathbf{I}(t)$ are non-negative, (3.2.2a) implies that $\mathbf{S}(t)$ is a non-increasing function of time. Thus, $S_j(t) = 0$ if $S_j(0) = 0$ for any j. Using the argument in the above paragraph and starting from a $t' \in [0, T)$ where $S_j(t') > 0$, or $I_j(t') > 0$, it may be shown that $S_j(t) > 0$ or

$I_j(t) > 0$ respectively for all $t > t'$. □

The above proof allows for choices of T that depend on the controls $\mathbf{u}$, provided such controls result in finite T. For the problem to be non-trivial, we assume henceforth that there exist $i \geq r$, $j \geq s$ for which $S_i(0) > 0$ and $I_j(0) > 0$.

We finish this section with a technical lemma for later:

Lemma 10. For all $t \in (0, T)$ and all i, $|\dot{I}_i(t^+)|$ and $|\dot{I}_i(t^-)|$ exist and are bounded, as is $|\dot{I}_i(T^-)|$.

Proof. The states are admissible (Theorem 4) and continuous, and the controls are bounded by definition. Hence, due to (3.2.2), $|\dot{I}_i(t)|$ exists and is bounded at all points except the finite set of points of discontinuity of the controls, and continuous over intervals over which $\mathbf{u}$ is continuous. Thus, $|\dot{I}_i(t^+)|$ and$|\dot{I}_i(t^-)|$ exist and are bounded for all $t \in (0, T)$. With the same reasoning, $|\dot{I}_i(T^-)|$ also exists and is bounded. □

3.2.2 Throughput constraint and objective functions

The objective function of the network can represent both a measure of the efficacy of the policy in ensuring timely message delivery, and the effect of the policy on the residual energy reserves of the nodes. We first develop measures for each of these cases, and then utilize them to define an objective function and a constraint on the achieved network throughput.

Throughput constraint One plausible measure of QoS in the context of DTNs is the probability of delivery of the message to the destination before a terminal time T. We examine two cases: one in which a minimum probability of delivery is mandated on the message before a fixed terminal time T, and another in which the time-frame of message delivery is flexible and the goal is to meet the minimum probability of delivery requirement as soon as possible. In what follows, we discuss these two cases.

Let $\hat{\beta}_0$ be the rate of contact of a node with the destination, potentially different from $\hat{\beta}$, and define $\beta_0 := N\hat{\beta}_0$.

Following from the exponential distribution of the inter-contact times, the *mandated probability of delivery* constraint $\mathbb{P}(\text{delivery}) \geq p$ (i.e., the message being delivered to the destination with probability greater than or equal to p within $[0, T]$) implies that:

$1 - \exp\left(-\int_0^T \beta_0 \sum_{i=s}^{B} I_i(t)\, dt\right) \geq p$. [4]

Note that the exponential term in the LHS is the probability that no contact occurs between the destination and any infective with sufficient energy during the interval of $[0, T]$.

Also notice that similar to (3.2.1), $\hat{\beta}_0$ is inversely proportional to the roaming area, which itself scales with N. Another point to note is that the summation

[4] Because $P(\text{delivery}) = \mathbb{E}\{\mathbf{1}_{\sigma=t}\}$, where σ is the time the message reaches the destination. So, $P(\text{delivery}) = \int_0^T P(\sigma = t)\, dt = \int_0^T \exp(-\hat{\beta}_0 \int_0^t \sum_{i=s}^{B} N I_i(\xi)\, d\xi) \cdot \hat{\beta}_0 \sum_{i=s}^{B} N I_i(t)\, dt = 1 - \exp(-\int_0^T \beta_0 \sum_{i=s}^{B} I_i(t)\, dt)$. A special case of this was shown in [33, App. A] and [1, §II.A].

inside the integral starts from index s, since infective nodes with less than s units of energy cannot forward their message to the destination upon potential contact. This is equivalent to a throughput constraint:

$$\int_0^T \sum_{i=s}^{B} I_i(t)\, dt \geq -\ln(1-p)/\beta_0. \tag{3.2.6}$$

In the first case, referred to as the *fixed terminal time* problem, the terminal time T is fixed and the throughput constraint is satisfied (along with minimizing the adverse effects on the residual energy of the nodes which we will discuss next) through appropriate choice of control function $\mathbf{u}$, if any such functions exist. In the second case, referred to as the *optimal stopping time* problem, for every choice of the control function $\mathbf{u}$, the terminal time T is chosen to satisfy (3.2.6) with equality. The terminal time is therefore variable and depends on the choice of $\mathbf{u}$. Such a T exists for a given control $\mathbf{u}$ if and only if for the resulting states

$$\lim_{T' \to \infty} \int_0^{T'} \sum_{i=s}^{B} I_i(t)\, dt \geq -\ln(1-p)/\beta_0. \tag{3.2.7}$$

The throughput constraint will not be satisfied in any finite time horizon for controls that do not satisfy the above. We will therefore exclude such controls in the optimizations we formulate next. Note that if the system uses a zero-control (i.e., $\mathbf{u}(t) = (0, \ldots, 0)$ at all t) then $S_i(t) = S_i(0)$ and $I_i(t) = I_i(0)$ for all t; thus, since $\sum_{i=s}^{B} I_i(0) > 0$, (3.2.7) holds. Therefore, there exists at least one control that satisfies (3.2.7). Since T is finite for every control that satisfies (3.2.7), the system is admissible for each such control as well.

Energy cost of the policy In the simplest representation of the trade-off with the energy overhead, one can think of maximizing the aggregate remaining energy in the network at the terminal time, irrespective of how it is distributed. It is however desirable for the network to avoid creating nodes with critically low energy reserves. We capture the impact of a forwarding policy on the residual energy reserves of the nodes by penalizing the nodes that have lower energy levels. Specifically, denoting the terminal time as T, the overall penalty associated with the distribution of the residual energies of nodes at T, henceforth referred to as the *energy cost* of the policy, is captured by: $\sum_{i=0}^{B} a_i \left(S_i(T) + I_i(T)\right)$, in which, $\{a_i\}$ is a *decreasing* sequence in i, i.e., a higher penalty is associated with lower residual energies at T.

The trade-off can now be stated as follows: by using a more aggressive forwarding policy (i.e., higher $u_i(t)$'s and for longer durations), the message propagates faster and there is a greater chance of delivering the message to the destination in a timely manner. However, this will lead to lesser overall remaining energy in the nodes upon delivery of the message, and it will potentially push the energy reserves of some nodes to critically low levels, degrading the future performance of the network.

Overall Objective and Problem Statements We now state the two optimization problems for which we provide necessary structural results for optimal forwarding policies in §3.3.

Problem 1: Fixed Terminal Time Considering a fixed terminal time T, we seek to maximize the following utility:

$$R = -\sum_{i=0}^{B} a_i \left(S_i(T) + I_i(T)\right) \tag{3.2.8}$$

by dynamically selecting the vector $\mathbf{u}(t) = (u_s(t), \ldots, u_B(t))$ of piece-wise continuous controls subject to control constraints $0 \leq u_i(t) \leq 1$ for all $s \leq i \leq B$, $0 \leq t \leq T$ and throughput constraint (3.2.6). States $\mathbf{S}(t)$ and $\mathbf{I}(t)$ satisfy state dynamics (3.2.2) and positivity and normalization conditions (3.2.4).

Problem 2: Optimal Stopping Time We seek to minimize a combination of a penalty associated with the terminal time T (the time taken to satisfy the throughput constraint (3.2.6)) and one associated with the adverse effects on the residual energy of nodes through choice of the control $\mathbf{u}$. We represent the penalty associated with terminal time T as $f(T)$. We make the natural assumption that $f(T)$ is *increasing* in T. We further assume that $f(T)$ is differentiable (thus $f'(T) > 0$). Considering a variable terminal time T that is selected to satisfy (3.2.6) with equality, the system seeks to maximize:

$$R = -f(T) - \sum_{i=0}^{B} a_i(S_i(T) + I_i(T)) \tag{3.2.9}$$

by dynamically regulating the piecewise continuous set of controls $\mathbf{u}(t) = (u_s(t),$ $\ldots, u_B(t))$ subject to the control constraints $0 \leq u_i(t) \leq 1$ for all $s \leq i \leq B$, $0 \leq t \leq T$ and (3.2.7). As in Problem 1, states $\mathbf{S}(t)$ and $\mathbf{I}(t)$ satisfy state dynamics (3.2.2) and positivity and normalization conditions (3.2.4).

3.3 Optimal Forwarding Policies

We identify the structure of the optimal forwarding policies in §3.3.1 and prove them in §3.3.2 and $3.3.3 respectively. Our theorems apply to both the Fixed Terminal Time and Optimal Stopping Time problem statements.

3.3.1 Structure of the optimal controls

We establish that the optimal dynamic forwarding policies require the nodes to opportunistically forward the message to any node that they encounter until a threshold time that depends on their current remaining energy.[5] Once the threshold is passed, they cease forwarding the message until the time-to-live (TTL) of the message. In the language of control theory, we show that, excluding the optimal controls related to energy levels for which the fraction of infectives is zero throughout, all optimal controls are bang-bang with at most one jump from one to zero. In the excluded cases, optimal controls do not affect the evolution of states or objective values.

Theorem 5. Suppose the set $\mathcal{U}^*$ of optimal controls is not empty.[6] Then for all

[5] As an infective node transmits, its energy level sinks; the threshold of each infective node should therefore be measured with regards to the *residual* level of energy (and not, for example, the starting level).

[6] If $\mathcal{U}^*$ is non-empty, the problem is feasible, i.e., there exists at least one control for which the throughput constraint holds. But, even if the problem is feasible, $\mathcal{U}^*$ may be empty, albeit rarely.

optimal controls $\mathbf{u}$ in $\mathcal{U}^*$, and for all $s \leq i \leq B$ such that $I_i \not\equiv 0$, there exists a $t_i \in [0, T]$ such that $u_i(t) = 1$ for $0 < t < t_i$ and $u_i(t) = 0$ for $t_i < t \leq T$.[7] Moreover, under any optimal control, for all $s \leq i \leq B$, either $I_i(t) = 0$ for all $t \in [0, T]$ or $I_i(t) > 0$ for all $t \in (0, T]$.

Given any optimal control $\mathbf{u}$, we define a set $\mathcal{Z}(\mathbf{u})$ such that $\mathcal{Z}(\mathbf{u}) = \{i : s \leq i \leq B, I_i(t) > 0, \forall t \in (0, T]\}$. The above theorem implies that the population of the infectives is zero throughout for any index outside $\mathcal{Z}(\mathbf{u})$ (i.e., if $i \notin \mathcal{Z}(\mathbf{u}), I_i(t) = 0$ for all $t \in [0, T]$), and we therefore characterize the optimal control only for the indices that are in $\mathcal{Z}(\mathbf{u})$. Also, for each $i \in \mathcal{Z}(\mathbf{u})$, t_i is the threshold time associated with the optimal control u_i. Intuitively, we would expect each optimal control to be a non-increasing function of time, since if a control is increasing over an interval, flipping that part of the control in time would result in earlier propagation of the message and a higher throughput with the same final state energies. The theorem, however, goes beyond this intuition in that it establishes

For example, there may be an infinite sequence of optimal controls such that the objective values constitute a bounded increasing sequence of positive real numbers; such a sequence will have a limit but the limiting value may not be attained by any control.

[7] Since the optimal controls associated with energy levels for which the population of the infectives is zero throughout do not influence the evolution of states or the objective values, this theorem implies that unless $\mathcal{U}^*$ is empty, there exists an optimal control in $\mathcal{U}^*$ that will have the reverse-step function structure posited in the theorem for all $s \leq i \leq B$. Note that the irrelevance of optimal controls associated with energy levels with zero population of infectives implies that the optimal controls are not, in general, unique.

that optimal controls are at their maximum value up to certain threshold times and then drop abruptly to zero (Fig. 3.1-(a)). For the fixed terminal time problem, the optimal controls can therefore be represented as a vector of $B - s + 1$ threshold times corresponding to different energy levels. This vector can be calculated through an optimization in the search space of $[0, T]^{B-s+1}$. For the optimal stopping time problem, there is an additional degree of freedom; the stopping time T itself. Note that $T \in [0, T_0]$, where T_0 satisfies (3.2.6) with equality if all controls are always zero. This is because no optimal control can have $T > T_0$, as in that case both the energy cost and the penalty associated with terminal time will exceed that of the all-zero controls case. Thus, the optimal stopping time and the thresholds can be calculated through an optimization in the space of $\{(T, \underline{t}) : 0 \leq T \leq T_0,\ \underline{t} \in [0, T]^{B-s+1}\}$. The one-time calculation of the threshold levels (and the optimal stopping time as appropriate) at the origin can be done by estimating the fractions of nodes with each energy level irrespective of their identities. This data can then be added to the message as a small overhead. Therefore, optimal message forwarding has the following structure:

Intuitively, it appears that the threshold-times will be non-decreasing functions of the energy levels, since lower levels of residual energy are penalized more and the energy consumed in each transmission and reception is the same irrespective of the energy levels of the nodes. The optimal controls depicted in Fig. 3.1-(a) suggest the same: $t_2 < t_3 < t_4 < t_5$. We now confirm the above intuition in the

Algorithm 1 Source Node

1: **Given:** $\mathbf{I}_0 := (I_{00}, \ldots, I_{0B})$.

2: Estimate the distribution of energy among nodes.

3: Find the best set of thresholds $\{t_i\}$ (and optimal stopping time T in the optimal stopping time problem).

4: Append the header, which contains the destination, T, and $\{t_i\}$, to the message.

5: Create an initial distribution of messages such that for $j = 0, \ldots, B$, infectives of energy level j constitute a fraction I_{0j} of the whole population.

case that the terminal-time penalty sequence $\{a_i\}$ satisfies certain properties:

Theorem 6. Assume that the sequence $\{a_i\}$ in (3.2.8) is strictly convex.[8] Then, for any optimal control $\mathbf{u}$, the sequence $\{t_i\}$ for $i \in \mathcal{Z}(\mathbf{u})$ is non-decreasing in i.

Fig. 3.1-(a) illustrates the threshold times for a strictly convex and decreasing sequence of terminal penalties. The naive intuition provided before Theorem 6 will however mislead us in general — we now present examples that show when the strict convexity requirement of the terminal-time penalty sequence is not satisfied, the claim of the theorem may not hold. One sample configuration is when we have a sharp reduction in penalty between two consecutive final energy levels, with penalties on either side being close to each other, e.g.,

[8] A sequence $\{a_i\}$ is strictly convex (resp. strictly concave) if the difference between the penalties associated with consecutive energy levels increases (resp. decreases) with a decrease in energy levels, i.e., for each $2 \leq i \leq B$, $a_{i-1} - a_i < a_{i-2} - a_{i-1}$ (resp. $a_{i-1} - a_i > a_{i-2} - a_{i-1}$).

Algorithm 2 Infective Nodes

On receipt of the message, extract destination, thresholds $\{t_i\}$, and stopping time T from the header.
Measure own residual energy i.
while $i \geq s$ **and** $t \leq T$ **do**
    if node n encountered **then**
        query its state [low cost].
        if n = {destination} **then**
            if n has not received the message yet **then**
                transmit the message.
            end if
            exit.
        else if n = {S with energy $j \geq r$} **and** $t < t_i$ **then**
            forward message.
            $i \leftarrow (i - s)$.
        end if
    end if
end while

$a_0 \approx a_1 \approx a_2 \gg a_3 \approx a_4 \approx a_5$ in Fig. 3.1-(b). The motivation for such a setting could be the case where the system is primarily interested in ensuring that it retains a certain minimum amount of energy (e.g., 3 units in Fig. 3.1-(b)) at the terminal time: energy values above the requisite threshold (e.g., $4, 5$ in Fig. 3.1-(b)) acquire insignificant additional rewards and energy values below the threshold (e.g., $0, 1, 2$ in Fig. 3.1-(b)) incur insignificant additional penalties, but the penalty at the threshold amount is substantially lower than that at the next lowest value. Fig. 3.1-(b) reveals that Theorem 6 need not hold for such a setting, as nodes with energy values that are either higher or lower than 3 would be incentivized to propagate the message (because of the low loss incurred for propagation in terms of final states), but those with exactly 3 units of energy would be extremely conservative, as there is a large penalty associated with any further propagation of the message. Thus, $t_3 < \min(t_2, t_4, t_5)$. The sequence of terminal-time penalties in Fig. 3.1-(b) is neither convex nor concave. But, Theorem 6 does not hold for concave terminal-time penalties either (Table 3.1). Therefore, the convexity of the terminal-time penalty sequence is integral to the result of Theorem 6.

3.3.2 Proof of Theorem 5

We prove Theorem 5 using tools from classical optimal control theory, specifically Pontryagin's Maximum Principle (stated in §3.3.2). We provide the full proof for the fixed terminal time problem (3.2.8) in §3.3.2, and specify the modifications

	Threshold Times of Controls	
	Energy Level 4	Energy Level 5
$\alpha = 0.5$	5.75	1.75
$\alpha = 1.5$	2.5	2.75
$\alpha = 2$	2.5	2.75

Table 3.1: An example for non-ordered threshold times of the optimal controls for concave terminal time penalties in the settings of Theorem 6 for the fixed terminal time problem. The parameters were exactly the same as those used in Fig. 3.1-(a), with the difference that $a_i = (B-i)^\alpha$, α is varied over the values $\{0.5, 1.5, 2\}$, $\mathbf{I_0} = (0, 0, 0, 0, 0, 0.1)$ and $\mathbf{S_0} = (0, 0, 0, 0.3, 0.3, 0.3)$. For $\alpha = 0.5$, the terminal time penalties become concave, and $t_4 > t_5$. For $\alpha = \{1.5, 2\}$, the terminal time penalties are strictly convex, and $t_4 < t_5$ as Theorem 6 predicts.

for the optimal stopping time problem in §3.3.2.

Pontryagin's Maximum Principle with Terminal Constraint

We start by stating the problem for a fixed terminal time t_1. Let $\mathbf{u}^*$ be a piecewise continuous control solving:

$$\text{maximize} \int_{t_0}^{t_1} f_0(\mathbf{x}(t), \mathbf{u}(t), t) + S_1(\mathbf{x}(t_1)) \tag{3.3.1}$$

$$\dot{\mathbf{x}}(t) = f(\mathbf{x}(t), \mathbf{u}(t), t), \quad \mathbf{x}(t_0) = \mathbf{x}^0, \quad \mathbf{u} \in \mathcal{U},$$

$$x_i^1(t_1) = x_i^1 \qquad 1 \leq i \leq l,$$

$$x_i^1(t_1) \geq x_i^1 \qquad l+1 \leq i \leq m,$$

$$x_i^1(t_1) \text{ free} \qquad i = m+1 \leq i \leq n,$$

and let $\mathbf{x}^*(t)$ be the associated optimal path. Define

$$\mathcal{H}(\mathbf{x}(t),\mathbf{u}(t), \mathbf{p}(t), t) :=$$

$$p_0 f_0(\mathbf{x}(t), \mathbf{u}(t), t) + \mathbf{p}^T(t) f(\mathbf{x}(t), \mathbf{u}(t), t) \tag{3.3.2}$$

to be the Hamiltonian, with $\mathbf{p} = \{p_i\}_{i=1}^n$.

Theorem 7. [78, p.182] There exist a constant p_0 and a continuous and piecewise continuously differentiable vector function $\mathbf{p}(t) = (p_1(t), \ldots, p_n(t))$ such that for all $t \in [t_0, t_1]$,

$$(p_0, p_1(t), \ldots, p_n(t)) \neq \vec{0}, \tag{3.3.3}$$

$$\mathcal{H}(\mathbf{x}^*, \mathbf{u}^*, \mathbf{p}(t), t) \geq \mathcal{H}(\mathbf{x}^*, \mathbf{u}, \mathbf{p}(t), t) \qquad \forall \mathbf{u} \in \mathcal{U}. \tag{3.3.4}$$

Except at the points of discontinuities of $\mathbf{u}^*(t)$, for $i = 1, \ldots, n$: $\dot{p}_i(t) = -\dfrac{\partial \mathcal{H}(\mathbf{x}^*, \mathbf{u}^*, \mathbf{p}(t), t)}{\partial x_i}$.

Furthermore, $p_0 = 0$ or $p_0 = 1$, and, finally, the following transversality condi-

tions are satisfied,

$$\begin{aligned} p_i(t_1) \text{ no condition} \qquad & 1 \le i \le l, \\ p_i(t_1) - p_0 \frac{\partial S_1(\mathbf{x}^*(t_1))}{\partial x_i} \ge 0 \qquad & \\ (= 0 \text{ if } x_i^*(t_1) > x_i^1) \quad & l+1 \le i \le m, \\ p_i(t_1) - p_0 \frac{\partial S_1(\mathbf{x}^*(t_1))}{\partial x_i} = 0 \qquad & m+1 \le i \le n. \end{aligned} \tag{3.3.5}$$

Now, we state the analogous theorem when t_1 is not fixed in (3.3.1), and $S_1(\mathbf{x}(t_1))$ is replaced with $S_1(\mathbf{x}(t_1), t_1)$, allowing explicit dependence of the cost on the terminal time:

Theorem 8. [78, p.183] Let $(\mathbf{x}^*(t), \mathbf{u}^*(t), t_1^*)$ be an admissible triple solving (3.3.1) (with $S_1(\mathbf{x}(t_1), t_1)$) with $t_1 \in [T_1, T_2]$, $t_0 \le T_1 < T_2$, T_1, T_2 fixed. Then the conclusions in Theorem 7 hold, with $S_1(\mathbf{x}^*(t_1), t_1)$ replacing $S_1(\mathbf{x}^*(t_1))$. In addition:

$$\mathcal{H}(\mathbf{x}^*, \mathbf{u}^*, \mathbf{p}, t_1^*) + p_0 \frac{\partial S_1(\mathbf{x}^*(t_1), t_1)}{\partial t} \begin{cases} \le 0 & \text{if } t_1^* = T_1 \\ = 0 & \text{if } t_1^* \in (T_1, T_2) \\ \ge 0 & \text{if } t_1^* = T_2 \end{cases}. \tag{3.3.6}$$

Fixed Terminal Time Problem

For every control $\tilde{\mathbf{u}}$, we define $\tau_i(\mathbf{I}(0), \mathbf{S}(0), \tilde{\mathbf{u}}) \in [0, T]$ as follows: If $I_i(0) > 0$, and therefore $I_i(t) > 0$ for all $t > 0$ due to Theorem 4, we define $\tau_i(\mathbf{I}(0), \mathbf{S}(0), \tilde{\mathbf{u}})$ to be 0. Else, $\tau_i(\mathbf{I}(0), \mathbf{S}(0), \tilde{\mathbf{u}})$ is the maximum t for which $I_i(t) = 0$. It follows from

Theorem 4 that $I_i(t) = 0$ for all $t \leq \tau_i(\mathbf{I}(0), \mathbf{S}(0), \tilde{\mathbf{u}})$ and all i such that $I_i(0) = 0$, and $I_i(t) > 0$ for all $\tau_i(\mathbf{I}(0), \mathbf{S}(0), \tilde{\mathbf{u}}) < t \leq T$. We begin with the hypothesis that there exists at least one optimal control, say $\tilde{\mathbf{u}} \in \mathcal{U}^*$, and construct a control $\mathbf{u}$ that chooses $u_i(t) := 0$ for $t \leq \tau_i(\mathbf{I}(0), \mathbf{S}(0), \tilde{\mathbf{u}})$ and $u_i(t) := \tilde{u}_i(t)$ for $t > \tau_i(\mathbf{I}(0), \mathbf{S}(0), \tilde{\mathbf{u}})$. Clearly, the states $\mathbf{S}(t), \mathbf{I}(t)$ corresponding to $\tilde{\mathbf{u}}$ also constitute the state functions for $\mathbf{u}$, as the state equations only differ at $t = 0$, a set of measure zero. Thus, $\mathbf{u}$ is also an optimal control, and $\tau_i(\mathbf{I}(0), \mathbf{S}(0), \tilde{\mathbf{u}}) = \tau_i(\mathbf{I}(0), \mathbf{S}(0), \mathbf{u})$ for each i. Henceforth, for notational convenience, we will refer to $\tau_i(\mathbf{I}(0), \mathbf{S}(0), \tilde{\mathbf{u}}), \tau_i(\mathbf{I}(0), \mathbf{S}(0), \mathbf{u})$ as τ_i. Note that the definition of this control completely specifies the values of each u_i in $[0, \tau_i]$. We will prove the following lemmas.

Lemma 11. For each $s \leq i \leq B$, if $\tau_i < T$ there exists a $t_i \in [\tau_i, T]$ such that $u_i(t) = 1$ for $\tau_i < t < t_i$ and $u_i(t) = 0$ for $t > t_i$.

Lemma 12. For all $s \leq i \leq B$, $\tau_i \in \{0, T\}$.

If $\tau_i = 0$ for some $i \geq s$, $\tilde{u}_i(t) = u_i(t)$, and $I_i(t) > 0$, for all $t \in (0, T]$. If $\tau_i = T$, $I_i(t) = 0$ for all $t \in [0, T]$. So the theorem follows from these lemmas, which we prove next.

Proof of Lemma 11 The lemma clearly holds if $\mathbf{u} \equiv 0$ (with $t_i = \tau_i$ for all $i \geq s$); we therefore consider the case that $\mathbf{u} \not\equiv 0$.[9] We proceed in the following steps:

1) Applying standard results from optimal control theory, we show that each optimal control u_i assumes the maximum value (1) when a *switching function*

[9]Note that $\mathbf{u} \equiv 0$ in $(\tau_i, T]$ does not imply $\tau_i = T$.

(denoted φ_i) is positive and the minimum value (0) when the switching function is negative. However, standard optimal control results do not specify the nature of the optimal control when the corresponding switching function is at 0 or the durations for which the switching function is positive, zero, or negative. The next step answers these questions using specifics of the problem.

2) The switching functions turn out to be continuous functions of time. We want to show that for each $i \geq s$, there exists $t_i \in [\tau_i, T]$ such that the relevant switching function (φ_i) is positive for $t \in (\tau_i, t_i)$, negative for $t \in (t_i, T]$, and equal to zero at t_i only if $t_i \in (\tau_i, T)$. Lemma 11 now follows from the relation between the optimal control and the switching function obtained in the first step.[10]

Step 1 Consider the system in (3.2.2) and the objective function in (3.2.8). To make the analysis more tractable, we introduce the following new state variable: $\dot{E} := \sum_{i=s}^{B} I_i$, with $E(0) := 0$.

Therefore, our throughput constraint (3.2.6) simply becomes: $E(T) \geq -\ln(1-p)/\beta_0$.

To facilitate an appeal to Theorem 7, we take $\mathbf{x}^T = (E, \mathbf{S}^T, \mathbf{I}^T)$, $\mathbf{u} = \mathbf{u}$, $p_0 = \bar{\lambda}_0$, $\mathbf{p} = (\lambda_E, \boldsymbol{\lambda}, \boldsymbol{\rho})$, $l = 0$, $m = 1$, $x_1^1 = -\ln(1-p)/\beta_0$, $f_0 \equiv 0$, $t_0 = 0$, $t_1 = T$, and $S_1(\mathbf{x}^*(t_1)) = R$, the optimization objective. In this case, $\{f_i\}_{i=1}^{2N+3}$ are given by the $\dot{E}$ equation above and by (3.2.2).

[10] We still do not know the value of u_i at time t_i at which the corresponding switching function φ_i may be zero. This is not a serious deficiency as the value of the optimal control in a measure zero set does not affect state evolution.

Using these replacements, the Hamiltonian (3.3.2) becomes

$$\begin{aligned}\mathcal{H} =&\lambda_E \sum_{i=s}^{B} I_i - \sum_{i=r}^{B}[\beta\lambda_i S_i \sum_{j=s}^{B} u_j I_j] + \sum_{i=r}^{B}[\beta\rho_{i-r} S_i \sum_{j=s}^{B} u_j I_j] \\ &+ \sum_{i=s}^{B}[\beta u_i \rho_{i-s} I_i \sum_{j=r}^{B} S_j] - \sum_{i=s}^{B}[\beta u_i \rho_i I_i \sum_{j=r}^{B} S_j] \end{aligned} \tag{3.3.7}$$

where, at the points of continuity of the controls, the absolutely continuous co-state functions λ_i, ρ_i and λ_E satisfy

$$\begin{aligned}\dot{\lambda}_i &= -\frac{\partial \mathcal{H}}{\partial S_i} = \beta\lambda_i \sum_{j=s}^{B} u_j I_j - \beta\rho_{i-r} \sum_{j=s}^{B} u_j I_j \\ &\quad - \beta \sum_{j=s}^{B} u_j \rho_{j-s} I_j + \beta \sum_{j=s}^{B} u_j \rho_j I_j \qquad (r \le i \le B) \\ \dot{\lambda}_i &= -\frac{\partial \mathcal{H}}{\partial S_i} = 0 \qquad (i < r) \\ \dot{\rho}_i &= -\frac{\partial \mathcal{H}}{\partial I_i} = \beta u_i \sum_{j=r}^{B} \lambda_j S_j + \beta u_i \rho_i \sum_{j=r}^{B} S_j \\ &\quad - \lambda_E - \beta u_i \sum_{j=r}^{B} \rho_{j-r} S_j - \beta u_i \rho_{i-s} \sum_{j=r}^{B} S_j \quad (s \le i \le B) \\ \dot{\rho}_i &= -\frac{\partial \mathcal{H}}{\partial I_i} = 0 \qquad (i < s) \\ \dot{\lambda}_E &= -\frac{\partial \mathcal{H}}{\partial E} = 0 \end{aligned} \tag{3.3.8}$$

with the final constraints:

$$\begin{aligned} &\lambda_i(T) = -\bar{\lambda}_0 a_i, \quad \rho_i(T) = -\bar{\lambda}_0 a_i, \quad \forall i = 0, \ldots, B \\ &\lambda_E(T) \ge 0, \quad \lambda_E(T)\,[E(T) + \ln(1-p)/\beta_0] = 0, \end{aligned} \tag{3.3.9}$$

and $\bar{\lambda}_0 \in \{0, 1\}$.

We formally define the switching functions φ_i as follows:

$$\varphi_i := \frac{\partial \mathcal{H}}{\partial u_i} = \beta I_i \left[\sum_{j=r}^{B} \left(-\lambda_j + \rho_{j-r} + \rho_{i-s} - \rho_i \right) S_j \right],$$

$$(s \leq i \leq B). \tag{3.3.10}$$

Note that $\varphi_i(t)$ is continuous for $s \leq i \leq B$. From (3.3.7):

$$\mathcal{H} = \lambda_E \sum_{i=s}^{B} I_i + \sum_{i=s}^{B} \varphi_i u_i. \tag{3.3.11}$$

From Theorem 7, maximizing the Hamiltonian (3.3.4) yields

$$u_i(t) = \begin{cases} 1 \text{ for } \varphi_i(t) > 0 \\ \\ 0 \text{ for } \varphi_i(t) < 0. \end{cases} \tag{3.3.12}$$

Furthermore, $\varphi_i(t) u_i(t) \geq 0$ for each $s \leq i \leq B$ and all $t \in [0, T]$; otherwise the value of the Hamiltonian can be increased at t by choosing $u_i(t) = 0$.

Equations (3.3.10, 3.3.12) reveal an accessible intuition about the logic behind the decision process: at any given time, by choosing a non-zero u_i, infectives with energy level $i \geq s$ forward the message to susceptibles of any energy level $j \geq r$ and turn into infectives with $i - s$ energy units, with the susceptibles turning into infectives of energy level $j - r$. The optimal control determines whether such an action is *beneficial*, taking into account the advantages (positive terms) and disadvantages (negative terms).

Step 2 To establish this claim, we prove the following lemma:

Lemma 13. Let $\mathbf{u} \not\equiv 0$. For all $i \geq s$, if $\varphi_i(t') = 0$ for $t' \in (\tau_i, T)$, then $\varphi_i(t) < 0$ for all $t > t'$. Also, if $\varphi_i(T) = 0$, $\varphi_i(t) > 0$ for $t \in (\tau_i, T)$.

For $i \geq s$, we show that for $t \in (\tau_i, T)$ at which $\varphi_i(t) = 0$, $\dot{\varphi}_i(t^+) < 0$ and $\dot{\varphi}_i(t^-) < 0$.[11] Furthermore, we show that if $\varphi_i(T) = 0$, $\dot{\varphi}_i(T^-) < 0$. We state and prove a property of real-valued functions which we will use in proving Lemma 13.

Property 3. If $g(x)$ is a continuous and piecewise differentiable function over $[a, b]$ such that $g(a) = g(b)$ while $g(x) \neq g(a)$ for all x in (a, b), $\frac{dg}{dx}(a^+)$ and $\frac{dg}{dx}(b^-)$ cannot be negative simultaneously.

Proof. We denote the value of $g(a)$ and $g(b)$ by L. If $\frac{dg}{dx}(a^+) < 0$, there exists $\epsilon > 0$ such that $g(x) < L$ for all $x \in (a, a + \epsilon)$, and if $\frac{dg}{dx}(b^-) < 0$, there exists $\alpha > 0$ such that $g(x) > L$ for all $x \in (b - \alpha, b)$. Now $g(a + \frac{\epsilon}{2}) < L$ and $g(b - \frac{\alpha}{2}) > L$; thus, due to the continuity of $g(t)$, the intermediate value theorem states that there must exist a $y \in (a + \frac{\epsilon}{2}, b - \frac{\alpha}{2})$ such that $g(y) = L$. This contradicts $g(x) \neq g(a)$ for $x \in (a, b)$. The property follows. □

If $\varphi_i(t) = 0$ and $\dot{\varphi}_i(t^+) < 0$ for $t < T$, we have:

$$\varphi(t + \Delta t) = \varphi_i(t) + \int_t^{t+\Delta t} \dot{\varphi}_i(x)\,\mathrm{d}x = \int_t^{t+\Delta t} \dot{\varphi}_i(x)\,\mathrm{d}x,$$

which proves the existence of an interval $(t, t + \epsilon]$ over which φ_i is negative. If $t + \epsilon \geq T$, then the claim holds, otherwise there must exist a t', $t < t' \leq T$ such that $\varphi_i(t') = 0$ and $\varphi(\bar{t}) \neq 0$ for $t < \bar{t} < t'$ (from the continuity of $\varphi_i(t)$). Note that

[11] $x(a^+) = \lim_{t \downarrow a} x(t)$, $x(a^-) = \lim_{t \uparrow a} x(t)$.

because $\varphi_i(t') = 0$, we have $\dot{\varphi}_i(t'^-) < 0$. This contradicts Property 3, completing the proof of the first part of the lemma. For the second part, note that if $\varphi_i(T) = 0$ and $\dot{\varphi}_i(t^-) < 0$, there exists an interval $(T - \epsilon, T)$ over which φ_i is positive. If $T - \epsilon \leq \tau_i$, then the claim holds, otherwise there must exist a $t' \in (\tau_i, T)$ such that $\varphi_i(t') = 0$ and $\varphi(\bar{t}) \neq 0$ for $t' < \bar{t} < T$ (from the continuity of $\varphi_i(t)$). Note that because $\varphi_i(t') = 0$, as we show we have $\dot{\varphi}_i(t'^+) < 0$. This contradicts Property 3, completing the proof of the second part of the lemma.

We now seek to upper bound $\dot{\varphi}_i(t^+)$ and $\dot{\varphi}_i(t^-)$ for $t \in (\tau_i, T)$ at which $\varphi_i(t) = 0$, and subsequently prove that the upper bound is negative. For $t = T$, we only consider the left hand limit of the derivative. Keeping in mind that $I_i(t) > 0$ for $t > \tau_i$, at any $t > \tau_i$ at which $\mathbf{u}$ is continuous,

$$\dot{\varphi}_i = \frac{\dot{I}_i \varphi_i}{I_i} - \varphi_i \beta \sum_{j=s}^{B} u_j I_j + \beta I_i \sum_{j=r}^{B} (\dot{\rho}_{j-r} - \dot{\lambda}_j + \dot{\rho}_{i-s} - \dot{\rho}_i) S_j.$$

From the expressions for the time derivative of the co-states in (3.3.8) combined with the expression for the switching functions in (3.3.10), and using (from (3.3.7)) that $\sum_{j=r}^{B} -\dot{\lambda}_j(t) S_j(t) = \mathcal{H}(t) - \lambda_E(t) \sum_{j=s}^{B} I_j(t)$, we can write:

$$\begin{aligned}
\dot{\varphi}_i = {} & \beta I_i \left(\mathcal{H}(t) - \lambda_E \sum_{j=s}^{B} I_j - \lambda_E \sum_{j=r}^{B} S_j \right) \\
& + \dot{I}_i \frac{\varphi_i}{I_i} - \varphi_i \beta \sum_{j=s}^{B} u_j I_j + \varphi_i u_i \beta \sum_{j=r}^{B} S_j \\
& - \beta^2 I_i \sum_{j=r}^{B} S_j u_{j-r} \Big(\sum_{k=r}^{B} \left[-\lambda_k + \rho_{k-r} + \rho_{j-r-s} - \rho_{j-r} \right] S_k \Big) \\
& - \beta^2 I_i \Big(\sum_{j=r}^{B} S_j \Big) u_{i-s} \Big(\sum_{k=r}^{B} \left[-\lambda_k + \rho_{k-r} + \rho_{i-2s} - \rho_{i-s} \right] S_k \Big).
\end{aligned}$$

Now, consider a $t \in (\tau_i, T)$ at which $\varphi_i(t) = 0$. We show that the right and left-hand limits of all terms in the second line are zero at t:

From the continuity of I_i and since $t > \tau_i$, $I_i(t) > 0$. Thus $I_i(t')$ is positive and bounded away from 0 for t' in a neighborhood of t. Furthermore, Lemma 10 shows that $|\dot{I}_i(t^+)|$ and $|\dot{I}_i(t^-)|$ exist and are bounded for all $t \in (0, T)$. Thus, from the continuity of φ_i at t and since $\varphi_i(t) = 0$, $\dot{I}_i(t^+)\frac{\varphi_i(t^+)}{I_i(t^+)}$ and $\dot{I}_i(t^-)\frac{\varphi_i(t^-)}{I_i(t^-)}$ equal zero. Due to Theorem 4, since the states and controls are bounded and since $\varphi_i(t) = 0$, the right hand and left hand limits at t of the second and third terms in the second line are also zero. We now argue that the right hand and left hand limits of lines 3 and 4 are non-positive. Starting with line 3, this is because for $j \geq r$,

$$I_{j-r}\left(u_{j-r}\sum_{k=r}^{B}\left[\rho_{k-r} - \lambda_k + \rho_{j-r-s} - \rho_{j-r}\right]S_k\right) = \varphi_{j-r}u_{j-r}.$$

The right hand side is non-negative at each t, as argued after (3.3.12). For $t > \tau_{j-r}$, $I_{j-r}(t) > 0$. Thus for all such t,

$$(u_{j-r}\sum_{k=r}^{B}\left[\rho_{k-r} - \lambda_k + \rho_{j-r-s} - \rho_{j-r}\right]S_k) \geq 0. \tag{3.3.13}$$

For $0 < t \leq \tau_{j-r}$, $u_{j-r}(t) = 0$. Thus, at all $t > 0$, (3.3.13) holds.

Now, since $\mathbf{I}$, $\mathbf{S}$ are continuous and $\mathbf{u}$ has right and left hand limits at each t, the right and left hand limits of the LHS above exist; such limits are clearly non-negative at each t. The same arguments apply for line 4 as well (except that $i - s$ must be considered instead of $j - r$, with $i \geq s$). It follows that at any $t > \tau_i$

at which $\varphi_i(t) = 0$,

$$\dot{\varphi}_i(t^+) \leq \beta I_i(t^+)(\mathcal{H}(t^+) - \lambda_E[\sum_{j=s}^{B} I_j(t^+) + \sum_{j=r}^{B} S_j(t^+)]),$$
$$\dot{\varphi}_i(t^-) \leq \beta I_i(t^-)(\mathcal{H}(t^-) - \lambda_E[\sum_{j=s}^{B} I_j(t^-) + \sum_{j=r}^{B} S_j(t^-)].$$

Using the same arguments it may also be shown that the latter inequality holds at $t = T$ if $\varphi_i(T) = 0$.

The lemma now follows once we prove:

Lemma 14. If $\mathbf{u} \not\equiv 0$, then for all $t \in (0, T)$, we have:

$$\mathcal{H}(t^-) - \lambda_E(t^-) \left[\sum_{j=s}^{B} I_j(t^-) - \sum_{j=r}^{B} S_j(t^-) \right] < 0. \tag{3.3.14}$$
$$\mathcal{H}(t^+) - \lambda_E(t^+) \left[\sum_{j=s}^{B} I_j(t^+) - \sum_{j=r}^{B} S_j(t^+) \right] < 0. \tag{3.3.15}$$

Furthermore, (3.3.14) applies for $t = T$.

Proof. We only prove (3.3.14); the proof for (3.3.15) is exactly the same and therefore omitted for brevity. We first establish:

Lemma 15. If $\bar{\lambda}_0 = 1$, for each $j \geq s$ there exists a positive-length interval containing T in which u_j equals 0. In addition, irrespective of the value of $\bar{\lambda}_0$ and for all t,

$$\mathcal{H}(t^-) = \mathcal{H}(T) = \lambda_E(T) \sum_{k=s}^{B} I_k(T). \tag{3.3.16}$$

Proof. Since the system is *autonomous*[12], the Hamiltonian is continuous in time

[12]An autonomous optimal control problem is one whose dynamic differential equations and objective function do not explicitly vary with time t.

and $\mathcal{H}(t) = \mathcal{H}(T)$ for all $t \in [0, T]$ [78, p. 86 & p. 197]. We separately consider: $\bar{\lambda}_0 = 1$ and 0.

1) $\bar{\lambda}_0 = 1$**.** The first part of the lemma clearly holds for $j \geq s$ if $\tau_j = T$, since then $u_j(t) = 0$ for all $t \in [0, T]$. We now seek to establish the same in the case that $\tau_j < T$, and therefore $I_j(T) > 0$. At $t = T$, for $s \leq j \leq B$ we have:

$$\varphi_j(T) = \beta I_j(T) \bar{\lambda}_0 \sum_{k=r}^{B} \left(a_k - a_{k-r} - a_{j-s} + a_j\right) S_k(T). \tag{3.3.17}$$

Recall that a_k is decreasing in k. Hence, since $\mathbf{S}(0) \neq \mathbf{0}$, and so for at least one $k \geq r$, $S_k(T) > 0$ (from Theorem 4), for all $j \geq s$ we have $\varphi_j(T) < 0$. [13] Since φ_j is a continuous function, φ_j is negative in an interval of positive length including T. The first part of the lemma follows from (3.3.12).

Now, since $u_k(T) = 0$ for all $k \geq s$ from the first part of this lemma, (3.3.7) simplifies to (3.3.16).

2) $\bar{\lambda}_0 = 0$**.** Replacing $\bar{\lambda}_0 = 0$ in (3.3.17), it follows that $\varphi_j(T) = 0$ for all $j \geq s$; the expression for the Hamiltonian in (3.3.11) would thus lead again to (3.3.16). □

From (3.3.8), we have $\dot{\lambda}_E = 0$, except at the points of discontinuity of $\mathbf{u}$ – a countable set – leading to $\lambda_E(t) = \lambda_E(T)$ for all $t \in [0, T]$ due to the continuity of the co-states. Hence, from Lemma 15, the LHS in (3.3.14) becomes

$$\lambda_E(T) \left(\sum_{j=s}^{B} I_j(T) - \sum_{j=r}^{B} S_j(t^-) - \sum_{j=s}^{B} I_j(t^-) \right). \tag{3.3.18}$$

[13] Each term is negative as $a_{k-r} > a_k$, $a_{j-s} > a_j$ for $k \geq r$ and $j \geq s$.

The lemma follows from two subsequently established facts:

(A) $\lambda_E(T) > 0$,[14] and

(B) $\sum_{j=s}^{B} I_j(T) - \sum_{j=r}^{B} S_j(t^-) - \sum_{j=s}^{B} I_j(t^-) < 0$.

In order to establish (A), we rule out $\lambda_E(T) = 0$; it must therefore be positive by (3.3.9). We again consider two cases: (i) $\bar{\lambda}_0 = 0$ and (ii) $\bar{\lambda}_0 = 1$. (i) If $\bar{\lambda}_0 = 0$, $\lambda_E(T) = 0$ would lead to $(\bar{\lambda}_0, \vec{\lambda}(T), \vec{\rho}(T), \lambda_E(T)) = \vec{0}$, which contradicts (3.3.3). (ii) Otherwise (i.e., for $\bar{\lambda}_0 = 1$), let $\lambda_E(T) = 0$. Then, $\lambda_E(t) = 0$ for all $t \in [0, T]$. Thus, from (3.3.11), $\mathcal{H}(t) = \sum_{j=r}^{B} \varphi_j(t) u_j(t)$. Furthermore, since our system is autonomous and from Lemma 15, $\mathcal{H}(t) = \mathcal{H}(T) = 0$ for all $t \in [0, T]$. But, as argued after (3.3.12), $\varphi_j(t) u_j(t) \geq 0$, for all $t \in [0, T]$ and all $j \geq s$. Hence, we have $\varphi_j(t) u_j(t) = 0$ for all such t and j. From Lemma 15 and since $\mathbf{u} \not\equiv 0$, there exists $t' \in (0, T)$ such that $u_j(t) = 0$ for all $t \in (t', T]$ and all $j \geq s$ and for some $k \geq s$, there exists a non-zero value of u_k in every left neighborhood of t'. At any $t \in (t', T]$ at which $\mathbf{u}$ is continuous and from equations (3.3.8), $\dot{\rho}_j(t) = \dot{\lambda}_j(t) = 0$ for $0 \leq j \leq B$. Since $\mathbf{u}$ may be discontinuous only at a countable number of points and due to the continuity of the co-states, $\rho_j(t') = \rho_j(T) = \lambda_j(T) = \lambda_j(t') = -a_j$ for all $j \geq s$.

For $j \geq r$ and $k \geq s$, define $\Omega_{j,k}(t) := \lambda_j(t) - \rho_{j-r}(t) - \rho_{k-s}(t) + \rho_k(t)$. For all such j, k, we know that $\Omega_{j,k}(t') = (-a_j + a_{j-r} + a_{k-s} - a_k) > 0$. Hence, due to continuity

[14] In this part we show that $\lambda_E(T) > 0$ whenever $\mathbf{u} \not\equiv 0$. This combined with (3.3.9) leads to $E(T) = -ln(1-p)/\beta_0$. Therefore, the delivery probability of the optimal control at the given terminal time T equals the mandated probability of delivery except possibly when $\mathbf{u} \equiv 0$.

of the co-states, there exists $\epsilon > 0$ such that for all $t \in (t'-\epsilon, t')$ and all j, k, we have $\Omega_{j,k}(t) > 0$. But for all t, we had: $\mathcal{H}(t) = -\sum_{j=r}^{B} \left[\beta \sum_{k=s}^{B} \Omega_{j,k}(t) u_k(t) I_k(t)\right] S_j(t) = -\sum_{r \leq j \leq B: S_j(0)>0} \left[\beta \sum_{k=s}^{B} \Omega_{j,k}(t) u_k(t) I_k(t)\right] S_j(t)$.

The last equality follows since for each $j \geq 0$, $S_j(t) = 0$ at each $t \in (0, T]$ if $S_j(0) = 0$ (Theorem 4). Since $\mathbf{S}(0) \neq \mathbf{0}$ there exists $k \geq r$ such that $S_k(0) > 0$. We examine a point $\bar{t} \in (t' - \epsilon, t')$ for which $u_l(\bar{t}) > 0$ for some $l \geq s$. Since $\mathcal{H}(\bar{t}) = 0$, and every variable in the above summation is non-negative, $\Omega_{k,l}(\bar{t}) u_l(\bar{t}) I_l(\bar{t}) S_k(\bar{t}) = 0$. Since $u_l(\bar{t}) > 0$, $I_l(\bar{t}) > 0$ by definition of $\mathbf{u}$, and $\Omega_{k,l}(\bar{t}) > 0$, therefore $S_k(\bar{t}) = 0$. This contradicts $S_k(0) > 0$ (Theorem 4). Thus, (A) holds.

We now seek to establish (B). The proof follows from the key insight that it is not possible to convert all of the susceptibles to infectives in a finite time interval, and hence at the terminal time the total fraction of infectives with sufficient energy reserves for transmitting the message is less than the sum fraction of susceptibles and infectives with energy reserves greater than r, s respectively at any time before T. To prove this, note that for all $t \in [0, T]$, from (3.2.2) we have: $\sum_{j=s}^{B} \dot{I}_j + \sum_{j=r}^{B} \dot{S}_j = -\beta(\sum_{j=r}^{s+r-1} S_j \sum_{k=s}^{B} u_k I_k + \sum_{j=s}^{2s-1} u_j I_j \sum_{k=r}^{B} S_k) \leq 0$. Thus $(\sum_{j=s}^{B} I_j + \sum_{j=r}^{B} S_j)$ is a decreasing function of time, leading to $\sum_{j=s}^{B} I_j(T) - \sum_{j=s}^{B} I_j(t^-) - \sum_{j=r}^{B} S_j(t^-) \leq -\sum_{j=r}^{B} S_j(T)$. Now, since there exists $k \geq r$ such that $S_k(0) > 0$, there will exist $k \geq r$ such that $S_k(T) > 0$ (Theorem 4). Also, from the same theorem, we have $S_m(T) \geq 0$ for all m. Thus, $\sum_{j=r}^{B} S_j(T) > 0$. The result follows. □

Proof of Lemma 12 We start by creating another control $\bar{\mathbf{u}}$ from $\mathbf{u}$ such that for every $i \geq s$, for every $t \leq \tau_i$, $\bar{u}_i(t) := 1$, and for every $t > \tau_i$, $\bar{u}_i(t) := u_i(t)$. We prove by contradiction that $\tau_i(\mathbf{I}(0), \mathbf{S}(0), \bar{\mathbf{u}}) \in \{0, T\}$ for each $i \geq s$. Since $\bar{u}_i \not\equiv u_i$ only in $[0, \tau_i]$ and $I_i(t) = 0$ for $t \in (0, \tau_i]$ when $\mathbf{u}$ is used, the state equations can only differ at a solitary point $t = 0$, and therefore both controls result in the same state evolutions. Thus, for each $i \geq s$, $\tau_i(\mathbf{I}(0), \mathbf{S}(0), \bar{\mathbf{u}}) = \tau_i(\mathbf{I}(0), \mathbf{S}(0), \mathbf{u})$, and $\tau_i(\mathbf{I}(0), \mathbf{S}(0), \bar{\mathbf{u}})$ may be denoted as τ_i as well. The lemma therefore follows.

For the contradiction argument, assume that the control is $\bar{\mathbf{u}}$ and that $\tau_i \in (0, T)$ for some $i \geq s$. Our proof relies on the fact that if $\bar{u}_i(t') = 0$ at some $t' \in (0, T)$, then $\bar{u}_i(t) = 0$ for $t > t'$, which follows from Lemma 11 and the definition of $\bar{\mathbf{u}}$. We break the proof into three parts:

Case 1: $i > B - r$

Here, for $t \in [0, T]$ (3.2.2c) leads to: $I_i(t) = I_i(0) e^{-\beta \int_0^t \bar{u}_i(t'') \sum_{j=r}^{B} S_j(t'')\, dt''}$. Since $I_i(t) = 0$ for $t \in [0, \tau_i]$, $I_i(0) = 0$. Thus, $I_i(t) = 0$ for all $t \in [0, T]$. So $\tau_i = T$ which contradicts our assumption that $\tau_i \in (0, T)$.

Case 2: $B - s < i \leq B - r$

For $t \in [0, \tau_i]$, since $I_i(t) = 0$ for $t \leq \tau_i$, (3.2.2d) becomes:

$$\dot{I}_i = \beta S_{i+r} \sum_{j=s}^{B} \bar{u}_j I_j = 0$$

in this interval. Now, since all elements in $\beta S_{i+r} \sum_{j=s}^{B} \bar{u}_j I_j$ are non-negative, we must either have (i) $S_{i+r}(t) = 0$ for some $t \in [0, \tau_i]$, or (ii) for all $s \leq k \leq B$, $\bar{u}_k(t) I_k(t) = 0$ for all $t \in [0, \tau_i]$.

(i) In the first case, from two appeals to Theorem 4, $S_{i+r}(0) = 0$ and therefore $S_{i+r}(t) = 0$ for all $t \in [0, T]$. So in $[\tau_i, T]$, (3.2.2d) becomes $\dot{I}_i = -\beta \bar{u}_i I_i \sum_{j=r}^{B} S_j$, leading to

$$I_i(t) = I_i(\tau_i) e^{-\beta \int_{\tau_i}^{t} \bar{u}_i(t'') \sum_{j=r}^{B} S_j(t'')\, dt''}. \tag{3.3.19}$$

Since $I_i(\tau_i) = 0$, $I_i(t) = 0$ for all $t \in [\tau_i, T]$. Therefore $\tau_i = T$ which contradicts our assumption that $\tau_i \in (0, T)$.

(ii) In this case, from (3.2.2a) to (3.2.2f), it follows that for all $k \geq 0$, $\dot{I}_k = 0$ and $\dot{S}_k = 0$ in $[0, \tau_i]$, leading to $\mathbf{I}(t) = \mathbf{I}(0)$ and $\mathbf{S}(t) = \mathbf{S}(0)$ for $t \in [0, \tau_i]$. Also, since $I_k(t) > 0$ for all $t > \tau_k$, we know that for all $k \geq s$ such that $\tau_k < \tau_i$, $I_k(t) > 0$ for $t \in (\tau_k, \tau_i]$ and therefore $\bar{u}_k(t) = 0$ for $t \in (\tau_k, \tau_i]$. This leads to $\bar{u}_k(t) = 0$ for $t \geq \tau_i$ (since Lemma 11 and the definition of $\bar{\mathbf{u}}$ show that if $\bar{u}_k(t') = 0$ at some $t' \in (\tau_k, T)$, then $\bar{u}_k(t) = 0$ for $t > t'$). Especially notice that for all $k \geq s$ such that $I_k(0) > 0$, $\tau_k = 0$ and this would apply. Thus, for each k, either $I_k(0) = 0$ or $\bar{u}_k(t) = 0$ for all $t \geq \tau_i$, and hence $I_k(0)\bar{u}_k(t) = 0$ for all $t \geq \tau_i$. Looking at the interval $[\tau_i, T]$, we prove that $\mathbf{S} \equiv \mathbf{S}(0)$ and $\mathbf{I} \equiv \mathbf{I}(0)$ constitute solutions to the system of differential equations (3.2.2) in this interval. Replacing these functions and $\bar{\mathbf{u}}$ into the RHS of equations (3.2.2), all terms will be zero (since $I_k(0)\bar{u}_k(t) = 0$ for all $k \geq s$, $t \geq \tau_i$), leading to $\dot{I}_k = 0$ and $\dot{S}_k = 0$ for all $k \geq s$, which in turn leads to $(\mathbf{S}(t), \mathbf{I}(t)) = (\mathbf{S}(\tau_i), \mathbf{I}(\tau_i)) = (\mathbf{S}(0), \mathbf{I}(0))$ for all $t \in [\tau_i, T]$. Thus, $\mathbf{S} \equiv \mathbf{S}(0)$ and $\mathbf{I} \equiv \mathbf{I}(0)$ are the unique solutions to the system of differential equations (3.2.2) in $[0, T]$, wherein uniqueness follows from Theorem 4. So $\tau_k \in \{0, T\}$ for these state

solutions; a contradiction.

Case 3: $s \leq i \leq B - s$

We prove this case using induction on i. In the induction case, we will consider i such that $\tau_l \in \{0, T\}$ for all l such that $i < l \leq B$. From the arguments for the previous cases, we know that $i = B - s$ satisfies the above criterion and therefore constitutes our base case. We only present the proof for the induction case as that for the base case is identical. For $t \in [0, \tau_i]$, since $I_i(t) = 0$, (3.2.2e) becomes $\dot{I}_i = \beta S_{i+r} \sum_{j=s}^{B} \bar{u}_j I_j + \beta \bar{u}_{i+s} I_{i+s} \sum_{j=r}^{B} S_j = 0$. Now, since both of these terms are non-negative, each must be equal to zero in $[0, \tau_i]$. As there exists $k \geq r$ such that $S_k(0) > 0$, there will exist $k \geq r$ such that $S_k(t) > 0$ for all $t \in [0, \tau_i]$ (due to Theorem 4). Also from the same theorem, we have $S_m(t) \geq 0$ for all m. Thus, $\sum_{j=r}^{B} S_j(t) > 0$ for all $t \in [0, \tau_i]$, and hence the second term is zero contingent on $\bar{u}_{i+s}(t) I_{i+s}(t) = 0$ for all t in this interval. So we must either have (I) $S_{i+r}(t) = 0$ for some t and $\bar{u}_{i+s}(t) I_{i+s}(t) = 0$ for all t in this interval, or (II) for all $s \leq k \leq B$, $\bar{u}_k(t) I_k(t) = 0$ over this interval. Note that the condition on (II) is exactly the same as in (ii) of Case 2, and following the same argument it may be shown that $\tau_k \in \{0, T\}$ for each $k \geq s$ in this case. So we focus on (I):

In (I), again with two appeals to Theorem 4, we see that $S_{i+r}(0) = 0$ and therefore $S_{i+r}(t) = 0$ for all $t \in [0, T]$. Thus, for all $t \in [0, T]$, $\dot{I}_i = -\beta \bar{u}_i I_i \sum_{j=r}^{B} S_j + \beta \bar{u}_{i+s} I_{i+s} \sum_{j=r}^{B} S_j$. If $\tau_{i+s} < \tau_i$, $I_{i+s}(t) > 0$ for all $t \in (\tau_{i+s}, \tau_i]$ and therefore $\bar{u}_{i+s}(t) = 0$ for $t \in (\tau_{i+s}, \tau_i]$, leading to $\bar{u}_{i+s}(t) = 0$ for $t \geq \tau_i$. So again, we have

(3.3.19) and therefore $\tau_i = T$, a contradiction. If $\tau_{i+s} > \tau_i$, on the other hand, for $t \in [\tau_i, \tau_{i+s}]$, (3.2.2e) becomes $\dot{I}_i = -\beta \bar{u}_i I_i \sum_{j=r}^{B} S_j$, again leading to (3.3.19) and thus $I_i(t) = 0$ for all $t \in [\tau_i, \tau_{i+s}]$, a contradiction. Thus, we are left with $\tau_i = \tau_{i+s}$. But, since $i < i + s \leq B$, $\tau_{i+s} \in \{0, T\}$. Thus, $\tau_i \in \{0, T\}$, which contradicts our assumption that $0 < \tau_i < T$. This completes our proof.

Optimal Stopping Time Problem

Using Theorem 8 (with $S_1(\mathbf{x}^*(t_1), t_1) = R$), the proof differs from the fixed terminal time case only in the arguments used to establish $\bar{\lambda}_0 = 1$ and $\lambda_E > 0$ in the proof of Lemma 14 in Step 2. Note that we need separate arguments since the problem is no longer autonomous. Equation (3.3.3) along with $\bar{\lambda}_0 \geq 0$ leads to $\bar{\lambda}_0 = 1$, because $\bar{\lambda}_0 = 0$ would imply:

(i) $\lambda_i(T) = \rho_i(T) = 0, \quad \forall i = 0, \ldots, B$,

(ii) $\mathcal{H}(T) = \lambda_E(T) \sum_{i=s}^{B} I_i(T) = \bar{\lambda}_0 f'(T) = 0$. The first equality in (ii) comes from replacing $\lambda_i(T) = \rho_i(T) = 0$ for all i into (3.3.7), and the second from (3.3.6). Now, there exists a $j \geq s$ such that $I_j(0) > 0$, and due to Theorem 4, $I_j(T) > 0$, and $I_m(T) \geq 0$ for all m. Thus, $\sum_{i=s}^{B} I_i(T) > 0$, leading to $\lambda_E(T) = 0$. This, combined with $\bar{\lambda}_0 = 0$ and (i), contradicts (3.3.3) at $t = T$.

Thus, henceforth we consider $\bar{\lambda}_0 = 1$. As in Lemma 15, it can be shown that $u_i(T) = 0$ for all $i \geq s$. So we again have

$$H(T) = \lambda_E(T) \sum_{i=s}^{B} I_i(T),$$

and, from (3.3.6), $\bar{\lambda}_0 f'(T) = \lambda_E(T) \sum_{i=s}^{B} I_i(T)$. Since $f'(T) > 0$ and $\sum_{i=s}^{B} I_i(T) > 0$, $\lambda_E(T) > 0$. The rest of the proof is identical to that for the fixed terminal time case.

3.3.3 Proof of Theorem 6

We present the proof without explicitly mentioning which version of the optimal control problem (fixed terminal time or optimal stopping time) we are considering since the proof is identical. We will use Lemma 13, (3.3.10), (3.3.12), and the values of $\lambda_i(T), \rho_i(T)$ from (3.3.9) which hold for both versions.

We will prove this theorem for an optimal control $\mathbf{u}$ such that $u_i \equiv 0$ for all $i \notin \mathcal{Z}(\mathbf{u})$. It is sufficient to consider only such optimal controls because for any optimal control $\tilde{\mathbf{u}}$ we can construct a control $\mathbf{u}$ such that $u_i(t) := 0$ for $i \notin \mathcal{Z}(\tilde{\mathbf{u}})$ and $u_i := \tilde{u}_i$ for $i \in \mathcal{Z}(\tilde{\mathbf{u}})$. Since $\mathbf{u}$ leads to the same state evolutions as $\tilde{\mathbf{u}}$, $\mathbf{u}$ is optimal, $\mathcal{Z}(\tilde{\mathbf{u}}) = \mathcal{Z}(\mathbf{u})$, and both controls have identical threshold times for $i \in \mathcal{Z}(\tilde{\mathbf{u}}) = \mathcal{Z}(\mathbf{u})$. The theorem therefore follows for $\tilde{\mathbf{u}}$ if it is proven for $\mathbf{u}$.

The result clearly holds if $\mathbf{u} \equiv 0$ as then $t_i = t_j = 0$ for all $i, j \in \mathcal{Z}(\mathbf{u})$. We therefore assume that $\mathbf{u} \not\equiv 0$. It suffices to show that if $\varphi_i(t) = 0$ for some $t > 0$ and for $i \in \mathcal{Z}(\mathbf{u})$, we have $\varphi_k(t) \leq 0$ for any $k < i$ where we have $k \in \mathcal{Z}(\mathbf{u})$. From the definition of $\mathcal{Z}(\mathbf{u})$, $\tau_i = \tau_k = 0$. Then, from Lemma 13 and (3.3.12), the threshold time for u_k will precede that of u_i.

To prove the above, we examine two cases: (1) $\bar{\lambda}_0 = 0$ and (2) $\bar{\lambda}_0 = 1$. In case

(1), $\rho_i(T) = \lambda_i(T) = 0$ for all i, leading to $\varphi_i(T) = 0$ for all $i \geq s$ from (3.3.10). From Lemma 13, this means that $\varphi_i(t) > 0$ for all $0 < t < T$ and all $i \in \mathcal{Z}(\mathbf{u})$ (note that $\tau_i = 0$ if $i \in \mathcal{Z}(\mathbf{u})$). Therefore, from (3.3.12), $u_i(t) = 1$ for all $t \in (0, T)$; thus $t_i = T$ for all $i \in \mathcal{Z}(\mathbf{u})$. Thus, henceforth we focus on the case where $\bar{\lambda}_0 = 1$.

Consider an $i \in \mathcal{Z}(\mathbf{u})$ and a time $\sigma_i > 0$ such that $\varphi_i(\sigma_i) = 0$. From (3.3.10) we have: $\varphi_i(\sigma_i) = \beta I_i \left(\sum_{j=r}^{B} \left(-\lambda_j + \rho_{j-r} + \rho_{i-s} - \rho_i \right) S_j \right) \Big|_{t=\sigma_i} = 0$. Note that $I_i(\sigma_i) > 0$ (since $i \in \mathcal{Z}(\mathbf{u})$, $\sigma_i > 0$); thus, at $t = \sigma_i$, $\sum_{j=r}^{B} \left(-\lambda_j + \rho_{j-r} \right) S_j = -\sum_{j=r}^{B} \left(\rho_{i-s} - \rho_i \right) S_j$. Using the above and (3.3.10), it turns out that for all $k \in \mathcal{Z}(\mathbf{u})$, $\varphi_k(\sigma_i) = \beta I_k \psi_{i,k}(\sigma_i) \sum_{j=r}^{B} S_j$, where $\psi_{i,k}$, for $s \leq k < i$, is defined as: $\psi_{i,k}(\sigma_i) := -\rho_{i-s} + \rho_i + \rho_{k-s} - \rho_k$. We know that $\sum_{j=r}^{B} S_j(\sigma_i) \geq 0$, $I_k(\sigma_i) > 0$ (from Theorem 4). The theorem now follows from the following lemma:

Lemma 16. For any $k < i$ such that $i, k \in \mathcal{Z}(\mathbf{u})$ and for $\sigma_i > 0$ such that $\varphi_i(\sigma_i) = 0$, we have $\psi_{i,k}(\sigma_i) \leq 0$.

Proof. At $t = T$, following (3.3.9), we have: $\psi_{i,k}(T) = -\rho_{i-s}(T) + \rho_i(T) + \rho_{k-s}(T) - \rho_k(T) = [a_{i-s} - a_i - (a_{k-s} - a_k)]$, which due to the properties assumed for a_i (a_i decreasing and strictly convex in i), yields $\psi_{i,k}(T) < 0$. This also holds on a sub-interval of nonzero length that extends to $t = T$, owing to the continuity of $\psi_{i,k}$. We now prove the lemma by contradiction: going back in time from $t = T$ towards $t = \sigma_i$, suppose a $\psi_{i,k}$ becomes non-negative at time $\bar{\sigma} > \sigma_i$ for some

$k < i$, $k \in \mathcal{Z}(\mathbf{u})$. That is, for at least one such k we have:

$$\begin{aligned}(-\rho_{i-s} + \rho_i + \rho_{l-s} - \rho_l) < 0 \\ \forall l < i,\ l \in \mathcal{Z}(\mathbf{u})\ , \forall t\ \ \sigma_i < \bar{\sigma} < t \leq T;\end{aligned} \tag{3.3.20}$$

and at $t = \bar{\sigma}$,

$$\begin{cases}(-\rho_{i-s} + \rho_i + \rho_{k-s} - \rho_k) = 0 \\ (-\rho_{i-s} + \rho_i + \rho_{l-s} - \rho_l) \leq 0, \forall\ l < i, l \in \mathcal{Z}(\mathbf{u}).\end{cases} \tag{3.3.21}$$

We show that the time derivative of $\psi_{i,k}$ is non-negative over the points of continuity of the controls in the interval $[\bar{\sigma}, T]$. Note that this, plus the continuity of $\psi_{i,k}$, leads to a contradiction with the existence of $\bar{\sigma}$ and hence proves the lemma, since: $\psi_{i,k}(\bar{\sigma}) = \psi_{i,k}(T) - \int_{t=\bar{\sigma}}^{T} \dot{\psi}_{i,k}(\nu)\, d\nu \leq \psi_{i,k}(T) < 0$. We now investigate $\dot{\psi}_{i,k}$ over the points of continuity of the controls in $[\bar{\sigma}, T]$.[15] For $s \leq k < i < 2s$ such that $k \in \mathcal{Z}(\mathbf{u})$:

$$\dot{\psi}_{i,k} = -\frac{\varphi_i u_i}{I_i} + \frac{\varphi_k u_k}{I_k}, \tag{3.3.22}$$

and for $s \leq k < 2s \leq i$ such that $k \in \mathcal{Z}(\mathbf{u})$ it follows that:

$$\begin{aligned}\dot{\psi}_{i,k} =& \beta u_{i-s}(\sum_{m=r}^{B} \left[-\lambda_m + \rho_{m-r} + \rho_{i-2s} - \rho_{i-s}\right] S_m) \\ &+ \lambda_E - \frac{\varphi_i u_i}{I_i} + \frac{\varphi_k u_k}{I_k}.\end{aligned} \tag{3.3.23}$$

The RHS of (3.3.22-3.3.23) is non-negative because:

[15] Note that since $i, k \in \mathcal{Z}(\mathbf{u})$, $I_i(t) > 0$ and $I_k(t) > 0$ for all $t > 0$.

(A) $\frac{\varphi_k u_k}{I_k}$ is non-negative due to (3.3.12) for all $k \geq s$,

(B) $u_{i-s}(\sum_{m=r}^{B}[-\lambda_m + \rho_{m-r} + \rho_{i-2s} - \rho_{i-s}]\, S_m)$ is non-negative for $i \geq 2s$. To see this, note that for i such that $I_{i-s}(t) > 0$ for $t > 0$ this term is equal to $\frac{\varphi_{i-s} u_{i-s}}{I_{i-s}}$ which is non-negative, again as imposed by the optimizations in (3.3.12); else $(i-s) \notin \mathcal{Z}(\mathbf{u})$ and $u_{i-s} \equiv 0$;

(C) $\varphi_i(t) u_i(t) = 0$ for $t \geq \sigma_i$. To see this note that $\varphi_i(\sigma_i) = 0$. For $t > \sigma_i$, from Lemma 13, we have $\varphi_i(t) < 0$, which together with (3.3.12) leads to $u_i(t) = 0$,

(D) $\lambda_E = \lambda_E(T) > 0$, as established after (3.3.18) for the fixed terminal time problem and in §3.3.2 for the optimal stopping time problem.

For $i > k \geq 2s$ we have:

$$\begin{aligned}
\dot{\psi}_{i,k} &= \beta u_{i-s}(\sum_{m=r}^{B}[-\lambda_m + \rho_{m-r} + \rho_{i-2s} - \rho_{i-s}]\, S_m) \\
&\quad - \beta u_{k-s}(\sum_{m=r}^{B}[-\lambda_m + \rho_{m-r} + \rho_{k-2s} - \rho_{k-s}]\, S_m) \\
&\quad - \frac{\varphi_i u_i}{I_i} + \frac{\varphi_k u_k}{I_k} \\
&\geq -\beta u_{k-s}(\sum_{m=r}^{B}[-\lambda_m + \rho_{m-r} + \rho_{k-2s} - \rho_{k-s}]\, S_m). \qquad (3.3.24)
\end{aligned}$$

The above inequality follows from (A), (B), (C) above. Now we show that the RHS in the last line is zero over the interval of $[\bar{\sigma}, T]$, completing the argument. If $k - s \notin \mathcal{Z}(\mathbf{u})$, then $u_{k-s} \equiv 0$. Else, $I_{k-s}(t) > 0$ for all $t > 0$, and the RHS equals

$\frac{\varphi_{k-s}u_{k-s}}{I_{k-s}}$. We now show that $\varphi_{k-s}(t) \leq 0$ for all $t \in [\bar{\sigma}, T]$; thus (3.3.12) leads to $\varphi_{k-s}(t)u_{k-s}(t) = 0$, for all $t \in [\bar{\sigma}, T]$. The result follows.

From (3.3.10), we have:

$$\begin{cases} \varphi_i & = \beta I_i \left(\sum_{j=r}^{B} \left(-\lambda_j + \rho_{j-r} + \rho_{i-s} - \rho_i \right) S_j \right) \\ \varphi_{k-s} & = \beta I_{k-s} \left(\sum_{j=r}^{B} \left(-\lambda_j + \rho_{j-r} + \rho_{k-2s} - \rho_{k-s} \right) S_j \right) \end{cases}$$

Now, since $I_i(t) > 0$ for $t > 0$, $\varphi_i(t) \leq 0$ leads to:

$$\sum_{j=r}^{B} \left(-\lambda_j + \rho_{j-r} + \rho_{i-s} - \rho_i \right) S_j \leq 0.$$

From (3.3.20, 3.3.21) and for $k' = k - s < i$, we have $\rho_{k-2s} - \rho_{k-s} \leq \rho_{i-s} - \rho_i$ over the interval of $[\bar{\sigma}, T]$. Hence we now have: $\sum_{j=r}^{B} \left(-\lambda_j + \rho_{j-r} + \rho_{k-2s} - \rho_{k-s} \right) S_j \leq 0,$ which together with $I_{k-s}(t) \geq 0$ for $t > 0$ results in $\varphi_{k-s}(t) \leq 0$.

This concludes the lemma, and hence the theorem. □

3.4 Numerical Investigations

Numerous heuristic policies have been proposed for message passing in DTNs in prior literature [1, 7, 9, 19, 20, 60, 61, 67, 68, 82–84, 88, 90, 96]. Many of these heuristics are simpler to implement than our optimal control as they employ controls that either do not depend on residual energy levels or do not change with time. We start by experimentally validating the mean-field deterministic model we used (§3.4.1) and quantifying the benefit of our optimal policy relative to

some of these heuristics (§3.4.2). Next, we investigate the sensitivity of our optimal control to errors in clock synchronization and residual energy determination among nodes (§3.4.3). Finally, in §3.4.4, we investigate the sending of multiple messages over successive time intervals empirically, and assess the performance of a natural generalization of our policy (which is optimal for the transmission of a *single* message) relative to that of the mentioned heuristics.

We focus on the fixed terminal time problem and derive the optimal controls using the GPOPS software [12, 28–30, 73] with INTLAB [75]. Unless otherwise stated, our system used parameters: $B = 5$, $s = 2$, and $r = 1$ (note that $s \geq r$, as demanded by our system model), $\mathbf{S_0} = (0, 0, 0, 0.3, 0.3, 0.35)$, and $a_i = (B - i)^2$. Note that βT denotes the average number of contacts of each node in the system in the time interval $[0, T]$. Thus, as expected we observed that changing β and T had very similar effects on the costs and the drop-off points of the optimal controls. We further assumed that $\beta = \beta_0$ (i.e., the rate of contact between any two nodes is the same as the rate of contact of the destination and any given node). We compared policies based on the difference between $\sum_{i=s}^{B} a_i(S_i(T) + I_i(T))$ and $\sum_{i=s}^{B} a_i(S_i(0) + I_i(0))$ (which, as the initial penalty function value, is the same for all policies) for each policy, which we call the "Unbiased Energy Cost".

3.4.1 Validation of the mean-field deterministic model

We noted in §3.2.1 that assuming exponential contact among nodes leads to the system dynamics (3.2.2) (the mean-field deterministic regime) in the limit that the number of nodes, N, approach ∞. We therefore assess the applicability of (3.2.2) for exponential contact processes and large, but finite N (§3.4.1). Subsequently we assess the validity of (3.2.2) for a specific truncated power-law contact process that was experimentally observed for human mobility at INFOCOM 2005 [37] (§3.4.1). Under this model, nodes do not mix homogeneously, as those that have met in the past are more likely to meet in the future, and their convergence to ODEs like ours has not been established.

For each contact process, we simulated 100 runs of the evolution of the states with forwarding probabilities provided by the optimal control for the fixed terminal time problem and state equations (3.2.2). We compared the average state evolutions and unbiased energy costs of these cases with those obtained from (3.2.2) under the same control. We describe the results below.

Exponential Contact Process

For a system with $N = 160$ nodes, $\mathbf{I_0} = (0, 0, 0, 0.0125, 0.0125, 0.025)$, $\beta = 2$, and $T = 5$, leading to an average 10 meetings per node, Fig. 3.2 and Fig. 3.3 show that the results obtained from the simulation of the exponential contact process and (3.2.2) are similar, as expected.

Truncated Power Law Contact Process

We consider the truncated power-law contact process observed in [37] for a network with $N = 41$ nodes and $\alpha = 0.4$. The power-law process was truncated in that the contact times are restricted to be between 2 minutes and 24 hours. We use $\beta = 4.46$ in our differential equations (3.2.2) so that $1/\beta$ equals the expected inter-contact time between any pair of nodes under this distribution. Also, $\mathbf{I_0} = (0, 0, 0, 0, 0.025, 0.025)$. Even though N is small and the contact process is not memoryless, Fig. 3.4 shows that the states derived from this simulation and (3.2.2) follow the same trends, but there is a gap, which is to be expected because this contact model does not have the homogeneity of the exponential case, and the number of nodes is small ($N = 41$, since the experimental data in [37] was obtained for this N). Fig. 3.5 show that the costs in this model are, however, quite close to those derived from our equations, suggesting the robustness of energy cost to the change in contact process.

3.4.2 Performance advantage of optimal control over heuristics

Description of Heuristics

We propose two classes of heuristic policies, and describe sub-classes that correspond to policies in prior literature. In all classes and sub-classes, we define the *best* policy to be that which minimizes the unbiased energy cost subject to

satisfying the throughput constraint (3.2.6).

I- Static Across Energy Levels: Policies that choose a one jump (from a fixed value in $[0, 1]$ to zero) control that is the same for all energy levels. In these policies, nodes do not need to know their residual energy level. The best policy in this class is selected through a search over the range $[0, T] \times [0, 1]$, which is less than that of the optimal control ($[0, T]^{B-s+1}$).

II- Static Across Time: Policies that force all controls to be at a fixed value (potentially different for each energy level) throughout $[0, T]$. These policies are inherently robust to errors in clock synchronization, and the best policy in this class can be determined through a search over the range $[0, 1]^{B-s+1}$, which is similar to that of the optimal control.

Policies where controls depend on residual energy levels, e.g., those in (II), have not been proposed in existing literature. Several sub-classes of (I) have been proposed, however:[16]

1) Probability Threshold (*optimized flooding*): Policies whose controls drop from 1 to 0 when the probability of message delivery in $[0, T]$ passes a certain threshold (e.g., [90]).

2) Infection Threshold: Policies whose controls drop from 1 to 0 when the total number of infected nodes with enough energy to transfer the message to the destination surpasses a certain threshold (e.g., [67]).

[16]Sub-classes inherit constraints of classes from which they are descended.

3) Static Across Time and Energy Levels: Policies that force all energy levels to choose the same fixed control (between 0 and 1) throughout $[0, T]$ (e.g., [67]).

4) One Control (*flooding*, *epidemic routing*): The single policy that sets all controls to one. (Originally in [88], also in [20] and [90].)

5) Zero Control (*Spray and Wait*, *two-hop transmission*, *direct transmission*): The single policy that sets all controls to zero. (Originally in [84], also in [20] and [90].)

The best policy in the Probability and Infection Threshold classes can be determined through a search over $[0, T]$, and that in the Static Across Time and Energy Levels class through a search over $[0, 1]$. However, the Zero Control policy fails to attain the mandated probability of delivery in settings that we consider (small to moderate values of initial infection and T), and is thus excluded from Fig. 3.6 and 3.9 presented below.

Relative Performance

In Fig. 3.6, the costs associated with energy consumption for the optimal policy and also the best policies in each of the proposed classes are compared as β is varied. We use the name of the class/sub-class to refer to the best policy in that class/sub-class. The mandated probability of delivery is 90%, while $\mathbf{I_0} = (0, 0, 0.0125, 0.0125, 0.0125, 0.0125)$. As the number of contacts increases, forwarding the message at every available opportunity becomes less desirable as it

leads to massive energy consumption. The "One Control" policy, therefore, acts as a battery depletion attack on the nodes, using up all of their energy reserves and leading to significantly higher cost (over 30% worse than the second worst heuristic), and therefore it is left out of the figure for illustrative purposes. We see that the optimal policy significantly outperforms the best of the rest of the heuristic for low and moderate values of β (for $\beta \leq 2.5$), e.g., the performance difference is 50% for $\beta \approx 2$. We also see that the Static Across Energy Levels and Static in Time heuristics respectively outperform all other heuristics for low and high values of β. As contacts (βT) increase, the flexibility to adapt the control in accordance with the residual energy of the nodes provided by Static in Time turns out to be beneficial, as the mandated probability of delivery can be achieved by utilizing higher energy nodes. In fact, Static in Time performs close to the optimal for large values of β. In summary, the improvement in performance attained by the optimal control over simpler heuristics justifies its utilization of time-dependent and residual-energy-dependent decisions except for relatively large values of β where there is less need to spread the message due to more frequent meetings with the destination. In this case, near-optimal performance can be achieved by choosing controls based only on residual energy and not time, as is the case for Static in Time. Such choices may be used instead of the optimal policy for more robustness to clock synchronization errors, an issue we visit next.

3.4.3 Sensitivity of the optimal control to synchronization and residual energy determination errors

We will consider a system with $N = 500$ nodes, $\mathbf{I}_0 = (0, 0, 0, 0.0125, 0.0125, 0.025)$, $T = 5$, mandated probability of delivery 75% and $\beta = 2$ simulated over 200 runs.

Synchronization Errors

We allow each node to have a clock synchronization error that manifests itself as a time-shift in implementing the control decisions.[17] Thus, the optimal policy may incur a higher energy cost than the optimal value and provide a probability of delivery which is lower than the mandated value. We assess the extent of the deviations considering node time-shifts as mutually independent and uniformly distributed in $[-\theta^*, \theta^*]$; θ^* represents a measure of the magnitude of the synchronization errors. Fig. 3.7 reveals that the network's performance is remarkably robust in terms of both unbiased energy cost and probability of delivery (with maximum standard deviations of 0.5 for the unbiased energy cost and 0.03 for the probability of delivery) for θ^* up to 10% of the TTL T. This suggests that the optimal policy does not have a significant operational drawback compared to the Static In Time heuristics that incur substantially higher energy costs except for

[17] In other words, if a node has a time-shift of Δ, while implementing the optimal control it uses a threshold time of $t_i + \Delta$ instead of t_i when it has i units of residual energy.

large values of β.

Energy Determination Errors

Now we examine the case where each node is uncertain about its residual energy level, as may be the case for nodes with dated hardware. We assume each node under/over-estimates its residual energy level by one unit, each with probability p^*, independent of others. Specifically, if a node has i units of energy, where $0 < i < B$, it estimates its energy availability as $i-1$, i and $i+1$ with probabilities p^*, $1-2p^*$ and p^* respectively.[18] Fig. 3.8 reveals that the network's performance is robust to such errors in terms of probability of message delivery, though the unbiased energy cost incurred increases slightly with p^* (a change of less than 10% for $p^* < 0.15$). The maximum standard deviations of both cases are similar to their analogs from §3.4.3, confirming the previous observation. This suggests that the optimal policy does not suffer from any significant operational drawbacks as compared to the Static Across Energy Levels heuristics, which attain substantially higher energy costs.

3.4.4 Multiple Message Transmission

We now consider a scenario where the network seeks to successively transmit M messages, where M is a system parameter. Each message is associated with a

[18] If a node has B (respectively 0) units of energy, it estimates its energy to be $B-1$ and B (respectively 0 and 1) energy units with probabilities p^* and $1-p^*$ (respectively $1-p^*$ and p^*).

TTL of T and all nodes drop the message at the end of the TTL. The transmission of the i-th message starts at the end of the TTL of the $(i-1)$-th message. The transmission of each message must satisfy the throughput requirement (3.2.6).

We assume that at its initial time each message is uniformly spread to a fixed, say Υ, fraction of the nodes that have at least $s+r$ units of energy. Since each initial reception consumes r units of energy, the nodes that receive the initial copies of a message have enough (i.e., at least s units of) energy to subsequently forward the message after reception.[19] Once the network cannot guarantee the mandated probability of delivery for a message, we consider it to have been exhausted.

In these settings, we consider the natural generalization of our single transmission policies: the "Myopic Optimal" policy uses the one-step optimal for the transmission of each message, while others use the single-transmission best policy in their corresponding class (from §3.4.2). Our metric for comparing the performance of policies is the unbiased energy cost $\sum_{i=s}^{B} a_i \left(S_i(MT) + I_i(MT)\right) - \sum_{i=s}^{B} a_i(S_i(0) + I_i(0))$. We only consider the cost of messages that can be forwarded to the destination before network exhaustion.

We plot the performance of each policy for $\{a_i\}$ that are quadratic functions of $B-i$ (Fig. 3.9), though similar results are seen for linear and exponential

[19] Here, $r+s=3$. Thus, for example, if 50% of nodes have 4 units of energy and 80% of nodes have at least 3 units of energy at the beginning of transmission of a message, and $\Upsilon = 0.01$, then 1.25% of the nodes with 4 units of energy receive the initial copy of the message. So at the beginning of this transmission, $I_3 = 0.00625$ and $S_4 = 0.04375$.

functions of $B - i$ [21]. Here, $T = 100$, $\beta = 3, \Upsilon = 0.001$, and the mandated probability of delivery for each message is 95%. Also, before the initial copies of the first message are distributed, all nodes have at least 3 units of energy - 33%, 33%, and 34% of the nodes have 3, 4, and 5 units of energy respectively. We see that the Myopic Optimal policy outperforms all the other policies that we consider in terms of the unbiased energy cost for each fixed number of transmissions and also the number of messages transmitted till exhaustion. Note that as M increases, the difference between the unbiased energy costs of the Myopic Optimal policy and other policies becomes substantial, e.g., the difference is around 90% for around 10 transmissions. The number of messages forwarded to the destination till exhaustion by the Myopic Optimal policy is also slightly greater than that of the Static Across Time policy, and 60% better than the best of the rest.

3.5 Conclusion

We formulated the problem of energy-dependent message forwarding with (delay sensitive) throughput guarantees in energy-constrained DTNs as a resource-heterogeneous epidemic using a deterministic mean-field model. We analytically established that optimal forwarding decisions are composed of simple threshold-based policies, where the threshold used by a node depends only on its residual energy. We also proved that the thresholds are monotonic in the energy levels for a large class of cost functions associated with the energy consumed in transmis-

sion of the message. Our simulations reveal that the optimal control substantially outperforms state-of-the-art heuristic strategies and are reasonably robust to possible errors that may arise in implementation.

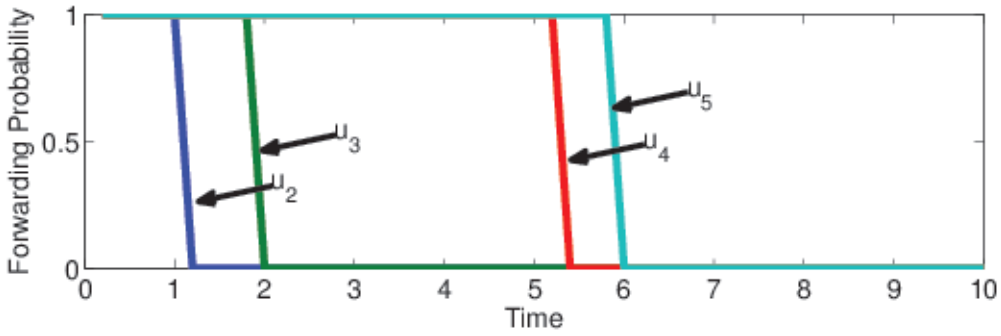

(a) convex terminal-time penalties

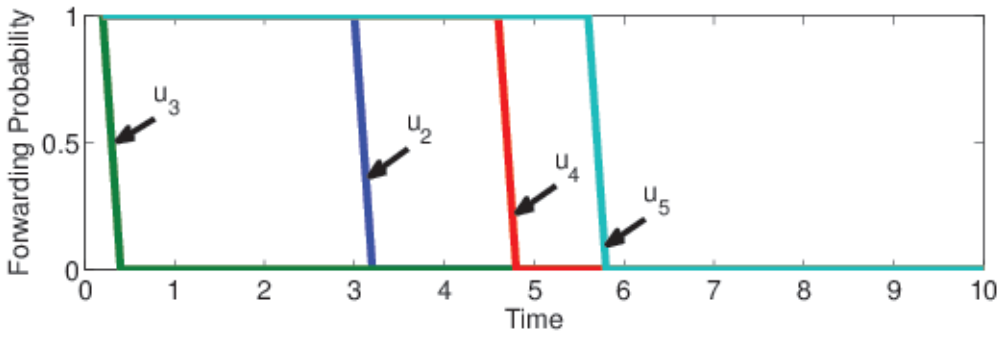

(b) non-convex terminal-time penalties

Figure 3.1: Illustrative examples for Theorems 5 and 6 for the fixed terminal time problem. The controls are plotted for a system with parameters: $B = 5$, $r = 1$, $s = 2$, $\beta = \beta_0 = 2$, $T = 10$, and $\mathbf{S_0} = (0, 0, 0, 0.55, 0.3, 0.1)$, with the mandated probability of delivery being 90%. In (a), the terminal time penalty sequence was $a_i = (B - i)^2$ and $\mathbf{I_0} = (0, 0, 0, 0, 0, 0.05)$, while in (b) the terminal time penalty sequence was $a_0 = 4.4$, $a_1 = 4.2$, $a_2 = 4$, $a_3 = 1.2$, $a_4 = 1.1$, $a_5 = 1$ (i.e., the $\{a_i\}$ sequence was neither convex nor concave) and $\mathbf{I_0} = (0, 0, 0, 0, 0.025, 0.025)$.

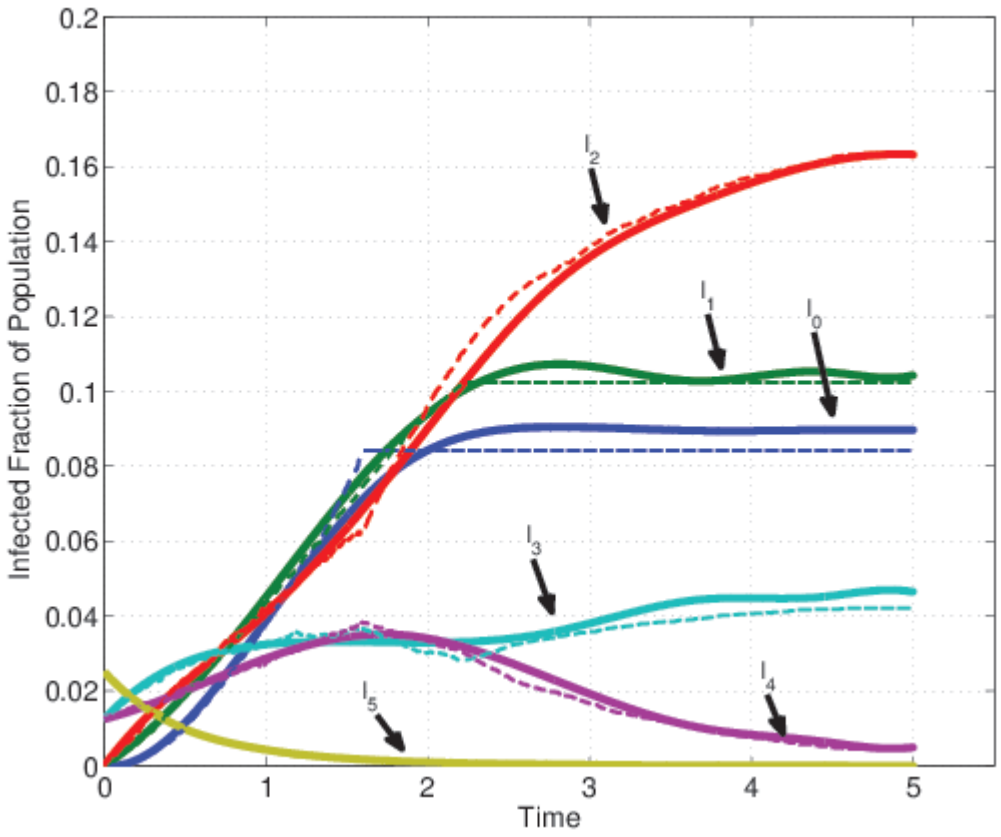

Figure 3.2: Comparison of the state processes for the mean-field deterministic regime (dashed lines) and simulated exponential contact process. We consider a mandated probability of delivery of 80%.

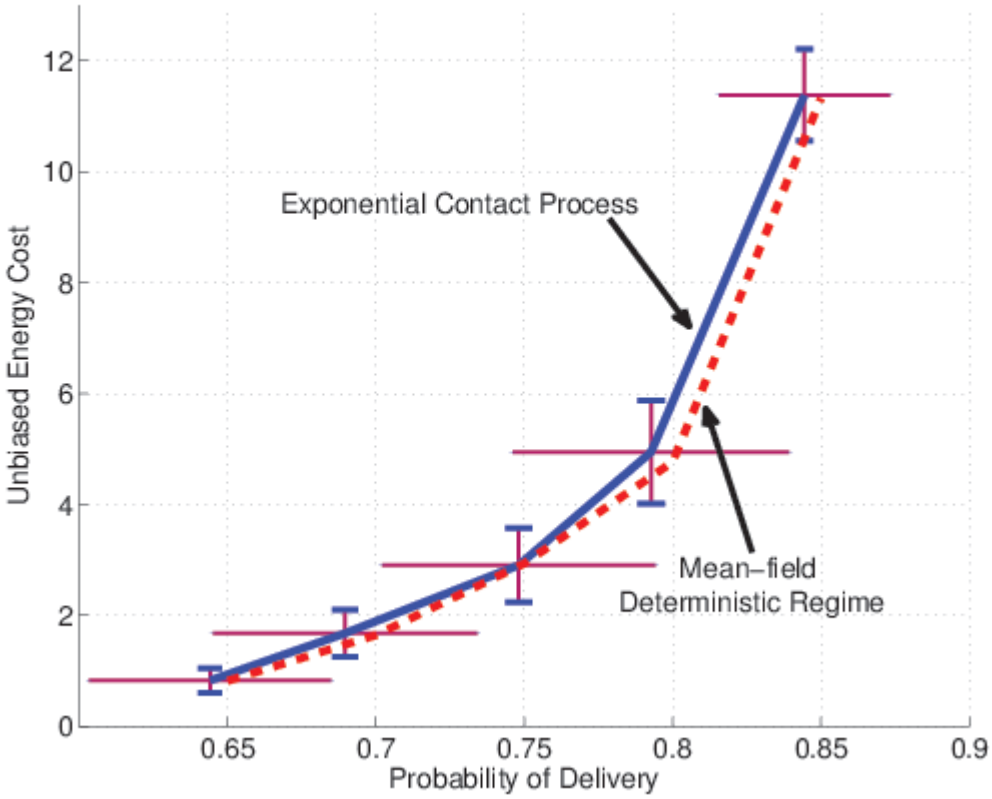

Figure 3.3: Comparing the costs of the mean-field deterministic regime (dashed line) and simulated exponential process as a function of the mandated probability of delivery. The error bars represent the standard deviations of the statistical simulations.

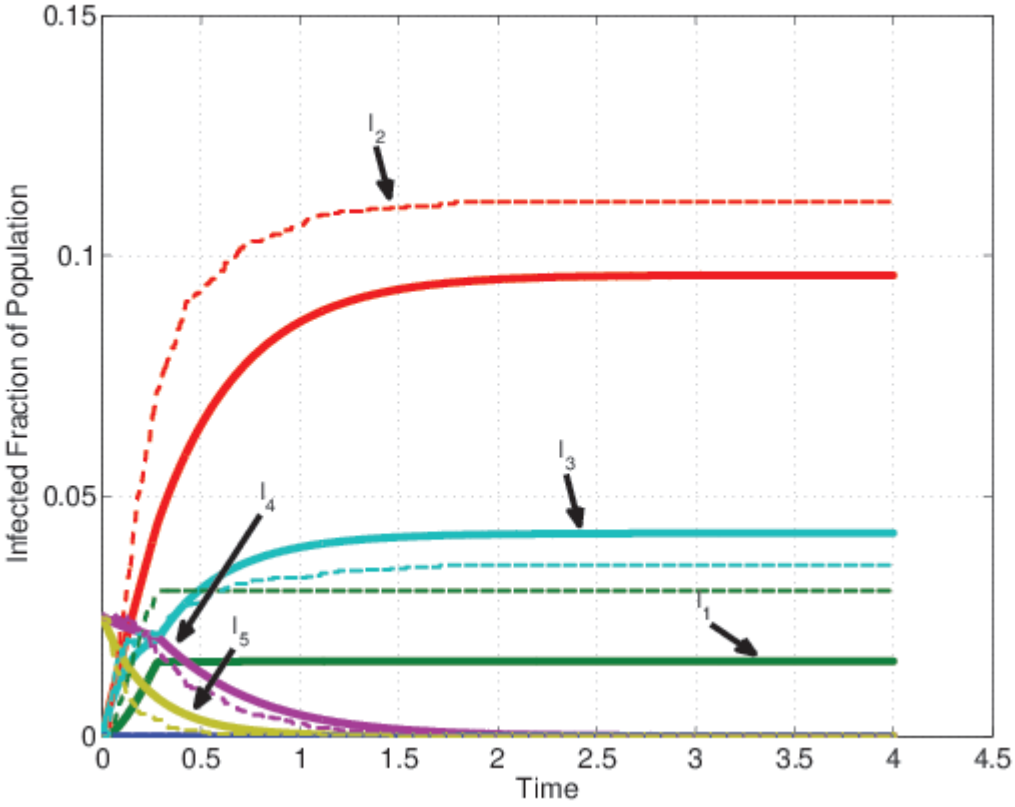

Figure 3.4: Comparison of the evolution of the infection in a mean-field deterministic regime (dashed lines) and the power-law contact process observed in [37]. We use a mandated probability of delivery of 90%.

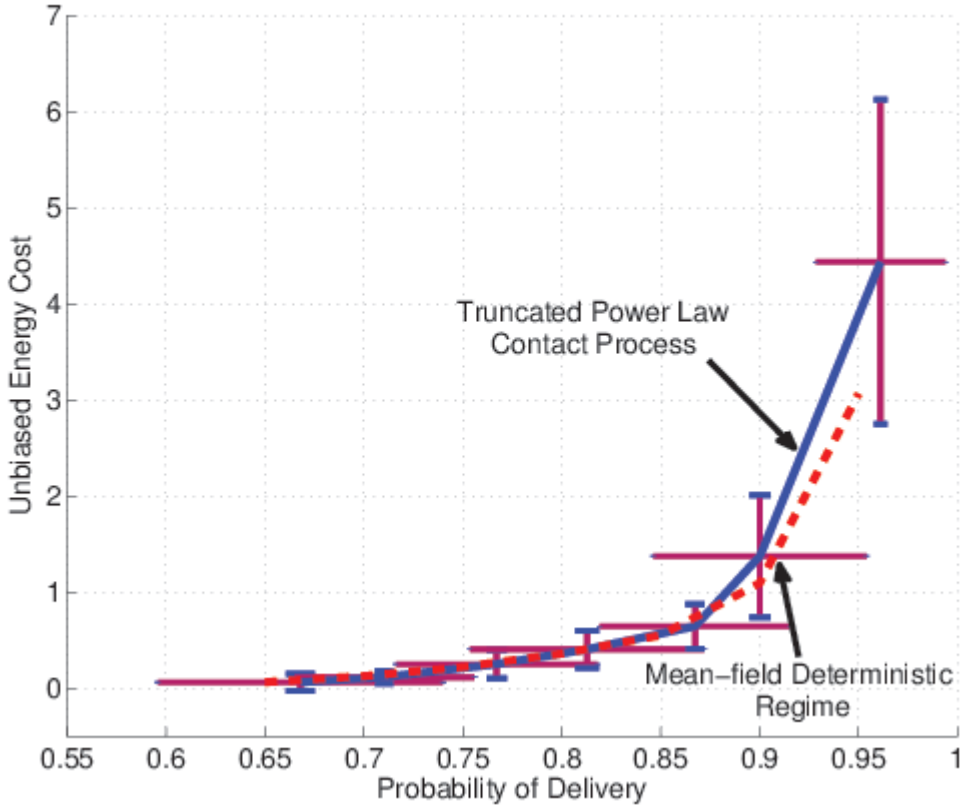

Figure 3.5: Comparing the costs of the mean-field deterministic regime (dashed line) and a simulated truncated power law contact process as a function of the mandated probability of delivery. The error bars represent the standard deviations of the statistical simulations.

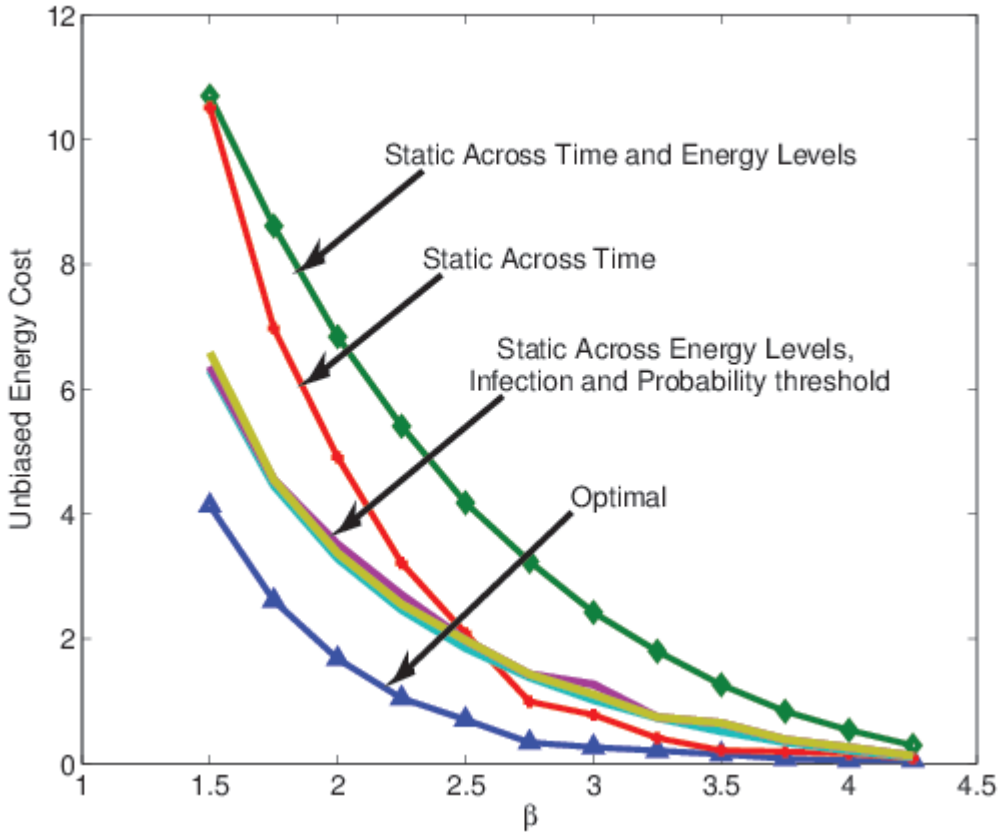

Figure 3.6: Performance of the optimal and heuristic controls. The performances of the "Static Across Energy Levels", "Infection Threshold", and "Probability Threshold" policies are very close, and they are indicated with a single arrow.

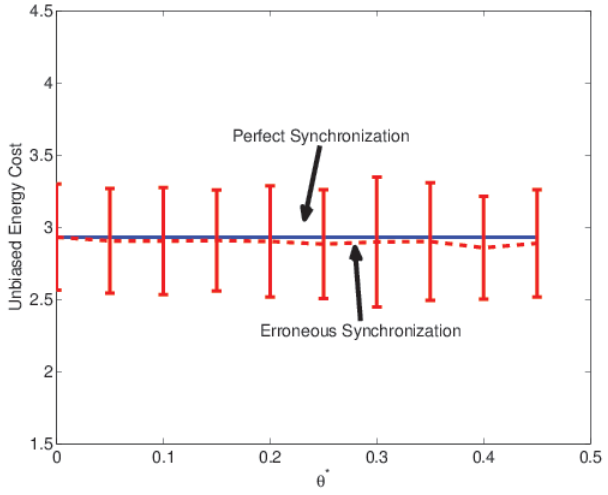

(a) Unbiased energy cost

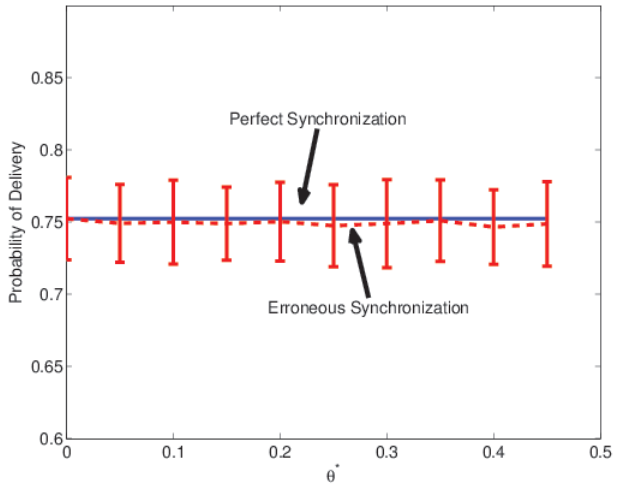

(b) Probability of delivery

Figure 3.7: Comparison of the performance of the optimal policy when we have perfect synchronization (solid line) and an implementation with synchronization errors, in terms of both unbiased energy cost and probability of message delivery. θ^* is the range of the synchronization error for each node, and the error bars represent standard deviations.

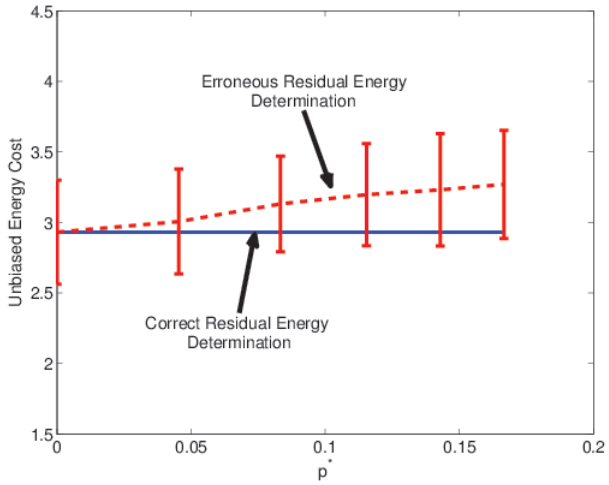

(a) Unbiased energy cost

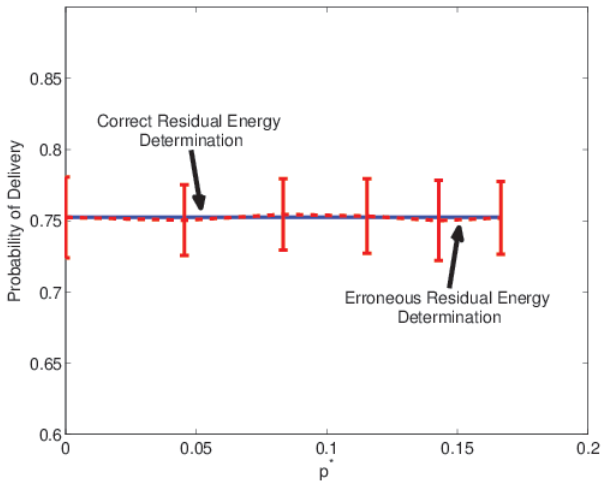

(b) Probability of delivery

Figure 3.8: Comparison of the performance of the optimal policy when nodes have correct knowledge of their residual energy (solid line) with cases where each node can makes a one unit error in determining its residual energy level (with probability p^*). Again, the error bars represent the standard deviations of each parameter.

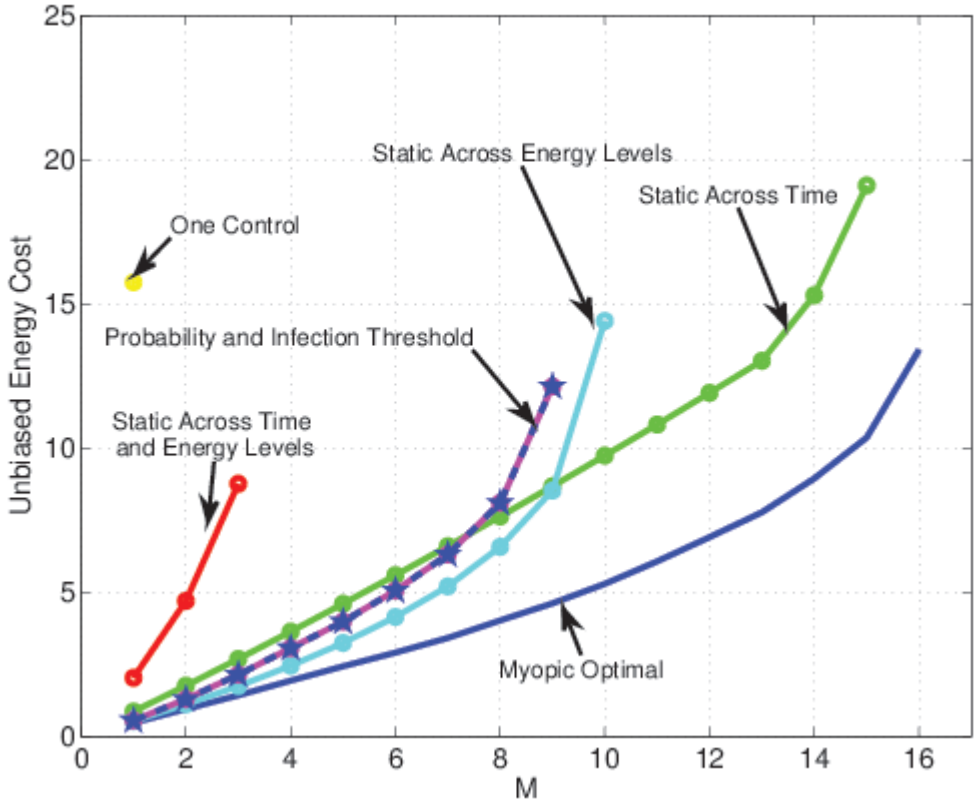

Figure 3.9: The figures plot the unbiased energy cost as a function of M, the number of messages transmitted, for different policies. The battery penalties were $a_i = (B - i)^2$.

Chapter 4

Epidemic-Heterogeneity: Visibility-Aware Optimal Contagion of Malware Epidemics[1]

4.1 Introduction

Epidemics that spread among a population may be *heterogeneous* themselves, with their interactions playing a critical role in their spread. Multiple epidemics spreading in one population can either compete with each other, amplify each other's effects/spread, or they may spread *in conjunction* with each other, where their relative spread is coordinated and controlled. This latter case arises uniquely

[1]Presented at Information Theory and Application Workshop (ITA) 2015 and submitted to IEEE Transactions on Automatic Control, July 2015 [23].

within the realm of malware. In this chapter, we examine how the heterogeneity of malware variants in terms of visibility to the network defender is being used by attackers in an emerging stealth-conscious generation of malware, and how this heterogeneity affects their particular spreading policies.

Malware (i.e., viruses, worms, trojans, etc.) has been a prominent feature of computer networks since the 1980's [66], and has evolved with the growing capabilities of computing technology. Anderson *et al.* [4] estimated that malware caused $370m of damage globally in 2010 alone. Traditionally, malware was designed with the express aim of infecting as many machines as possible, leading to the mass epidemics of the early 2000's (e.g., Blaster [6]). More recently, the focus has shifted to more "surgical" strikes where visibility is highly undesirable, as awareness can lead the intended target to cease communication (e.g., by quarantining the targets). The malware Regin was only discovered (in 2014) after operating since at least 2008, and was so complex that even when its presence was detected, it was not possible to ascertain what it was doing and what it was targeting [87]. Stuxnet, as another example, was designed to attack a specific control software used in centrifuges [25] and did not steal or manipulate data, or receive any command instructions from remote sources so as to maintain stealth [53]. Yet, it was discovered and remedied after it spread outside its target area [76] (cf. Duqu, Flame, and Gauss [11]). Thus there is a new trade-off for the attacker — to ensure maximum damage while minimizing visibility to the

defender.

We now describe different dimensions of this trade-off. Malware spreads from one computing device to another when there is a communication opportunity between the devices. In networks, both wired and wireless, inter-node communication can be visible to the network administrator, and can serve as a way of detecting the presence of malware before its function is fully understood. However, the attacker also has a conflicting onus to ensure the rapid propagation of her program, as computer systems evolve at a rapid pace, and the exploit(s) that the malware targets will be noticed and patched in due course. Furthermore, some malware designers work to specific deadlines — e.g., Stuxnet was due to become inoperational in June 2012 [95]. Thus, an attacker will seek to minimize her communication footprint while still trying to ensure the timely spread of the malware.

In particular, we consider the case where two variants of a single malware spread in a network. One spreads aggressively in every contact, and is thus visible to the network due to its communications, while the other, passive, variant does not spread subsequent to infecting a node. Coordinating distributed attacks comes at the cost of added visibility due to communication and is susceptible to timing errors in the hosts. Thus, we focus on the case where distributed nodes that are infected are not asked to coordinate, as was the case in Regin and Stuxnet. The natural question that arises is to characterize the structure of the optimal mal-

ware variant mix that the attacker will spread at each instant depending on their goal structures and the communication mechanisms that they may have at their disposal. This is an imperative first step to devising remedies for such attacks.

4.1.1 Problem Description

We consider a network under attack by these two variants of a malware. Depending on their infection status, nodes can be divided into 4 groups: Germinators (G), Susceptibles (S), Zombies (Z), and Passives (P). We now describe these states, as well as their dynamics and the impact of the attacker's control (as will be elucidated in §4.3.1). We also outline an augmentation to the model that is considered in §4.3.2 and adds a further possible mechanism of interaction and control to the dynamics:

1. *Germinators* (G):

    - are a *fixed* (potentially very small) fraction of nodes,
    - are the only nodes under the attacker's direct control,
    - are the only nodes that can *choose* how to interact with susceptibles and zombies depending on the goal of the attacker: at each encounter with a susceptible, they decide whether to turn it into a zombie or a passive, or to leave it as a susceptible.
    - damage the network by executing malicious code,

- are visible to the network due to their communications.
- in an augmentation in §4.3.2, we add a further mechanism of interaction (*halting*) whereby the germinators, upon contact with zombies, can turn them into passives (i.e., stopping them from spreading the message any further). This can potentially lead to the attacker initially utilizing epidemic spreading and then halting the spread once the marginal benefit of infection is overtaken by the marginal effect of visibility, leading to to a potentially longer propagation of the zombies.

2. *Susceptibles* (S):

- are nodes that have not received any variant of the malware,
- upon receipt of the malware from germinators, they can turn into zombies (Z) or passives (P).
- upon receipt of the malware from zombies, they will turn into zombies (Z).

3. *Zombies* (Z):

- have received the aggressive malware variant,
- damage the network by executing malicious code,
- will continue to propagate the aggressive variant indiscriminately (i.e., upon meeting a susceptible, will turn into a zombie),

- are visible to the network due to their communications.
- in the augmentation in §4.3.2, the additional mechanism of *halting* can turn zombies into passives.

4. *Passives* (P):

   - have received the passive variant of the malware,
   - damage the network by executing malicious code,
   - will *not* propagate the malware variant any further,
   - contrary to germinators and zombies, are *invisible* to the network as they do not communicate with other nodes to spread the malware henceforth.

These states and their properties are summarized in Table 4.1.

In these models, the attacker *controls* the mixture of zombie and passive malware variants through the germinators under its direct control. Whenever a germinator meets a susceptible, based on the control chosen by the attacker, it spreads either the zombie or passive variant of the malware to the susceptible, or leaves it as it is. In the dynamics in §4.4.3, the germinator has an additional controlled mechanism of action, whereby upon meeting a node with the zombie variant of the malware, it can replace the variant with the passive one (a "halting" mechanism). These controls are assumed to be *piecewise continuous*, but they can take any value between zero and one, which determines the percentage of rele-

State	Visibility	Growth over time	Propagation
S	N	Only decrease	-
G	Y	Fixed	Y
Z	Y	Increase or decrease	Y
P	N	Only increase	N

Table 4.1: The states of the SGZP model and their characteristics. "Visibility" denotes whether the infection state of the node is detectable by the network defender. "Growth over time" determines the possible changes in the fraction of nodes in each state over time (note that the only case in which zombies can decrease is the dynamics outlined in §4.4.3). Finally, "Propagation" determines whether a node in that state can spread the malware to a susceptible node upon contact.

vant interactions for which the specified action happens. We do not assume that all nodes make the same spreading decision at each time instance: the attacker can assign a certain uniformly distributed and possibly varying fraction of germinators to make the same decision at each time, or it could allow all agents to make one of the two decisions with a certain, possibly varying probability at each time. The outcome of both cases is that a certain uniformly distributed percentage of interactions (derived from the attacker's controls) lead to the creation of zombies and passives, and the rest have no effect on the potential target.

Later, we also investigate the effect of defense strategies on the optimal spread of malware variants (§4.3.3). In these defense strategies, the defender limits the effective contacts of nodes using a pre-determined function of malware visibility (which changes over time) as a means to limit the spread of malware. We consider two classes of network defense functions: affine and sigmoid. These defense strategies, however, come at the cost of stopping legitimate communication within the network. This is akin to choosing the communication ranges of nodes as a decreasing function of the visibility of the malware, which is a form of *quarantine*.

We allow the attacker to choose the malware spreading controls so as to maximize a measure of overall damage (described in §4.3.5). We first consider a damage function that depends on a) malware efficacy, which is a function of the aggregate number of zombies and passives, and b) malware visibility, which is a function of the number of zombies (for the models in §4.3.1 and §4.3.2). Then, we

consider a damage function where malware efficacy is the attacker's only direct concern, and is thus the damage function to be maximized, for the case where visibility is built into the network dynamics through a network defense policy which is a function of the fraction of zombies (as in the model in §4.3.3). These formulations, to the best of our knowledge, have no precedent in the epidemics literature, and can be used to further investigate the effects of malware visibility in networks.

An advantageous feature of all these models is that the malware designer only requires synchronized actions from a fixed number of nodes that are under its control from the outset. This decreases the risks of detection and policy implementation errors arising from coordinating synchronized distributed actions among a varying set of nodes.

4.1.2 Results

We then derive necessary structures for optimal solutions for each of the cases, using Pontryagin's Maximum Principle and custom arguments constructed for each case (in §4.4). We show that the attacker's optimal strategy in all of these models is for the germinators to spread only one variant of the epidemic at each time: the germinators will create zombies up to a certain threshold time, and then only create passives (including by halting zombies) from then on. That is, the optimal controls are *bang-bang* (i.e., only taking their minimal and maximum values) with

only one jump. Note that the controls can take any value between 0 and 1 at each point in time, and this bang-bang structure is one that emerges from the dynamics of the problem. These structural results are without precedent in the literature, both due to the uniqueness of the model, as well as the constraints placed on the *vector* of optimal controls.

It is interesting to note that in each of the variations we consider, our analysis reveals that all the controls in each model have the same threshold, a fact that is not at all clear *a priori*. Thus the entire control space can be described by one time threshold. This structure is invaluable for deriving the optimal controls computationally. Furthermore, the controls are easy to implement as the germinators need to be programmed with just one time instant for all of their controls.

Finally, we investigate the performance of the derived optimal controls using numerical simulations (in §4.5). We first investigate the effect of the additional halting action on the optimal attack policies. We show that for both the simple and halting models, as the rate of contact between zombies and susceptibles increases, zombies are created for a shorter time period. We also show that the halting control adds to the length of time the zombie variant should optimally be propagated, with the additional propagation time depending on some system parameters. We then compare the optimal control with heuristics, and show that even without the halting control, the optimal solution performs 10% better than the leading heuristic, with the performance differential being larger for more naive heuristics. We

then consider errors in the implementation of the network defense strategy outlined in §4.3.3, and investigate their effects on the malware spread. We show that erroneous estimations on the part of the defender only slightly affect the damage inflicted by the attacker, which points towards the robustness of the attack policies to errors in estimations by the network defense. Finally, we quantify the effect of synchronization errors among the relatively small number of germinators on the efficacy of the malware attack. We show that any such attack is robust to small errors among the germinators, sounding an alarm to the fact that these malware attacks are less vulnerable to implementation issues that may arise from synchronization errors than previous generations of malware.

4.2 Literature Review

Multiple interacting epidemics that spread among a single population have been considered in the fields of biology (e.g., multiple strains of a viral epidemic [40, 41]) and sociology (e.g., competition among memes in a world with limited attention span [91]). The *key* distinction between the control of biological epidemics [10, 36, 65, 92, 93] and that of malware ones is that in malware epidemics the *attacker* can also decide to *use her resources optimally* and to *adapt* to foresee the response of the defender. In the realm of sociology, the control of information epidemics offers closer parallels to that of malware. For example, Kandhway and Kuri [39] model how an erroneous rumor may be optimally stifled by the

spread of correct information, which is a secondary epidemic that interacts with the naturally occurring rumor epidemic. However, in this case *only one* of the epidemics can be controlled, while the malware attacker can possibly simultaneously control the spread of *all* malware variants. When there are multiple controllable epidemics, the resulting simultaneous controls are interdependent, and focusing on one control and characterizing its structure does not lead to a characterization of the optimal action. Thus, in malware epidemics there are *vectors* of controls available to the attacker, which requires new approaches and techniques compared to the other fields discussed.

Even within the majority of malware epidemic models, e.g., [27, 34, 48, 51, 62, 77, 98], the spread of *only one* malware has been examined, while we focus on the case where two variants are spreading in conjunction with each other. This presents a fundamentally different choice to the attacker, and so the model presented for the spread of visibility-heterogeneous malware variants has no precedent in literature. Accordingly, the questions we asked and the solutions we obtained are substantially different to prior work.

Nonetheless, we still distinguish other aspects of our work from those considering a single type of malware: in these papers: 1- it is assumed that the attacker's sole aim is to maximize the spread of the malware, which is no longer the case for the emerging class of surgical malware such as Regin [87] and Stuxnet [25] and 2- attackers have a mechanism to control the spread of the malware remotely in

the future, e.g., through a timer in the code which would be executed in infected machines (as in [22]). Any such code would have to interact with the operating system of the infected node, the configuration of which might not be known to the attacker, and can thus create a point of failure for the malware. The failure of such a mechanism of control was key to the overspread and subsequent remedy of Stuxnet [76].

Among the work on the control of a single-type/variant of malware (and the closely related literature on the spread of a message in Delay Tolerant Networks [**?**, 82] and the spread of a rumor [39]), the closest work to this topic (in terms of approach and spreading models) was by Khouzani and Sarkar [48]. They, however assume that the malware can control the transmission range of infected nodes[2] and *patching* is the major defense of the network and starts as soon as the epidemic spreads[3]. Thus, their models and their results apply to a fundamentally different class of malware.

Finally, the very strict structure we prove for the vector of malware optimal control, which restricts the search space for computational methods to a single

[2]We assume that the control affects the mix of malware variants and that the communication ranges of nodes are outside the malware's control, perhaps even being controlled by the defender as a mitigation mechanism. Thus, the control and the trade-off to the malware designer is fundamentally different.

[3]This may not be the case for an emerging stealthy epidemic like Stuxnet that is very large and extremely hard to decipher, let alone mitigate [15, 95]. In our model, the network only becomes aware of the malware as it becomes more visible (i.e., as the visible variant spreads).

parameter, is without precedent in any of the aforementioned literature.

4.3 System Model and Objective Formulation

In this section we model the spread of malware in a homogeneous network with random contacts. This can be the case where malware spreads among mobile devices with proximity-based communication, or where random contacts in an address-book are utilized. The virus propagates in the network between times 0 and T. We represent the fraction of *susceptible*, *germinator*, *zombie*, and *passive* nodes with S, G, Z, and P respectively, and assume that they are differentiable. We assume that for any pair of states, the statistics of meeting times between all pairs of nodes of those two states are identical and exponentially distributed, where the mean is equal to the *homogeneous mixing rate* of those two states. Groenevelt *et al.* [33] have shown that homogeneous mixing holds under the common Random Way-point and Random Direction mobility models (when the communication range of the fast-moving nodes is small compared to the total region). Note that the zombies can be programmed to only spread the malware at a fraction of the times they meet susceptibles, slowing their spread, or they can be programmed to use resources that are not utilized by the rest of the network to spread faster. Therefore we take the mixing rate between Z and S to be potentially different from the other pairs of states.

We describe the state dynamics of such systems as an epidemic for the cases

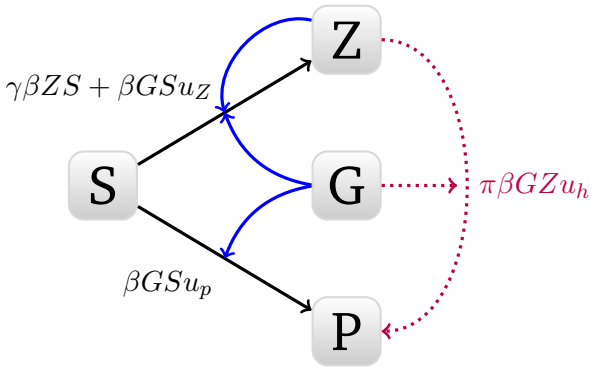

Figure 4.1: The solid lines show the dynamics in §4.3.1. The dotted lines show the additional halting action in §4.3.2. The model in §4.3.3 has the same dynamics as the solid lines, but with β being a function of Z (i.e., $\beta(Z)$).

where: 1) germinator agents can only interact with susceptible agents (§4.3.1), 2) germinator agents can also interact with zombies as well (§4.3.2), and 3) effective network contact rates are a function of the infection spread, mirroring the response of a network defender (§4.3.3) (Figure 4.1). We state and prove a key observation about all these dynamics (§4.3.4). We next formulate the aggregate damage of attack efficacy and the ensuing visibility (§4.3.5). Finally, we lay out the optimization problem in §4.3.6.

4.3.1 SGZP Model with no halting

The attacker can spread the malware in two ways: 1- upon encountering a susceptible, she can, through the control variable u_Z, turn that susceptible node into a zombie, i.e., one that will henceforth propagate that infection to susceptibles it

meets. 2- upon encountering a susceptible, she can, through the control variable u_P, turn that susceptible into a *Passive*, P. These control variables — $(u_Z, u_P) \in \mathcal{U}$, where $\mathcal{U}$ is the set of piecewise continuous controls — can be thought of as the respective probabilities of infection, and to maintain such an intuition, we constrain their sum to be less than one.[4]

$$\dot{S} = -\beta GS(u_P + u_Z) - \gamma\beta ZS \tag{4.3.1a}$$

$$\dot{Z} = \beta GSu_Z + \gamma\beta ZS \tag{4.3.1b}$$

$$\dot{P} = \beta GSu_P \tag{4.3.1c}$$

$$u_P + u_Z \leq 1 \tag{4.3.2a}$$

$$0 \leq u_P \leq 1 \;\; 0 \leq u_Z \leq 1 \tag{4.3.2b}$$

Here, β is the mixing rate between S and G, and $\gamma\beta$ is the mixing rate between Z and S (with $\gamma > 0$).

[4]Our models are based on results that show in the population (mean-field) limit and where state transitions occur according to a Poisson contact process, the fractions of agents in each state converges path-wise (with probability of path-divergence divergence going to zero) to the results of the deterministic ordinary differential equation derived from the dynamics on any limited time period (c.f. [52, p.1], [32]).

4.3.2 SGZP Model with halting

This model is akin to the previous one, with one more mechanism added: germinator nodes (G) can force a zombie (Z) to become passive (P) through a process we will call "halting". This happens through another control variable u_h, which, in keeping with the intuition, can be thought of as the probability of halting encountered zombies at each instant. Again, we take $(u_Z, u_P, u_h) \in \mathcal{U}'$, where $\mathcal{U}'$ is the set of piecewise continuous controls. The system dynamics become:

$$\dot{S} = -\beta GS(u_P + u_Z) - \gamma\beta ZS \tag{4.3.3a}$$

$$\dot{Z} = \beta GSu_Z + \gamma\beta ZS - \pi\beta GZu_h \tag{4.3.3b}$$

$$\dot{P} = \beta GSu_P + \pi\beta GZu_h, \tag{4.3.3c}$$

with $0 < \pi \leq 1$ signifying the extent to which the zombies can be stopped when encountered by the original germinators. This model is similar to the Daley-Kendall rumor model [18], where repeated interaction with active agents can turn an active spreader of the rumor into an agent that is aware of the rumor, but has no interest in spreading it any further. The constraints now become:

$$u_P + u_Z \leq 1 \tag{4.3.4a}$$

$$0 \leq u_P \leq 1,\ 0 \leq u_Z \leq 1,\ 0 \leq u_h \leq 1. \tag{4.3.4b}$$

4.3.3 SGZP Model with no halting and adaptive defense

Instead of allowing a constant rate of interactions β, the network defender can choose the effective mixing rate β to be a function of the fraction of zombies as her defense policy ($\beta(Z)$). In these policies, the network defender regulates the rate of contact between nodes based on the proportion of zombie nodes it has observed. The network can determine the fraction of the network that has been infected by zombies by observing the chatter among nodes and the extra communications whose purpose is unknown, either in the whole network or among a representative subset of nodes.

We consider the system dynamics described in the no-halting model, and adapt them accordingly:

$$\dot{S} = -\beta(Z)GS(u_P + u_Z) - \gamma\beta(Z)ZS \tag{4.3.5a}$$

$$\dot{Z} = \beta(Z)GSu_Z + \gamma\beta(Z)ZS \tag{4.3.5b}$$

$$\dot{P} = \beta(Z)GSu_P \tag{4.3.5c}$$

The controls available are also the same as those in (4.3.2). In particular, they are still assumed to be piecewise continuity.

We consider two classes of $\beta(Z)$ functions: 1) Affine functions, of the form $\beta(Z) = -aZ + \beta_{max}$ for $0 \leq a \leq \beta_{max}$ (a natural assumption, as the contact rate cannot be negative). If $a = 0$, the affine case simplifies to the constant β case. 2) Exponential sigmoids, of the form $\beta_Z = \frac{\beta_0}{1 + e^{\alpha(Z - Z_{th})}}$, with $0 < Z_{th} < 1$ being a

fixed threshold and $\alpha > 0$ denoting the sharpness of the cut-off. As α increases, $\beta(Z)$ can become arbitrarily close to $\beta(Z) = \beta_0 \mathbf{1}_{Z \leq Z_{th}}$, an all-or-nothing policy. Both of these classes satisfy $\beta(Z) > 0$ for all Z (i.e., the network never shuts down completely due to the infection) and $\frac{d\beta(Z)}{dZ} < 0$ for all Z (except for the trivial case of constant $\beta(Z)$), as more visibility should lead to more communication restrictions from the network. In mobile epidemics, this is equivalent to nodes decreasing their communication range upon the detection of an infection, e.g. as in [49]. In practice, the network will have an estimate $\hat{Z}$ of the fraction of zombies. Our simulations reveal that the sub-optimality induced by the estimation error is small (§4.5).

4.3.4 Key observations

We start with a theorem that holds for all the models presented above, and which will be used as a building block to obtain structural results in §4.4.

Theorem 9. For a system with the mechanics described in either §4.3.1, §4.3.2, or §4.3.3, with initial conditions $S(0) = S_0 > 0$, $G(0) = G_0 > 0$, $Z(0) = Z_0 \geq 0$, and $P(0) = P_0 \geq 0$, and $S_0 + G_0 + Z_0 + P_0 = 1$, and with piecewise continuous controls u_P, u_Z (and in (4.3.3), u_h), the dynamical systems (4.3.1), (4.3.3), and (4.3.5) have unique state solutions $(S(t), G(t), Z(t), P(t))$, with $S(t) > 0$, $Z(t) \geq 0$, $P(t) \geq 0$, and $(S + G + Z + P)(t) = 1$ for all $t \in [0, T]$.

The assumptions $S_0 > 0$ and $G_0 > 0$ are natural, otherwise there is no in-

teraction to control. Henceforth, we will assume these, as well as $Z_0 \geq 0$ and $P_0 \geq 0$.

Proof. The uniqueness follows from standard results in the theory of ordinary differential equations [78, Theorem A.8, p. 419] given the observation that the RHS of the dynamic systems is comprised of quadratic forms and is thus Lipschitz over $[0, T] \times \mathbf{S}$, where $\mathbf{S}$ is the set of states such that the boundary conditions hold.

We provide the proof for the case of §4.3.1, and note the changes for §4.3.2. First of all, $(\dot{S} + \dot{Z} + \dot{P})(t) = 0$ and $(S + Z + P)(0) = 1 - G_0$, so $(S + G + Z + P)(t) = 1$ for all t. We know that $\dot{S} = -\beta GS(u_P + u_Z) - \gamma\beta ZS \geq -MS$, where M is the upperbound of $\beta G + \gamma\beta Z$ (because $(u_P + u_Z) \leq 1$). Therefore, $S(t) \geq S_0 e^{-Mt} > 0$ for all t. Therefore, $\dot{Z} = \beta GSu_Z + \gamma\beta ZS \geq \gamma\beta ZS \geq MZ$, where M is a lowerbound on $\gamma\beta S$ which exists due to continuity (respectively, $\dot{Z} = \beta GSu_Z + \gamma\beta ZS - \pi\beta ZGu_h \geq Z(\gamma\beta S - \beta\pi Gu_h) \geq M'Z$, where M' is a lowerbound on $(\gamma\beta S - \beta\pi Gu_h)$ which again exists due to continuity). Note that the first inequality resulted from $u_Z(t) \geq 0$ for all t. Therefore, $Z(t) \geq Z_0 e^{Mt} \geq 0$ (respectively $Z(t) \geq Z_0 e^{M't} \geq 0$) for all t. Finally, $\dot{P} = \beta GSu_P \geq 0$ for all t (respectively, $\dot{P} = \beta GSu_P + \pi\beta ZGu_h \geq 0$ for all t), as $u_Z(t) \geq 0$, so $P_0 \geq 0$ leads to $P(t) \geq 0$ for all t.

Theorem 9 can be proved very similarly for the model in §4.3.3 using the reasoning we used for the model in §4.3.1, with the difference that in the arguments, β is replaced by $\beta(Z)$, which is lower-bounded away from zero for positive Z. □

4.3.5 Utility Function

As we discussed, the attacker tries to maximize attack efficacy while minimizing visibility. We capture efficacy as a function $f(\cdot)$ of the aggregate number of zombies (Z) and passives (P) at each time instant. Meanwhile, visibility is only a function of zombies that re-spread the malware. This means that we can capture instantaneous visibility as a function $g(\cdot)$ of the number of zombies at that instant. This formulation is comprehensive because the fixed number of Germinators (G) both cause damage and are visible, and are implicitly a term that is added to the variable of both functions. This leads to the following aggregate damage function that the attacker seeks to maximize:

$$J = \int_0^T (f(Z(t) + P(t)) - g(Z(t)))\, dt. \tag{4.3.6}$$

We have some natural assumptions on $f(.)$ and $g(.)$:

$$\frac{dg(Z)}{dZ} > 0, \quad \frac{\partial f(Z+P)}{\partial Z} = \frac{\partial f(Z+P)}{\partial P} > 0 \tag{4.3.7}$$

$$f(0) = g(0) = 0 \tag{4.3.8}$$

We assume that $f(x)$ is **concave**, which means that incremental damage does not increase as the number of infected agents increases [i.e., the pay-off per infected agent decreases].

In §4.4.1: We assume $g(x)$ is **convex**. This means that an increment in the zombies is costlier (results in more visibility) when the infection is already more

visible. This could be the case when the network becomes more wary of the infection as it progresses and becomes more visible.

In §4.4.3: We simplify g to be **linear**, $g(x) = k_g x$, $k_g > 0$.

In §4.4.5: We set $g(x) \equiv 0$, as the effects of visibility have been built into the network dynamics through $\beta(Z)$. This leaves us with:

$$J = \int_0^T f(Z(t) + P(t))\, dt. \tag{4.3.9}$$

4.3.6 Problem statement

In §4.4.1 and §4.4.5, the attacker seeks to choose controls $(u_Z, u_P) \in \mathcal{U}$ *satisfying* (4.3.2) *so as to maximize* J *(respectively,* (4.3.6) *and* (4.3.9)*), while in §4.4.3, she seeks to maximize* J (4.3.6) *through a choice of* $(u_Z, u_P, u_h) \in \mathcal{U}'$ *that satisfies* (4.3.4).

4.4 Structural Results

Using Pontryagin's Maximum Principle and custom arguments specific to each case, we obtain the *one-jump bang-bang* structure of the optimal controls for the various cases in §4.3.1, §4.3.2, and §4.3.3. We provide the proof for §4.4.1 in §4.4.2) and the ones for §4.4.3 and §4.4.5 in §4.4.4 and §4.4.6 respectively.

Intuition is unclear in determining these structures: while intuitively creating zombies at the beginning of the time period allows the malware to benefit from

their epidemic spread, it also penalizes the malware more because of its prolonged visibility. This is further complicated by the fact that the controls can take any value between 0 and 1, and thus it is possible for the attacker to have any mix of malware spread at each instance in time. The strict structures that arise from the analysis are counter-intuitive and interesting both theoretically and from an implementation standpoint.

4.4.1 Results for the no halting model (proved in §4.4.2)

Theorem 10. Any optimal control in $\mathcal{U}$ will satisfy

$$u_P(t) = \begin{cases} 0 & t \in [0, t^*) \\ \\ 1 & t \in (t^*, T) \end{cases} \qquad u_Z(t) = \begin{cases} 1 & t \in [0, t^*) \\ \\ 0 & t \in (t^*, T) \end{cases}$$

for some $t^* \in [0, T)$.

This result means that for any optimal control, there exists a time threshold t^* such that prior to t^*, the germinators convert all the susceptibles they encounter to zombies, and subsequent to it they convert the susceptibles to passives.

The fact that creating zombies starts from the initial time for all interactions, that passives are created for a time period leading up to the terminal time for all interactions, and that the switch between creating zombies and passives is instantaneous – with no gap between, and no over-lap in, the intervals in which these variants are propagated, as well as no intermediate propagation rates – is not at all *a priori* obvious.

Note that we prove a *necessary* condition for any optimal control, thus reducing the search space of controls from a vector of functions to a scalar (t^*). This is a cause for concern, as the latter is much more computationally tractable for the attacker, and shows that any optimal policy will also be simple for the attacker to execute.

4.4.2 Proof of Theorem 10 for the no halting model

Proof. This proof utilizes the necessary conditions for an optimal control derived from Pontryagin's maximum principle. In particular, we explicitly characterize the optimal controls as functions of the optimal states and *co-states* (akin to Lagrange multipliers). Subsequently, we start at terminal time, where the co-states are known, and follow their evolution backward in time till we arrive at the initial time, thereby implicitly characterizing the necessary structure of the optimal controls.

Define continuous co-states $(\lambda_S, \lambda_P, \lambda_Z, \lambda_0)$ such that at points of continuity of the controls:

$$\begin{aligned}
\dot{\lambda}_S &= \beta[(\lambda_S - \lambda_P)Gu_P + (\lambda_S - \lambda_Z)Gu_Z + (\lambda_S - \lambda_Z)\gamma Z] \\
\dot{\lambda}_Z &= -f'(Z+P) + g'(Z) + (\lambda_S - \lambda_Z)\gamma\beta S \\
\dot{\lambda}_P &= -f'(Z+P), \qquad (4.4.1)
\end{aligned}$$

with final co-state constraints:

$$\lambda_S(T) = \lambda_Z(T) = \lambda_P(T) = 0. \tag{4.4.2}$$

Towards characterizing properties of optimal solutions, we define the *Hamiltonian* as:

$$\mathcal{H}(t) := \lambda_0(f(Z+P) - g(Z)) + (\lambda_P - \lambda_S)\beta GSu_P + (\lambda_Z - \lambda_S)\beta GSu_Z + (\lambda_Z - \lambda_S)\gamma\beta ZS. \tag{4.4.3}$$

Pontryagin's Maximum Principle [78, p.182] states that any optimal control vector u^* must satisfy the following necessary conditions:

$$(\lambda_S, \lambda_P, \lambda_Z, \lambda_0) \neq \vec{0}, \tag{4.4.4}$$

$$\forall_{u\in\mathcal{U}, t\in[0,T]}\ \mathcal{H}(S^*, Z^*, P^*, u^*, \lambda_S(t), \lambda_P(t), \lambda_Z(t), \lambda_0, t) \geq \mathcal{H}(S^*, Z^*, P^*, u, \lambda_S(t), \lambda_P(t), \lambda_Z(t), \lambda_0, t). \tag{4.4.5}$$

$$\lambda_0 \in \{0, 1\} \tag{4.4.6}$$

But if $\lambda_0 = 0$, $(\lambda_S(T), \lambda_P(T), \lambda_Z(T), \lambda_0) = \vec{0}$, a contradiction, so $\lambda_0 = 1$.

Structure of the optimal control

If we define:

$$\varphi_P = (\lambda_P - \lambda_S)\beta GS \tag{4.4.7a}$$

$$\varphi_Z = (\lambda_Z - \lambda_S)\beta GS, \tag{4.4.7b}$$

then, the Hamiltonian becomes:

$$\mathcal{H}(t) = f(Z+P) - g(Z) + \varphi_P u_P + \varphi_Z u_Z + (\lambda_Z - \lambda_S)\gamma\beta ZS. \tag{4.4.8}$$

The maximization of the Hamiltonian (4.4.5), added to the sum constraints for the controls (4.3.2a), leads to the following optimality conditions for the controls:[5]

$$(u_P, u_Z) = \begin{cases} (0,0) & \varphi_P < 0, \;\; \varphi_Z < 0 & \text{(4.4.9a)} \\ (1,0) & \varphi_P > 0, \;\; \varphi_P > \varphi_Z & \text{(4.4.9b)} \\ (0,1) & \varphi_Z > 0, \;\; \varphi_Z > \varphi_P & \text{(4.4.9c)} \\ (?,?) & \varphi_Z = \varphi_P \geq 0 & \text{(4.4.9d)} \\ (?,0) & \varphi_P = 0, \;\; \varphi_Z < 0 & \text{(4.4.9e)} \\ (0,?) & \varphi_Z = 0, \;\; \varphi_P < 0 & \text{(4.4.9f)} \end{cases}$$

From (4.4.7) and the state (4.3.1) and costate (4.4.1) evolution equations and after some manipulations, we have:[6]

$$\dot{\varphi}_P = \beta[Gu_Z(\varphi_Z - \varphi_P) + \gamma Z(\varphi_Z - \varphi_P) - GSf'(Z+P)] \tag{4.4.10a}$$

$$\dot{\varphi}_Z = \beta[GS(g'(Z) - f'(Z+P)) + Gu_P(\varphi_P - \varphi_Z) - \gamma S\varphi_Z] \tag{4.4.10b}$$

$$\dot{\varphi}_P - \dot{\varphi}_Z = -(\varphi_P - \varphi_Z)(\beta Gu_Z + \gamma\beta Z + \beta Gu_P) - \beta GSg'(Z) + \gamma\beta S\varphi_Z, \tag{4.4.10c}$$

[5]The question marks (?) denote singular controls. These can occur when the coefficient of a control variable in the *augmented Hamiltonian* (which includes the constraints) is zero over an interval, and thus the control has no effect on the Hamiltonian maximizing condition of the PMP.

[6]$g'(Z) := \frac{dg(Z)}{dZ}, \quad f'(Z+P) := \frac{\partial f(Z+P)}{\partial Z} = \frac{\partial f(Z+P)}{\partial P}$

Proof methodology outline

From here on, we will use the necessary optimality conditions to obtain timing conditions for phase transitions among the conditions in (4.4.9). We show that a time t^* exists such that, for $t \in (t^*, T)$, we have $u_P(t) = 1$ and $u_Z(t) = 0$ (§4.4.2). If $t^* = 0$, we have finished characterizing optimal controls. If not (i.e., $t^* > 0$), we prove that a time t'' exists such that for $t \in (t'', t^*)$, we have $u_P(t) = 0$ and $u_Z(t) = 1$ (in §4.4.2). Finally, we show that t'' must be equal to zero (in §4.4.2), leading to all possible optimal controls agreeing with the structure laid out in Theorem 10.

Time interval leading up to T and the existence of t^*

We now follow the evolution of φ_Z and φ_P for a time interval leading to T in order to characterize necessary conditions for the optimal controls and to prove the existence of t^*. From the terminal time costate conditions (4.4.2):

$$\varphi_P(T) = \varphi_Z(T) = 0,$$

$$\dot{\varphi}_P(T^-) = -f'((Z+P)(T^-))\beta GS(T^-) < 0,$$

$$\dot{\varphi}_P(T^-) - \dot{\varphi}_Z(T^-) = -\beta GS(T^-)g'(Z(T^-)) < 0.$$

Therefore, $\varphi_P(t) > max\{\varphi_Z(t), 0\}$ for some interval leading up to T due to the continuity of the states and costates and using the definition of a left derivative. Let (t^*, T) be the largest interval over which this holds for $t \in (t^*, T)$ for some

$t^* < T$, leading to the fact that for all such t, $u_P(t) = 1$ and $u_Z(t) = 0$ due to (4.4.9b).

For $t \in (t^*, T)$, (4.4.10) becomes:

$$\dot{\varphi}_P = -\beta G S f'(Z + P) + \gamma\beta Z(\varphi_Z - \varphi_P) \tag{4.4.11a}$$

$$\dot{\varphi}_Z = \beta G S(g'(Z) - f'(Z + P)) + \beta G(\varphi_P - \varphi_Z) - \gamma\beta S\varphi_Z \tag{4.4.11b}$$

$$\dot{\varphi}_P - \dot{\varphi}_Z = \gamma\beta S\varphi_Z - (\varphi_P - \varphi_Z)(\gamma\beta Z + \beta G) - \beta G S g'(Z). \tag{4.4.11c}$$

Recall that $\varphi_P(t) > 0$ for $t \in (t^*, T)$, so due to continuity, we either have $\varphi_P(t^*) > 0$ or $\varphi_P(t^*) = 0$. We now rule out $\varphi_P(t^*) = 0$. If $\varphi_P(t^*) = 0$, Rolle's Mean Value Theorem [86, p. 215] applies over the interval (t^*, T): as $\varphi_P(t^*) = \varphi_P(T) = 0$ and φ_P is continuous and differentiable over this interval, there must exist $\tau \in (t^*, T)$ such that $\dot{\varphi}_P(\tau) = 0$. However, from (4.4.11a), it can be seen that $\dot{\varphi}_P(t) < 0$ for $t \in (t^*, T)$, a contradiction. Therefore, $\varphi_P(t^*) > 0$.

Thus, either $t^* = 0$ or $\varphi_Z(t^*) = \varphi_P(t^*)$. If $t^* = 0$, due to (4.4.9b), we have $u_P(t) = 1$ and $u_Z(t) = 0$ for all t which agrees with the structure in Theorem 10, so henceforth we focus on **the case where** $\varphi_Z(t^*) = \varphi_P(t^*) > 0$.

First, we derive a property that will prove useful later on. We have $\dot{Z}(t) \geq 0$ from (4.3.1b) and Theorem 9, and thus due to the convexity of $g(\cdot)$ for $t < t^*$:

$$\frac{G g'(Z(t^*))}{\gamma} \geq \frac{G g'(Z(t))}{\gamma}. \tag{4.4.12}$$

Next, $Z(t^*)$ can either be equal to zero or strictly positive. We first show that if $Z(t^*) = 0$, the structure holds.

If $Z(t^*) = 0$, we have $\dot{Z} = \gamma\beta SZ$ for $t \in (t^*, T)$ as $u_Z(t) = 0$ in this interval. Consider $M_1 > 0$ to be an upper-bound on the continuous $\gamma\beta S$ in this interval, so we must have $Z(t) \leq Z(t^*)e^{M_1(t-t^*)} = 0$, and therefore $Z(T) = 0$ due to continuity and the uniqueness of solutions of first-order initial value problems. Thus, as $\dot{Z} \geq 0$ for $t \in (0, T)$, we must have $\dot{Z} = 0$ over this interval, which from (4.3.1b) and Theorem 9 leads to $u_Z(t) = 0$ for $t \in (0, T)$ and $Z_0 = 0$. This also means that from (4.4.11a), $\dot{\varphi}_P(t) = -\beta GSf'(Z + P) < 0$ in this interval, leading to $\varphi_P(t) > \varphi_P(T) = 0$, and from (4.4.9), to $u_P(t) = 1$ over this interval. Thus, again $t^* = 0$, agreeing with the structure predicted by Theorem 10. So from now on we will **consider** $Z(t^*) > 0$.

Now, we examine $g'(Z(t^*)) - f'((Z+P)(t^*))$, noting that it can either be positive or strictly negative, and investigate both cases in turn.

If $g'(Z(t^*)) - f'((Z + P)(t^*)) \geq 0$, then $g'(Z(t)) - f'((Z + P)(t)) \geq 0$ for all $t \in (t^*, T)$. This is because from (4.3.1), $\dot{P}(t) + \dot{Z}(t) \geq 0$ and $\dot{Z}(t) \geq 0$ over this interval, which coupled with the convexity of $g(\cdot)$ and $-f(\cdot)$ in their arguments gives the aforementioned result. From (4.4.11b) and the definition of t^*, $\dot{\varphi}_Z > -\gamma\beta S\varphi_Z \geq -M_2\varphi_Z$ in this interval, with $M_2 > 0$ being an upper-bound on $\gamma\beta S$. Therefore, $\varphi_Z(t^*) \leq \varphi_Z(T)e^{-M_2(t^*-T)} = 0$ due to an integral argument, which means that $\varphi_P(t^*) > 0 \geq \varphi_Z(t^*)$. Note that this would contradict the starting assumption of this segment, which was $\varphi_P(t^*) = \varphi_Z(t^*)$

Therefore, from here on we will **examine the case of** $g'(Z(t^*)) < f'((Z +$

$P)(t^*)$).

Time interval leading up to $t^* > 0$ and the existence of t''

We now look at the evolution of φ_Z and φ_P for a time interval leading to $t^* > 0$, and show that t'' exists such that t for $t \in (t'', t^*)$, we have $u_P(t) = 0$ and $u_Z(t) = 1$. Furthermore, in these cases we showed $\varphi_Z(t^*) = \varphi_P(t^*)$, $Z(t^*) > 0$, and $g'(Z(t^*)) < f'((Z + P)(t^*))$. At such a point t^*, from (4.4.10b) and the continuity of the states and co-states:

$$(\dot{\varphi}_P(t^{*+}) - \dot{\varphi}_Z(t^{*+})) = \beta S(t^*)[\gamma\varphi_Z(t^*) - Gg'(Z(t^*))]. \tag{4.4.13}$$

Now, (4.4.13) should be positive, because if this derivative was strictly negative, the definition of the right-derivative would show that $\varphi_Z(t) > \varphi_P(t)$ for t in an interval starting from t^*, a contradiction. Because from Theorem 9, $S(t^*) > 0$:

$$\beta S(t^*)[\gamma\varphi_Z(t^*) - Gg'(Z(t^*))] \geq 0 \quad \Rightarrow \quad \varphi_Z(t^*) \geq \frac{Gg'(Z(t^*))}{\gamma}. \tag{4.4.14}$$

Now, we can see from a continuity argument on (4.4.10b) (given that $\varphi_Z(t^*) = \varphi_P(t^*) > 0$) that $\dot{\varphi}_Z(t^{*-}) < 0$. Thus $\varphi_Z(t) > \varphi_Z(t^*)$ for some interval leading up to t^* due to the definition of a left-derivative.

From (4.4.10b), (4.4.12), and (4.4.14), we must have: $\varphi_Z(t) > \dfrac{Gg'(Z(t))}{\gamma}$ for t in some interval leading up to t^*. Let (t', t^*) be the maximal such interval. In this interval, from (4.4.10c), $\dot{\varphi}_P - \dot{\varphi}_Z > -(\varphi_P - \varphi_Z)(\gamma\beta Z + \beta G) \geq -M_3(\varphi_P - \varphi_Z)$, where $M_3 > 0$ is an upper-bound on the continuous expression $\gamma\beta Z + \beta G$. So

for any t in this interval, $(\varphi_P(t) - \varphi_Z(t)) < (\varphi_P(t^*) - \varphi_Z(t^*))e^{-M_3(t-t^*)} = 0$. Thus, $\varphi_P(t) < \varphi_Z(t)$ for $t \in (t', t^*)$. As $\varphi_Z(t^*) > 0$, due to the continuity of the states and co-states, there exists a maximal interval (t'', t^*) such that $\varphi_Z(t) > \max\{\varphi_P(t), 0\}$. Following from (4.4.9c), for $t \in (t'', t^*)$ we must have $u_P(t) = 0$ and $u_Z(t) = 1$.

Proof that $t'' = 0$

If $t'' = 0$, the above concludes our specification of the structure, which agrees with Theorem 10. Thus, henceforth we assume $t'' > 0$, and thus **either** $\varphi_Z(t'') = \varphi_P(t'')$ **or** $\varphi_Z(t'') = 0$.

For $t \in (t'', t^*)$, (4.4.10) becomes:

$$\dot{\varphi}_P = \beta[-GSf'(Z + P) + G(\varphi_Z - \varphi_P) + \gamma Z(\varphi_Z - \varphi_P)] \tag{4.4.15a}$$

$$\dot{\varphi}_Z = \beta[GS(g'(Z) - f'(Z + P)) - \gamma S\varphi_Z] \tag{4.4.15b}$$

$$\dot{\varphi}_P - \dot{\varphi}_Z = \beta[\gamma S\varphi_Z - (\varphi_P - \varphi_Z)(G + \gamma Z) - GSg'(Z)], \tag{4.4.15c}$$

Now, for $t \in (t'', t^*)$, $g'(Z(t)) - f'((Z + P)(t)) < g'(Z(t^*)) - f'((Z + P)(t^*)) < 0$. This is because $\dot{Z}(t) > 0$ as $u_Z(t) = 1$, and $\dot{P}(t) = 0$ as $u_P(t) = 0$, so $g(\cdot) - f(\cdot)$ is convex in the strictly increasing Z in this interval. So from (4.4.15b), $\dot{\varphi}_Z < -\gamma\beta S\varphi_Z \leq -M_4\varphi_Z$ with $M_4 > 0$ being the upper-bound of the continuous $\gamma\beta S$, and therefore for all $t \in (t'', t^*)$, $\varphi_Z(t) \geq \varphi_Z(t^*)e^{-M_4(t-t^*)}$, and therefore by continuity, $\varphi_Z(t'') \geq \varphi_Z(t^*)e^{-M_4(t''-t^*)}$. Thus, we can conclude that $\varphi_Z(t'') > 0$, as $\varphi_Z(t^*) > 0$.

So for $t'' > 0$, **we must have** $\varphi_P(t'') = \varphi_Z(t'')$. In this case, we have $(\dot{\varphi}_P(t''^+) -$

$\dot{\varphi}_Z(t''^+)) \leq 0$, as if it is strictly positive, an integral argument will lead to a contradiction with $\varphi_P(t) < \varphi_Z(t)$ for $t \in (t'', t^*)$. Using the continuity of the states and co-states and as from Theorem 9, $S(t'') > 0$, (4.4.15b) becomes:

$$\dot{\varphi}_P(t''^+) - \dot{\varphi}_Z(t''^+) = \beta S(t'')[\gamma\varphi_Z(t'') - Gg'(Z(t''))] \leq 0$$

$$\Rightarrow \quad \varphi_Z(t'') \leq \frac{Gg'(Z(t''))}{\gamma}, \tag{4.4.16}$$

We know that for all $t \in (t'', t^*)$, $g'(Z(t)) - f'(Z + P(t)) < 0$, so from (4.4.15b), $\dot{\varphi}_Z(t) < -\gamma\beta S\varphi_Z < -M_5\varphi_Z < 0$, where $M_5 > 0$ is an upper-bound on the continuous $\gamma\beta S$. Thus,

$$\varphi_Z(t'') > \varphi_Z(t^*). \tag{4.4.17}$$

But (4.4.12), (4.4.16), and (4.4.17) lead to $\varphi_Z(t^*) < \frac{Gg'(Z(t^*))}{\gamma}$, which contradicts (4.4.14).

Thus $t'' = 0$, and this concludes our specification of the structure of the optimal controls which conform to the structure set out in Theorem 10. □

4.4.3 Results for the halting model (proved in §4.4.4)

Theorem 11. Any optimal control in $\mathcal{U}'$ will satisfy

$$u_P(t) = u_h(t) = \begin{cases} 0 \; t \in [0, t^*) \\ \\ 1 \; t \in (t^*, T) \end{cases} \qquad u_Z(t) = \begin{cases} 1 \; t \in [0, t^*) \\ \\ 0 \; t \in (t^*, T) \end{cases}$$

for some $t^* \in [0, T)$, except in the case where $Z(t) = 0$ for all $t \in [0, T]$, in which case u_h can be arbitrary with the other two structures holding.

This means that there exists a time threshold t^* such that prior to t^*, the germinators again convert all the susceptibles they encounter to zombies while not halting any zombies they meet, and subsequent to it they convert both the susceptibles and zombies they encounter to passives. Here, the added halting control can be used to slow the spread of zombies.

The fact that the same result as Theorem 10 holds for u_Z and u_P in the presence of u_h is not clear *a priori*. Furthermore, the fact that the halting optimal control is bang-bang and that the switching time is the same as the other controls is surprising.

4.4.4 Proof of Theorem 11

Proof. This proof follows the same structure as that of Theorem 10.

As before, we define continuous co-states $(\lambda_S, \lambda_P, \lambda_Z, \lambda_0)$ such that at points of continuity of the controls:

$$\begin{aligned}
\dot{\lambda}_S &= (\lambda_S - \lambda_P)\beta G u_P + (\lambda_S - \lambda_Z)[\beta G u_Z + \gamma\beta Z] \\
\dot{\lambda}_Z &= \lambda_0 g'(Z) - \lambda_0 f'(Z+P) + (\lambda_S - \lambda_Z)\gamma\beta S + (\lambda_Z - \lambda_P)\pi\beta G u_h \\
\dot{\lambda}_P &= -\lambda_0 f'(Z+P),
\end{aligned} \tag{4.4.18}$$

with final state constraints:

$$\lambda_S(T) = \lambda_Z(T) = \lambda_P(T) = 0. \tag{4.4.19}$$

To characterize optimal controls, we define the Hamiltonian to be:

$$\mathcal{H}(t) = \lambda_0(f(Z+P) - g(Z)) + (\lambda_P - \lambda_Z)\pi\beta G Z u_h + (\lambda_Z - \lambda_S)[\beta G S u_Z + \gamma\beta Z S] + (\lambda_P - \lambda_S)\beta G S u_P. \tag{4.4.20}$$

Pontryagin's Maximum Principle again gives the following necessary conditions for an optimal control vector u^*:

$$(\lambda_S, \lambda_P, \lambda_Z, \lambda_0) \neq \vec{0}, \tag{4.4.21}$$

$$\forall_{u\in\mathcal{U}, t\in[0,T]}\ \mathcal{H}(S^*, Z^*, P^*, u^*, \lambda_S(t), \lambda_P(t), \lambda_Z(t), \lambda_0, t) \geq \mathcal{H}(S^*, Z^*, P^*, u, \lambda_S(t), \lambda_P(t), \lambda_Z(t), \lambda_0, t). \tag{4.4.22}$$

$$\lambda_0 \in \{0, 1\} \tag{4.4.23}$$

Again, if $\lambda_0 = 0$, $(\lambda_S(T), \lambda_P(T), \lambda_Z(T), \lambda_0) = \vec{0}$, a contradiction, so $\lambda_0 = 1$.

Now, we have:

$$\dot{\lambda}_P - \dot{\lambda}_Z = -g'(Z) - (\lambda_S - \lambda_Z)\gamma\beta S - (\lambda_Z - \lambda_P)\pi\beta G u_h$$

$$\dot{\lambda}_S - \dot{\lambda}_Z = f'(Z+P) - g'(Z) + (\lambda_S - \lambda_P)\beta G u_P + (\lambda_S - \lambda_Z)\beta G u_Z + (\lambda_S - \lambda_Z)\gamma\beta(Z - S) - (\lambda_Z - \lambda_P)\pi\beta G u_h$$

$$\dot{\lambda}_S - \dot{\lambda}_P = f'(Z+P) + (\lambda_S - \lambda_Z)[\beta G u_Z + \gamma\beta Z] + (\lambda_S - \lambda_P)\beta G u_P,$$

Structure of the optimal control

If we define:

$$\varphi_P = (\lambda_P - \lambda_S)\beta GS \tag{4.4.24a}$$

$$\varphi_Z = (\lambda_Z - \lambda_S)\beta GS \tag{4.4.24b}$$

$$\varphi_h = (\lambda_P - \lambda_Z)\pi\beta GZ, \tag{4.4.24c}$$

then, the Hamiltonian becomes:

$$\mathcal{H}(t) = f(Z+P) - g(Z) + \varphi_P u_P + \varphi_Z u_Z + \varphi_h u_h + (\lambda_Z - \lambda_S)\gamma\beta ZS. \tag{4.4.25}$$

Also notice that:

$$\varphi_h = \pi\frac{Z}{S}(\varphi_P - \varphi_Z). \tag{4.4.26}$$

The maximization of the Hamiltonian (4.4.22), added to the sum constraints for the controls (4.3.2a), leads to the following optimality conditions for the controls:

$$(u_P, u_Z) = \begin{cases} (0,0) & \varphi_P < 0, \;\; \varphi_Z < 0 & \text{(4.4.27a)} \\ (1,0) & \varphi_P > 0, \;\; \varphi_P > \varphi_Z & \text{(4.4.27b)} \\ (0,1) & \varphi_Z > 0, \;\; \varphi_Z > \varphi_P & \text{(4.4.27c)} \\ (?,?) & \varphi_Z = \varphi_P \geq 0 & \text{(4.4.27d)} \\ (?,0) & \varphi_P = 0, \;\; \varphi_Z < 0 & \text{(4.4.27e)} \\ (0,?) & \varphi_Z = 0, \;\; \varphi_P < 0 & \text{(4.4.27f)} \end{cases}$$

Furthermore,

$$\varphi_Z(t) > 0 \text{ or } \varphi_P(t) > 0 \Rightarrow u_P(t) + u_Z(t) = 1, \tag{4.4.28}$$

as if that is not true, we can increase $\mathcal{H}(t)$ by adding to either $u_P(t)$ or $u_Z(t)$, a contradiction with the Hamiltonian maximization condition of the Maximum Principle (4.4.22).

Also,

$$u_h = \begin{cases} 0 & \varphi_h < 0 \\ 1 & \varphi_h > 0 \\ ? & \varphi_h = 0 \end{cases} . \tag{4.4.29}$$

Using (4.4.26), we can rewrite (4.4.29) as:

$$u_h = \begin{cases} 0 & \varphi_P < \varphi_Z \ \& \ Z(t) > 0 \quad \text{(4.4.30a)} \\ 1 & \varphi_P > \varphi_Z \ \& \ Z(t) > 0 \quad \text{(4.4.30b)} \\ ? & \varphi_P = \varphi_Z \text{ or } Z(t) = 0 \quad \text{(4.4.30c)} \end{cases}$$

. From (4.4.24) and the state and costate evolution equations and after trite

manipulation, we have:

$$\dot{\varphi}_P = -\beta G S f'(Z+P) + \beta G u_Z(\varphi_Z - \varphi_P) + \gamma\beta Z(\varphi_Z - \varphi_P) \tag{4.4.31a}$$

$$\dot{\varphi}_Z = \beta G S(k_g - f'(Z+P)) - \gamma\beta S\varphi_Z + \beta G(u_P - \pi u_h)(\varphi_P - \varphi_Z) \tag{4.4.31b}$$

$$\dot{\varphi}_P - \dot{\varphi}_Z = -(\varphi_P - \varphi_Z)(\beta G u_Z + \gamma\beta Z + \beta G u_P - \beta G u_h) - \beta G S k_g + \gamma\beta S\varphi_Z \tag{4.4.31c}$$

$$\dot{\varphi}_h = -\pi\beta G Z k_g + \pi\beta G u_Z(\varphi_P - \varphi_Z) + \pi\gamma\beta Z\varphi_P. \tag{4.4.31d}$$

From here on, the proof follows the same outline laid out in §4.4.2 (in terms of finding t^* and t'' and proving $t'' = 0$); however, the algebraic expressions for $\dot{\varphi}_Z$, $\dot{\varphi}_P$ are different and $\varphi_h(t)$ is introduced in the dynamics, necessitating the use of different and context-specific analytical arguments.

Time interval leading up to T and the existence of t^*

We follow the evolution of φ_Z, φ_P, and φ_h for a time interval leading to T and prove the existence of t^* such that we have $u_P(t) = 1$, $u_Z(t) = 0$, and, if $Z(T) > 0$, $u_h(t) = 1$ for all $t \in (t^*, T)$ (otherwise, u_h can be arbitrary over this interval).

From the terminal time costate conditions (4.4.19):

$$\varphi_P(T) = \varphi_Z(T) = \varphi_h(T) = 0, \tag{4.4.32a}$$

$$\dot{\varphi}_P(T^-) = -f'((Z+P)(T^-))\beta GS(T^-) < 0, \tag{4.4.32b}$$

$$\dot{\varphi}_P(T^-) - \dot{\varphi}_Z(T^-) = -\beta GS(T^-)k_g < 0, \tag{4.4.32c}$$

$$\dot{\varphi}_h(T^-) = -\pi\beta GZ(T^-)k_g \leq 0. \tag{4.4.32d}$$

Now, we may either have $Z(T) = 0$ or $Z(T) > 0$ due to Theorem 9.

We start by **considering the case where** $Z(T) = 0$. From (4.3.3b) we have

$$\dot{Z} \geq Z(\gamma\beta S - \pi\beta G u_h) \geq M_6 Z$$

for $t \in [0, T]$, where $M_6 > 0$ is an upper-bound on the $\gamma\beta S$ over the whole interval. Therefore, $Z(t)e^{M_6(t-T)} \leq Z(T) = 0$. Thus we must have $Z(t) = 0$ for all $t \in [0, T]$. This means that $\dot{Z}(t) = \beta GSu_Z = 0$ over this interval, which from Theorem 9 leads to $u_Z(t) = 0$ for all $t \in [0, T]$. Furthermore, as $Z(t)$ is never positive, $u_h(t)$ will have no effect on the dynamics of the system, and can thus be arbitrary. Finally, (4.4.31a) and (4.4.32a) tell us that $\varphi_P(T) = 0$ and $\dot{\varphi}_P(t) = -\beta GSf'(P) < 0$ over this interval, which leads to $\varphi_P(t) > 0$ for $t \in [0, T)$ due to continuity of the states and co-states and the differentiability of $\varphi_P(t)$ using an integral argument. This, along with $u_Z(t) = 0$ for all $t \in [0, T]$ and (4.4.28) leads to $u_P(t) = 1$ for all $t \in [0, T)$ (and therefore $t^* = 0$). So in sum, for all $t \in [0, T)$, $u_P(t) = 1$, $u_Z(t) = 0$, with $u_h(t)$ taking any arbitrary value. This agrees with the structure set forth in Theorem 11.

Henceforth, **we examine the case where** $Z(T) > 0$. From (4.4.32a) and (4.4.32c), as before, $\varphi_P(t) > max\{\varphi_Z(t), 0\}$ for some interval leading up to T due to the continuity of the states and costates and using the definition of a left derivative. Let (t^*, T) be the largest interval over which this holds for $t \in (t^*, T)$ for some $t^* < T$, leading to the fact that for all such t, $u_P(t) = 1$ and $u_Z(t) = 0$ due to (4.4.27b).

We now prove that for $t \in [t^*, T]$, $Z(t) > 0$. If $Z(\tau) = 0$ at any $\tau \in (t^*, T)$, as $u_Z(t) = 0$ in this interval and from (4.3.3b) we will have $\dot{Z} = Z(\gamma\beta S - \pi\beta G u_h) < M_7 Z$ for $t \in [\tau, T]$ and for some $M_7 > 0$ which is an upper-bound to $\gamma\beta S$. This leads to $Z(t) \leq Z(\tau)e^{M_7(t-\tau)} = 0$, or $Z(t) = 0$ for all $t \in [\tau, T]$ and especially $Z(T) = 0$ which is a contradiction. The same reasoning also applies to $t = t^*$ due to continuity. So for $t \in [t^*, T]$, $Z(t) > 0$. Thus, from (4.4.30b) and the definition of t^*, we have $u_h(t) = 1$ for all $t \in (t^*, T)$.

So **if** $t^* = 0$, we have $u_P(t) = 1$, $u_Z(t) = 0$, and $u_h(t) = 1$ for all $t \in [0, T)$, which agrees with Theorem 11. Now **we consider** $t^* > 0$.

Time interval leading up to $t^* > 0$ and the existence of t''

We now look at the evolution of φ_Z, φ_P, and φ_h for a time interval leading to $t^* > 0$, and show t'' exists such that for $t \in (t'', t^*)$ we must have $u_P(t) = 0$, $u_h(t) = 0$, and $u_Z(t) = 1$. For $t \in (t^*, T)$, and after replacing optimal controls,

(4.4.31) becomes:

$$\dot{\varphi}_P = -\beta G S f'(Z+P) + \gamma\beta Z(\varphi_Z - \varphi_P) \tag{4.4.33a}$$

$$\dot{\varphi}_Z = \beta G S(k_g - f'(Z+P)) + \beta G(1-\pi)(\varphi_P - \varphi_Z) - \gamma\beta S\varphi_Z \tag{4.4.33b}$$

$$\dot{\varphi}_P - \dot{\varphi}_Z = -(\varphi_P - \varphi_Z)(\gamma\beta Z + \beta G(1-\pi)) - \beta G S k_g + \gamma\beta S\varphi_Z, \tag{4.4.33c}$$

$$\dot{\varphi}_h = \pi Z(\gamma\beta\varphi_P - \beta G k_g). \tag{4.4.33d}$$

It can be seen that $\dot{\varphi}_P(t) < 0$ for $t \in (t^*, T)$ (as $\varphi_P(t) > \varphi_Z(t)$ and $f'(Z(t) + P(t)) > 0$ in this interval). This, coupled with $\varphi_P(T) = 0$ ((4.4.32a)) leads to $\varphi_P(t^*) > 0$ due to continuity and an integral argument. Thus, we must have $\varphi_Z(t^*) = \varphi_P(t^*) > 0$ for $t^* > 0$.

For $t \in (t^*, T)$:

$$\dot{Z} + \dot{P} = \beta G S + \gamma\beta Z S > 0. \tag{4.4.34}$$

Now, **if** $k_g - f'((Z+P)(t^*)) \geq 0$, then $k_g - f'((Z+P)(t)) \geq 0$ for all $t \in (t^*, T)$ due to the convexity of $k_g - f(\cdot)$ in its argument and as $Z + P$ is strictly increasing in this interval (from (4.4.34)). From (4.4.33b), $\dot{\varphi}_Z > -\gamma\beta S\varphi_Z \geq -M_8\varphi_Z$ for all $t \in (t^*, T)$, with M_8 being an upper-bound on $\gamma\beta S$. Therefore, $\varphi_Z(t^*) < \varphi_Z(T)e^{-M_8(t^*-T)} = 0$ due to an integral argument, which means that $\varphi_P(t^*) > 0 \geq \varphi_Z(t^*)$. This contradicts the starting assumption of this argument, which was $\varphi_P(t^*) = \varphi_Z(t^*)$.

Therefore, from here on we will **consider** $k_g < f'((Z+P)(t^*))$. At such a point

t^*, from (4.4.33b) and the continuity of the states and co-states:

$$(\dot{\varphi}_P(t^{*+}) - \dot{\varphi}_Z(t^{*+})) = \beta S(t^*)[\gamma\varphi_Z(t^*) - Gk_g]. \tag{4.4.35}$$

Now, (4.4.35) should be positive, because if this derivative was strictly negative, the definition of the right-derivative would show that $\varphi_Z(t) > \varphi_P(t)$ for t in an interval starting from t^*, a contradiction with the definition of t^*. So, as $S(t^*) > 0$ from Theorem 9:

$$\beta S(t^*)[\gamma\varphi_Z(t^*) - Gk_g] \geq 0 \Rightarrow \varphi_Z(t^*) \geq \frac{Gk_g}{\gamma}. \tag{4.4.36}$$

Now, we can see from a continuity argument on (4.4.33b) (given that $\varphi_Z(t^*) = \varphi_P(t^*) > 0$) that $\dot{\varphi}_Z(t^{*-}) < 0$. Thus $\varphi_Z(t) > \varphi_Z(t^*) > 0$ for some interval leading up to t^* due to the definition of a left-derivative. Thus, from (4.4.36) we must have: $\varphi_Z(t) > \frac{Gk_g}{\gamma}$ (and therefore also $\varphi_Z(t) > 0$) for t in some interval leading up to t^*. Let (t', t^*) be the maximal such interval. In this interval, from (4.4.33c), we have

$$\dot{\varphi}_P - \dot{\varphi}_Z > -(\varphi_P - \varphi_Z)(\gamma\beta Z + \beta G(1-\pi)) \geq -M_9(\varphi_P - \varphi_Z),$$

where $M_9 > 0$ is an upper-bound on the continuous expression $\gamma\beta Z + \beta G(1-\pi)$. So for any t in this interval, $(\varphi_P(t) - \varphi_Z(t)) < (\varphi_P(t^*) - \varphi_Z(t^*))e^{-M_9(t-t^*)} = 0$.

Thus, $\varphi_P(t) < \varphi_Z(t)$ for $t \in (t', t^*)$. As $\varphi_Z(t^*) > 0$, due to the continuity of the states and co-states, there exists a maximal interval (t'', t^*) such that $\varphi_Z(t) > \max\{\varphi_P(t), 0\}$. Following from (4.4.27c) , for $t \in (t'', t^*)$ we must have $u_P(t) = 0$ and $u_Z(t) = 1$.

As $\varphi_Z(t) > \varphi_P(t)$, from (4.4.30a) and (4.4.30c) we have $Z(t)u_h(t) = 0$ for $t \in (t'', t^*)$. This leads to $\dot{Z}(t) > 0$ in this interval (from (4.3.3b)), which combined with Theorem 9 leads to $Z(t) > 0$ in this interval. Therefore, from (4.4.30a) we can also conclude that in this interval, $u_h(t) = 0$.

Proof of $t'' = 0$

If $t'' = 0$, this concludes our specification of the structure, which agrees with Theorem 11. Thus, henceforth we **consider the case where** $t'' > 0$, and thus **either** $\varphi_Z(t'') = \varphi_P(t'')$ **or** $\varphi_Z(t'') = 0$.

For $t \in (t'', t^*)$, (4.4.31) becomes:

$$\dot{\varphi}_P = -\beta GSf'(Z+P) + \beta G(\varphi_Z - \varphi_P) + \gamma\beta Z(\varphi_Z - \varphi_P) \tag{4.4.37a}$$

$$\dot{\varphi}_Z = \beta GS(k_g - f'(Z+P)) - \gamma\beta S\varphi_Z \tag{4.4.37b}$$

$$\dot{\varphi}_P - \dot{\varphi}_Z = -(\varphi_P - \varphi_Z)(\beta G + \gamma\beta Z) - \beta GSk_g + \gamma\beta S\varphi_Z \tag{4.4.37c}$$

$$\dot{\varphi}_h = -\pi\beta GZk_g + \pi\beta G(\varphi_P - \varphi_Z) + \pi\gamma\beta Z\varphi_P, \tag{4.4.37d}$$

Now, for $t \in (t'', t^*)$,

$$k_g - f'((Z+P)(t)) < k_g - f'((Z+P)(t^*)) < 0 \tag{4.4.38}$$

as $k_g - f(\cdot)$ is convex and in this interval and $\dot{P}(t) + \dot{Z}(t) = \dot{Z}(t) = \beta GS + \gamma\beta ZS > 0$ as $u_Z(t) = 1$, and $u_P(t) = u_h(t) = 0$. So from (4.4.37b), $\dot{\varphi}_Z < -\gamma\beta S\varphi_Z \leq -M_{10}\varphi_Z$ with $M_{10} > 0$ being the upper-bound of the continuous $\gamma\beta S$, and therefore for all $t \in (t'', t^*)$, $\varphi_Z(t) \geq \varphi_Z(t^*)e^{-M_{10}(t-t^*)}$. As $\varphi_Z(t^*) > 0$, $\varphi_Z(t)$ is bounded away from

zero, which **leads to** $\varphi_Z(t'') > 0$ due to continuity.

So we **must have** $\varphi_P(t'') = \varphi_Z(t'')$. In this case, from (4.4.37c) we have $(\dot{\varphi}_P(t''^+) - \dot{\varphi}_Z(t''^+)) \leq 0$, as if it is strictly positive, an integral argument will lead to a contradiction with $\varphi_P(t) < \varphi_Z(t)$ for $t \in (t'', t^*)$. Using the continuity of the states and co-states, as well as the fact that $S(t'') > 0$ from Theorem 9, (4.4.15b) becomes:

$$\dot{\varphi}_P(t''^+) - \dot{\varphi}_Z(t''^+) = \beta S(t'')[\gamma\varphi_Z(t'') - Gk_g] \leq 0 \quad \Rightarrow \varphi_Z(t'') \leq \frac{Gk_g}{\gamma}, \quad (4.4.39)$$

From (4.4.38) and (4.4.37b), $\dot{\varphi}_Z < -\gamma\beta S\varphi_Z < -M_{10}\varphi_Z < 0$. So,

$$\varphi_Z(t'') > \varphi_Z(t^*). \quad (4.4.40)$$

But (4.4.36) and (4.4.39) lead to $\varphi_Z(t'') \leq \varphi_Z(t^*)$, which contradicts (4.4.40).

Thus $t'' = 0$, and this concludes our specification of the structure of the optimal controls which conform to the structure set out in Theorem 11. □

4.4.5 Results for the adaptive defense model

Theorem 10 holds (with the difference that $t^* \in [0, T]$***) for constant, affine, and sigmoid*** $\beta(Z)$**.** This is remarkable given that here, β changes as a function of Z. This result is proved in §4.4.6.

4.4.6 Proof of Theorem 10 for the adaptive defense model

Proof. We first provide a general framework (akin to the one presented for Theorem 10), and then we differentiate the analysis based on the type of adaptive defense used by the network: Constant $\beta(Z)$ in §4.4.6, affine $\beta(Z)$ in §4.4.6, and sigmoid $\beta(Z)$ in §4.4.6

As before, define the continuous co-states $(\lambda_S, \lambda_P, \lambda_Z, \lambda_0)$ such that at points of continuity of the controls:

$$\begin{aligned}
\dot{\lambda}_S &= \beta(Z)[(\lambda_S - \lambda_P)Gu_P + (\lambda_S - \lambda_Z)(Gu_Z + \gamma Z)] \\
\dot{\lambda}_Z &= -\lambda_0 f'(Z+P) + (\lambda_S - \lambda_Z)\gamma\beta(Z)S + \beta'(Z)[(\lambda_S - \lambda_P)GSu_P \\
&\quad + (\lambda_S - \lambda_Z)GSu_Z + (\lambda_S - \lambda_Z)\gamma ZS] \\
\dot{\lambda}_P &= -\lambda_0 f'(Z+P),
\end{aligned} \tag{4.4.41}$$

with final co-state constraints:

$$\lambda_S(T) = \lambda_Z(T) = \lambda_P(T) = 0. \tag{4.4.42}$$

To characterize optimal controls, we define the *Hamiltonian*:

$$\begin{aligned}
\mathcal{H}(t) :=& \lambda_0 f(Z+P) + (\lambda_P - \lambda_S)\beta(Z)GSu_P + (\lambda_Z - \lambda_S)\beta(Z)GSu_Z \\
&+ (\lambda_Z - \lambda_S)\gamma\beta(Z)ZS
\end{aligned} \tag{4.4.43}$$

Pontryagin's Maximum Principle [78, p.182] gives us the following necessary

conditions for optimality for an optimal control vector u^*:

$$(\lambda_S, \lambda_P, \lambda_Z, \lambda_0) \neq \vec{0}, \tag{4.4.44}$$

$$\forall_{u \in \mathcal{U}, t \in [0,T]} \ \mathcal{H}(S^*, Z^*, P^*, u^*, \lambda_S(t), \lambda_P(t), \lambda_Z(t), \lambda_0, t)$$

$$\geq \mathcal{H}(S^*, Z^*, P^*, u, \lambda_S(t), \lambda_P(t), \lambda_Z(t), \lambda_0, t). \tag{4.4.45}$$

$$\lambda_0 \in \{0, 1\} \tag{4.4.46}$$

But if $\lambda_0 = 0$, $(\lambda_S(T), \lambda_P(T), \lambda_Z(T), \lambda_0) = \vec{0}$, a contradiction, so $\lambda_0 = 1$.

General structure of the optimal control

If we define:

$$\varphi_P = (\lambda_P - \lambda_S)\beta(Z)GS \tag{4.4.47a}$$

$$\varphi_Z = (\lambda_Z - \lambda_S)\beta(Z)GS, \tag{4.4.47b}$$

then, the Hamiltonian becomes:

$$\mathcal{H}(t) = f(Z + P) + \varphi_P u_P + \varphi_Z u_Z + (\lambda_Z - \lambda_S)\gamma\beta(Z)ZS. \tag{4.4.48}$$

The maximization of the Hamiltonian (4.4.45), added to the sum constraints for the controls (4.3.2a), leads to (4.4.9) as the optimality conditions for the controls:

$$\varphi_Z(t) > 0 \text{ or } \varphi_P(t) > 0 \Rightarrow u_P(t) + u_Z(t) = 1, \tag{4.4.49}$$

as if that is not true, we can add to the instantaneous value of $\mathcal{H}(t)$ by adding to either $u_P(t)$ or $u_Z(t)$, a contradiction with the Hamiltonian maximization condition (4.4.45).

From (4.4.47) and the state (4.3.5) and costate (4.4.41) evolution equations and after some manipulation, we have:

$$\dot{\varphi}_P = -\beta(Z)GSf'(Z+P) + \beta'(Z)S\varphi_P[Gu_Z + \gamma Z] - (\varphi_P - \varphi_Z)\beta(Z)[Gu_Z + \gamma Z] \tag{4.4.50a}$$

$$\dot{\varphi}_Z = -\beta(Z)GSf'(Z+P) - \varphi_P Gu_P\beta'(Z)S - \varphi_Z\beta(Z)\gamma S + (\varphi_P - \varphi_Z)\beta(Z)Gu_P, \tag{4.4.50b}$$

$$\begin{aligned}\dot{\varphi}_P - \dot{\varphi}_Z = &-(\varphi_P - \varphi_Z)\beta(Z)[G(u_Z + u_P) + \gamma(Z+S)] \\ &+\varphi_P S\big[\gamma\beta(Z) + \beta'(Z)[G(u_Z + u_P) + \gamma Z]\big]\end{aligned} \tag{4.4.50c}$$

Again, the proof follows the outline laid out in §4.4.2 (i.e., proving the existence of t^* and t', which are, however, defined differently, and proving $t' = 0$ for $t^* > 0$), with the difference that the algebraic expressions for $\dot{\varphi}_Z$ and $\dot{\varphi}_P$, and therefore all subsequent analytical arguments, will change.

Time interval leading up to T and the existence of t^*

We follow the evolution of φ_Z and φ_P for a time interval leading to T and prove the existence of t^* such that we have $u_P(t) = 1$, and $u_Z(t) = 0$ for all $t \in (t^*, T)$.

From the terminal time costate conditions (4.4.42) and their directional derivatives (4.4.50), we have:

$$\varphi_P(T) = \varphi_Z(T) = 0, \tag{4.4.51a}$$

$$\dot{\varphi}_P(T^-) = \dot{\varphi}_Z(T^-) = -\beta(Z)GSf'(Z+P) < 0. \tag{4.4.51b}$$

So, due to continuity of the states and co-states, there is an interval leading up to T, over which we have $\varphi_P(t) > 0$ and $\varphi_Z(t) > 0$. Let (t^*, T) be the maximal length interval with this property. Equation (4.4.49) leads to

$$u_Z(t) + u_P(t) = 1 \tag{4.4.52}$$

for $t \in (t^*, T)$.

Now, for $t \in (t^*, T)$, (4.4.50c) becomes:

$$\dot{\varphi}_P(t) - \dot{\varphi}_Z(t) = -(\varphi_P - \varphi_Z)\beta(Z)[G + \gamma(Z + S)] + \varphi_P S\big[\gamma\beta(Z) + \beta'(Z)[G + \gamma Z]\big] \tag{4.4.53}$$

The rest of the analysis depends on the $\beta(Z)$ function - we present different arguments for $\beta(Z)$'s that are constant, affine, and sigmoid (§Appendices 4.4.6, 4.4.6, and 4.4.6, respectively). For the affine case (§4.4.6), the analysis needs to be broken down into different cases according to the value of $Z(T)$ in relation to the constant $\frac{1}{2}[\frac{\beta_{\max}}{a} - \frac{G}{\gamma}]$. When $\beta(Z)$ is a sigmoid (§4.4.6), we use different analytical arguments to prove the result depending on whether $e^{\alpha(Z(T)-Z_{th})}(1-\frac{\alpha}{\gamma}G-\alpha Z(T))+1$ is less than, equal to, or greater than zero. For the simple case of constant $\beta(Z)$ (§4.4.6), no such conditional arguments are needed.

Constant $\beta(Z)$

Assume $\beta(Z) = \beta$.[7] In this case, there is no penalty for creating zombies, and we expect zombies to be created for the whole time period. Then for $t \in (t^*, T)$,

[7]Note that this is a case of the model in §4.4.5 with $g \equiv 0$.

(4.4.53) becomes:

$$(\dot{\varphi}_P - \dot{\varphi}_Z)(t) = \varphi_P S\gamma\beta - (\varphi_P - \varphi_Z)\beta[G + \gamma(Z + S)] \geq -(\varphi_P - \varphi_Z)M_{11},$$

for all $t \in (t^*, T)$ and for some $M_{11} > 0$ that is an upper-bound for $\beta(G+\gamma(Z+S))$, as $\varphi_P(t)S(t)\gamma\beta > 0$ in this interval. Therefore, for $t \in (t^*, T)$, $\varphi_P(t) - \varphi_Z(t) < [\varphi_P(T) - \varphi_Z(T)]e^{-M_{11}(t-T)} = 0$ (from (4.4.51a)), and thus $\varphi_P(t) < \varphi_Z(t)$ for $t \in (t^*, T)$.

Due to the continuity of the states and co-states and from the definition of t^*, there exists an interval (t', T), with $t' \leq t^*$ such that $\varphi_Z > \varphi_P$ and $\varphi_Z > 0$. These conditions, coupled with (4.4.9c) lead to $u_P(t) = 0$ and $u_Z(t) = 1$ for all $t \in (t', T)$.

We now prove $t' = 0$. If this does not hold, either $\varphi_Z(t') = \varphi_P(t')$ or $\varphi_Z(t') = 0$ for some $t' > 0$ due to continuity of the states and co-states.

Since $u_P(t) = 0$ for $t \in (t', T)$, (4.4.50b) becomes:

$$\dot{\varphi}_Z(t) = -\beta(Z)GSf'(Z + P) - \varphi_Z\beta(Z)\gamma S < 0,$$

which leads to $\varphi_Z(t') > \varphi_Z(T) = 0$. Thus, $\varphi_Z(t')$ cannot be equal to zero.

If $\varphi_Z(t') = \varphi_P(t')$, then from (4.4.50c), $\beta'(Z) = 0$ for constant $\beta(Z)$, and the continuity of the states and co-states:

$$\left(\dot{\varphi}_P - \dot{\varphi}_Z\right)(t'^+) = \varphi_P(t')S(t')\gamma\beta = \varphi_Z(t')S(t')\gamma\beta > 0,$$

leading to the existence of an interval (t', t'') over which $\varphi_P(t) > \varphi_Z(t)$, a contradiction with the definition of t'.

Thus, $t' = 0$ and $u_Z(t) = 1$ and $u_P(t) = 0$ for all t, which agrees with the statement of Theorem 10 and our intuition that zombies will be created for the entire period. □

Affine $\beta(Z)$

Assume $\beta(Z) = -aZ + \beta_{\max}$, with $0 < a \leq \beta_{\max}$ (as $\beta_{\max}$ is an upperbound on this $\beta(Z)$ and $\beta(Z) > 0$). Then, for $t \in (t^*, T)$, (4.4.53) becomes:

$$\begin{aligned}\dot{\varphi}_P(t) - \dot{\varphi}_Z(t) = &- a\varphi_P S\big[\gamma(2Z - \frac{\beta_{\max}}{a}) + G\big] \\ &-(\varphi_P - \varphi_Z)(-aZ + \beta_{\max})[G + \gamma(Z + S)] \end{aligned} \tag{4.4.54}$$

Now we break down the situations that can arise based on the value of $Z(T)$ with respect to the fixed $\frac{1}{2}[\frac{\beta_{\max}}{a} - \frac{G}{\gamma}]$:

$Z(T) \leq \frac{1}{2}[\frac{\beta_{\max}}{a} - \frac{G}{\gamma}]$ Note that for this case, we must have $\frac{1}{2}[\frac{\beta_{\max}}{a} - \frac{G}{\gamma}] \geq 0$ due to Theorem 9.

We first consider the sub-case where $Z(T) = \frac{1}{2}[\frac{\beta_{\max}}{a} - \frac{G}{\gamma}] = 0$. Here, we must have $\dot{Z}(t) = 0$ for all t as $\dot{Z}(t) \geq 0$ for all t and as states are continuous. The only way for $\dot{Z}(t) = 0$ for all t is for us to have $Z_0 = 0$ and $u_Z(t) = 0$ for all $t < T$ (due to Theorem 9). This leads to (4.4.50a) becoming $\dot{\varphi}_P(t) = -\beta(0)GS(t)f'(P(t)) < 0$ for all $t < T$, and thus $\varphi_P(t) > 0$. This fact, combined with $u_Z(t) = 0$ for all t and (4.4.9b) leads to $u_P(t) = 1$ for all t (i.e., $t^* = 0$ in the statement of Theorem 10).

Otherwise, we either have (i) $Z(T) = \frac{1}{2}[\frac{\beta_{\max}}{a} - \frac{G}{\gamma}] > 0$ or (ii) $Z(T) < \frac{1}{2}[\frac{\beta_{\max}}{a} - \frac{G}{\gamma}]$.

(i) In this case, from (4.3.5) (for which $\beta(Z) > 0$ and $G > 0$), Theorem 9 (which specifies $S(T) > 0$), and continuity of the states, we have $\dot{Z}(T^-) > 0$. Thus $Z(t) < \frac{1}{2}[\frac{\beta_{\max}}{a} - \frac{G}{\gamma}]$ for some (t'', T). Therefore, as $\dot{Z}(t) \geq 0$ for all t, so $Z(t) < \frac{1}{2}[\frac{\beta_{\max}}{a} - \frac{G}{\gamma}]$ for all $t < T$.

(ii) Since $\dot{Z} \geq 0$ from (4.3.5) and Theorem 9, in this case we also have $Z(t) < \frac{1}{2}[\frac{\beta_{\max}}{a} - \frac{G}{\gamma}]$ for all $t < T$.

Therefore for both (i) and (ii), $\gamma\beta_{\max} - 2\gamma a Z(t) - Ga > 0$ for all $t < T$.

From (4.4.54) and for all $t \in (t^*, T)$:

$$\dot{\varphi}_P(t) - \dot{\varphi}_Z(t) > -(\varphi_P - \varphi_Z)\beta(Z)[G + \gamma(Z + S)] \geq -(\varphi_P - \varphi_Z)M_{12},$$

for some $M_{12} > 0$ which is an upper-bound to the continuous $\beta(Z)[G + \gamma(Z + S)]$ over this interval. Therefore, for $t \in (t^*, T)$, $\varphi_P(t) - \varphi_Z(t) < [\varphi_P(T) - \varphi_Z(T)]e^{-M_{12}(t-T)} = 0$, and thus $\varphi_P(t) < \varphi_Z(t)$ for $t \in (t^*, T)$.

Due to the continuity of the states and co-states and because for $t \in (t^*, T)$, $\varphi_Z(t) > 0$, there exists an interval (t', T), with $t' \leq t^*$ such that both $\varphi_Z(t) > \varphi_P(t)$ and $\varphi_Z(t) > 0$. These conditions, coupled with (4.4.9c) lead to $u_P(t) = 0$ and $u_Z(t) = 1$ for all $t \in (t', T)$.

We now prove $t' = 0$. If this does not hold, either $\varphi_Z(t') = 0$ or $\varphi_Z(t') = \varphi_P(t')$ for some $t' > 0$ due to continuity of the states and co-states.

For $t \in (t', T)$ (4.4.50b) becomes:

$$\dot{\varphi}_Z(t) = -\beta(Z)GSf'(Z + P) - \varphi_Z\beta(Z)\gamma S < 0,$$

which leads to $\varphi_Z(t') > \varphi_Z(T) = 0$.

So we must have $\varphi_Z(t') = \varphi_P(t')$ for $t' > 0$. From (4.4.54) and the continuity of the states and co-states:

$$\begin{aligned}\big(\dot{\varphi}_P - \dot{\varphi}_Z\big)(t'^{+}) &= \varphi_P(t')S(t')\big[\gamma\beta_{\max} - 2\gamma a Z(t') - Ga\big] \\ &= \varphi_Z(t')S(t')\big[\gamma\beta_{\max} - 2\gamma a Z(t') - Ga\big] > 0,\end{aligned}$$

leading to the existence of an interval (t', t'') over which $\varphi_P(t) > \varphi_Z(t)$, a contradiction with the definition of t'.

Thus, $t' = 0$ and $u_Z(t) = 1$ and $u_P(t) = 0$ for all t, which agrees with the statement of Theorem 10. □

$Z(T) > \frac{1}{2}[\frac{\beta_{\max}}{a} - \frac{G}{\gamma}]$ Due to the continuity of the states, $Z(t) > \frac{1}{2}[\frac{\beta_{\max}}{a} - \frac{G}{\gamma}]$ for $t \in (t_1, T)$ for some t_1. Recall that for $t \in (t^*, T)$, $\varphi_P(t) > 0$. Thus, for $t \in (t_2, T)$, where $t_2 = \max\{t^*, t_1\}$ and with M_{12} again defined as the upper-bound to the continuous $\beta(Z)[G + \gamma(Z + S)]$, (4.4.54) leads to:

$$\dot{\varphi}_P(t) - \dot{\varphi}_Z(t) < -(\varphi_P - \varphi_Z)\beta(Z)[G + \gamma(Z + S)] \leq -(\varphi_P - \varphi_Z)M_{12}.$$

Therefore, in this interval, $\varphi_P(t) - \varphi_Z(t) > [\varphi_P(T) - \varphi_Z(T)]e^{-M_{12}(t-T)} = 0$, and thus $\varphi_P(t) > \varphi_Z(t)$ and $\varphi_P(t) > 0$ for $t \in (t_2, T)$.

Now, due to the continuity of the states and co-states, define (t_3, T) to be the maximal length interval over which $\varphi_P(t) > \max\{\varphi_Z(t), 0\}$. Note that for $t \in (t_3, T)$ we have $u_Z(t) = 0$ and $u_P(t) = 1$ due to (4.4.9b).

Due to continuity of the states and co-states, either $t_3 = 0$, in which case $u_Z(t) = 0$ and $u_P(t) = 1$ for all t (agreeing with the structure of Theorem 10), or we have a $t_3 > 0$ such that $\varphi_P(t_3) = 0$ or $\varphi_P(t_3) = \varphi_Z(t_3) > 0$.

From (4.4.50a), Theorem 9, and from the definition of t_3, for $t \in (t_3, T)$ we have:

$$\begin{aligned}\dot{\varphi}_P &= -\beta(Z)GSf'(Z+P) - (\varphi_P - \varphi_Z)\beta(Z)\gamma Z - aS\varphi_P\gamma Z \\ &< -aS\varphi_P\gamma Z \leq -M_{13}\varphi_P,\end{aligned}$$

for some $M_{13} > 0$ that is an upper-bound to the continuous $a_1 S\gamma Z$ over this interval. Thus,

$$\varphi_P(t_3) > \varphi_P(T)e^{-M_{13}(t_3 - T)} = 0.$$

So for $t_3 > 0$, we must have $\varphi_P(t_3) = \varphi_Z(t_3) > 0$. From the continuity of the states and co-states, there must exist an interval leading up to t_3 such that $\varphi_Z(t) > 0$ and $\varphi_P(t) > 0$. Let (t_4, t_3) be the maximal-length interval with such a property. Notice that (4.4.49) also applies, leading to $u_P(t) + u_Z(t) = 1$ for $t \in (t_4, t_3)$.

Furthermore, also from continuity, (4.4.54) becomes:

$$(\dot{\varphi}_P - \dot{\varphi}_Z)(t_3^+) = -a\varphi_P(t_3)S(t_3)\big[\gamma(2Z(t_3) - \frac{\beta_{\max}}{a}) + G\big] \tag{4.4.55}$$

But if $\dot{\varphi}_P(t_3^+) - \dot{\varphi}_Z(t_3^+) < 0$, then due to continuity and the definition of the derivative, we must have an interval starting from t_3 where $\varphi_Z(t) > \varphi_P(t)$, which contradicts the definition of t_3 (which stated that over an interval starting at t_3,

$\varphi_P(t) > \max\{\varphi_P(t), 0\}$). So we must have $\dot{\varphi}_P(t_3^+) - \dot{\varphi}_Z(t_3^+) \geq 0$. From (4.4.55) this is equivalent to $[\gamma(2Z(t_3) - \frac{\beta_{\max}}{a}) + G] \leq 0$, or $Z(t_3) \leq \frac{1}{2}[\frac{\beta_{\max}}{a} - \frac{G}{\gamma}]$.

Following the same set of arguments as presented in §4.4.6 for the case of $Z(T) \leq \frac{1}{2}[\frac{\beta_{\max}}{a} - \frac{G}{\gamma}]$ and retracing them for $Z(t_3) \leq \frac{1}{2}[\frac{\beta_{\max}}{a} - \frac{G}{\gamma}]$ (with t_3 replacing T in all arguments) shows that the structure postulated in Theorem 10 holds.

Thus, all possible state and co-state trajectories lead to the structure postulated in Theorem 10. □

Sigmoid $\beta(Z)$

Assume $\beta_Z = \dfrac{\beta_0}{1 + e^{\alpha(Z - Z_{th})}}$, with $0 < Z_{th} < 1$ being a fixed threshold and $\alpha > 0$ denoting the sharpness of the cut-off. This simulates a threshold-like detection of zombies by a network administrator. In this case, (4.4.50c) becomes:

$$\begin{aligned}\dot{\varphi}_P - \dot{\varphi}_Z =& -(\varphi_P - \varphi_Z)\beta(Z)[G(u_Z + u_P) + \gamma(Z + S)] \\ &+ \frac{\beta_0 \gamma \varphi_P S\left[e^{\alpha(Z - Z_{th})}(1 - \frac{\alpha}{\gamma}G(u_z + u_P) - \alpha Z) + 1\right]}{(1 + e^{\alpha(Z - Z_{th})})^2}\end{aligned} \tag{4.4.56}$$

Define: $\Psi(Z, u_Z + u_P) := e^{\alpha(Z - Z_{th})}(1 - \frac{\alpha}{\gamma}G(u_z + u_P) - \alpha Z) + 1$. Then (4.4.56) becomes:

$$\begin{aligned}\dot{\varphi}_P - \dot{\varphi}_Z =& -(\varphi_P - \varphi_Z)\beta(Z)[G(u_Z + u_P) + \gamma(Z + S)] \\ &+ \frac{\beta_0 \gamma \varphi_P S}{(1 + e^{\alpha(Z - Z_{th})})^2}\Psi(Z, u_Z + u_P)\end{aligned} \tag{4.4.57}$$

Now, for possible intervals where $u_Z + u_P$ is a constant $c \in [0, 1]$, $\Psi(Z, c)$ is a function of one variable (Z). We can see that at points of continuity of the controls and

in intervals where it is defined, $\Psi(Z, c)$ is also continuous and differentiable. Furthermore, we can see that at points of continuity of the controls in these intervals, we have:

$$\frac{d\Psi(Z,c)}{dZ} = -\alpha^2 e^{\alpha(Z-Z_{th})}(\frac{G}{\gamma}c + Z) < 0 \tag{4.4.58}$$

Now we break down the situations that can arise based on the value of $\Psi(Z(T), 1)$:

$\Psi(Z(T), 1) > 0$ From $\dot{Z} \geq 0$ ((4.3.5) and Theorem 9) and the continuity of the states, we have $Z(t) \leq Z(T)$ for all t. Now for $t \in (t^*, T)$, as the sum of the controls is constant and equal to one due to (4.4.52), we will have $\Psi(Z(t), 1) \geq \Psi(Z(T), 1) > 0$ due to (4.4.58). Thus from (4.4.57) and for all $t \in (t^*, T)$ at which the controls are continuous:

$$\dot{\varphi}_P(t) - \dot{\varphi}_Z(t) > -(\varphi_P - \varphi_Z)\beta(Z)[G + \gamma(Z + S)] \geq -(\varphi_P - \varphi_Z)M_{14},$$

for some $M_{14} > 0$ which is an upper-bound to the continuous $\beta(Z)[G+\gamma(Z+S)]$. Therefore, for $t \in (t^*, T)$, $\varphi_P(t) - \varphi_Z(t) < [\varphi_P(T) - \varphi_Z(T)]e^{-M_{14}(t-T)} = 0$, and thus $\varphi_P(t) < \varphi_Z(t)$ for $t \in (t^*, T)$.

Due to the continuity of the states and co-states and from the definition of t^*, there exists an interval (t', T), with $t' \leq t^*$ such that $\varphi_Z(t) > \varphi_P(t)$ and $\varphi_Z(t) > 0$. These conditions, coupled with (4.4.9c) lead to $u_P(t) = 0$ and $u_Z(t) = 1$ for all $t \in (t', T)$, with the corollary that $u_P(t) + u_Z(t) = 1$.

We now prove $t' = 0$. If this does not hold, either $\varphi_Z(t') = 0$ or $\varphi_Z(t') = \varphi_P(t') > 0$ for $t' > 0$ due to continuity of the states and co-states.

For $t \in (t', T)$, as $u_P(t) = 0$, (4.4.50b) becomes:

$$\dot{\varphi}_Z(t) = -\beta(Z)GSf'(Z+P) - \varphi_Z\beta(Z)\gamma S < 0,$$

as each term in the right hand side is strictly positive in the interval. Now, if we have $\varphi_Z(t') = 0$, from this time-derivative and continuity of the states and co-states we must have $\varphi_Z(t') > \varphi_Z(T) = 0$. Thus, $\varphi_Z(t') = 0$ is ruled out.

On the other hand, if $\varphi_Z(t') = \varphi_P(t') > 0$, then from (4.4.57) and the continuity of the states and co-states:

$$\big(\dot{\varphi}_P - \dot{\varphi}_Z\big)(t'^+) = \frac{\beta_0\gamma\varphi_P(t')S(t')}{(1+e^{\alpha(Z(t')-Z_{th})})^2}\Psi(Z(t'),1) > 0$$

leading to the existence of an interval (t', t'') over which $\varphi_P(t) > \varphi_Z(t)$, a contradiction with the definition of t'.

Thus, $t' = 0$ and $u_Z(t) = 1$ and $u_P(t) = 0$ for all t, which agrees with the statement of Theorem 10.

$\Psi(Z(T),1) = 0$ **and** $Z(T) > 0$ We have $\dot{Z}(T^-) > 0$ (from (4.3.5), Theorem 9, and continuity) which leads to $Z(t) < Z(T)$ for an interval leading up to t. As $\dot{Z} \geq 0$, we can extend $Z(t) < Z(T)$ to all t. Now for $t \in (t^*, T)$, from (4.4.52), we will have $\Psi(Z(t),1) > \Psi(Z(T),1) = 0$ due to (4.4.58). We now prove $t' = 0$ and $u_Z(t) = 1$ and $u_P(t) = 0$ for all t.

From (4.4.52), (4.4.57), for all $t \in (t^*, T)$ (over which $\varphi_P(t) > 0$):

$$\dot{\varphi}_P(t) - \dot{\varphi}_Z(t) > -(\varphi_P - \varphi_Z)\beta(Z)[G + \gamma(Z+S)] \geq -(\varphi_P - \varphi_Z)M_{12},$$

for some $M_{12} > 0$ which is an upper-bound to the continuous $\beta(Z)[G + \gamma(Z + S)]$ over this interval. Therefore, for $t \in (t^*, T)$, $\varphi_P(t) - \varphi_Z(t) < [\varphi_P(T) - \varphi_Z(T)]e^{-M_{12}(t-T)} = 0$, and thus $\varphi_P(t) < \varphi_Z(t)$ for $t \in (t^*, T)$.

Due to the continuity of the states and co-states and because for $t \in (t^*, T)$, $\varphi_Z(t) > 0$, there exists an interval (t', T), with $t' \leq t^*$ such that both $\varphi_Z(t) > \varphi_P(t)$ and $\varphi_Z(t) > 0$. These conditions, coupled with (4.4.9c) lead to $u_P(t) = 0$ and $u_Z(t) = 1$ for all $t \in (t', T)$.

We now prove $t' = 0$. If this does not hold, either (i) $\varphi_Z(t') = 0$ or (ii) $\varphi_Z(t') = \varphi_P(t')$ for some $t' > 0$ due to continuity of the states and co-states.

For $t \in (t', T)$ (4.4.50b) becomes:

$$\dot{\varphi}_Z(t) = -\beta(Z)GSf'(Z + P) - \varphi_Z\beta(Z)\gamma S < 0,$$

which leads to $\varphi_Z(t') > \varphi_Z(T) = 0$.

So for $t' > 0$ we must have $\varphi_Z(t') = \varphi_P(t')$. From (4.4.57) and the continuity of the states and co-states:

$$\begin{aligned}\big(\dot{\varphi}_P - \dot{\varphi}_Z\big)(t'^+) &= \frac{\beta_0\gamma\varphi_P(t')S(t')}{(1 + e^{\alpha(Z(t')-Z_{th})})^2}\Psi(Z(t'), 1) \\ &= \frac{\beta_0\gamma\varphi_Z(t')S(t')}{(1 + e^{\alpha(Z(t')-Z_{th})})^2}\Psi(Z(t'), 1) > 0,\end{aligned}$$

leading to the existence of an interval (t', t'') over which $\varphi_P(t) > \varphi_Z(t)$, a contradiction with the definition of t'.

Thus, $t' = 0$ and $u_Z(t) = 1$ and $u_P(t) = 0$ for all t, which agrees with the statement of Theorem 10. □

$\Psi(Z(T),1) = 0$ **and** $Z(T) = 0$ We must have $\dot{Z}(t) = 0$ for all t as $\dot{Z} \geq 0$ and as states are continuous. The only way for $\dot{Z}(t) = 0$ for all t is for us to have $Z_0 = 0$ and $u_Z(t) = 0$ for all $t < T$ (due to Theorem 9). This leads to (4.4.50a) becoming $\dot{\varphi}_P(t) = -\beta(0)GS(t)f'(P(t)) < 0$ for all $t < T$, and thus $\varphi_P(t) > 0$. This fact, combined with $u_Z(t) = 0$ for all t and (4.4.9b) leads to $u_P(t) = 1$ for all t.

$\Psi(Z(T),1) < 0$ Due to the continuity of the states, $\Psi(Z(t),1) < 0$ for $t \in (t_1, T)$ for some t_1. Thus, (4.4.57) leads to $\dot{\varphi}_P(t) - \dot{\varphi}_Z(t) < -(\varphi_P - \varphi_Z)\beta(Z)[G + \gamma(Z + S)] \leq -(\varphi_P - \varphi_Z)M_{12}$, for $t \in (t_2, T)$, where $t_2 = \max\{t^*, t_1\}$ and with M_{12} defined as before (an upper-bound to the continuous $\beta(Z)[G+\gamma(Z+S)]$ over this interval). Therefore, in this interval, $\varphi_P(t) - \varphi_Z(t) > [\varphi_P(T) - \varphi_Z(T)]e^{-M_{12}(t-T)} = 0$, and thus $\varphi_P(t) > \varphi_Z(t)$ and $\varphi_P(t) > 0$ for $t \in (t_2, T)$.

Now, due to the continuity of the states and co-states, define (t_3, T) to be the maximal length interval over which $\varphi_P(t) > \varphi_Z(t)$ and $\varphi_P(t) > 0$. Note that for $t \in (t_3, T)$ we have (due to (4.4.9b)) $u_Z(t) = 0$ and $u_P(t) = 1$.

Due to continuity of the states and co-states, either $t_3 = 0$, in which case $u_Z(t) = 0$ and $u_P(t) = 1$ for all t, or we have a $t_3 > 0$ such that (i) $\varphi_P(t_3) = 0$ or (ii) $\varphi_P(t_3) = \varphi_Z(t_3) > 0$.

From (4.4.50a), Theorem 9, and from the definition of t_3, for $t \in (t_3, T)$ we

have:

$$\dot{\varphi}_P = -\beta(Z)GSf'(Z+P) - (\varphi_P - \varphi_Z)\beta(Z)\gamma Z - \frac{\alpha\beta_0\gamma e^{\alpha(Z-Z_{th})}}{(1+e^{\alpha(Z-Z_{th})})^2}S\varphi_P Z$$
$$< -\frac{\alpha\beta_0\gamma e^{\alpha(Z-Z_{th})}SZ}{(1+e^{\alpha(Z-Z_{th})})^2}\varphi_P \quad \leq -M_{15}\varphi_P,$$

for some $M_{15} > 0$ that is an upper-bound to the continuous $\frac{\alpha\beta_0\gamma e^{\alpha(Z-Z_{th})}SZ}{(1+e^{\alpha(Z-Z_{th})})^2}$. Thus, $\varphi_P(t_3) > \varphi_P(T)e^{-M_{15}(t_3-T)} = 0$.

So for $t_3 > 0$ we must have $\varphi_P(t_3) = \varphi_Z(t_3) > 0$. From the continuity of the states and co-states, there must exist an interval leading up to t_3 such that $\varphi_Z(t) > 0$ and $\varphi_P(t) > 0$. Let (t_4, t_3) be the maximal-length interval with such a property. Notice that (4.4.49) also applies, leading to $u_P(t) + u_Z(t) = 1$ for $t \in (t_4, t_3)$.

Furthermore, also from continuity, (4.4.57) becomes:

$$\dot{\varphi}_P(t_3^+) - \dot{\varphi}_Z(t_3^+) = \frac{\beta_0\gamma\varphi_P(t_3)S(t_3)}{(1+e^{\alpha(Z(t_3)-Z_{th})})^2}\Psi(Z(t_3),1) \tag{4.4.59}$$

But if $\dot{\varphi}_P(t_3^+) - \dot{\varphi}_Z(t_3^+) < 0$, then due to continuity and the definition of the derivative, we must have an interval starting from t_3 where $\varphi_Z(t) > \varphi_P(t)$, which contradicts the definition of t_3. So we must have $\dot{\varphi}_P(t_3^+) - \dot{\varphi}_Z(t_3^+) \geq 0$. From (4.4.55) this is equivalent to $\Psi(Z(t_3),1) \geq 0$.

Following the same set of arguments as presented in §4.4.6, §4.4.6, and §4.4.6 for the case of $\Psi(Z(T),1) \geq 0$ and retracing them for $\Psi(Z(t_3),1) \geq 0$ (with t_3 replacing T in all arguments) shows that the structure postulated in Theorem 10 holds.

Thus, all possible state and co-state trajectories lead to the structure postulated in Theorem 10.

□

4.5 Simulation

In the preceding sections, we showed that the optimal spreading controls of the malware in all of the described settings can be fully described by a scalar parameter t^*. In this section, we investigate the variation of t^* with respect to some system parameters and then compare the relative performance of the optimal spreading controls with simple heuristics (§4.5.1). In these studies, the main parameter of variation is γ, as a higher γ indicates that zombies spread at a faster rate than infection via germination, and thus γ represents a measure of the virility of the zombie malware variant. Varying γ changes the relative contact rates internal to the model and thus represents different possible dynamics of a malware attack. In contrast, varying β, the contact rate of germinators and susceptibles, changes the number of contacts across the board, which is equivalent to changing T. Thus any variation of β would only show how t^* changes for a specific epidemic. Finally, we numerically investigate the fragility of the optimal control to network estimation errors in the adaptive defense model and to synchronization errors among germinators (§4.5.2).

4.5.1 Structure of the optimal malware spread controls and their performance vs heuristics

We first computed t^* (the optimal switching time) as a function of the relative spread rate of the zombies γ for the problems in §4.3.1 and §4.3.2 (with different values of halting efficacy π), as well as the optimal controls, for a cost function for which both Theorem 10 and 11 apply (Figure 4.2). As γ increases, zombies are created for a shorter period due to the rapid explosion of their population later on. Furthermore, the addition of a halting control and its increased efficacy leads to the attacker creating zombies for longer, as she can control their spread (and thus their visibility) later on using the halting control.

We then compared the cost of these two optimal controls to that of simple heuristics: for the model in §4.3.1, *Always Zombie* and *Always Passive* represent the two most extreme policies - *Always Zombie* sets $u_Z(t) = 1$ and $u_P(t) = 0$ for all times, while *Always Passive* does the exact opposite. Thus, in these heuristics the germinators only ever propagate one fixed type of malware variant. In the *Optimal Static Mixing* heuristic, the attacker chooses a fixed ratio for u_Z and u_P at all times. Our optimal controls are titled *No Halting* and *Halting*, the latter indexed by the value of π (which represents the relative success of the germinators in halting zombies). The efficacy of the policies is evaluated as γ, the relative propagation rate of the zombies is varied (Figure 4.3, which is presented for the

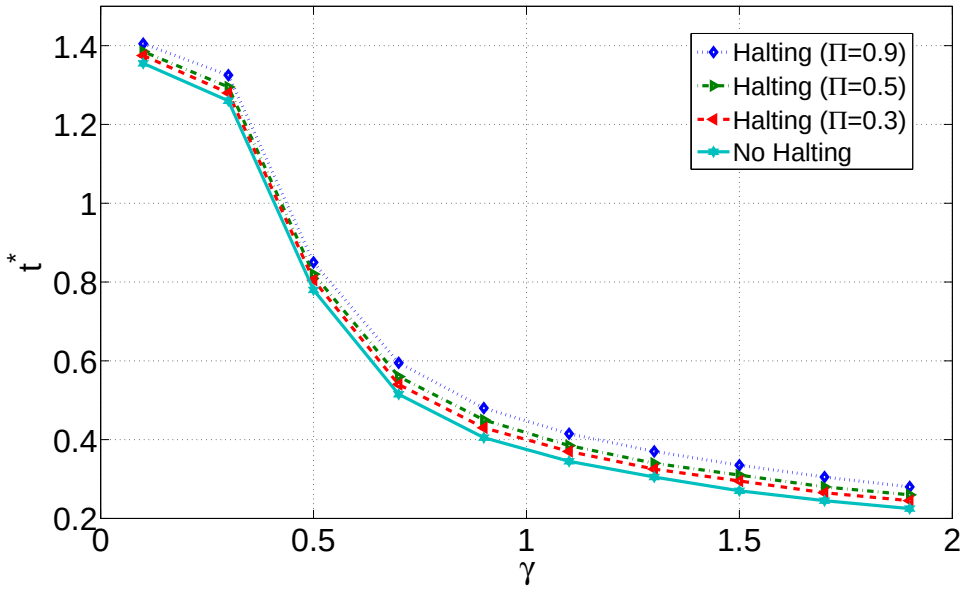

Figure 4.2: We compared t^* (the length of time the zombie control u_Z was equal to one) for the optiml no halting and halting controls as the secondary rate of spread of the zombies (γ) was varied. Here, $\beta = 2$, $T = 5$,$(S_0, G_0, Z_0, P_0) = (0.99, 0.01, 0, 0)$, $f(x) = x^{0.5}$, and $g(x) = k_g x = 0.7x$.

same parameters as those used in Figure 4.2).

The optimal controls perform much better than the heuristics, with the halting control outperforming the no-halting control for by as much as 10% for large values of π (where the halting control is efficient) and γ (where the zombie variant propagation is rapid), both factors which penalize sub-optimal decision-making. This vindicates the assumption that the attacker would be wise to utilize the halting control were it to be available. Out of the simple heuristics, optimal static mixing has the maximum utility, which is typically 10% below that of even the no-halting optimal control.

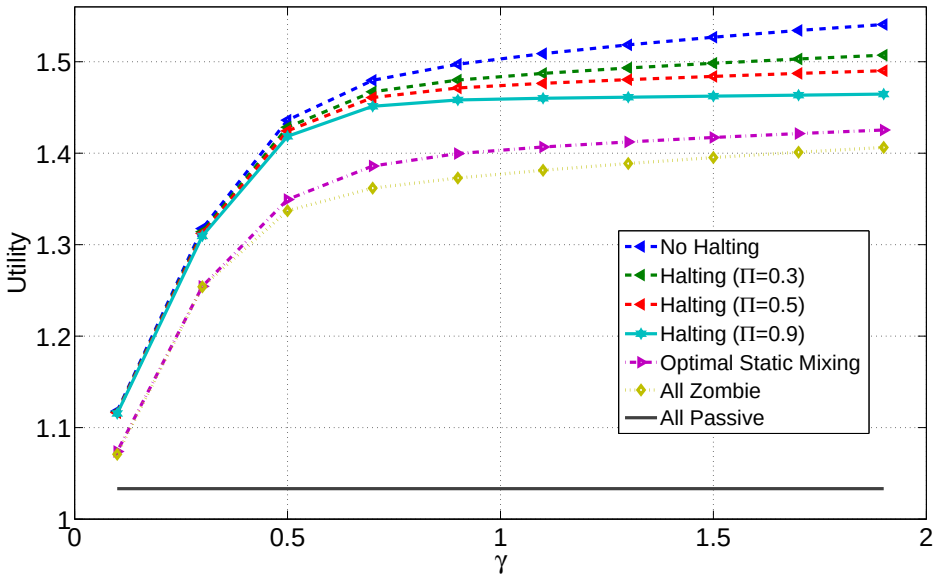

Figure 4.3: Comparison of the damage utilities across the optimal controls and heuristics for the parameters of Fig. 4.2.

4.5.2 Fragility of the optimal damage to network estimation errors and synchronization errors in the germinators

We then investigated how the optimal control would fare when the network, which is capable of adaptive defense (i.e., the model in §4.3.3), has an erroneous estimate of the fraction of zombies, and (Figure 4.4). The optimal attack policy is derived with the assumption that the network's defense policy is based on the correct observation of the visibility of the epidemic (i.e., the fraction of zombies), information that is rarely available. Figure 4.4 shows that the optimal control is remarkably robust to the network's estimation errors up, with an error of 5% even when the estimation error is 40%. In many cases, the performance is much better.

Finally, we examined how synchronization errors among germinators would affect the utility of the malware. One of the benefits of the malware spread models was that they assumed that only this small fraction of nodes, which is under the direct control of the attacker, has to coordinate their actions. To examine the fragility of the optimal control to this coordination, once the optimal policy is derived, random errors are introduced to the clocks of the germinators, and the resulting utilities are compared over 100 runs of the simulation (Figure 4.5). As can be seen, the damage of both the no halting ($\pi = 0$) and halting ($\pi = 0.5$) cases is distributed around the damage obtained by the calculated optimal control, and only suffers a 10-15% performance drop for synchronization errors of up to 30%

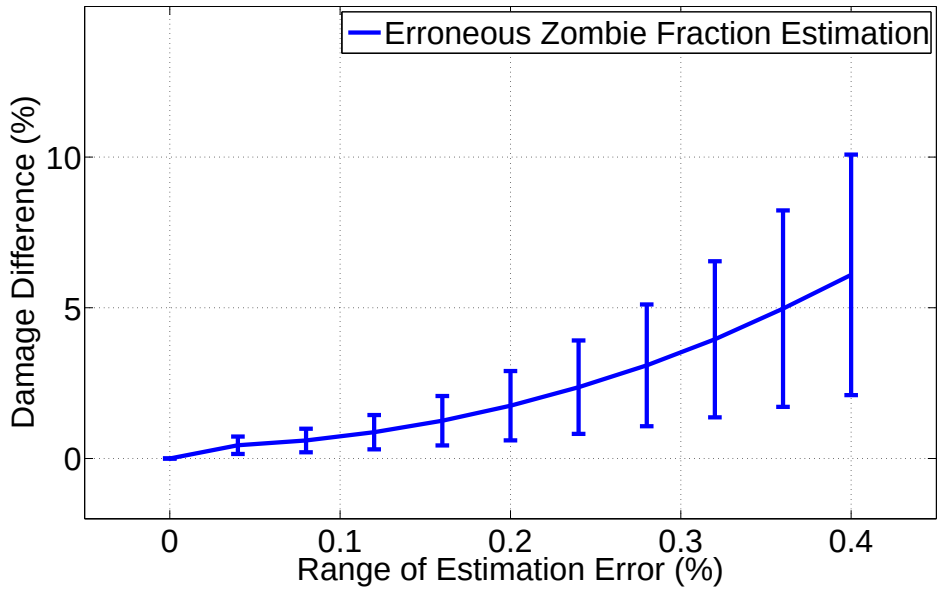

Figure 4.4: The network was assumed to make unbiased random estimation errors at each time instant with the range depicted on the x-axis. The solid line shows the average difference in damage relative to the optimal over 50 runs of the estimating network. Here, we used an exponential sigmoid $\beta(Z)$ with $\beta_0 = 1$, $\alpha = 100$, $T = 15$, $\gamma = 1.4$, $Z_{th} = 0.01$, $(S_0, G_0, Z_0, P_0) = (0.999, 0.001, 0, 0)$, and $f(x) = x^{0.9}$.

of t^* in the small number of germinators.

Furthermore, it can be seen that the synchronized infinite-node optimal control can actually perform slightly worse than the case where there are synchronization errors on a finite number of nodes, even in the mean. We can explain this as follows: in the previous sections, we characterized the optimal solution for the problem in §4.3.6 under the assumption that the number of nodes was infinite. For a finite number of nodes, even without synchronization errors, the damage sustained by the simulated network can be different from (and potentially less than) that computed using the computational optimal control framework.

These studies lead to the conclusion that an adversary will not be deterred by the possibility of errors in estimation and synchronization of the malware spread, further sounding the alarm about the emerging trend of visibility-aware malware.

4.6 Conclusion

We investigated the coordinated spread of malware variants in computer networks by focusing on the *heterogeneity* of these malware in terms of visibility to the network. We showed that policies that optimize the stealth-spread trade-off for a variety of malware variant models and objectives (with and without network defense) have very simple structures. In such optimal policies, only one variant of the malware is propagated at each point in time by all nodes under the attacker's control. Furthermore, the variant being spread changing abruptly at one and only

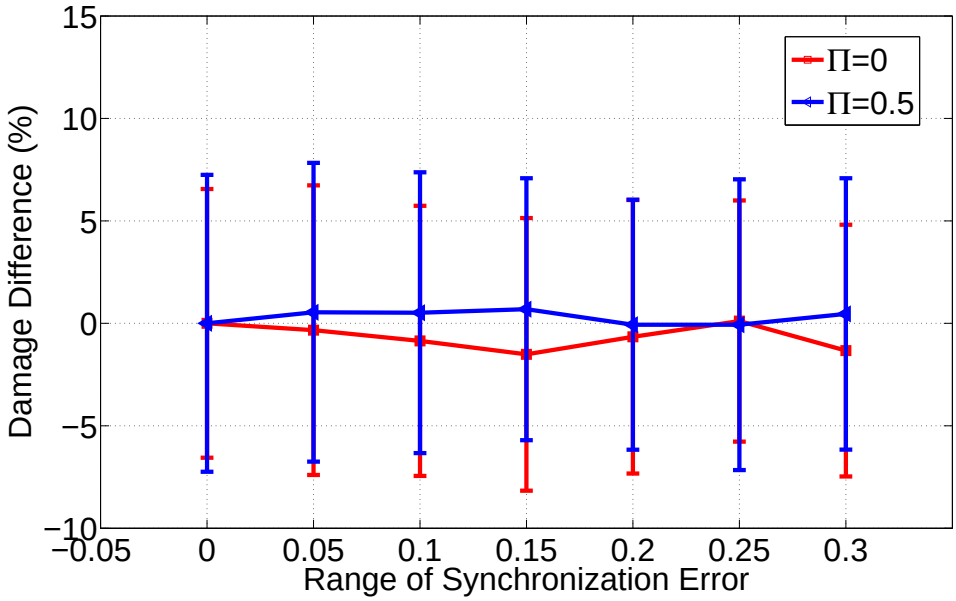

Figure 4.5: Germinators were assumed to have unbiased random synchronization errors at each time instant with the range depicted on the x-axis. The lines shows average damage over 100 runs with unsynchronized germinators. Here, $\beta = 2$, $\gamma = 0.5$, $T = 5$, $(S_0, G_0, Z_0, P_0) = (0.99, 0.01, 0, 0)$, $f(x) = x^{0.5}$, and $g(x) = k_g x = 0.7x$, and the simulation was run for 500 nodes (i.e., 5 germinators).

one instance in time, with spread being prioritized beforehand and stealth being prioritized afterwards. Finally, we showed through simulations that such optimal policies that are simple to compute, store, and implement provide a significant gain over naive heuristics and are also robust to clock synchronization errors and errors in network defense policies, underlining the threat posed by such policies.

Chapter 5

Summary and Future Directions

In this thesis, we examined the role of heterogeneity in the spread and control of epidemics. We first presented a taxonomy of heterogeneity, showing that heterogeneity can be manifested in contact rates, resources, and epidemics. In subsequent chapters, we sought to develop a theory of the optimal control of each of these types of heterogeneous epidemics by focusing on a particular problem within the domain. We showed that optimal patching controls against malware in a *rate-heterogeneous* epidemic, for classes of defenders that have different sensitivities to infection and differing control mechanisms at their disposal follow simple, implementable structures irrespective of the network topology and can result in significant benefits to the network. We showed that message delivery in a a Delay-Tolerant Network can be modeled as a *resource-heterogeneous* epidemic, focusing on a case where resource-heterogeneity results from differences in the

remaining energy of nodes. We proved that in such settings, optimal forwarding policies follow simple threshold-based structures, and in certain cases have an innate ordering. Finally, we showed that the spread of malware variants with differing visibility to the network can be modeled as a case where the *epidemic* itself is *heterogeneous*. We showed that the stealth-spread trade-off is optimized by simple threshold-based policies that are robust to errors in implementation and system parameters.

In Chapter 2, we proved structure for optimal patching controls regardless of network topology. The use of information gathered from particular topologies to restrict the policy search space is a promising avenue for future work. Furthermore, more efficient computational methods to compute the thresholds will also be crucial in practice. Finally, the contact rates among different types may not be fully known, so efficient computation of these rates from real-world data and trading off the estimation error against the sub-optimality losses that would arise from running our policies on noisy contact-rate data is a critical avenue for future work.

In Chapter 3, our analysis targeted the transmission of a single message, and our simulations reveal that a natural generalization of the corresponding optimal policy substantially outperforms heuristics even for sequential transmission of multiple messages. It would be of interest to characterize the optimal policy in this case and also for the transmission of multiple messages with overlap-

ping time-to-live intervals. Next, in order to attain an adequate balance between tractability and emulation of reality, we abstracted certain features that arise in practice. A case in point is that we ignored the energy dissipated in scanning the media in search of new nodes. We also assumed homogeneous mixing, i.e., the inter-contact times are similarly distributed for all pairs of nodes. Future research may be directed towards generalizing the analytical results for models that relax the above assumptions (e.g., with the rate-heterogeneous model of the previous chapter). Similarly, we demonstrated using simulations that our optimal control policy is robust to clock synchronization errors and also errors in the determination of a node's residual energy level. Designing policies that are provably robust to the above errors as per some formal robustness metric remains open.

In Chapter 4 we investigated the optimal controls for the SGZP model with and without halting with no explicit network defense (§4.3.1 and 4.3.2), and without halting for the case with adaptive network defense (§4.3.3). This leaves open the case of the SGZP model with halting and adaptive defense. Initial analytical investigations show that Theorem 11 is likely generalizable to this case, barring some technical issues that will be investigated in the future. The set-up and formulation of the visibility problem is, to the best of our knowledge, novel, and thus leads itself to analysis both in the mean-field regime and in more structured settings. In particular, in the mean-field case, possible patching will be addressed at a later stage, as well as the dynamic game that would result from such a competition.

Another possible direction is to look at the optimal control of such an epidemic in sub-populations with differentiating characteristics (e.g., location, contact rate). Such a generalization would better model Stuxnet in particular, with the goal being to maximize the number of infected agents in a particular region, while minimizing the total number of detectable zombies.

Bibliography

[1] E. Altman, A. P. Azad, T. Basar, and F. De Pellegrini, "Optimal activation and transmission control in delay tolerant networks," in *INFOCOM, 2010 Proceedings IEEE*. IEEE, 2010, pp. 1–5.

[2] E. Altman, G. Neglia, F. De Pellegrini, and D. Miorandi, "Decentralized stochastic control of delay tolerant networks," in *INFOCOM 2009, IEEE*. IEEE, 2009, pp. 1134–1142.

[3] M. Altunay, S. Leyffer, J. Linderoth, and Z. Xie, "Optimal response to attacks on the open science grid," *Computer Networks*, 2010.

[4] R. Anderson, C. Barton, R. Böhme, R. Clayton, M. van Eeten, M. Levi, T. Moore, and S. Savage, "Measuring the cost of cybercrime." in *WEIS*, 2012.

[5] H. Andersson and T. Britton, *Stochastic epidemic models and their statistical analysis*. Springer New York, 2000, vol. 151.

[6] M. Bailey, E. Cooke, F. Jahanian, and D. Watson, "The blaster worm: Then and now," *Security & Privacy, IEEE*, vol. 3, no. 4, pp. 26–31, 2005.

[7] A. Balasubramanian, B. Levine, and A. Venkataramani, "Dtn routing as a resource allocation problem," in *ACM SIGCOMM Computer Communication Review*, vol. 37, no. 4. ACM, 2007, pp. 373–384.

[8] F. Ball and D. Clancy, "The final size and severity of a generalised stochastic multitype epidemic model," *Advances in applied probability*, pp. 721–736, 1993.

[9] N. Banerjee, M. Corner, and B. Levine, "Design and field experimentation of an energy-efficient architecture for dtn throwboxes," *Networking, IEEE/ACM Transactions on*, vol. 18, no. 2, pp. 554–567, 2010.

[10] H. Behncke, "Optimal control of deterministic epidemics," *Optimal control applications and methods*, vol. 21, no. 6, pp. 269–285, 2000.

[11] B. Bencsáth, G. Pék, L. Buttyán, and M. Félegyházi, "The cousins of stuxnet: Duqu, flame, and gauss," *Future Internet*, vol. 4, no. 4, pp. 971–1003, 2012.

[12] D. Benson, G. Huntington, T. Thorvaldsen, and A. Rao, "Direct trajectory optimization and costate estimation via an orthogonal collocation method," *Journal of Guidance Control and Dynamics*, vol. 29, no. 6, p. 1435, 2006.

[13] D. Bernoulli and S. Blower, "An attempt at a new analysis of the mortality caused by smallpox and of the advantages of inoculation to prevent it," *Reviews in Medical Virology*, vol. 14, no. 5, pp. 275–288, 2004.

[14] B. Bollobás, *Modern graph theory*. Springer Verlag, 1998, vol. 184.

[15] T. M. Chen and S. Abu-Nimeh, "Lessons from stuxnet," *Computer*, vol. 44, no. 4, pp. 91–93, 2011.

[16] Z. Chen and C. Ji, "Spatial-temporal modeling of malware propagation in networks," *IEEE Transactions on Neural Networks*, vol. 16, no. 5, pp. 1291–1303, 2005.

[17] D. J. Daley, J. Gani, and J. M. Gani, *Epidemic modelling: an introduction*. Cambridge University Press, 2001, vol. 15.

[18] D. Daley and D. G. Kendall, "Stochastic rumours," *IMA Journal of Applied Mathematics*, vol. 1, no. 1, pp. 42–55, 1965.

[19] E. de Oliveira and C. de Albuquerque, "Nectar: a dtn routing protocol based on neighborhood contact history," in *Proceedings of the 2009 ACM symposium on Applied Computing*. ACM, 2009, pp. 40–46.

[20] F. De Pellegrini, E. Altman, and T. Başar, "Optimal monotone forwarding policies in delay tolerant mobile ad hoc networks with multiple classes of nodes," in *IEEE WiOpt'10*, 2010, pp. 497–504.

[21] S. Eshghi, M. Khouzani, S. Sarkar, N. B. Shroff, and S. S. Venkatesh, "Optimal energy-aware epidemic routing in dtns," *IEEE Transactions on Automatic Control*, vol. 60, no. 6, pp. 1554–1569, 2015.

[22] S. Eshghi, M. Khouzani, S. Sarkar, and S. S. Venkatesh, "Optimal patching in clustered malware epidemics," *IEEE Transactions on Networking*, 2014.

[23] S. Eshghi, S. Sarkar, and S. S. Venkatesh, "Visibility-aware optimal contagion of malware epidemics," *arXiv preprint arXiv:1507.03528*, 2015.

[24] M. Faghani and H. Saidi, "Malware propagation in online social networks," in *4th IEEE International Conference on Malicious and Unwanted Software (MALWARE)*, 2009, pp. 8–14.

[25] N. Falliere, L. O. Murchu, and E. Chien, "W32. stuxnet dossier," *White paper, Symantec Corp., Security Response*, 2011.

[26] G. Feichtinger, R. F. Hartl, and S. P. Sethi, "Dynamic optimal control models in advertising: recent developments," *Management Science*, vol. 40, no. 2, pp. 195–226, 1994.

[27] M. Garetto, W. Gong, and D. Towsley, "Modeling malware spreading dynamics," in *INFOCOM 2003. Twenty-Second Annual Joint Conference of the IEEE Computer and Communications. IEEE Societies*, vol. 3. IEEE, 2003, pp. 1869–1879.

[28] D. Garg, W. Hager, and A. Rao, "Pseudospectral methods for solving infinite-horizon optimal control problems," *Automatica*, vol. 47, no. 4, pp. 829–837, 2011.

[29] D. Garg, M. Patterson, W. Hager, A. Rao, D. Benson, and G. Huntington, "A unified framework for the numerical solution of optimal control problems using pseudospectral methods," *Automatica*, vol. 46, no. 11, pp. 1843–1851, 2010.

[30] D. Garg, M. Patterson, C. Francolin, C. Darby, G. Huntington, W. Hager, and A. Rao, "Direct trajectory optimization and costate estimation of finite-horizon and infinite-horizon optimal control problems using a radau pseudospectral method," *Computational Optimization and Applications*, vol. 49, no. 2, pp. 335–358, 2011.

[31] N. Gast and B. Gaujal, "A mean field approach for optimization in discrete time," *Discrete Event Dynamic Systems*, vol. 21, no. 1, pp. 63–101, 2011.

[32] N. Gast, B. Gaujal, and J. Le Boudec, "Mean field for Markov decision processes: from discrete to continuous optimization," *Arxiv preprint arXiv:1004.2342*, 2010.

[33] R. Groenevelt, P. Nain, and G. Koole, "The message delay in mobile ad hoc networks," *Performance Evaluation*, vol. 62, no. 1, pp. 210–228, 2005.

[34] K. J. Hall, "Thwarting network stealth worms in computer networks through biological epidemiology," Ph.D. dissertation, Citeseer, 2006.

[35] W. H. Hamer, *The Milroy lectures on epidemic disease in England: the evidence of variability and of persistency of type*. Bedford Press, 1906.

[36] H. W. Hethcote and P. Waltman, "Optimal vaccination schedules in a deterministic epidemic model," *Mathematical Biosciences*, vol. 18, no. 3, pp. 365–381, 1973.

[37] P. Hui, A. Chaintreau, J. Scott, R. Gass, J. Crowcroft, and C. Diot, "Pocket switched networks and human mobility in conference environments," in *ACM SIGCOMM Workshop on Delay-tolerant Networking*. ACM, 2005, p. 251.

[38] IFRC, "The link between tuberculosis and hiv."

[39] K. Kandhway and J. Kuri, "How to run a campaign: Optimal control of sis and sir information epidemics," *Applied Mathematics and Computation*, vol. 231, pp. 79–92, 2014.

[40] B. Karrer and M. Newman, "Competing epidemics on complex networks," *Physical Review E*, vol. 84, no. 3, p. 036106, 2011.

[41] W. Kendall and I. Saunders, "Epidemics in competition ii: the general epidemic," *Journal of the Royal Statistical Society. Series B (Methodological)*, pp. 238–244, 1983.

[42] J. O. Kephart and S. R. White, "Directed-graph epidemiological models of computer viruses," in *Research in Security and Privacy, 1991. Proceedings., 1991 IEEE Computer Society Symposium on*. IEEE, 1991, pp. 343–359.

[43] W. O. Kermack and A. G. McKendrick, "Contributions to the mathematical theory of epidemics. ii. the problem of endemicity," *Proceedings of the Royal society of London. Series A*, vol. 138, no. 834, pp. 55–83, 1932.

[44] M. Khouzani, S. Eshghi, S. Sarkar, N. B. Shroff, and S. S. Venkatesh, "Optimal energy-aware epidemic routing in dtns," in *Proceedings of the thirteenth ACM international symposium on Mobile Ad Hoc Networking and Computing*. ACM, 2012, pp. 175–182.

[45] M. Khouzani, S. Sarkar, and E. Altman, "Dispatch then stop: Optimal dissemination of security patches in mobile wireless networks," in *IEEE CDC'10*, 2010, pp. 2354–2359.

[46] ——, "Optimal control of epidemic evolution," in *IEEE INFOCOM*, 2011.

[47] M. Khouzani and S. Sarkar, "Dynamic malware attack in energy-constrained mobile wireless networks," in *Information Theory and Applications Workshop (ITA), 2010*. IEEE, 2010, pp. 1–11.

[48] ——, "Maximum damage battery depletion attack in mobile sensor networks," *Automatic Control, IEEE Transactions on*, vol. 56, no. 10, pp. 2358–2368, 2011.

[49] M. Khouzani, S. Sarkar, and E. Altman, "A dynamic game solution to malware attack," in *INFOCOM, 2011 Proceedings IEEE*. IEEE, 2011, pp. 2138–2146.

[50] ——, "Maximum damage malware attack in mobile wireless networks," *IEEE/ACM Transactions on Networking (TON)*, vol. 20, no. 5, pp. 1347–1360, 2012.

[51] J. Kim, S. Radhakrishnan, and S. K. Dhall, "Measurement and analysis of worm propagation on internet network topology," in *Computer Communications and Networks, 2004. ICCCN 2004. Proceedings. 13th International Conference on*. IEEE, 2004, pp. 495–500.

[52] T. Kurtz, "Solutions of ordinary differential equations as limits of pure jump markov processes," *Journal of Applied Probability*, pp. 49–58, 1970.

[53] R. Langner, "Stuxnet: Dissecting a cyberwarfare weapon," *Security & Privacy, IEEE*, vol. 9, no. 3, pp. 49–51, 2011.

[54] H. Leyden, "Blaster variant offers a fix for pox-ridden pcs," *http://www.theregister.co.uk/2003/08/19/blaster_variant_offers_fix/*, 2003.

[55] F. Li, Y. Yang, and J. Wu, "Cpmc: an efficient proximity malware coping scheme in smartphone-based mobile networks," in *INFOCOM, 2010 Proceedings IEEE*. IEEE, 2010, pp. 1–9.

[56] Y. Li, P. Hui, D. Jin, L. Su, and L. Zeng, "Optimal distributed malware defense in mobile networks with heterogeneous devices," *Mobile Computing, IEEE Transactions on*, vol. 13, no. 2, pp. 377–391, 2014.

[57] Y. Li, Y. Jiang, D. Jin, L. Su, L. Zeng, and D. O. Wu, "Energy-efficient optimal opportunistic forwarding for delay-tolerant networks," *Vehicular Technology, IEEE Transactions on*, vol. 59, no. 9, pp. 4500–4512, 2010.

[58] Y. Li, Z. Wang, D. Jin, L. Zeng, and S. Chen, "Collaborative vehicular content dissemination with directional antennas," *Wireless Communications, IEEE Transactions on*, vol. 11, no. 4, pp. 1301–1306, 2012.

[59] M. Liljenstam, Y. Yuan, B. Premore, and D. Nicol, "A mixed abstraction level simulation model of large-scale internet worm infestations," in *10th IEEE International Symposium on Modeling, Analysis and Simulation of Computer and Telecommunications Systems, MASCOTS 2002*. IEEE, 2002, pp. 109–116.

[60] A. Lindgren, A. Doria, and O. Schelén, "Probabilistic routing in intermittently connected networks," *ACM SIGMOBILE Mobile Computing and Communications Review*, vol. 7, no. 3, pp. 19–20, 2003.

[61] X. Lu and P. Hui, "An energy-efficient n-epidemic routing protocol for delay tolerant networks," in *Networking, Architecture and Storage (NAS), 2010 IEEE Fifth International Conference on*. IEEE, 2010, pp. 341–347.

[62] Z. Lu, W. Wang, and C. Wang, "How can botnets cause storms? understanding the evolution and impact of mobile botnets."

[63] H. Malchow, S. V. Petrovskii, and E. Venturino, *Spatiotemporal patterns in ecology and epidemiology: theory, models, and simulation*. Chapman & Hall/CRC Press London, 2008.

[64] J. Mickens and B. Noble, "Modeling epidemic spreading in mobile environments," in *Proceedings of the 4th ACM Workshop on Wireless Security*. ACM, 2005, pp. 77–86.

[65] R. Morton and K. Wickwire, "On the optimal control of a deterministic epidemic," *Advances in Applied Probability*, pp. 622–635, 1974.

[66] W. H. Murray, "The application of epidemiology to computer viruses," *Computers & Security*, vol. 7, no. 2, pp. 139–145, 1988.

[67] G. Neglia and X. Zhang, "Optimal delay-power tradeoff in sparse delay tolerant networks: a preliminary study," in *Proceedings of the 2006 SIGCOMM workshop on Challenged networks*. ACM, 2006, pp. 237–244.

[68] S. Nelson, M. Bakht, and R. Kravets, "Encounter-based routing in dtns," in *INFOCOM 2009, IEEE*. IEEE, 2009, pp. 846–854.

[69] H. Nguyen and Y. Shinoda, "A macro view of viral propagation and its persistence in heterogeneous wireless networks," in *Fifth International Conference on Networking and Services*. IEEE, 2009, pp. 359–365.

[70] A.-K. Pietilainen, "CRAWDAD data set thlab/sigcomm2009 (v. 2012-07-15)," Downloaded from http://crawdad.org/thlab/sigcomm2009/, Jul. 2012.

[71] K. Ramachandran and B. Sikdar, "Modeling malware propagation in networks of smart cell phones with spatial dynamics," in *IEEE INFOCOM'07*, 2007, pp. 2516–2520.

[72] ——, "On the stability of the malware free equilibrium in cell phones networks with spatial dynamics," in *ICC'07*, 2007, pp. 6169–6174.

[73] A. Rao, D. Benson, C. Darby, M. Patterson, C. Francolin, I. Sanders, and G. Huntington, "Algorithm 902: Gpops, a matlab software for solving multiple-phase optimal control problems using the gauss pseudospectral method," *ACM Transactions on Mathematical Software*, vol. 37, no. 2, pp. 1–39, 2010.

[74] R. E. Rowthorn, R. Laxminarayan, and C. A. Gilligan, "Optimal control of epidemics in metapopulations," *Journal of the Royal Society Interface*, vol. 6, no. 41, pp. 1135–1144, 2009.

[75] S. Rump, "Intlab - interval laboratory," *Developments in Reliable Computing*, pp. 77–104, 1999.

[76] D. Sanger, "Obama order sped up wave of cyberattacks against iran," *New York Times*, June 1st, 2012.

[77] H. C. Schramm and D. P. Gaver, "Lanchester for cyber: The mixed epidemic-combat model," *Naval Research Logistics (NRL)*, vol. 60, no. 7, pp. 599–605, 2013.

[78] A. Seierstad and K. Sydsaeter, *Optimal control theory with economic applications*. North-Holland Amsterdam, 1987, vol. 20.

[79] S. P. Sethi, "Dynamic optimal control models in advertising: a survey," *SIAM review*, vol. 19, no. 4, pp. 685–725, 1977.

[80] S. P. Sethi and P. W. Staats, "Optimal control of some simple deterministic epidemic models," *Journal of the Operational Research Society*, pp. 129–136, 1978.

[81] S. P. Sethi and G. L. Thompson, *Optimal control theory: applications to management science and economics*. Kluwer Academic Publishers Boston, 2000, vol. 101.

[82] C. Singh, A. Kumar, and R. Sundaresan, "Delay and energy optimal two-hop relaying in delay tolerant networks," in *Modeling and Optimization in Mobile, Ad Hoc and Wireless Networks (WiOpt), 2010 Proceedings of the 8th International Symposium on*. IEEE, 2010, pp. 256–265.

[83] C. Singh, A. Kumar, R. Sundaresan, and E. Altman, "Optimal forwarding in delay tolerant networks with multiple destinations," in *Modeling and Opti-*

mization in Mobile, Ad Hoc and Wireless Networks (WiOpt), 2011 International Symposium on. IEEE, 2011, pp. 228–235.

[84] T. Spyropoulos, K. Psounis, and C. Raghavendra, "Spray and wait: an efficient routing scheme for intermittently connected mobile networks," in *Proceedings of the 2005 ACM SIGCOMM workshop on Delay-tolerant networking*. ACM, 2005, pp. 252–259.

[85] R. Stengel, *Optimal control and estimation*. Dover Publications, 1994.

[86] J. Stewart, "Calculus early transcendentals, 6e," *Belmont, CA: Thompson Brooks/Cole*, 2006.

[87] Symantec, "Regin: Top-tier espionage toolenables stealthy surveillance," *White paper, Symantec Corp., Security Response*, 2014.

[88] A. Vahdat, D. Becker *et al.*, "Epidemic routing for partially connected ad hoc networks," Technical Report CS-200006, Duke University, Tech. Rep., 2000.

[89] P. Wang, M. C. González, C. A. Hidalgo, and A.-L. Barabási, "Understanding the spreading patterns of mobile phone viruses," *Science*, vol. 324, no. 5930, pp. 1071–1076, 2009.

[90] Y. Wang and H. Wu, "DFT-MSn: The delay fault tolerant mobile sensor network for pervasive information gathering," in *INFOCOM, Proceedings of IEEE*, 2006, pp. 1021–1034.

[91] L. Weng, A. Flammini, A. Vespignani, and F. Menczer, "Competition among memes in a world with limited attention," *Scientific Reports*, vol. 2, 2012.

[92] K. Wickwire, "Optimal isolation policies for deterministic and stochastic epidemics," *Mathematical biosciences*, vol. 26, no. 3, pp. 325–346, 1975.

[93] ——, "Optimal control policies for reducing the maximum size of a closed epidemic : I. deterministic dynamics," *Mathematical Biosciences*, vol. 30, no. 1, pp. 129–137, 1976.

[94] Y. Yang, S. Zhu, and G. Cao, "Improving sensor network immunity under worm attacks: a software diversity approach," in *Proceedings of the 9th ACM international symposium on Mobile ad hoc networking and computing*. ACM, 2008, pp. 149–158.

[95] K. Zetter, "Digital detectives deciphered stuxnet, the most menacing malware in history," *Wired Magazine*, 2011.

[96] X. Zhang, G. Neglia, J. Kurose, and D. Towsley, "Performance modeling of epidemic routing," *Computer Networks*, vol. 51, no. 10, pp. 2867–2891, 2007.

[97] Z. Zhu, G. Cao, S. Zhu, S. Ranjan, and A. Nucci, "A social network based patching scheme for worm containment in cellular networks," in *INFOCOM'09*. IEEE, 2009, pp. 1476–1484.

[98] C. C. Zou, W. Gong, and D. Towsley, "Code red worm propagation modeling and analysis," in *Proceedings of the 9th ACM conference on Computer and communications security*. ACM, 2002, pp. 138–147.

[99] G. Zyba, G. Voelker, M. Liljenstam, A. Méhes, and P. Johansson, "Defending mobile phones from proximity malware," in *INFOCOM 2009, IEEE*. IEEE, 2009, pp. 1503–1511.